NASA CONTRACTOR REPORT

NASA CR-2372

NASA CR-2372

SNAP-8 REFRACTORY BOILER DEVELOPMENT PROGRAM

by R. A. Fuller

Prepared by
GENERAL ELECTRIC COMPANY
Cincinnati, Ohio 45215
for Lewis Research Center

NATIONAL AERONAUTICS AND SPACE ADMINISTRATION • WASHINGTON, D. C. • APRIL 1974

1. Report No.	2. Government Accession No.	3. Recipient's Catalog No.
NASA CR-2372		

4. Title and Subtitle	5. Report Date
SNAP-8 REFRACTORY BOILER DEVELOPMENT PROGRAM	APRIL - 1974
	6. Performing Organization Code

7. Author(s)	8. Performing Organization Report No.
R. A. Fuller	None
	10. Work Unit No.
9. Performing Organization Name and Address	
General Electric Company P.O. Box 15132 Cincinnati, Ohio 45215	11. Contract or Grant No. NAS 3-10610
	13. Type of Report and Period Covered Contractor Report
12. Sponsoring Agency Name and Address	
National Aeronautics and Space Administration Washington, D.C. 20546	14. Sponsoring Agency Code

15. Supplementary Notes

Final Report. Project Manager, Edward R. Furman, Power Systems Division, NASA Lewis Research Center, Cleveland, Ohio

16. Abstract

Performance and endurance tests of the SNAP-8, SN-1 refractory metal boiler are described. The tests were successful and indicated that the boiler heat transfer area could be reduced significantly primarily because of the wetting characteristics of mercury on tantalum in a contaminant-free environment. A continuous endurance test of more than 10 000 hours was conducted without noticeable change in the thermal performance of the boiler. A conclusion of the metallographic examination of the boiler following the endurance test was that expected boiler life would be of the order of 40 000 hours at observed corrosion rates.

17. Key Words (Suggested by Author(s))	18. Distribution Statement
Mercury boiler; Tantalum tubes; Tantalum/ stainless steel bimetal joints; boiler hydraulic testing; Mercury corrosion testing	Unclassified - unlimited Cat. 03

19. Security Classif. (of this report)	20. Security Classif. (of this page)	21. No. of Pages	22. Price*
Unclassified	Unclassified	228	$5.75

* For sale by the National Technical Information Service, Springfield, Virginia 22151

Page Intentionally Left Blank

TABLE OF CONTENTS

LIST OF FIGURES

Figure

Figure

Figure

Figure

Figures

LIST OF TABLES

I. SUMMARY

The General Electric Company, under contract NAS 3-10610, has completed an analytical and experimental development program for NASA-Lewis Research Laboratory. The objectives of this program were:

A. To establish the performance and endurance capabilities of a full scale, multitube, double containment, NaK-Hg refractory metal boiler for the SNAP-8 Power Conversion System.

B. To investigate the effects of possible gaseous and solid contaminants on the containment material.

C. To determine the mechanical strength and corrosion resistance of the tantalum stainless steel transition sections employed in the boiler design.

This report details the performance and endurance tests of the SNAP-8 boiler and describes the test facility. In addition, summaries of work completed concurrently with the test program are included. These are: the corrosion resistance of tantalum to mercury and NaK, low cycle fatigue tests of tantalum, thermal shock testing of tantalum/Type 316 stainless steel bimetallic joints, shellside hydraulic studies of a full scale model boiler, a single tube boiler and the development of a mercury electromagnetic pump.

Initial boiler test results indicated that boiler performance characteristics were essentially the same as at NASA-LeRC, namely the lack of boiling and low pressure drop in the plug region, and an undesirable circumferential shell temperature distribution in the high heat transfer region of the boiler.

The failure of the mercury inlet tantalum/stainless steel transition joint required the rebuilding of the test boiler in the field. This rebuild included the recentering of the tube bundle within the shell,at which time a heavy deposit was discovered and removed from the tube bundle in the high heat transfer region. Subsequent tests showed a marked improvement in thermal performance as well as an improvement in the circumferential shell thermal gradient.

A 2500-hour endurance test was completed without thermal performance degradation, at which time the facility was secured in good working order. A radiographic examination of the boiler showed the mercury exit bellows to be distorted and the mercury inlet bellows to be deformed. A rebuild of the boiler in the field elim nated the exit bellows and the inlet of the boiler was made such that the bellows operates at the lower static NaK pressure rather than the high mercury pressure.

A subsequent 10,000-hour endurance test was completed without performance degradation,which concluded the test program. The boiler was removed from the facility, sectioned, examined metallurgically, and found to be completely satisfactory.

Some general conclusions can be drawn from this test program:

1. The double containment refractory metal boiler concept is completely satisfactory. The results of the metallurgical evaluation indicate a life expectancy of 40,000 hours at observed corrosion rates.
2. Refractory metal boilers can be successfully repaired in the field if access is provided.
3. The SNAP-8 boiler design is conservative thermally.
4. Precipitation of impurities in the primary NaK onto the boiler tubes, as well as mercury side contamination, may effect boiler performance.

Tantalum specimens with homogeneous oxygen concentrations ranging from 50-500 ppm were exposed to NaK at 1350°F to determine the threshold oxygen concentration for corrosion.[8] In addition, contaminated and uncontaminated specimens were welded in a pure helium and helium atmosphere contaminated with air to evaluate the combined effects of welding, welding gas purity and pre-weld oxygen concentration of the tantalum on the corrosion resistance of tantalum to NaK. Results of these tests have shown that oxygen dissolution will occur at the tantalum-NaK interface without corrosion if the oxygen concentration is below 270 ppm.

Specimens of tantalum, T-111 alloy and Cb-1Zr were strained 5 and 20% by bending.[9] A portion of the bent specimens was retained in the as-bent condition while portions of the remaining specimens were given selected vacuum anneals.

Specimens and mercury were encapsulated in tantalum capsules and tested at 1200°F for 1000 hours. Subsequent cleaning and post-test evaluation indicated no observable changes in any of the specimens as a result of the exposure to mercury.

The start-up procedure for the SNAP-8 power conversion system results in a severe thermal transient within the boiler when mercury at 70° F is injected into the 1300° F boiler. The refractory boiler design necessitates the use of tantalum/Type 316 stainless steel transition joints. This test[11] was conducted to evaluate two joint designs; one a coextruded joint, the other a brazed joint. The coextruded joint failed after 55 thermal cycles while two brazed joints survived 155 and 100 cycles each.

A water flow test was performed on a shell side mockup of the SNAP-8 boiler.[12] The purpose of this test was to visually study the shell side hydraulic characteristics, to attempt to understand the reasons for the circumferential shell temperature distribution, and to propose and test modifications to the boiler that would improve boiler performance. Several tube bundle supports and turbulators were studied, as was an exit plenum.

Elevated temperature, uniaxial, low cycle fatigue tests[14] were performed on unalloyed tantalum. The results of these tests showed that tantalum has high resistance to low cycle fatigue consistent with its high ductility.

A single tube test boiler was designed and fabricated by GE-NSP[15] based upon the premise that, if mercury "wetted" the tantalum, the boiler would perform thermally in a manner similar to the "high performance" alkali metal boilers designed, fabricated and tested at GE-NSP. The NaK-Hg test boiler was installed in the GE test facility in order to check out the facility prior to the installation of the SNAP-8, SN-1 seven tube boiler. The single tube boiler performance was as predicted. Thus, if a contaminant-free environment could be assured for the SNAP-8 boiler, a greatly shortened version of the present seven tube design could be used at a saving in space and weight.

One of the reasons for the loss of boiler performance in prior tests of SNAP-8 boilers is the lubricating oil contamination from mechanical pumps. To preclude this possibility an electromagnetic centrifugal mercury pump[17] was developed which eliminated the oil bearings and permitted the testing of the refractory metal boiler in a

controlled loop environment. This pump developed in excess of 530 psi at 12,500 lb/hr for the duration of the test program without a failure and was probably the prime reason for the lack of thermal performance degradation in the test boiler.

II. INTRODUCTION

Early experience at General Electric with the mercury Rankine cycle [1] for central power station use has shown that the thermal performance of mercury boilers is erratic and depends on the degree of "wetting" that occurs between the mercury and the containment material. (Wetting is defined as the contact angle between the mercury and the containment material approaching 0°). In some cases, thermal performance was enhanced by the addition of a "wetting" agent such as rubidiuum. However, maintenance of the mercury central station proved expensive, thus eventually causing shutdown of the central stations built.

The advent of the SNAP-8 program to provide a dynamic power generating system for use in long term space vehicles revived an interest in the Mercury Rankine Cycle. Tests at Aerojet General Corporation [2] using Chrome-Moly steels as the mercury containment material again demonstrated that the thermal performance was unpredictable and the containment materials were not compatible with mercury.

Therefore, NASA-LeRC, after evaluating the results of various metallurgical tests conducted on several materials, chose tantalum for the mercury containment material because of its good corrosion resistance, low solubility and good "wetting" properties with mercury. A seven tube boiler was designed and fabricated by NASA-LeRC to determine the thermal performance and compatibility of tantalum with mercury.

GE-NSP, with its considerable background in the testing of refractory alloy components and loops at high temperature in a contaminant-free environment, was chosen by NASA-LeRC to test the SNAP-8, SN-1 refractory alloy boiler for long term thermal performance and compatibility of the materials of construction with the working fluids.

Boiler SN-1 is a seven tube, counterflow NaK to mercury heat exchanger with a static NaK third fluid between the primary loop NaK and the mercury to meet the radioactive fluid isolation requirements for manned space missions. The primary NaK portion of the boiler consists of the shell, baffles and tube supports fabricated from Type 304 stainless steel and the outside of the static NaK tubes which are Type 321 stainless steel. The mercury portion of the boiler is fabricated from

unalloyed tantalum with the exception of a short section of stainless steel at each end of the boiler where a transition is made from tantalum to stainless steel. The static NaK fills the void between the tantalum and the Type 321 stainless steel tubes. Bellows are provided at each end of the boiler to accommodate the difference in thermal expansion between the unalloyed tantalum and the stainless steel.

The boiler was installed in the W-1 test facility at Lewis Research Center and tested for approximately 1445 hours prior to its installation in a modified heat transfer facility at GE-NSP. This boiler, SN-1, was performance and endurance tested for 13,680 hours and subsequently removed for metallurgical evaluation. These tests proved the adequacy of the boiler design and the compatibility of the materials with the working fluids.

Concurrently with the boiler test program, experimental investigations were carried out to evaluate the threshold corrosion resistance of contaminated tantalum to NaK, the corrosion resistance of other refractory materials to mercury, the adequacy of the tantalum/stainless steel transition joint, the development of a mercury electromagnetic pump, hydraulic studies of the shell side of the SNAP-8 boiler, and the design, fabrication and test of a "high performance" single tube boiler.

III. TEST FACILITY

A. FACILITY DESCRIPTION

The SNAP-8 refractory boiler test facility is composed of a NaK primary loop and a mercury secondary loop. The NaK is heated by a gas-fired heater designed for a thermal input of 550 KW. The mercury loop, in which vapor is generated, transfers its heat to an air cooled condenser. Figure 1 is an isometric view of the boiler test facility and illustrates the locations of the principal components.

The primary NaK loop, which simulates the reactor coolant loop of an actual SNAP-8 Electric Generating System, contains a NaK electromagnetic pump with a capacity of 200 gpm. This is sufficient to meet the required 50,000 lb/hr NaK flow at nominal system conditions. To assure adequate NaK purity, a columbium 1% zirconium hot trap was installed in the dump tank. The NaK loop was helium mass spectrometer tested after construction and after each facility or boiler repair. The NaK loop was then flushed and hot trapped prior to system operation. This was sufficient to maintain NaK purity between 10 and 25 ppm oxide. High purity argon is used as a cover gas to prevent air infusion and to prevent the NaK from boiling during operation.

The instrumentation necessary to determine the heat input to the boiler and boiler performance includes an electromagnetic flowmeter and thermocouples. In addition, loop operating instrumentation, such as pressure gages, liquid level gages, gas fired heater thermocouples, are provided to facilitate facility operation.

The mercury pump provides 12,500 lb/hr of mercury at 530 psi to the boiler. The liquid throttle valve serves to dampen boiler oscillations which may occur during operation by varying the liquid mercury pressure drop. The turbine simulator is a throttle valve which can be varied to maintain boiler exit and condenser pressures as required. The air cooled condenser condenses the mercury vapor for return to the boiler. A tank is provided for mercury storage. Instrumentation is provided to determine boiler performance and includes pressure gages, venturi meters and thermocouples. Also provided are liquid level gages, condenser pressure gages, pump pressure gages and thermocouples that are necessary for monitoring and controlling loop operation.

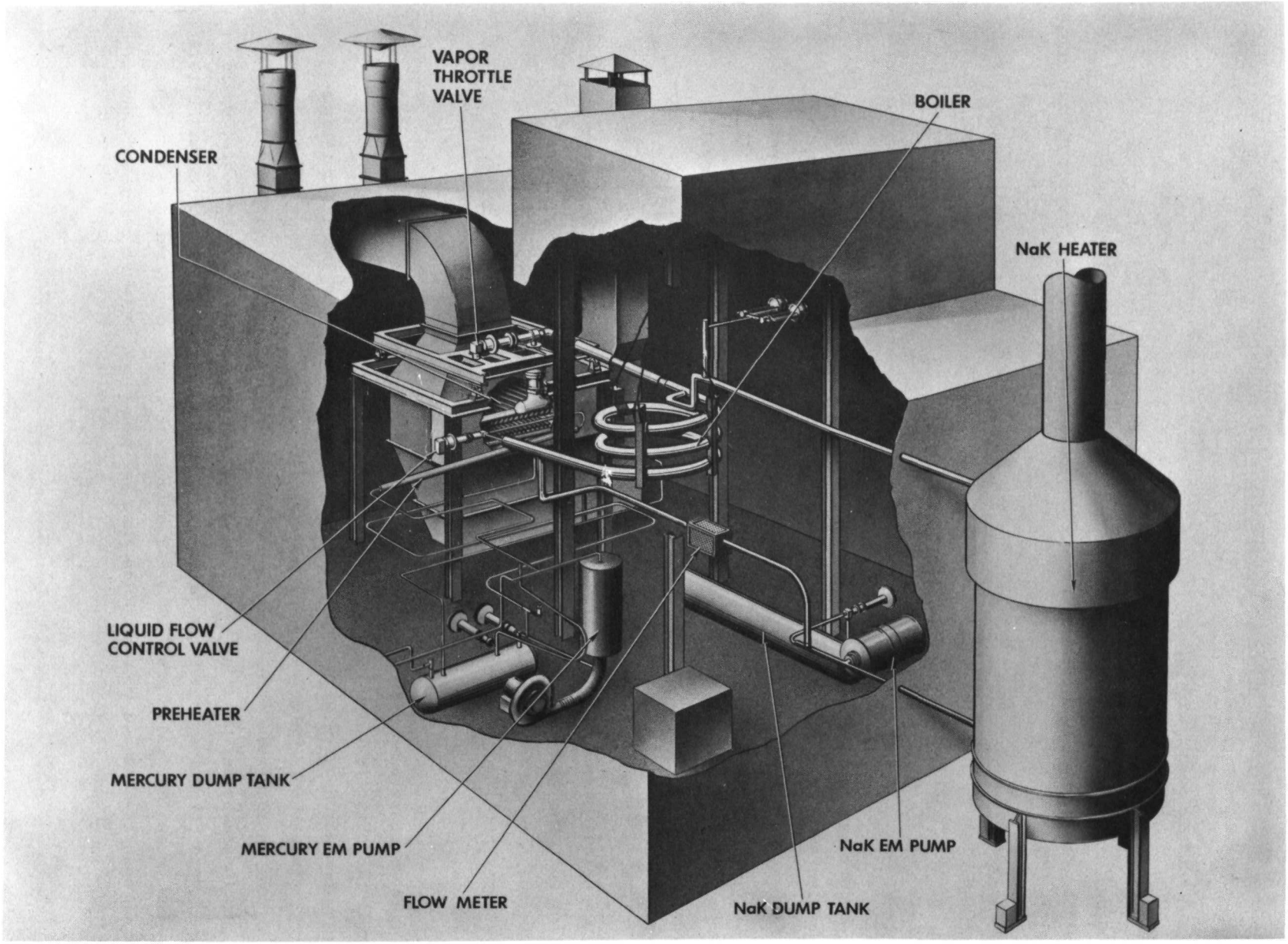

Figure 1. Isometric view of the SNAP-8 Refractory Boiler Test Facility.

The NaK loop, with the exception of the Type 316 stainless steel dump tank, is fabricated from L-605 alloy. The mercury loop,with the exception of the L-605 vapor line, turbine simulator and dump tank, is fabricated from Type 304 stainless steel. The facility is enclosed in a partitioned sheet metal enclosure. One section of the enclosure contains all the NaK components with the exception of the boiler; the other section contains all the mercury components and is coated with an epoxy paint to facilitate cleanup in the event of a mercury leak. In addition, all the air exhausted from the facility during operation is scrubbed prior to its release to the environment. To accommodate thermal expansion, the entire facility,with the exception of the gas fired heater and the mercury dump tank, is free to move.

COMPONENT DESCRIPTION

NaK LOOP

Heater - The gas fired heater, constructed by Struthers-Wells Corp., is shown schematically in Figure 2 and, as installed, in Figure 3. The tube bundle, fabricated completely from L-605, consists of two torroidal headers of 5-inch diameter pipes interconnected by 30 tubes of 1-inch diameter (inside) by 0.210-inch wall thickness. An 0.050-inch corrosion allowance and an 0.050-inch oxidation allowance are provided. To reduce thermal expansion stresses, the heater tubes have offset bends. The inlet header at the lower end is internally baffled for good flow distribution. The heater shell is air tight and the exhaust stack valved. In the event of a NaK leak inside the heater, all caustic fumes can be contained. An alternate vent line to a scrubber system serves to expedite cleanup. Automatic ignition and temperature control are provided to maintain constant NaK discharge temperature to the boiler. In addition, safety controls are provided to secure the heater in the event of a NaK or mercury pump failure, heater overtemperature, or flameout. The nominal rating of the heater is:

Heat Rate	550 KW
Fluid	NaK
Outlet Temperature	1350°F
Pressure	150 psi
Heat Transfer Area	120 ft^2

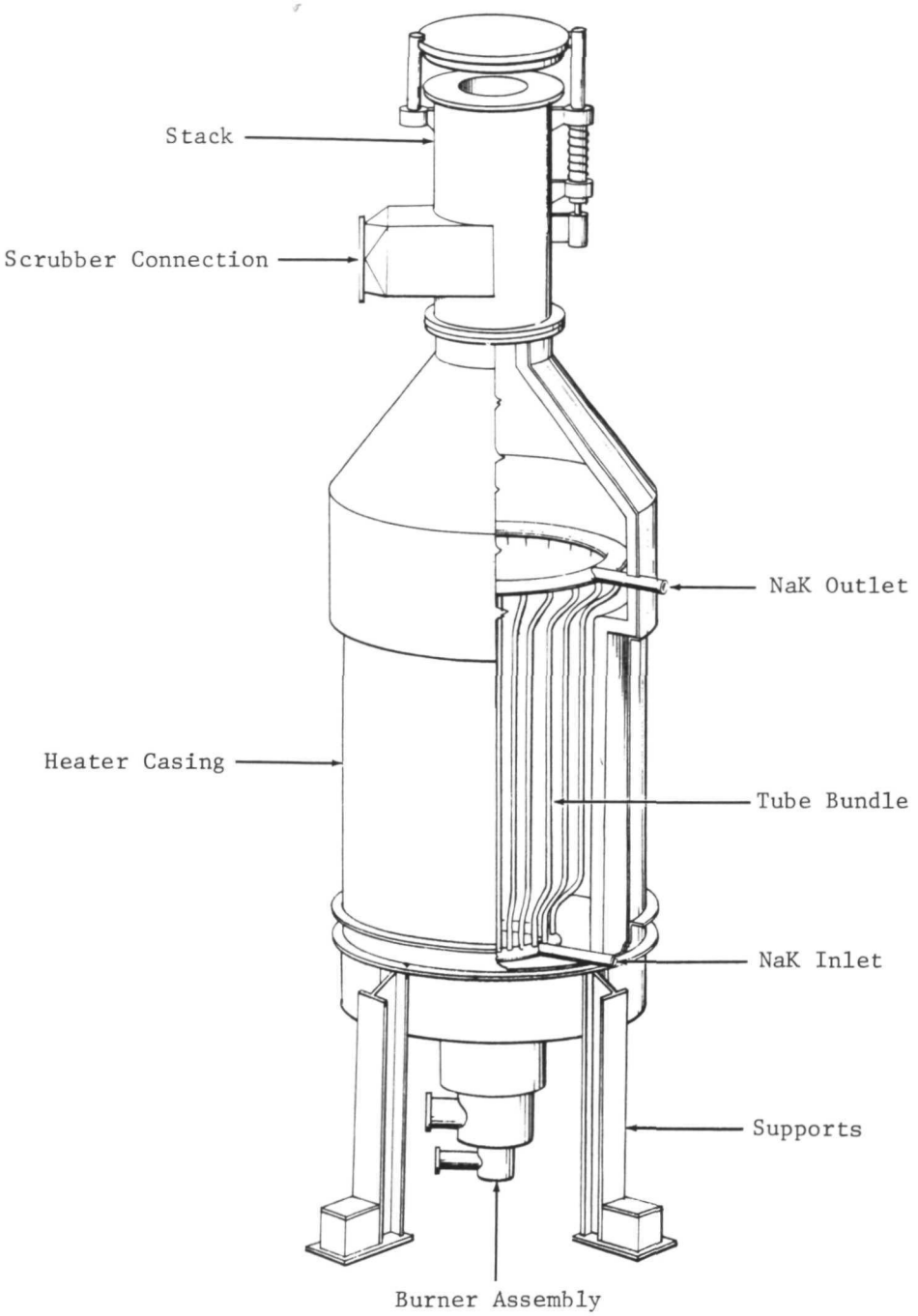

Figure 2. Schematic of facility gas fired heater.

Figure 3. Installation of facility gas fired heater.

The heater efficiency is approximately 30% and a large fraction of excess air is used to avoid carburation of the L-605 tube bundle and to limit flame temperature.

NaK Pump - A helical, induction, electromagnetic pump is used to circulate the NaK. Figure 4 shows the pump outline and pump duct detail. The pump, shown in Figure 5, consists of a polyphase stator, a pump duct made up of two concentric tubes with helical passages in the annulus, and suitable enclosing and supporting framework. The duct is fabricated from L-605 and operates at loop temperature. The stator uses conventional Class H electrical insulation and is thermally insulated from the duct. Compressed air is blown through passages in the stator laminations to keep the stator within the Class H insulation allowable temperature limits. Pump specifications are:

Working Fluid	NaK
Flow	200 gpm
Head	20 psi
Operating Temperature	1350°F
Power Input	35 KW, 440 Volt 60 Cycle

Valves - The valves utilized in the NaK loop were manufactured by either Fisher-Governor, Inc. or Hoke, Inc. The valves were designed for 1350°F at 100 psi operation and had stellited plugs and seats. These valves are of welded bellows design and were subjected to helium mass spectrometer leak testing prior to installation in the facility.

Dump Tank - The NaK dump tank, depicted along with other components in Figure 6, is sized to contain 650 lbs of NaK with ample volume for expansion in the event of an emergency dump. The dump tank consists of an 8-foot section of 18-inch diameter pipe by 0.500-inch wall pipe with 18 IPS pipe caps butt welded at each end. A fill and drain line, vent line, liquid level instrumentation and loop fill drain line are attached. Included in the dump tank is a hot trap of columbium 1% zirconium. The hot trap is shown in Figure 7. Heaters are attached to the lower half of the dump tank to promote natural circulation during hot

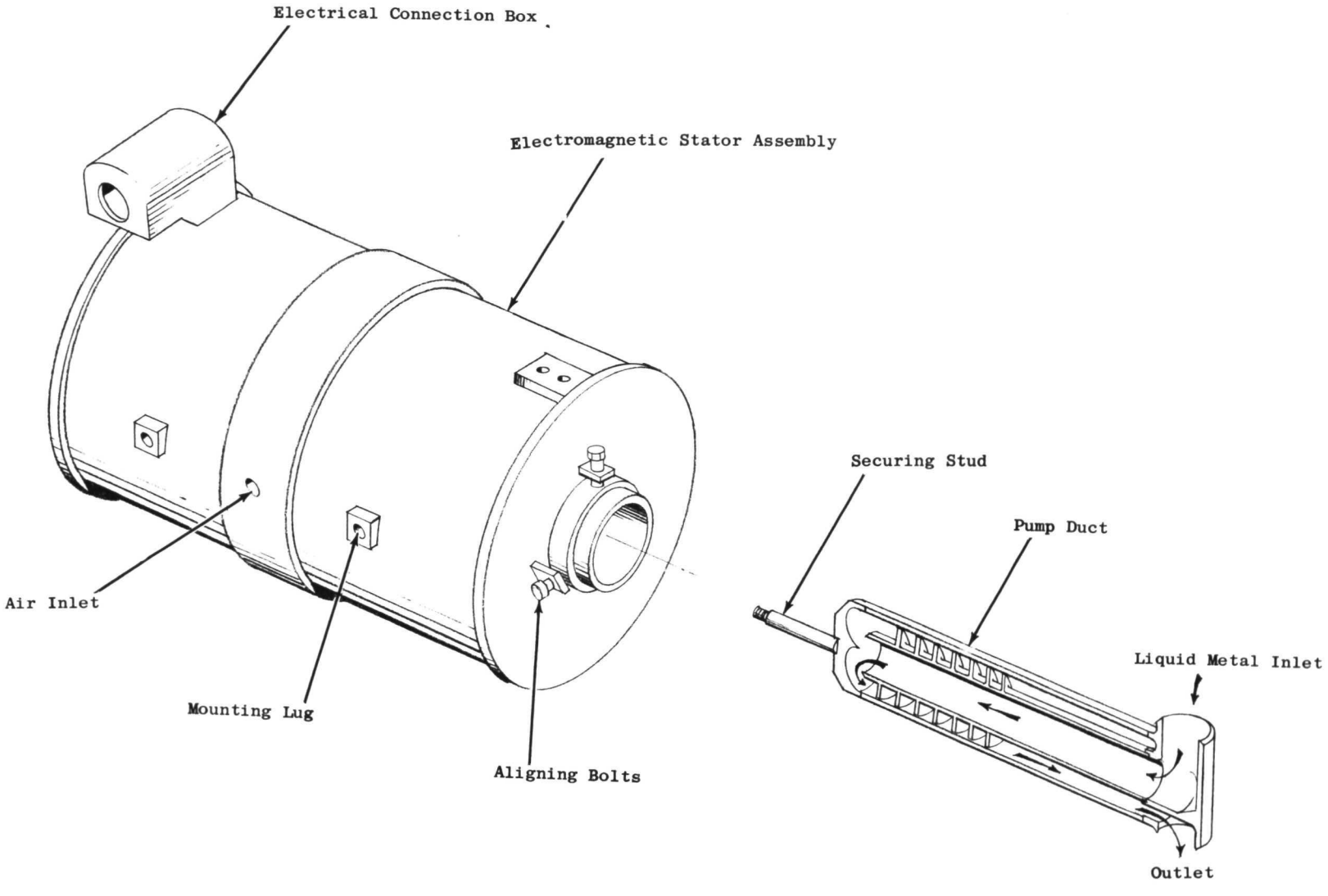

Figure 4. Schematic of facility NaK electromagnetic pump.

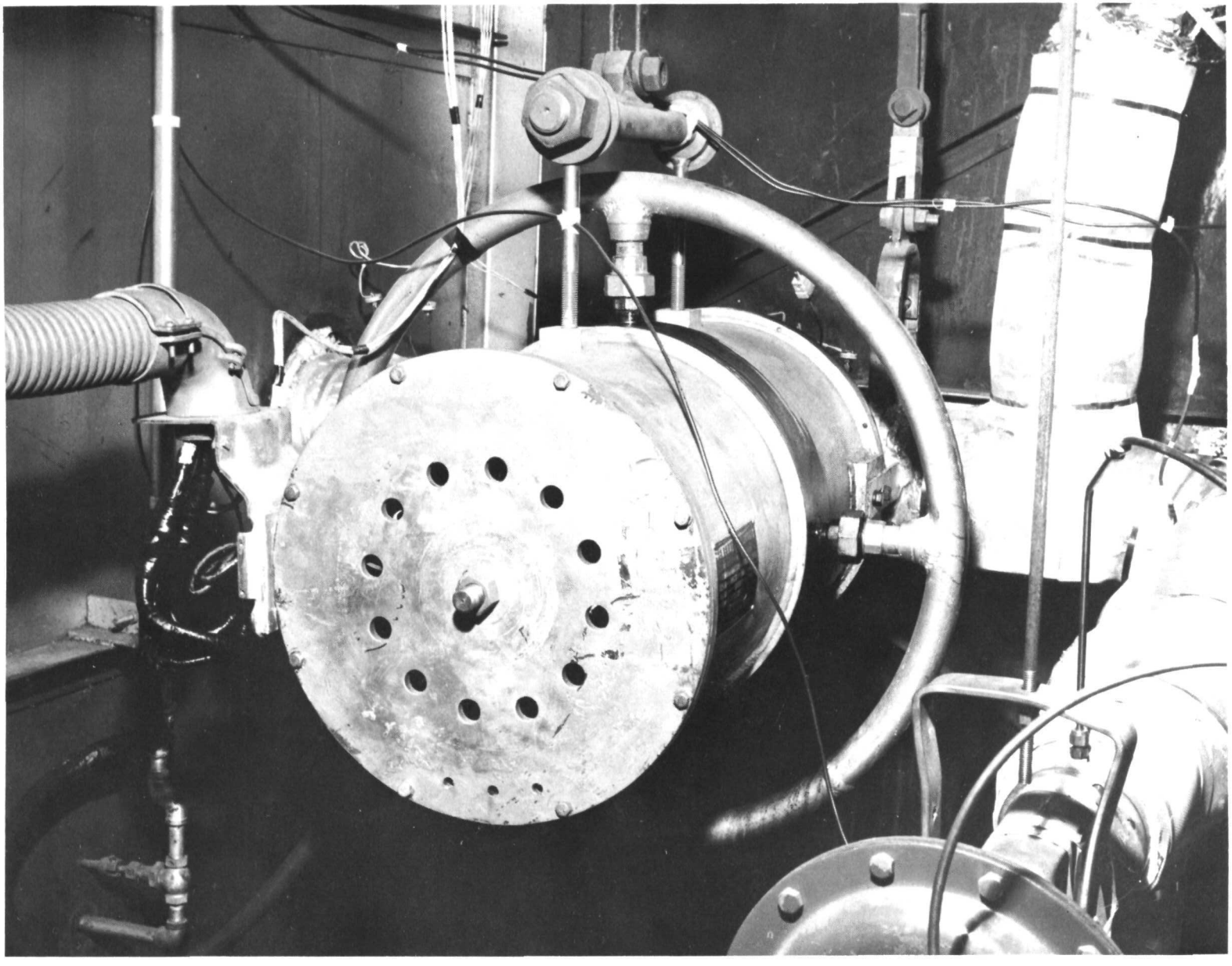

Figure 5. Installation of facility NaK electromagnetic pump.

Figure 6. SNAP-8 refractory boiler development test facility showing NaK dump tank and dump valve.

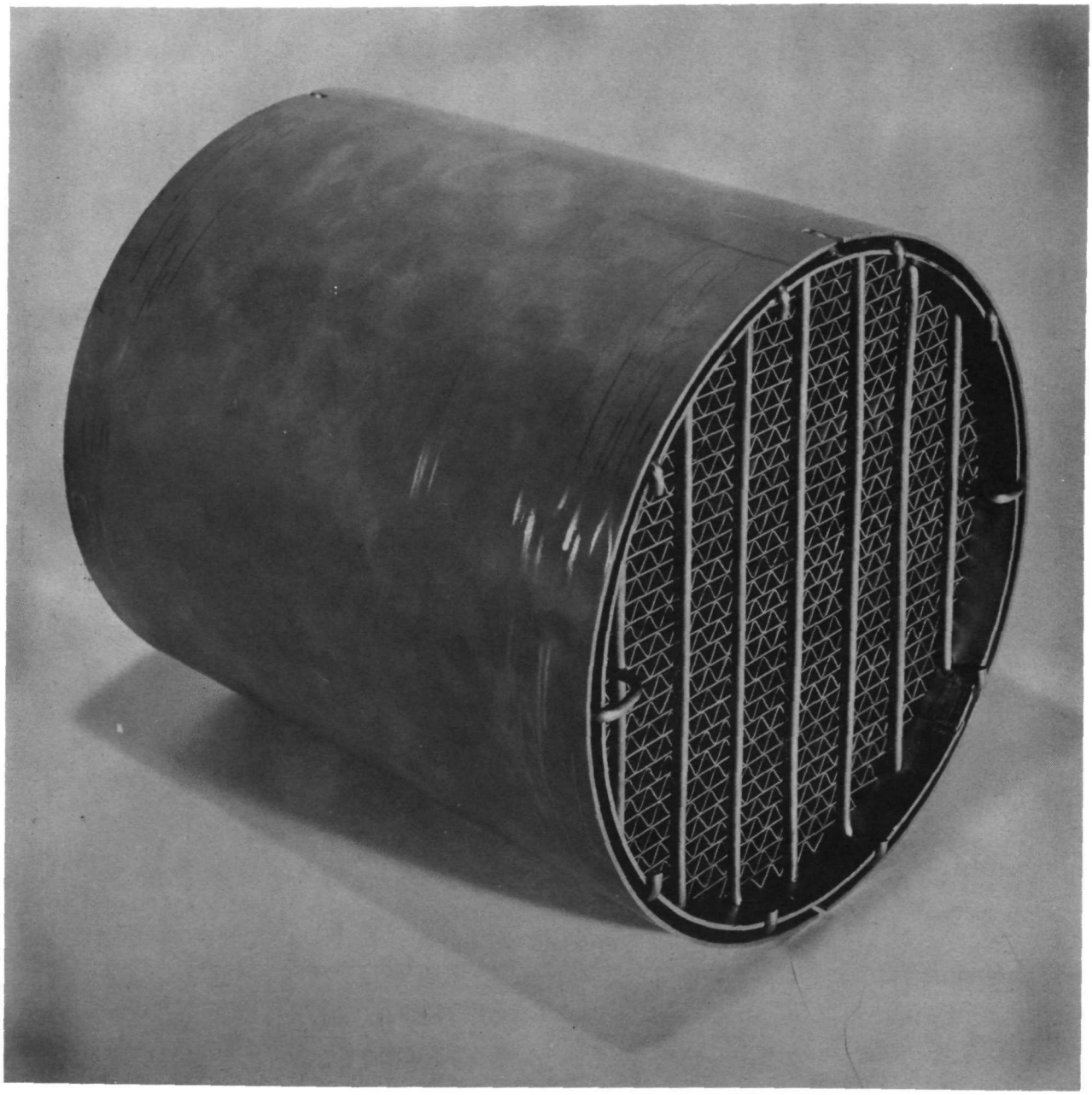

Figure 7. Typical refractory metal hot trap.

trapping. The electrical heaters are designed to maintain the dump tank at 1300°F. Automatic power controls are provided for temperature regulation.

MERCURY LOOP

Pump - A three stage mercury helical induction electromagnetic pump is shown schematically in Figure 8. The pump consists essentially of a polyphase stator, a pump duct consisting of two spiral diffusers and a flat plate with straightening vanes attached spaced within a section of 6-inch IPS pipe. Shown in Figure 9 are the diffusers. Attached at each end of the pipe section are two 6-inch IPS pipe caps with 3/4-inch pipe connections at the center of the caps. This pump resulted from a development test program[3] conducted by General Electric to develop a mercury electromagnetic pump primarily for this program. The performance curve for this pump is shown in Figure 10 and shows that the 530 psi developed head at 12,500 lbs/hr mercury flow can be achieved at approximately 535 volts. No difficulties were encountered in the operation of this pump for the entire program.

Condenser - The condenser installation, shown in Figure 11, was fabricated by Mine Safety Appliances Co. and consists of 30 1-1/2-inch outside diameter finned tubes connected in parallel to two 4-inch IPS headers. The condenser is suspended from a dolly to accommodate the facility thermal expansion and is totally enclosed in a sealed stainless steel sheet metal enclosure.

Valving is provided to introduce and remove inert gas from the lower header and a liquid level gage is installed to indicate the mercury inventory in the condenser. The condenser is cooled by two 8,000 CFM centrifugal blowers, shown in Figure 12. The blowers create a negative pressure inside the condenser box such that if condenser leak occurs, the mercury vapor is exhausted through the scrubber system. In addition, bypass air flow is provided to maintain the blower temperature within specified limits.

Valves - The mercury liquid throttle valve and turbine simulator are reworked L-605 alloy valves utilized on a previous program. The valves, shown in Figure 13, were manufactured by Fisher-Governor Co. and are all welded bellows sealed. The liquid throttle valve has a 3/8-inch diameter port with tapered plug to provide a method of varying the liquid pressure drop in the mercury loop to

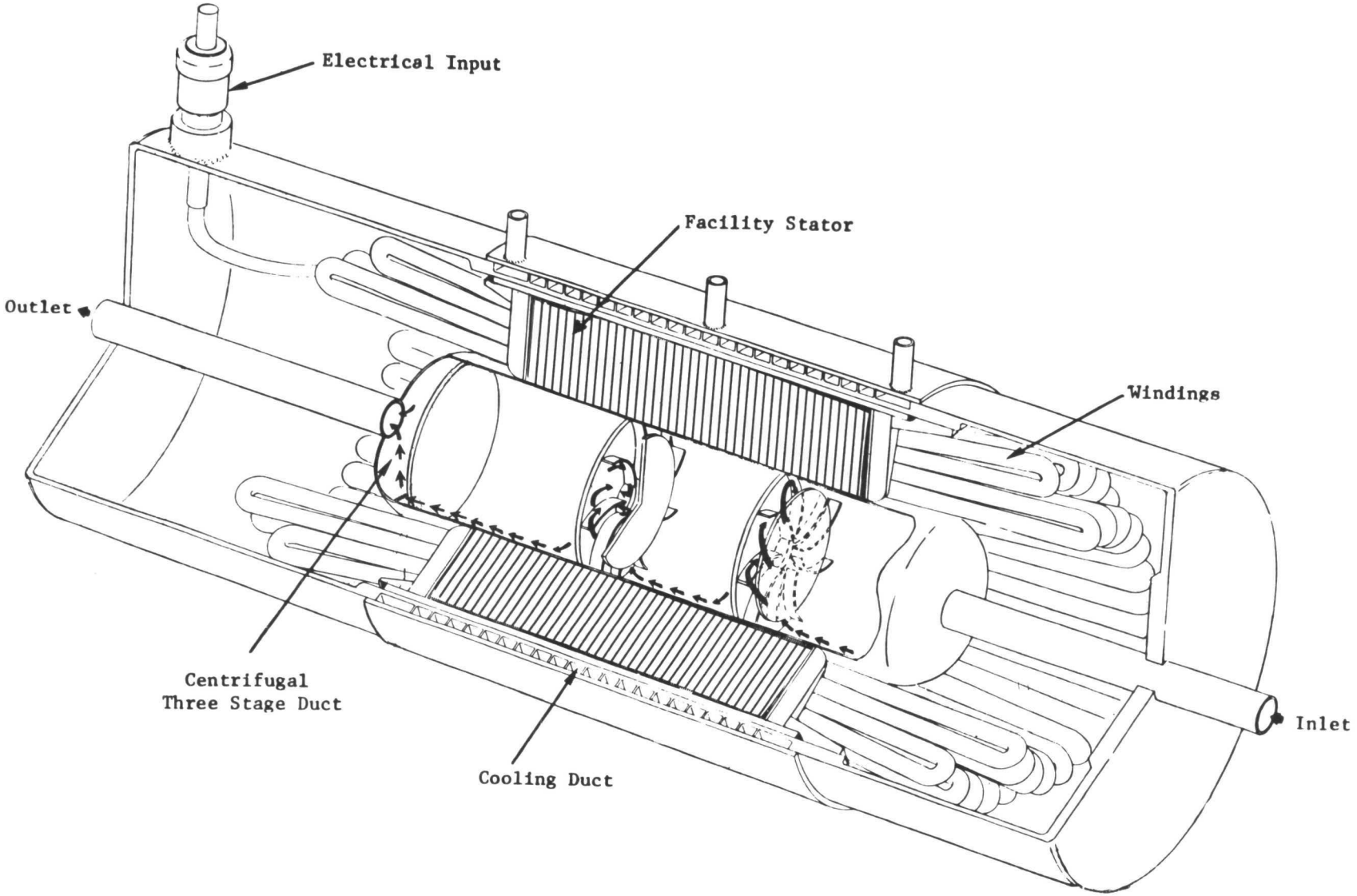

Figure 8. Three stage mercury centrifugal EM pump.

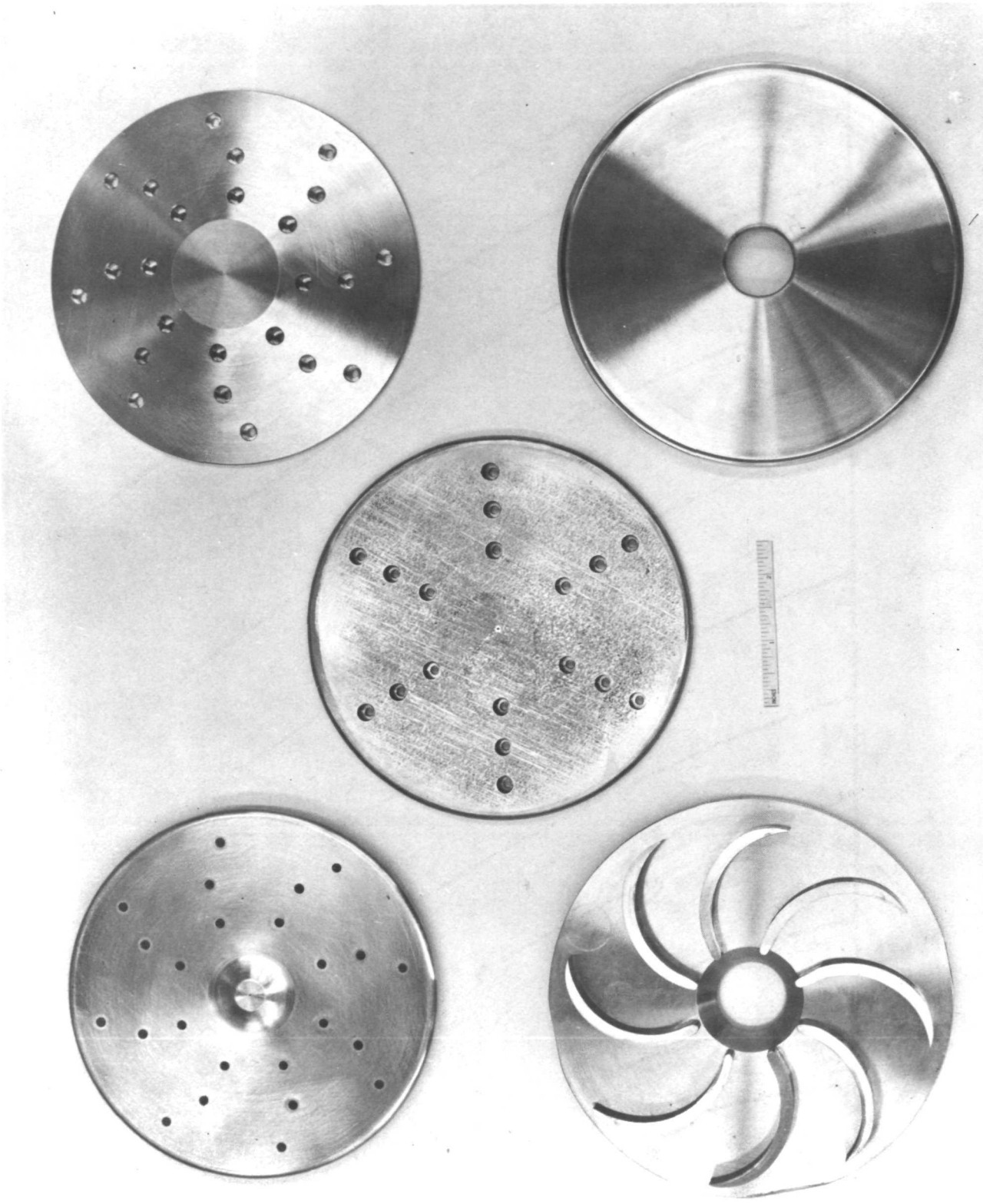

Figure 9. Diffusers for three stage centrifugal EM pump.

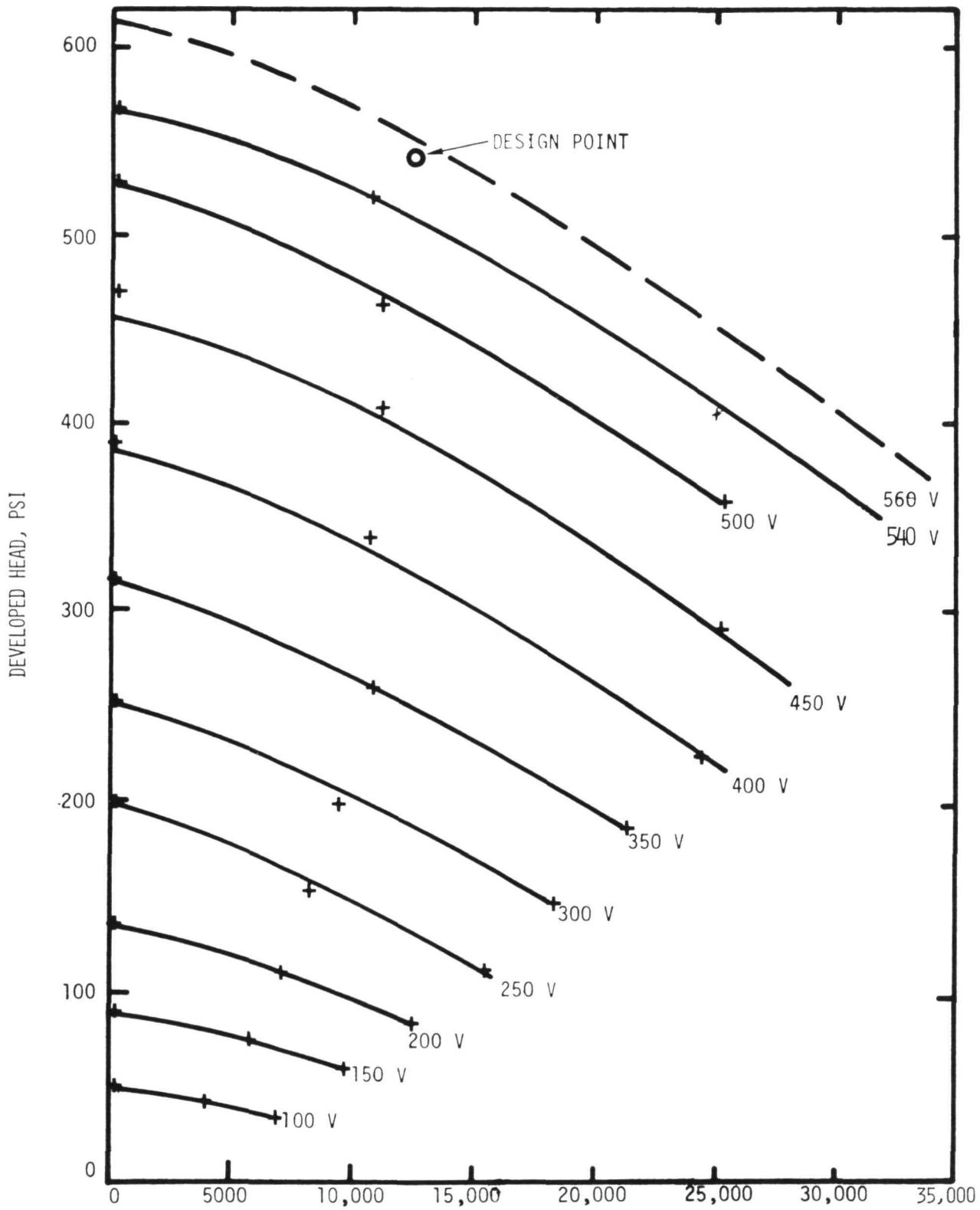

Figure 10. Performance curve for three stage centrifugal EM pump.

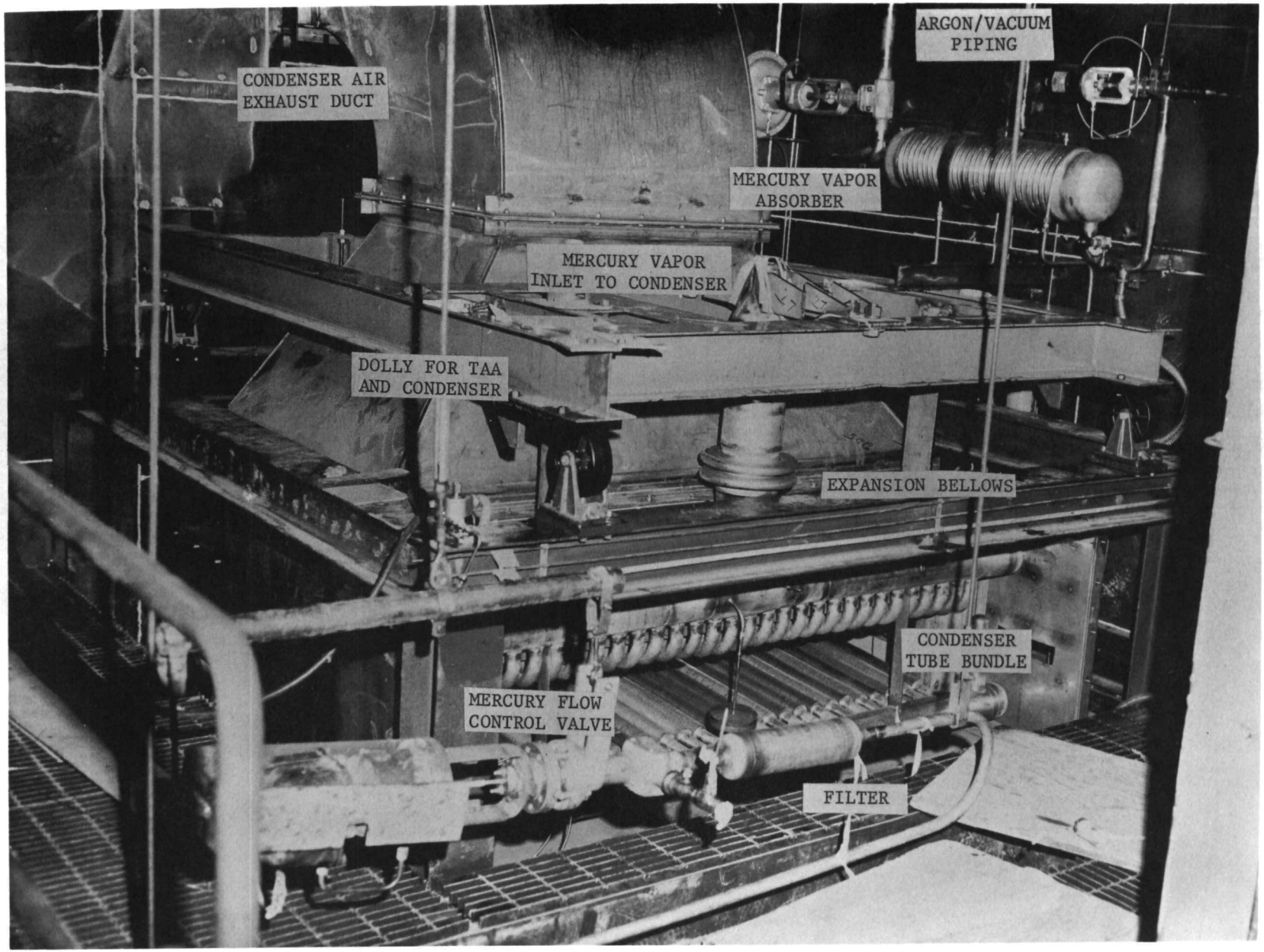

Figure 11. SNAP-8 refractory boiler development facility showing condenser, dolly, mercury piping, and argon/vacuum piping.

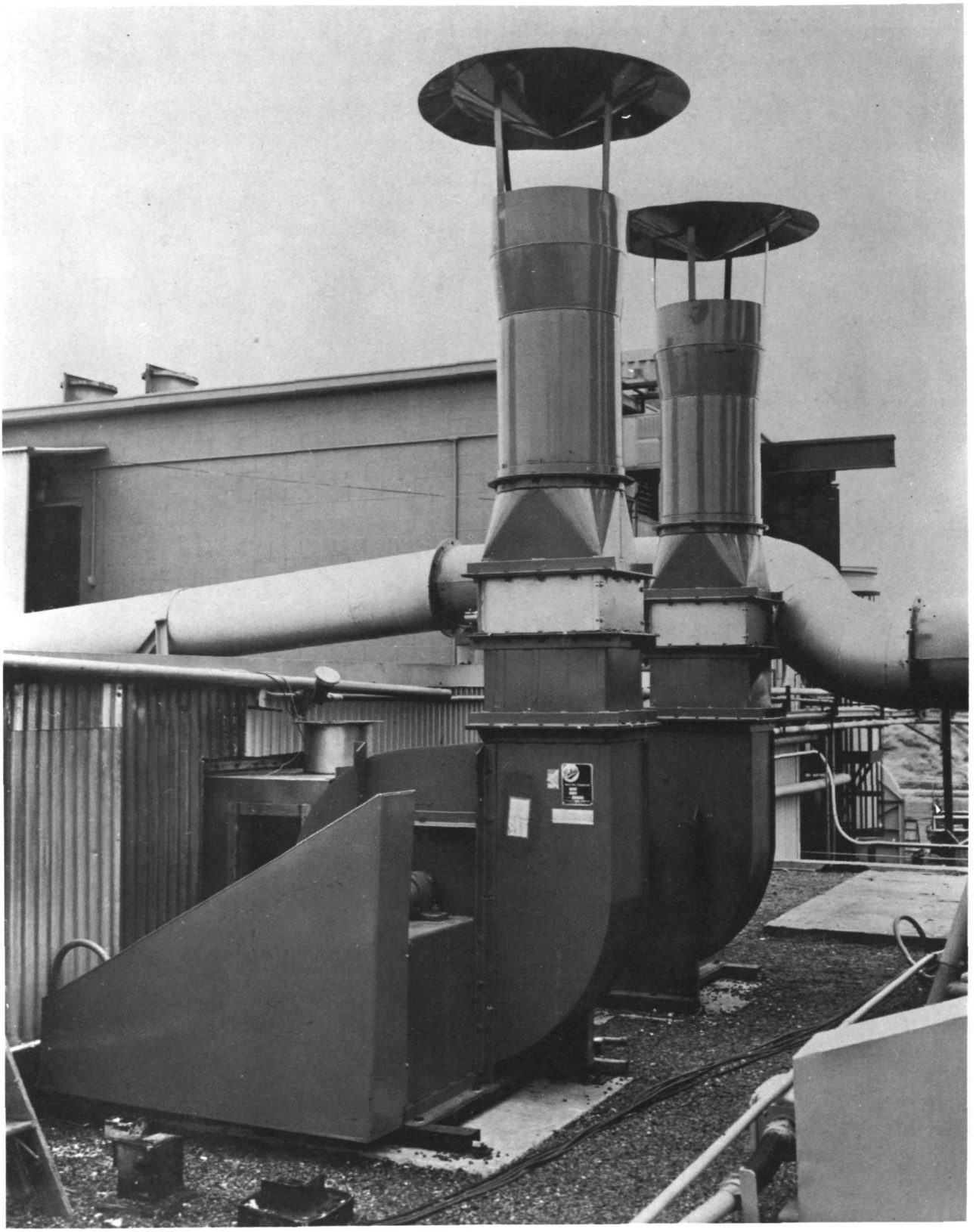

Figure 12. SNAP-8 refractory boiler development facility showing condenser air exhaust blower.

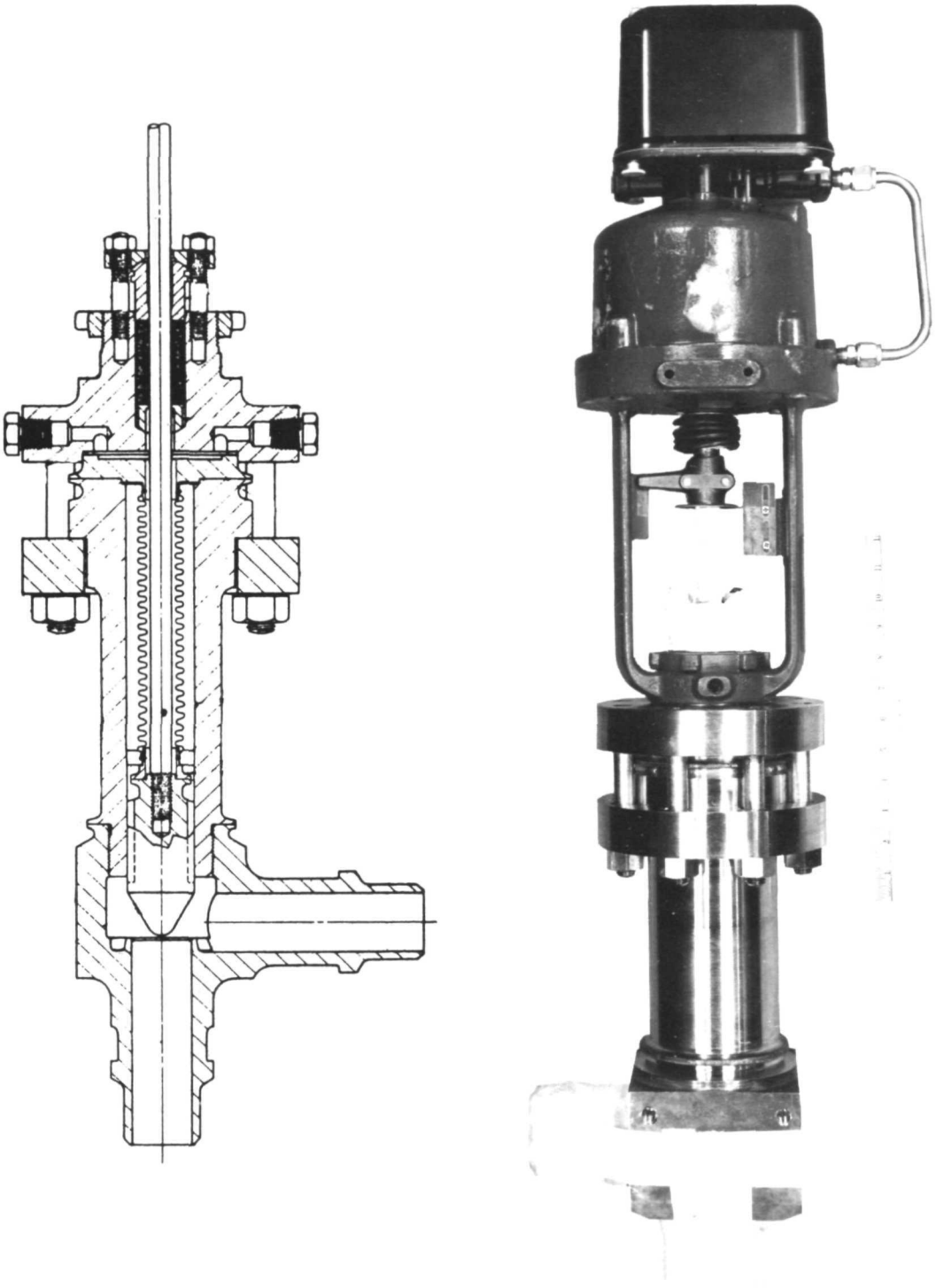

(a) Mercury Liquid Throttle Valve (b) Mercury Vapor Throttle Valve

Figure 13. Facility valves for SNAP-8 refractory boiler development facility.

stabilize the boiler. The plug and seat of this valve were stellited. The mercury vapor throttle valve has a 1-inch diameter port and tapered plug both fabricated from Stellite 6-B. This valve simulates the turbine pressure drop and permits the operation of the boiler and condenser at different pressures.

All other facility valves were manufactured by Hoke, Inc. and all bellows sealed valves were installed with the seat toward the working fluid.

Dump Tank - The mercury dump tank installation, shown in Figure 14, consists of a section of 18-inch diameter by 0.250-inch thick L-605 with 18-inch caps welded at each end. This tank was reworked from an earlier test program. Attached to the dump tank are the necessary loop fill and drain line, argon and vacuum vent lines, emergency dump line and tank fill and drain line.

Mercury Subcooler - The mercury subcooler, shown in Figure 14, consisted of a 1/4-inch tube helically wrapped and brazed to the 3/4-inch pipe line that ran from the condenser to the mercury pump and from the pump to the liquid throttle valve. The purpose of these coolers were to trim the mercury temperature to the pump suction to prevent cavitation at low condensing pressures and to control the boiler mercury inlet temperature.

Sampling System - Also shown in Figure 14 is the mercury sample line which is connected to a sample valve external to the enclosure for sampling during operation. Also provided at the sample station are valved argon and vacuum lines.

Filter - To protect the 7 orifices located at the mercury inlet to the boiler from blockage, a 40 micron filter was installed upstream of the boiler, as shown in Figure 11.

VACUUM - ARGON SYSTEM

The vacuum-argon system, shown in Figure 15, has a vacuum pump for both the NaK and mercury systems. The pumps are used to remove inert gases before and during operation. Liquid nitrogen filled cold traps are provided ahead of each vacuum to condense the vapors and prevent their exhaustion to the environment. The possibility of vapor exhaustion is greatest in the mercury condenser for it operates at a high temperature, low pressure and thus, during the removal of inert gases from the condenser, it is possible to exhaust mercury vapor. To minimize this possibility, a mercury adsorber (Figure 16), is installed. The

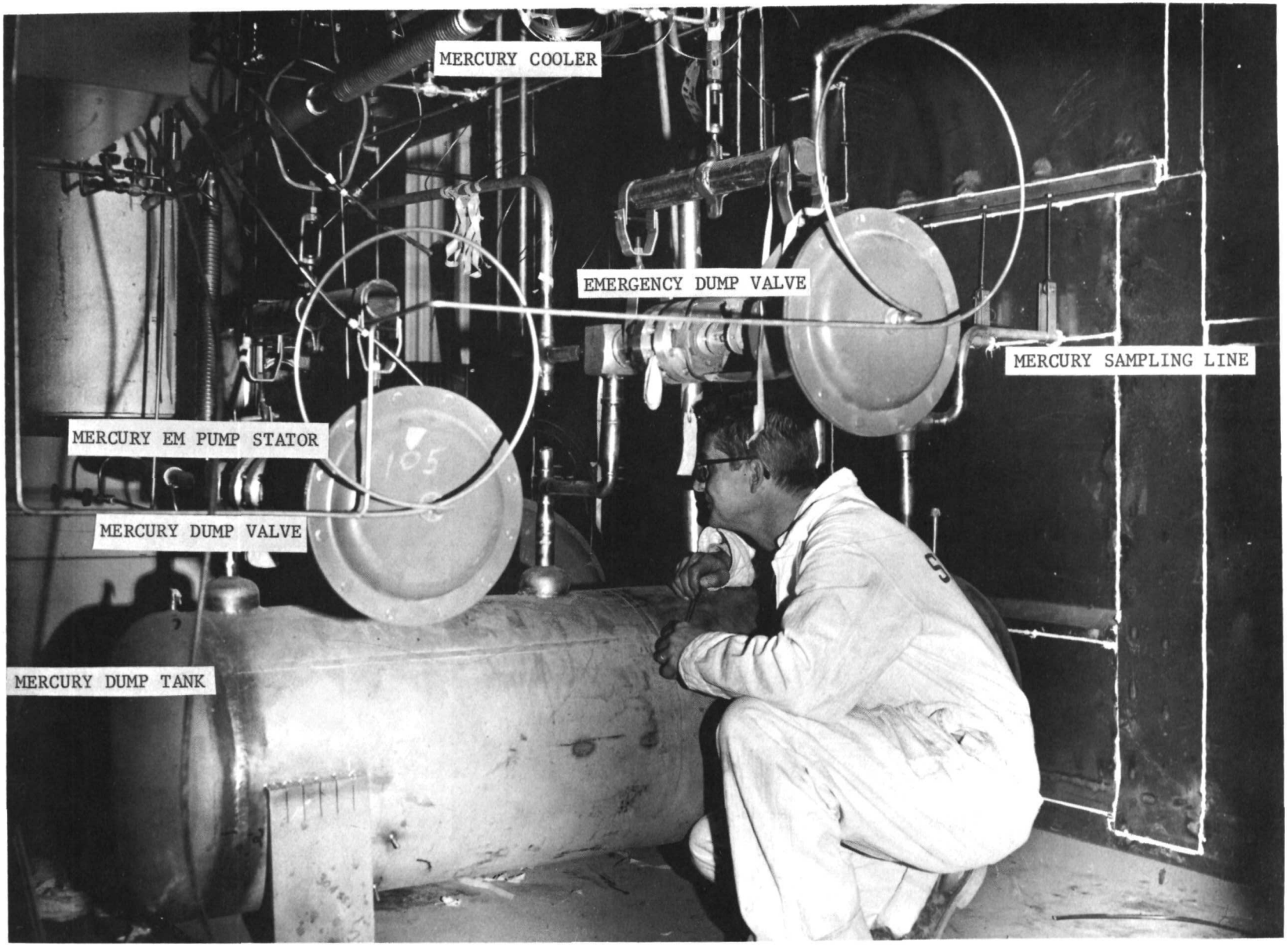

Figure 14. SNAP-8 refractory boiler development facility showing mercury dump tank with dump valves, EM pump stator, and sampling line.

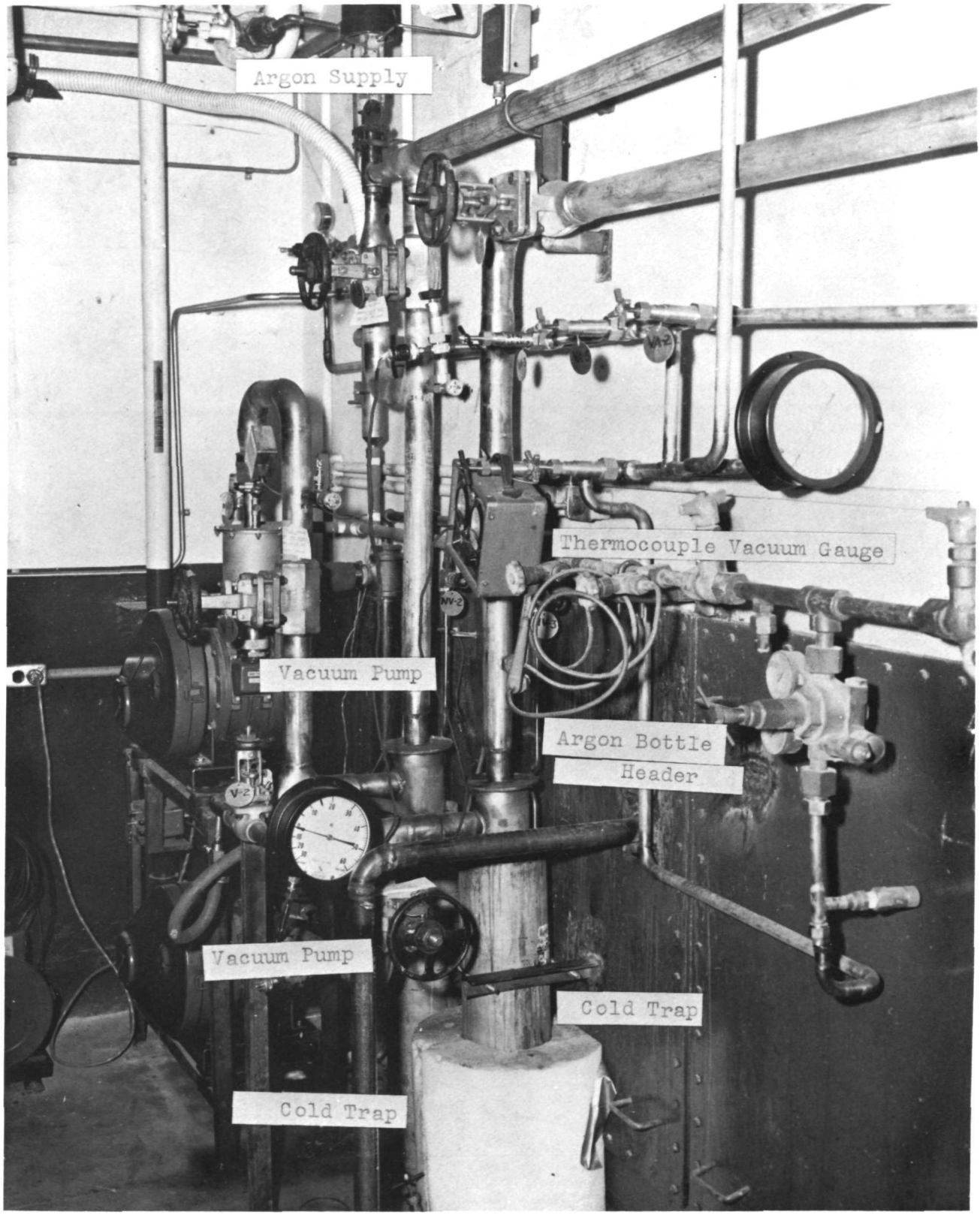

Figure 15. SNAP-8 refractory boiler development facility showing argon/vacuum system.

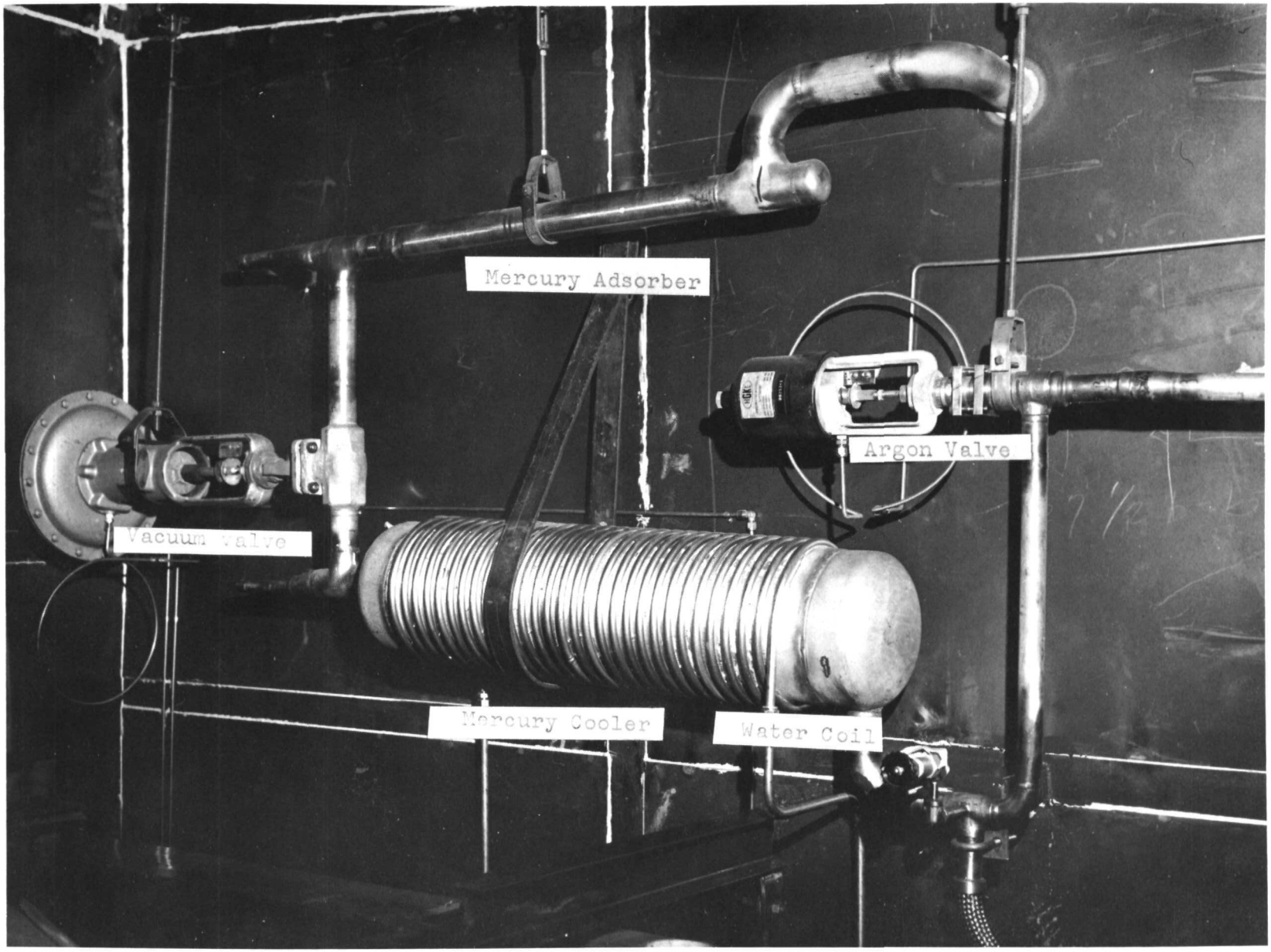

Figure 16. SNAP-8 refractory boiler development facility showing mercury vapor cooler and adsorber.

adsorber consists of a section of 2-inch IPS pipe with end caps and appropriate piping connections. The internals of the pipe are packed with copper mesh to collect mercury vapor. Also shown in Figure 16 is a mercury vapor condenser which is a section of 8-inch stainless steel pipe with end caps and piping connection. The cooler is wrapped with stainless steel tubing for water cooling. The cooler condenses extracted mercury vapor prior to its entering the mercury adsorber.

Inert gas is provided to the mercury loop at the dump tank and condenser to prevent the infusion of air into the system and to fill the mercury loop and control condensing pressures. Likewise, inert gas is provided at the NaK dump tank and stand pipe to prevent air infusion, to fill the loop and control loop pressure.

BOILER DESCRIPTION

Boiler SN-1, designed and fabricated by NASA-LeRC, is a floating head, double contained, refractory metal boiler. The boiler, shown in Figure 17, consists of a 5-inch outside diameter by 0.090-inch wall, Type 304 stainless steel shell. The shell is formed into a helix approximately 52 inches in diameter for 2-1/2-turns with a 3-foot straight section at the bottom of and tangent to the helix. Likewise, an 18-inch straight section is tangent at the top of the helix parallel to the 3-foot section and on the opposite side of the helix. The shell contains two fixed headers to which the seven flattened Type 321 stainless steel containment tubes are attached. Supporting the stainless steel tubes are the tube supports spaced equally throughout the assembly. Within the seven stainless steel tubes are seven unalloyed tantalum tubes attached to floating tantalum headers. Each tantalum tube contains at the mercury inlet a 0.060 inch diameter orifice and a 3-foot long plug with 16 parallel helical flow passages. Attached to each plug is a wire coil which extends downstream to the boiler exit. To each tantalum header a tantalum reducer is welded. A tantalum/stainless steel transition joint which is 2.5-inches in diameter is attached to the tantalum reducer. A stainless steel bellows connects the bimetal joints to the shell heads. Within the bellows, a stainless steel tube liner is utilized to guide and protect the bellows. Four pins are located at 90° intervals around each bimetal joint to further guide the tube. Convoluted zirconium fills the annulus between the bellows and the shell to act as an oxide getter for the static NaK system.

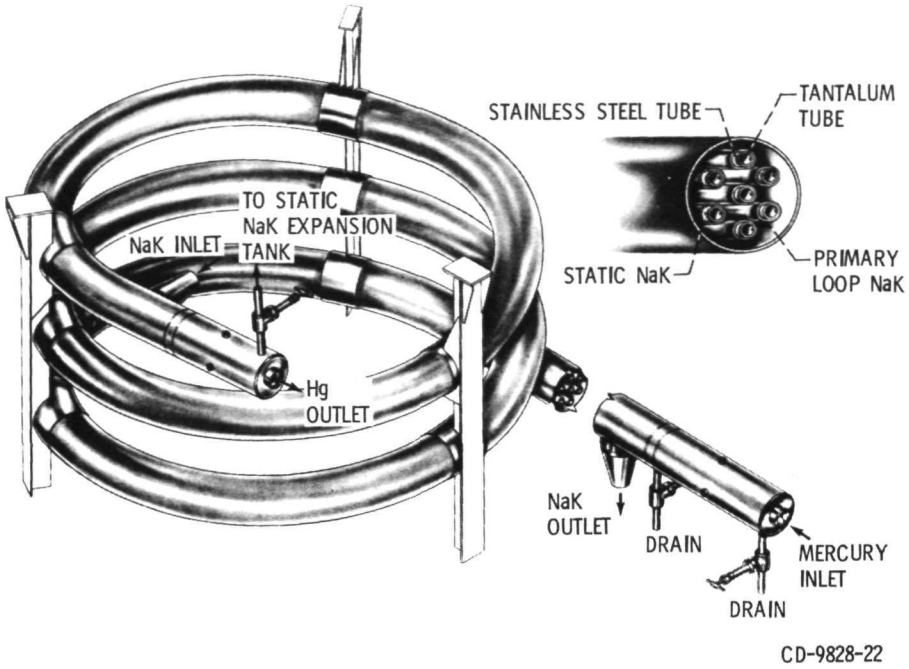

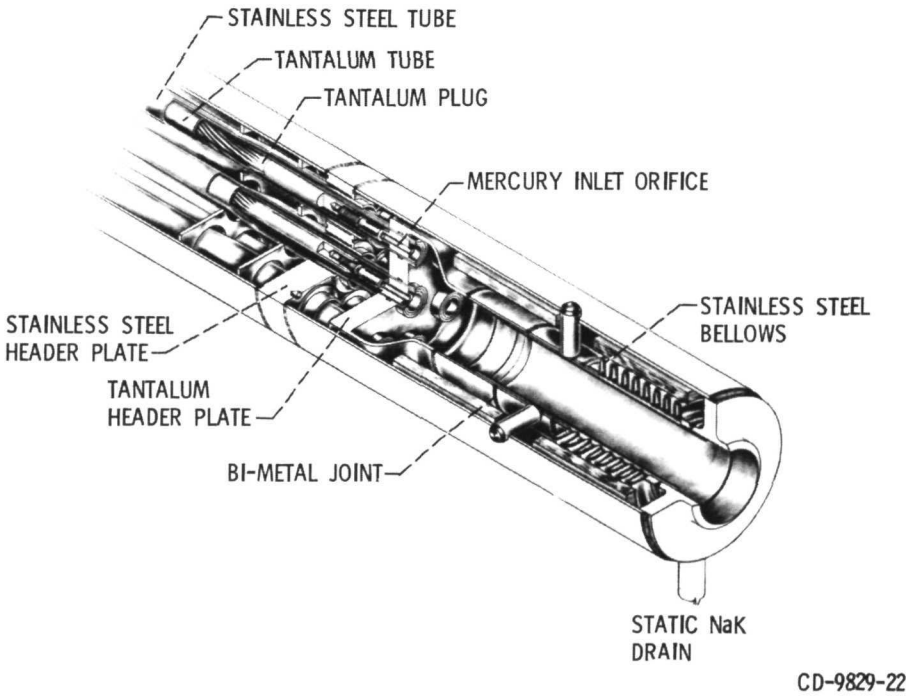

Figure 17. Schematic of SNAP-8, SN-1 refractory metal boiler.

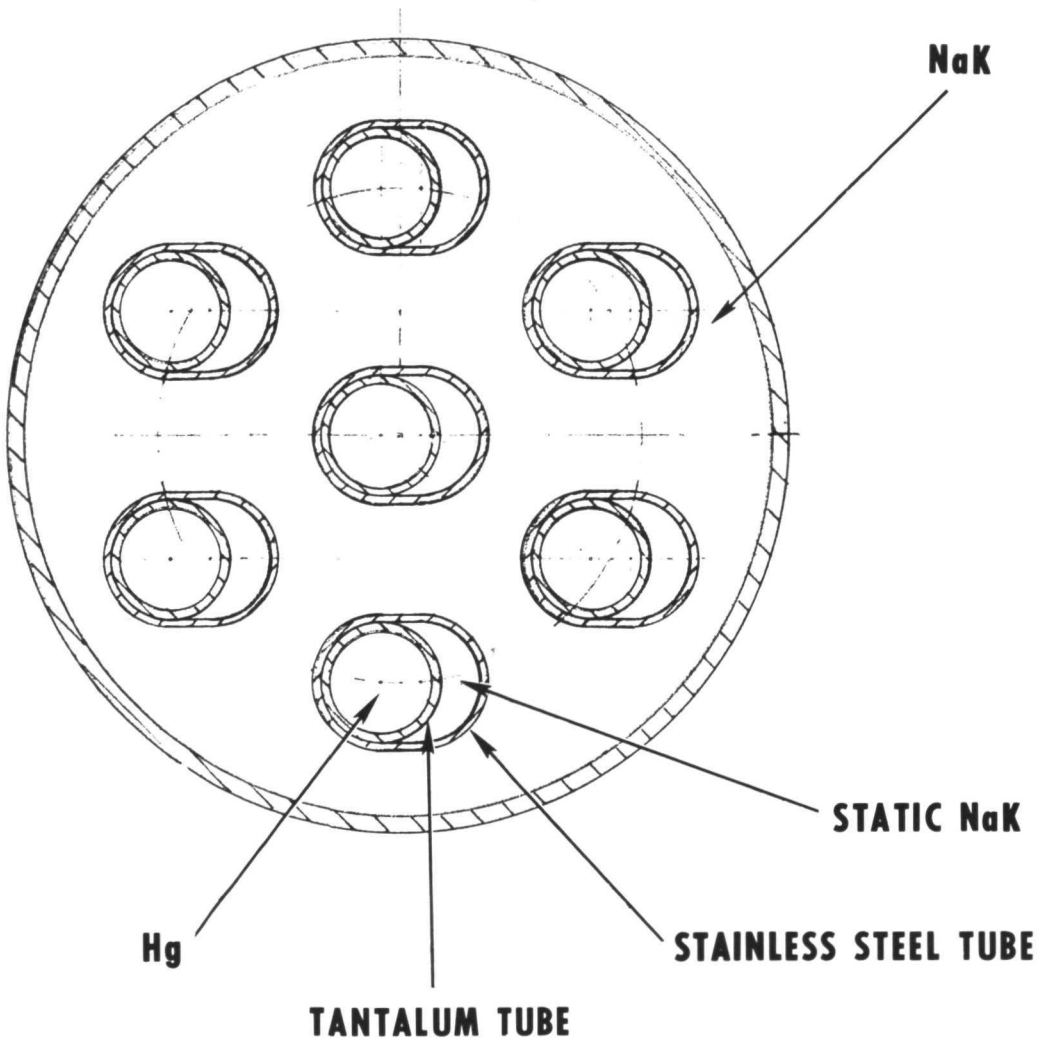

Figure 18. Cross section of SNAP-8 refractory metal boiler.

The primary NaK fills the area between the shell, the stainless steel tubes and the stainless tube headers. The static NaK fills the annulus between the stainless steel tubes, the tantalum tubes, and the shell between the stainless tube headers and the shell end caps. The boiler is shown in cross section in Figure 18, which depicts these areas.

The boiler was received at General Electric-NSP after approximately 1445 hours of testing at NASA-LeRC.

B. INSTRUMENTATION

A complete instrumentation layout for the test facility is shown on the loop schematic in Figure 19. Pressure gages, flowmeters, thermocouples, level controls and mercury vapor detectors are shown in their relative locations. The instrumentation installation consists of temperature, flow and pressure instruments which monitor operation and provide data for boiler performance.

Flow - A permanent magnet flowmeter was used to measure NaK flow. This flowmeter consists of a 3.513-inch OD x 2.812-inch ID 1605 pipe centered axially and vertically between the poles of a horn-type permanent magnet with a field strength of 728 Gauss.

A theoretical calculated sensitivity of 13.93 gpm/mv was calculated from the following equation:

Calculate Y at 200, 500 and 800°F

$$Y = \frac{3162\ d\ (1 + a\ (T_t - 77)\ )}{K_2\ K_1}$$

$$\frac{Y}{B} = \frac{GPM}{MV}$$

$$K_1 = \frac{2dD}{D^2 + d^2 + r_f/r_w\ (D^2 - d^2)}$$

Duct = L605

B = 828 GAUSS

K_2 = .995

d = 2.812 in

D = 3.513 in

r = resistivity, micro OHM CM of fluid

w = resistivity, micro OHM CM of wall

a = coefficient of thermal exp in/in/^{o}F

The calculated flow versus emf at four temperature curves for this flowmeter is shown in Figure 20. The instrumentation on the flowmeter consists of two emf electrodes which are attached to the duct perpendicular to the pole air gap flux-path. A thermocouple is attached to the duct and a thermocouple is attached to the magnet to assure that the magnet temperature remained well below the Curie point. Normally the magnet temperature was approximately 100°F to 150°F.

Two venturi nozzles were installed in the mercury loop. One measured the liquid flow rate; the other measured vapor flow rate. Each flowmeter was designed to provide a 20 psi differential pressure drop at 12,500 lbs/hr mercury flow. Each venturi was calibrated in a water flow test to determine its coefficient. The flow versus pressure drop for each meter is shown in Figures 21 and 22.

Temperature - With two exceptions, all thermocouples were chromel alumel with 0.125-inch, 0.062-inch or 0.04-inch diameters. One hundred and fifty thermocouples were installed on the entire facility. All thermocouples necessary to

Page Intentionally Left Blank

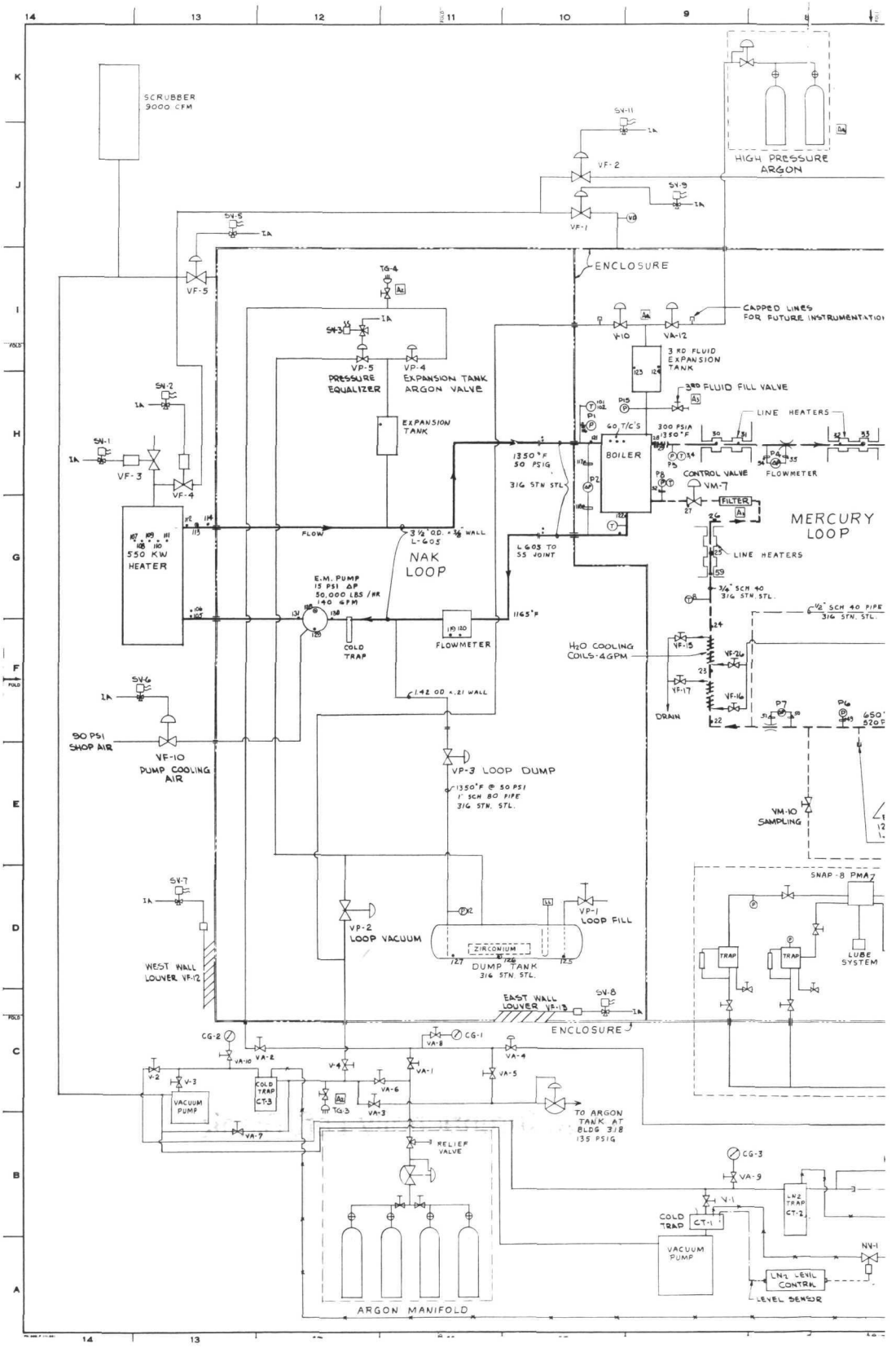

Figure 19. Schematic of 550 KW SNAP-8 refractory

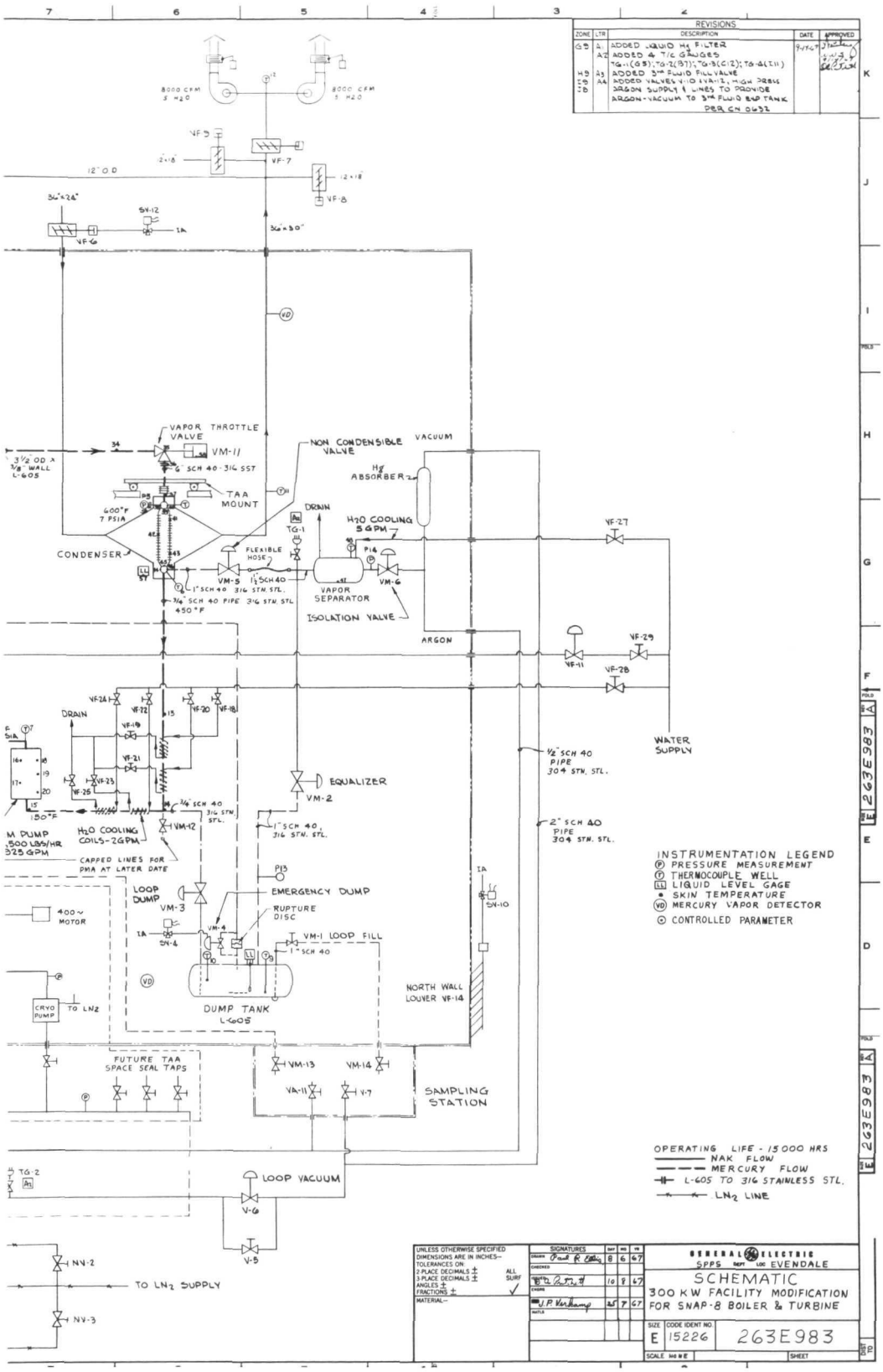

metal boiler test facility with instrumentation.

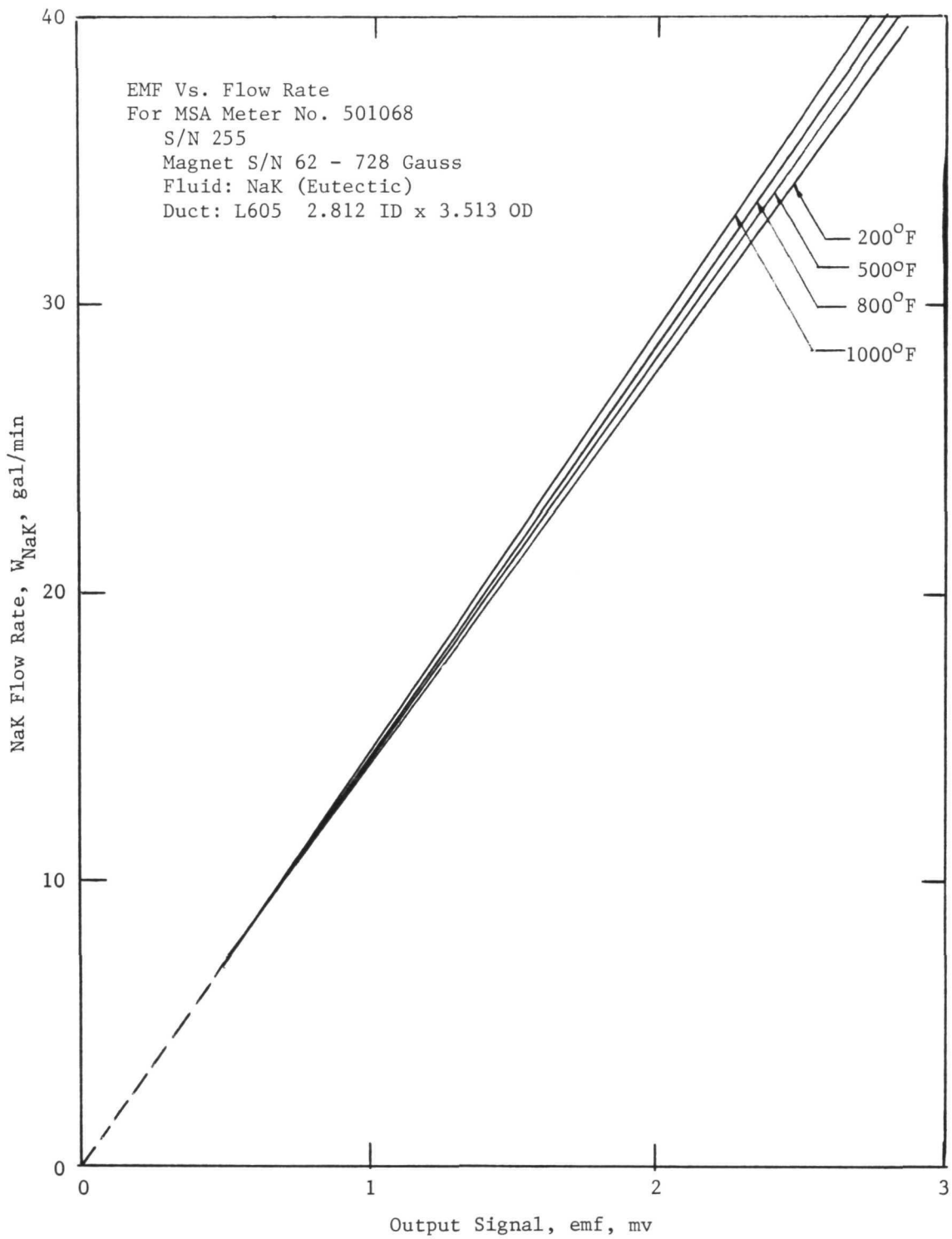

Figure 20. NaK EM flowmeter calibration.

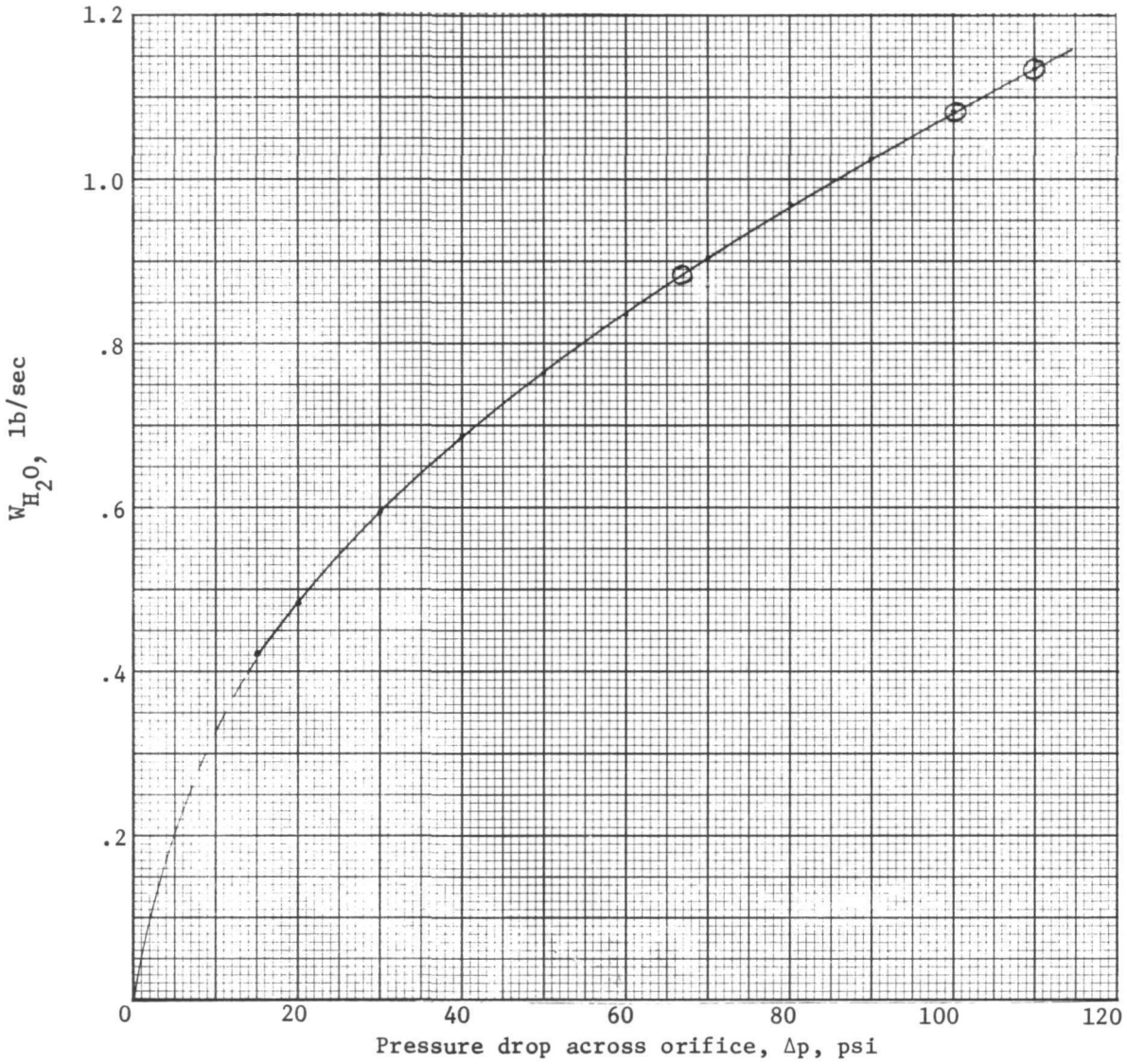

Figure 21. Mercury vapor Venturi flow calibration.

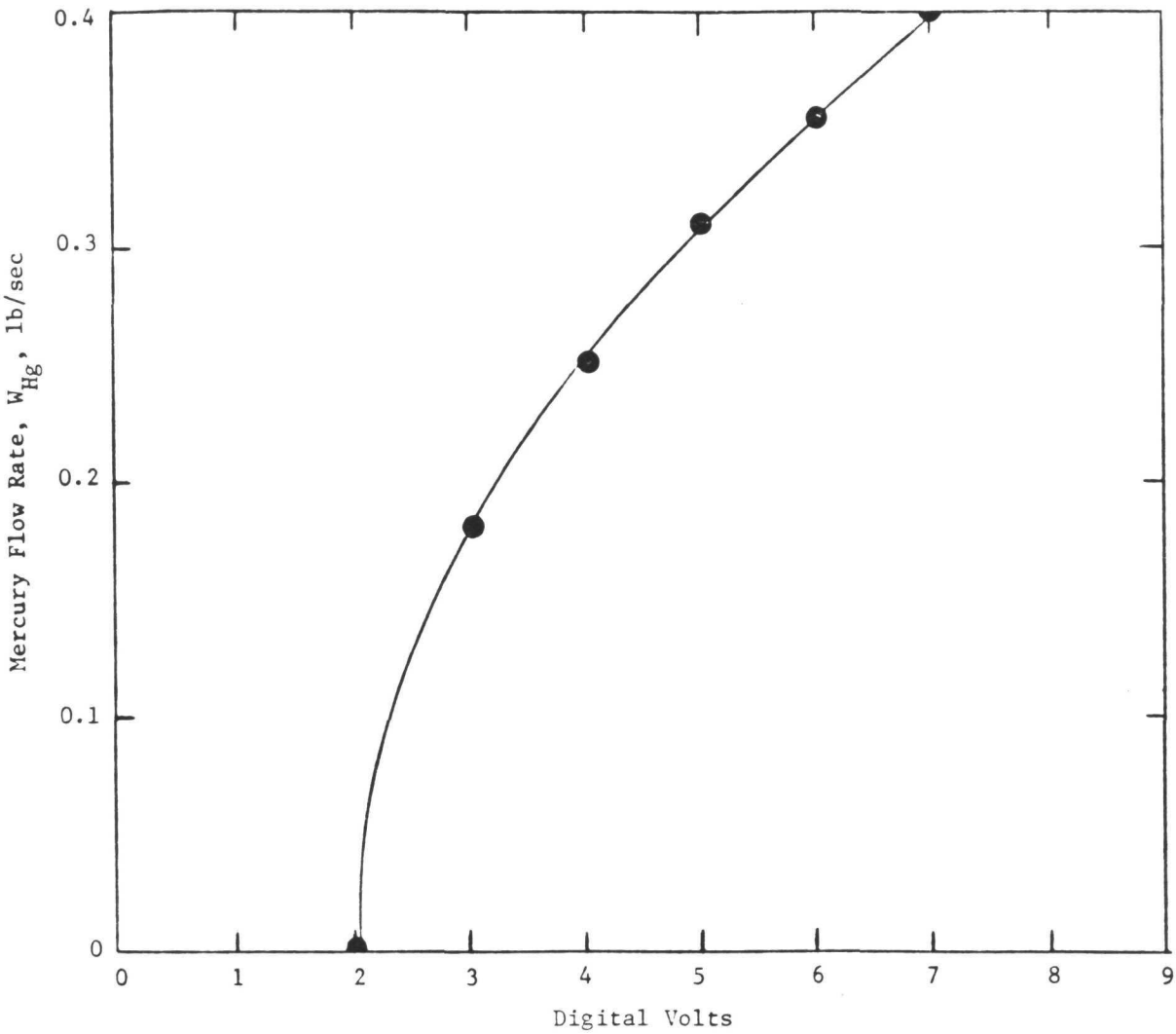

Figure 22. Mercury liquid Venturi flow calibration.

determine boiler performance were referenced to a 150° F temperature controlled box. (Thermocouple locations and circumferential positions are shown in Table I.) At locations where it was necessary to determine true fluid temperatures, wells were provided which were immersed in the fluid stream to at least 10 times the well diameter. The wells were made from 0.25-inch OD tubing and three 0.06-inch OD ungrounded sheathed thermocouples were installed. Two copper-Constantan thermocouples referenced to an ice bath were used to check the 150°F reference temperature. All other thermocouples were connected to various instruments to facilitate operation and to operate safety relays.

Approximately 50 of the thermocouples, which were required for performance calculations, were calibrated prior to installation at the freezing point of zinc (787.1°F) and aluminum (1220°F). The calibrated thermocouples included all the well thermocouples and a group of the boiler shell surface thermocouples. The results of these calibrations are summarized as follows:

0.062-inch OD well thermocouples plus or minus 3/8% tolerance except for two thermocouples which were within plus or minus 0.5%.

0.125-inch OD exposed junction thermocouples plus or minus 3/4%.

The o.125-inch OD exposed junction thermocouples were tack welded to the shell as shown in Figure 23.

Pressure Gages - The pressure gages on the NaK loop and the mercury loop are "Taylor" slack diagram units, as shown in Figure 24. These gages restrict the mercury or NaK to the sensing head which is welded to the facility at the point of measurement. An 0.005-inch thick diaphragm transmits the forces via a NaK filled capillary tube to a sensing chamber located outside the loop enclosure as shown in Figure 25. The sensing heads provide a pneumatic signal which varies from 3 to 15 psig over the calibrated range of the pressure transducer. The pneumatic signal is converted to a 4 to 20 milli-amp DC signal by a signal conditioning circuit in the control room. The DC current is then converted into a 10 to 50 millivolt signal for recording at the control console and a 2 to 10 volt signal for digital recording. In addition, the 4 to 20 milli-amp DC signal is used to operate meter relays which are part of the facility safety system. A typical circuit is shown in Figure 26.

TABLE I

LIST OF THERMOCOUPLE STATIONS AND RELATIVE POSITIONS

Station Number	Distance from Ref. Pt.* (inches)	T/C** Positions Occupied	Station Number	Distance from Ref. Pt.* (inches)	T/C Positions Occupied
0	-12	A	21	113 3/8	A,E
1	- 6	A	22	125 1/2	A,E
2	0	A	23	137 3/4	A,E,G
3	6 1/8	A,E	24	150	A,E
4	12	A,E	25	161 3/4	A,E,G
5	18	A	26	173 1/2	A,E
6	24	A,C,D,E,F,H	27	185 3/8	A,E,G
7	30	A,E	28	197 1/4	A,E
8	36	A,E	29	209 3/8	A,E,G
9	42	A,E	30	221 1/2	A,E
10	48	A,C,D,E,F,G	31	233 1/2	A,E,G
11	54	A,D,E,F,G	32	258 3/8	A,E,G
12	60	A	33	282	A,E
13	68	A,C,D,E,F.H	34	305 1/2	A,E,G
14	71 3/4	A	35	329 1/8	A,E
15	77 3/4	A,C,D,E,F,H	36	353 1/4	A,E,G
16	83 3/4	A	37	377 1/2	A,E
17	89 3/4	A,C,D,E,F,H	38	401 3/4	A,E,G
18	95 3/4	A,E	39	425 3/8	A,E
19	101 1/2	A,E	NaK Inlet	436	+
			40	437	B
20	107 5/8		41	449	A,E
			End of Boiler	453 5/8	-

*Reference Pt.: Location is 1/2" downstream of downstream face of Mercury Inlet Header (see Fig. 17).

**See legend in Figs. 52 to 107.

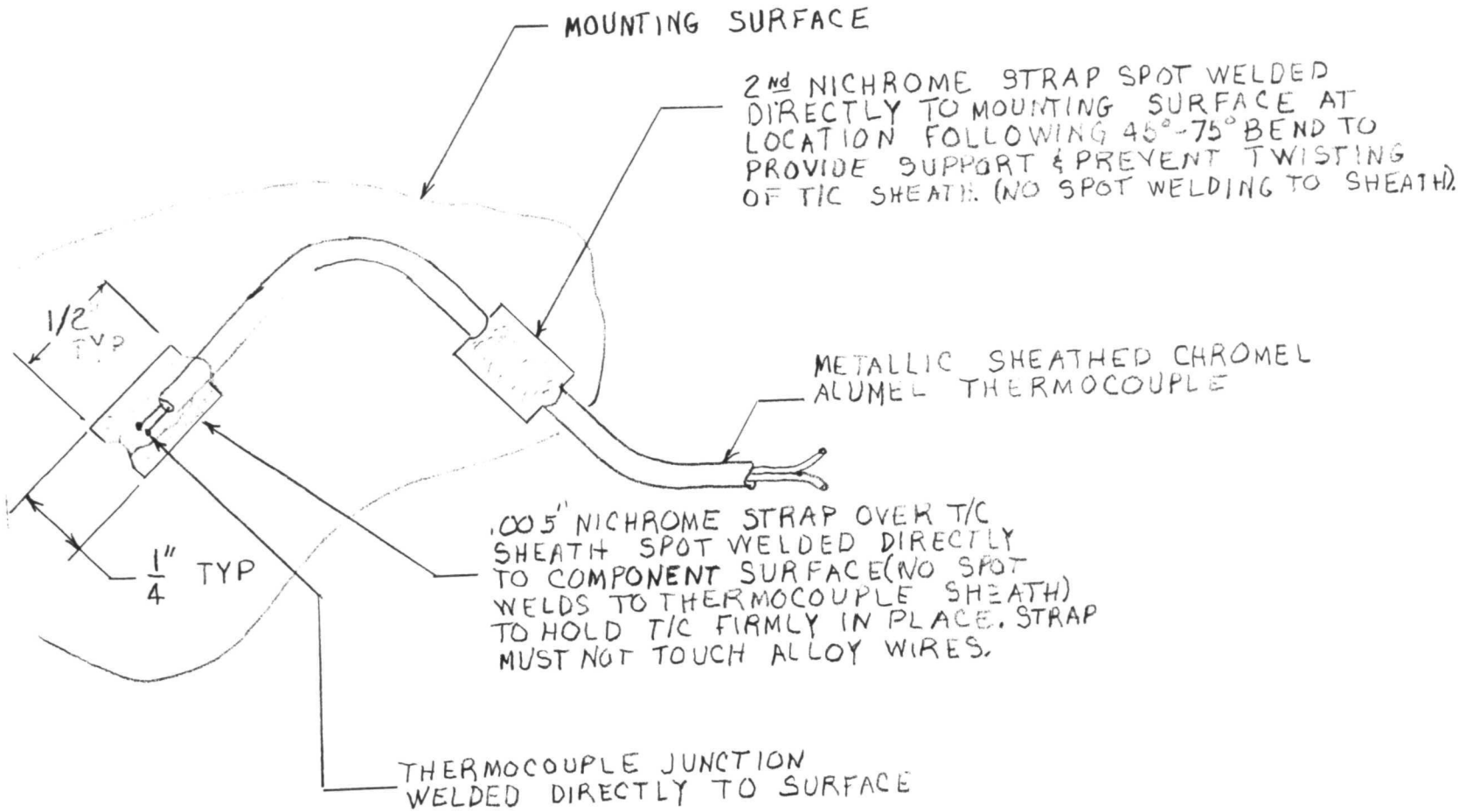

Figure 23. Typical thermocouple connection.

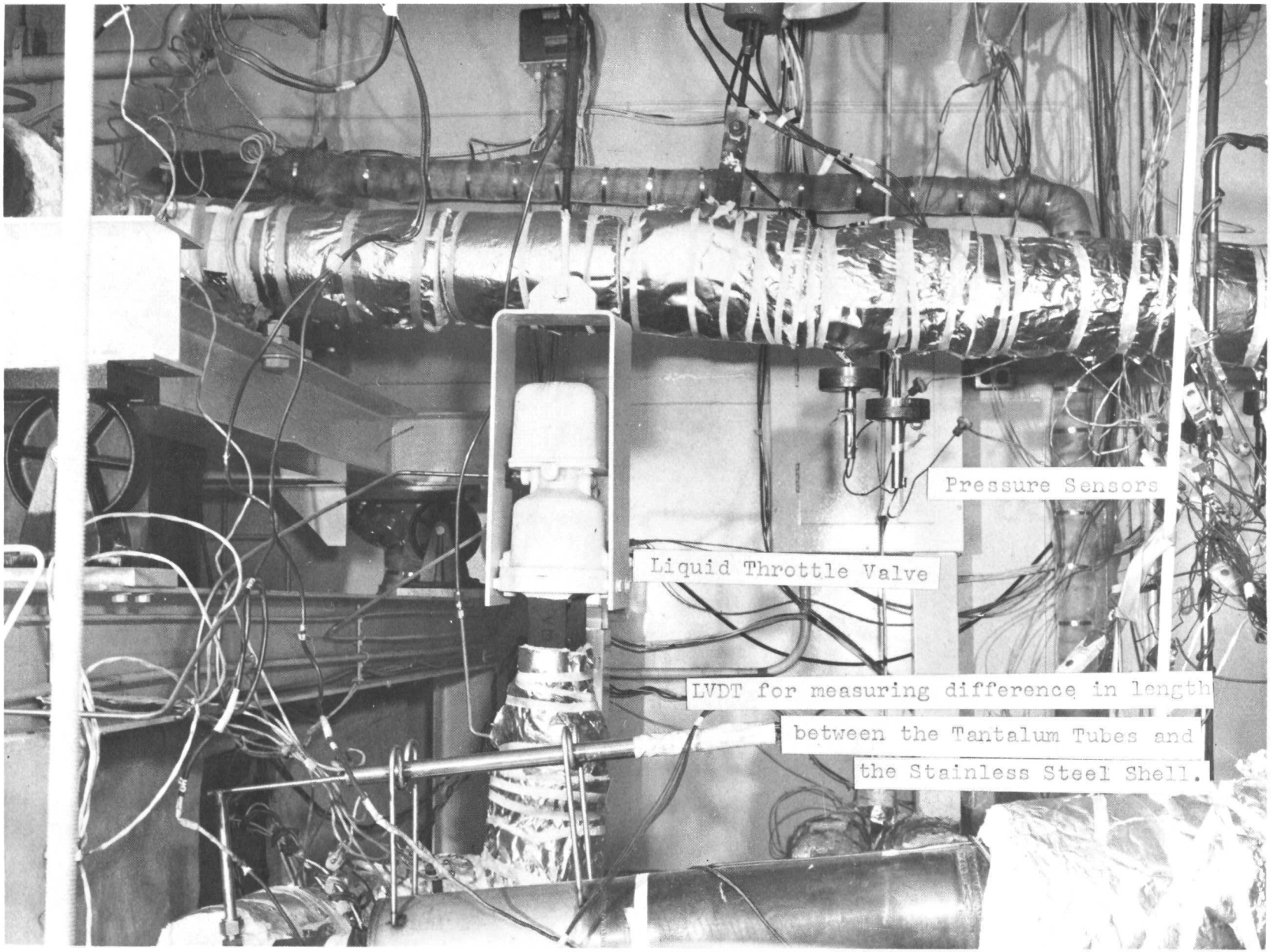

Figure 24. SNAP-8 refractory boiler development test facility showing "Taylor" pressure sensor installation.

Figure 25. SNAP-8 refractory boiler development facility showing mercury vapor detector and mercury pressure gages.

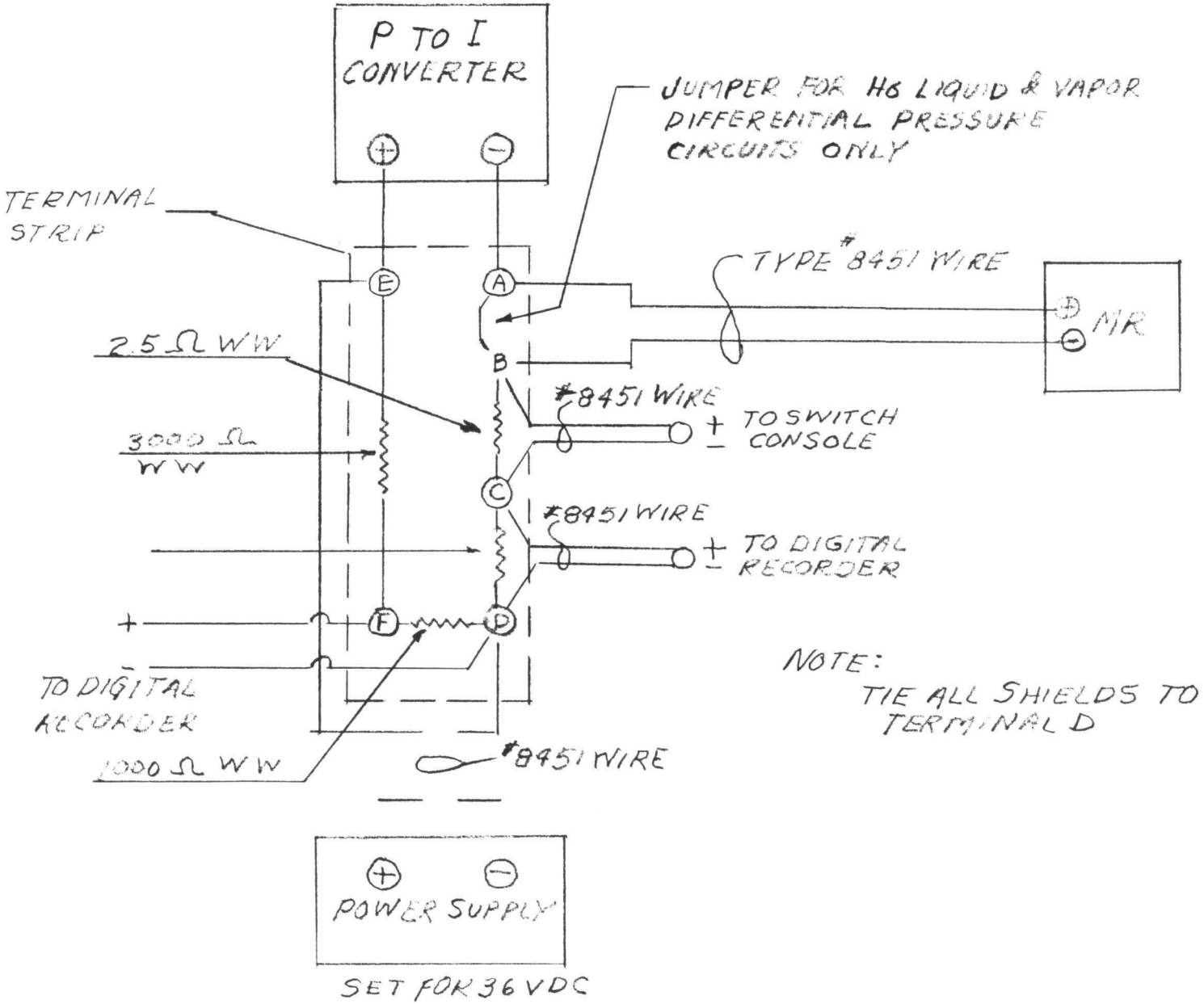

Figure 26. Schematic of pressure-to-current system.

All of the pressure transducers were calibrated prior to installation at ambient temperature and 500°F. The differential pressure transducers were calibrated by subjecting the high pressure transducer to pressure with the low pressure transducer vented to atmosphere. All calibration results showed that the transducers were linear and repeatable within plus or minus 1% throughout the calibration range. Typical calibration curves are shown in Figure 27. Final adjustments were made with the NaK loop filled and the mercury loop with operating inventory to account for static head variations.

Digital Readout - A digital readout system was used to record all the necessary facility and boiler instrumentation necessary to determine the SN-1 performance. The recording system records 2 items per second on punch tape and printed tapers. Table II shows all the parameters recorded on the digital system. The punched tape or printed tape was then processed through a data processing system to produce usable results.

Facility Instrumentation - Liquid level gages were provided in the NaK dump tank the mercury dump tank, the NaK stand pipe and the lower drum of the mercury condenser.

The NaK level proves are of the resistance type as shown in Figure 28. These probes generate an EMF according to the resistance as a function of immersion in the NaK. The electrical schematic for this circuit is also shown in Figure 28.

The mercury dump tank liquid level indicator and the condenser drum indicator were electromechanical gages in which a float pushed a metal rod into an LVDT. These probes proved unsuccessful, probably because the horizontal motion of the mercury within the drum during filling and in the dump tank during draining deformed the shaft. The drum probe was replaced during a shutdown with a high-low resistance probe which gave a signal change of approximately 25 millivolts when the mercury touched the high probe or exposed the low probe.

Automatic safety control circuits were installed in the power circuitry to provide securing of the facility if preset pressure or temperature were exceeded and if loss of flow occurred. If these preset limits were exceeded, the EM pumps and gas fired heater and mercury line electrical heat were secured. The parameters which would shut down the facility are:

TABLE II

Digital Col	T/C #	Symbol	CATS	Location
456	1	TBIW1	B	Hg Inlet Well 1
457	2	TBIW2	B	Hg Inlet Well 2
458	3	TBEW1	B	Hg Exit Well 1
459	4	IBEW2	B	Hg Exit Well 2
460	101	TNaKIN1	B	NaK Inlet Well 1
461	102	TNaKIN2	B	NaK Inlet Well 2
462	103	TNaKX1	B	NaK Exit Well 1
463	104	TNaKX2	B	NaK Exit Well 2
464	106	TGHIN	B	NaK Gas Heater Inlet
465	119	TFMD	B	NaK Flowmeter Duct Temp.
466	116	T(P1)	B	Pressure Gage P1 Temp.
467	117	T(P2HI)	B	Pressure Gage P2 Temp., (high)
468	118	T(P2LO)	B	Pressure Gage P2 Temp., (low)
469	53	T(P3)	B	Pressure Gage P3 Temp.
470	54	T(P4HI)	B	Pressure Gage P4 Temp., (high)
471	55	T(P4LO)	B	Pressure Gage P4 Temp., (low)
472	56	T(P5)	B	Pressure Gage P5 Temp.
473	49	T(P6)	B	Pressure Gage P6 Temp.
474	52	T(P8)	B	Pressure Gage P8 Temp.
475	50	T(P7HI)	B	Pressure Gage P7 Temp., (high)
476	51	T(P7LO)	B	Pressure Gage P7 Temp., (low)
477		T(PHEX)	B	Preheater Exit Temp.
478		478	B	Cell Temp. Near NASA Boiler
479		⎪	B	Cell Temp. Near NASA Boiler
480		⎪	B	
481		⎪	B	
482		⎪	B	
483		⎪	B	
484		⎪	B	
485		485	B	
486	110	TBSOA	B	N-Boiler Shell T/C, Station 0, Cir. Loc. A
487	111	TBSIA	B	N-Boiler Shell T/C, Station 1, Cir. Loc. A
488	112	TBS2A	B	N-Boiler Shell T/C, Station 2, Cir. Loc. A
489	113	TBS3A	B	N-Boiler Shell T/C, Station 3, Cir. Loc. A
490	331	TBS3E	B	G-Boiler Shell T/C, Station 3, Cir. Loc. E
491	114	TBS4A	B	N-Boiler Shell T/C, Station 4, Cir. Loc. A
492	310	TBS4E	B	N-Boiler Shell T/C, Station 4, Cir. Loc. E
493	115	TBS4A	B	N-Boiler Shell T/C, Station 5, Cir. Loc. A
494	116	TBS6A	B	N-Boiler Shell T/C, Station 6, Cir. Loc. A
495	203	TBS6C	B	G-Boiler Shell T/C, Station 6, Cir. Loc. C
496	203	TB56D	B	G-Boiler Shell T/C, Station 6, Cir. Loc. D
497	311	TBS6E	B	N-Boiler Shell T/C, Station 6, Cir. Loc. E
498	204	TBS6F	B	G-Boiler Shell T/C, Station 6, Cir. Loc. F
499	205	TBS6H	B	G-Boiler Shell T/C, Station 6, Cir. Loc. H
500		500	C	

TABLE II. - Continued.

Digital Col	T/C #	Symbol	CATS	Location
501	117	TBS7A	C	N-Boiler Shell T/C, Station 7, Cir. Loc. A
502	312	TBS7E	C	N-Boiler Shell T/C, Station 7, Cir. Loc. E
503	118	TBS8A	C	N-Boiler Shell T/C, Station 8, Cir. Loc. A
504	313	TBS8E	C	N-Boiler Shell T/C, Station 8, Cir. Loc. E
505	119	TBS9A	C	N-Boiler Shell T/C, Station 9, Cir. Loc. A
506	314	TBS9E	C	N-Boiler Shell T/C, Station 9, Cir. Loc. E
507	120	TBS10A	C	N-Boiler Shell T/C, Station 10, Cir. Loc. A
508	206	TBS10C	C	G-Boiler Shell T/C, Station 10, Cir. Loc. C
509	207	TBS10D	C	G-Boiler Shell T/C, Station 10, Cir. Loc. D
510	315	TBS10E	C	N-Boiler Shell T/C, Station 10, Cir. Loc. E
511	332	TBS10F	C	G-Boiler Shell T/C, Station 10, Cir. Loc. F
512	209	TBS10G	C	G-Boiler Shell T/C, Station 10, Cir. Loc. G
513	121	TBS11A	C	N-Boiler Shell T/C, Station 11, Cir. Loc. A
514	122	TBS11D	C	N-Boiler Shell T/C, Station 11, Cir. Loc. B
515	316	TBS11E	C	N-Boiler Shell T/C, Station 11, Cir. Loc. E
516	210	TBS11F	C	G-Boiler Shell T/C, Station 11, Cir. Loc. F
517	123	TBS11G	C	N-Boiler Shell T/C, Station 11, Cir. Loc. G
518	124	TBS12A	C	N-Boiler Shell T/C, Station 12, Cir. Loc. A
519	125	TBS13A	C	N-Boiler Shell T/C, Station 13, Cir. Loc. A
520	211	TBS13C	C	G-Boiler Shell T/C, Station 13, Cir. Loc. C
521	212	TBS13O	C	G-Boiler Shell T/C, Station 13, Cir. Loc. D
522	317	TBS13E	C	N-Boiler Shell T/C, Station 13, Cir. Loc. E
523	213	TB513F	C	G-Boiler Shell T/C, Station 13, Cir. Loc. F
524	214	TBS13H	C	G-Boiler Shell T/C, Station 13, Cir. Loc. H
525	126	TB514A	C	N-Boiler Shell T/C, Station 14, Cir. Loc. A
526	127	TBS15A	C	N-Boiler Shell T/C, Station 15, Cir. Loc. A
527	215	TBS15C	C	G-Boiler Shell T/C, Station 15, Cir. Loc. C
528	216	TBS15D	C	G-Boiler Shell T/C, Station 15, Cir. Loc. D
529	318	TBS15E	C	N-Boiler Shell T/C, Station 15, Cir. Loc. E
530	217	TBS15F	C	G-Boiler Shell T/C, Station 15, Cir. Loc. F
531	218	TBS15H	C	G-Boiler Shell T/C, Station 15, Cir. Loc. H
532	128	TBS16A	C	N-Boiler Shell T/C, Station 16, Cir. Loc. A
533	129	TBS17A	C	N-Boiler Shell T/C, Station 17, Cir. Loc. A
534	219	TBS17C	C	G-Boiler Shell T/C, Station 17, Cir. Loc. C
535	220	TBS17D	C	G-Boiler Shell T/C, Station 17, Cir. Loc. D
536	319	TBS17E	C	N-Boiler Shell T/C, Station 17, Cir. Loc. E
537	221	TBS17F	C	G-Boiler Shell T/C, Station 17, Cir. Loc. F
538	222	TBS17H	C	G-Boiler Shell T/C, Station 17, Cir. Loc. H
539	130	TBS18A	C	N-Boiler Shell T/C, Station 18, Cir. Loc. A
540	223	TBS18E	C	G-Boiler Shell T/C, Station 18, Cir. Loc. E
541	131	TBS19A	C	N-Boiler Shell T/C, Station 19, Cir. Loc. A
542	320	TBS19E	C	N-Boiler Shell T/C, Station 19, Cir. Loc. E
543	132	TBS20A	C	N-Boiler Shell T/C, Station 20, Cir. Loc. A
544	224	TBS20E	C	G-Boiler Shell T/C, Station 20, Cir. Loc. E
545	133	TBS21A	C	N-Boiler Shell T/C, Station 21, Cir. Loc. A

TABLE II. - Concluded.

Digital Col.	T/C #	Symbol	CATS	Location
546	321	TBS21E	C	N-Boiler Shell T/C, Station 21, Cir. Loc. E
547	134	TBS22A	C	N-Boiler Shell T/C, Station 22, Cir. Loc. A
548	225	TBS22E	C	G-Boiler Shell T/C, Station 22, Cir. Loc. E
549	135	TBS23A	C	N-Boiler Shell T/C, Station 23, Cir. Loc. A
550	322	TBS23E	C	N-Boiler Shell T/C, Station 23, Cir. Loc. E
551	226	TBS23G	D	G-Boiler Shell T/C, Station 23, Cir. Loc. G
552	136	TBS24A	D	N-Boiler Shell T/C, Station 24, Cir. Loc. A
553	227	TBS24E	D	G-Boiler Shell T/C, Station 24, Cir. Loc. E
554	137	TBS25A	D	N-Boiler Shell T/C, Station 25, Cir. Loc. A
555	323	TBS25E	D	N-Boiler Shell T/C, Station 25, Cir. Loc. E
556	228	TBS25G	D	G-Boiler Shell T/C, Station 25, Cir. Loc. G
557	138	TBS26A	D	N-Boiler Shell T/C, Station 26, Cir. Loc. A
558	229	TBS26E	D	G-Boiler Shell T/C, Station 26, Cir. Loc. E
559	139	TBS27A	D	NOBoiler Shell T/C, Station 27, Cir. Loc. A
560	324	TBS27E	D	N-Boiler Shell T/C, Station 27, Cir. Loc. E
561	230	TBS27G	D	G-Boiler Shell T/C, Station 27, Cir. Loc. G
562	360	TBS28A	D	N-Boiler Shell T/C, Station 28, Cir. Loc. A
563	231	TBS28E	D	G-Boiler Shell T/C, Station 28, Cir. Loc. E
564	361	TBS29A	D	N-Boiler Shell T/C, Station 29, Cir. Loc. A
565	325	TBS29E	D	N-Boiler Shell T/C, Station 29, Cir. Loc. E
566	232	TBS29G	D	G-Boiler Shell T/C, Station 29, Cir. Loc. G
567	362	TBS30A	D	N-Boiler Shell T/C, Station 30, Cir. Loc. A
568	233	TBS30E	D	G-Boiler Shell T/C, Station 30, Cir. Loc. E
569	363	TBS31A	D	N-Boiler Shell T/C, Station 31, Cir. Loc. A
570	326	TBS31E	D	N-Boiler Shell T/C, Station 31, Cir. Loc. E
571	234	TBS31G	D	G-Boiler Shell T/C, Station 31, Cir. Loc. G
572	364	TBS32A	D	N-Boiler Shell T/C, Station 32, Cir. Loc. A
573	327	TBS32E	D	N-Boiler Shell T/C, Station 32, Cir. Loc. E
574	235	TBS32G	D	G-Boiler Shell T/C, Station 32, Cir. Loc. G
575	365	TBS33A	D	N-Boiler Shell T/C, Station 33, Cir. Loc. A
576	236	TBS33E	D	G-Boiler Shell T/C, Station 33, Cir. Loc. E
577	366	TBS34A	D	N-Boiler Shell T/C, Station 34, Cir. Loc. A
578	328	TBS34E	D	N-Boiler Shell T/C, Station 34, Cir. Loc. E
579	237	TBS34G	D	G-Boiler Shell T/C, Station 34, Cir. Loc. G
580	367	TBS35A	D	N-Boiler Shell T/C, Station 35, Cir. Loc. A
581	238	TBS35E	D	G-Boiler Shell T/C, Station 35, Cir. Loc. E
582	368	TBS36A	D	N-Boiler Shell T/C, Station 36, Cir. Loc. A
583	329	TBS36E	D	N-Boiler Shell T/C, Station 36, Cir. Loc. E
584	239	TBS36G	D	G-Boiler Shell T/C, Station 36, Cir. Loc. G
585	369	TBS37A	D	N-Boiler Shell T/C, Station 37, Cir. Loc. A
586	240	TBS37E	D	G-Boiler Shell T/C, Station 37, Cir. Loc. E
587	370	TBS38A	D	N-Boiler Shell T/C, Station 38, Cir. Loc. A
588	330	TBS38E	D	N-Boiler Shell T/C, Station 38, Cir. Loc. E
589	241	TBS38G	D	G-Boiler Shell T/C, Station 38, Cir. Loc. G
590	371	TBS39A	D	N-Boiler Shell T/C, Station 39, Cir. Loc. A
591	242	TBS39E	D	G-Boiler Shell T/C, Station 39, Cir. Loc. E
592	372	TBS40B	D	N-Boiler Shell T/C, Station 40, Cir. Loc. B
593	373	TBS41A	D	N-Boiler Shell T/C, Station 41, Cir. Loc. A
594	243	TBS41E	D	G-Boiler Shell T/C, Station 41, Cir. Loc. E
595	595			
596				
597				
598				
599	599			

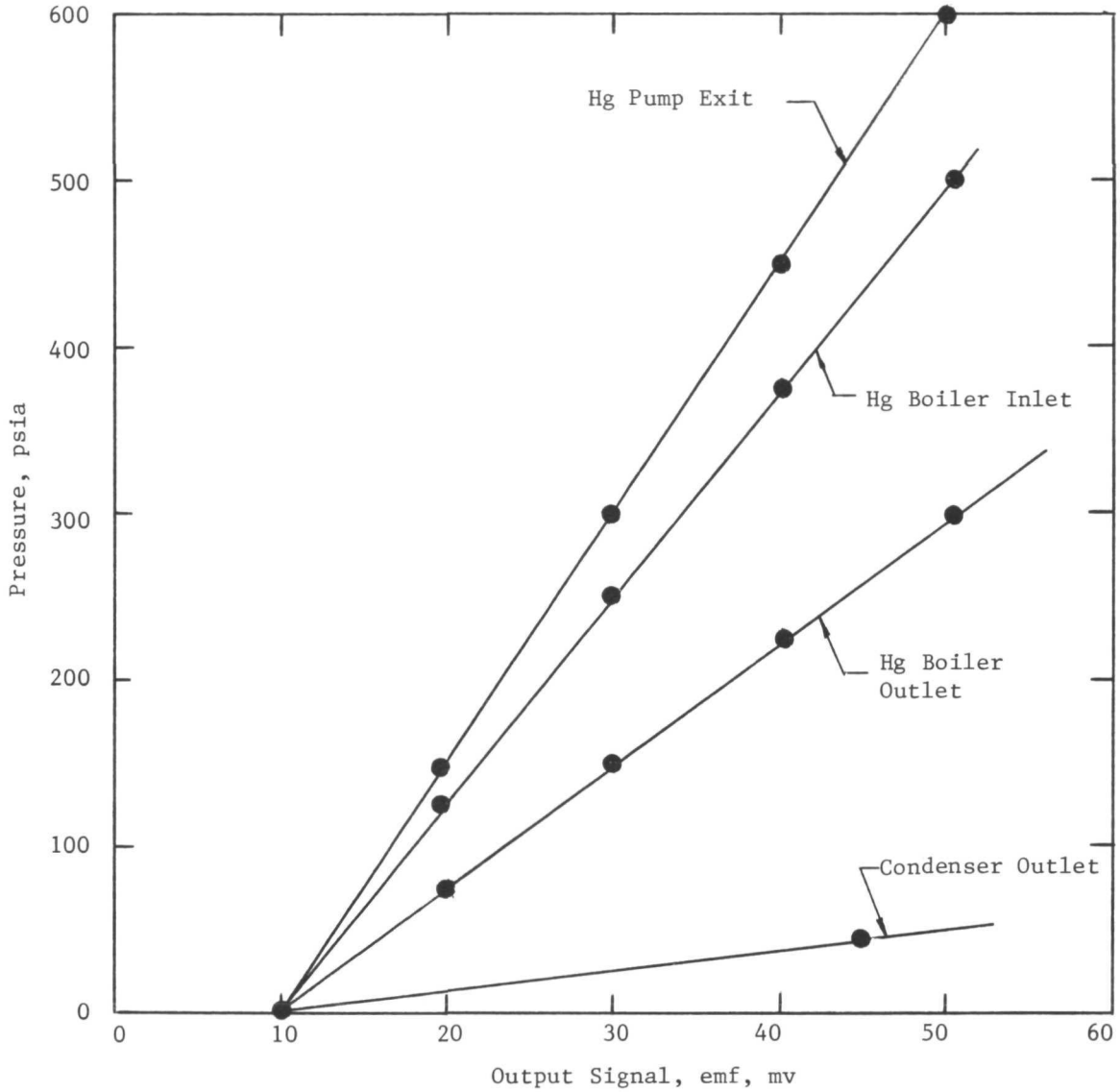

Figure 27. Calibration of pressure transducers.

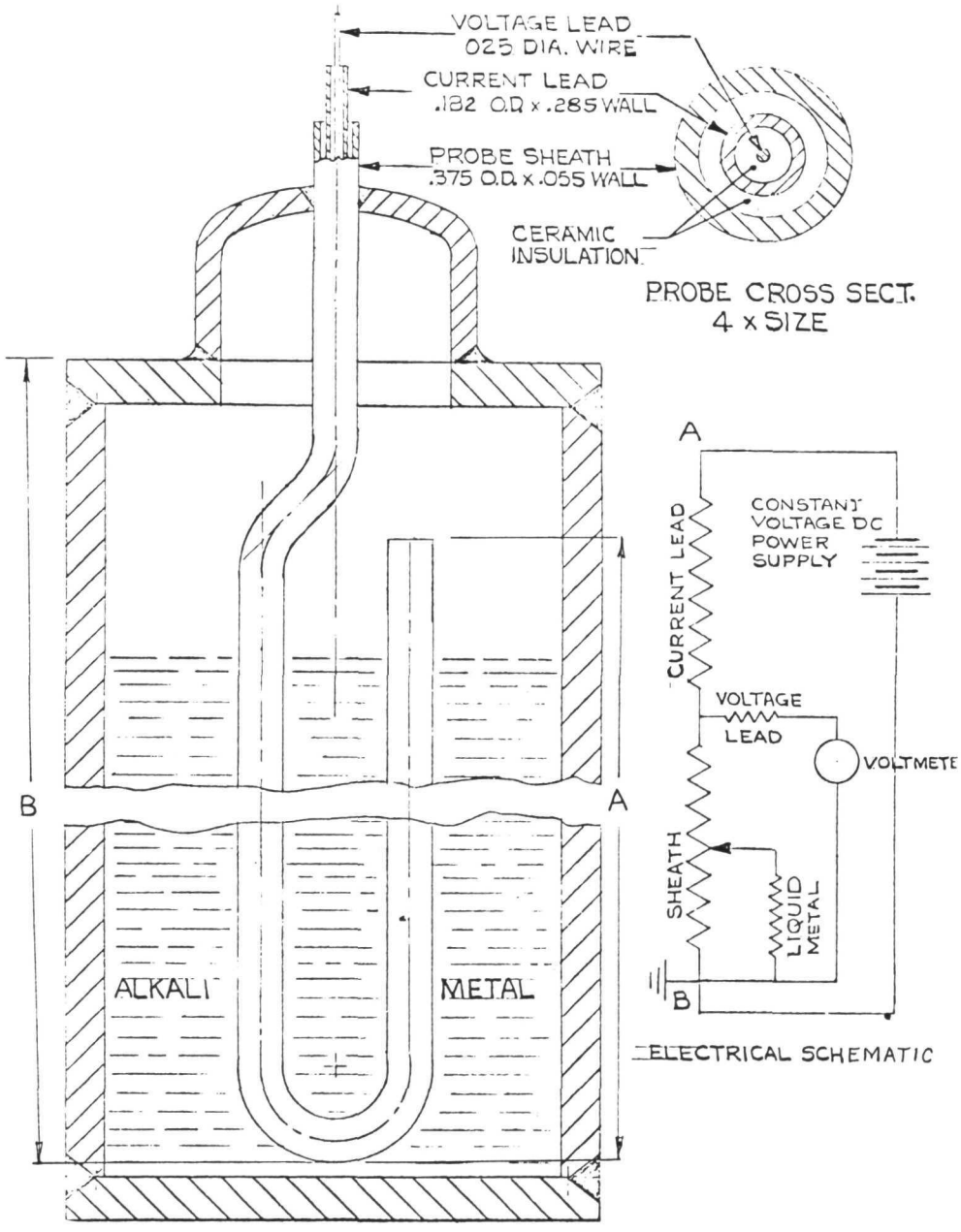

Figure 28. Schematic of liquid level probe and electrical circuit.

1. Loss of flame in gas fired heater
2. Loss of gas pressure in gas fired heater
3. Loss of air blower in gas fired heater
4. Overtemperature gas fired heater tube bundle
5. Loss of mercury or NaK flow
6. Loss of pump power
7. Mercury inlet overpressure
8. Mercury exit overpressure
9. Mercury condenser overpressure
10. Mercury vapor line heater overtemperature.

These were all annunciated for the operator at the console. In addition, smoke detectors were provided in the gas fired heater and the NaK portion of the test cell which would annunciate to the operator in the control room if smoke were detected. Also, mercury vapor detection was provided (Figure 29) in the test cell and exhaust duct of the mercury condenser. The cell level was indicated and the operator was able to determine the mercury vapor level within the cell prior to entering. The condenser exhaust detector annunciated to alert the operator to instigate emergency proceedings.

The NaK dump tank, mercury preheater and mercury vapor line heater would automatically control a preset temperature.

The argon and vacuum system pressures were read at the console via conventional pneumatic transmitters rated 30 inches vacuum to 160 psig. These transmitters transmitted a 3 to 15 psig signal in proportion to loop pressure to a receiver gage in the control room. Additional direct reading gages were located on the argon-vacuum system for operator convenience.

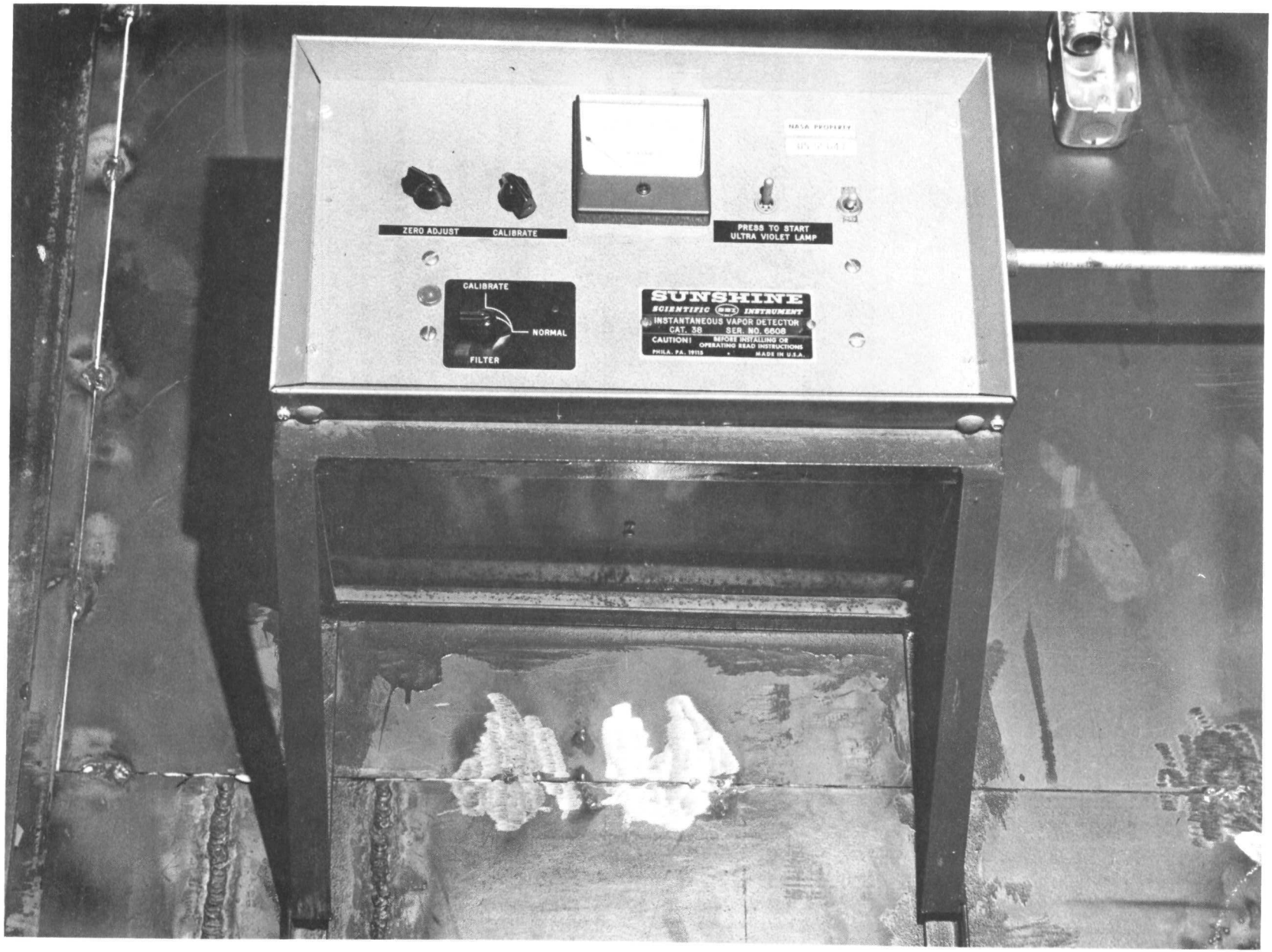

Figure 29. Mercury vapor detector for cell monitoring.

C. FACILITY CHECKOUT AND OPERATION

Facility checkout and operating procedures were established to minimize facility problems during construction and to provide instructions to the facility operator that would cover actions to be taken during emergencies that would minimize the possibility of damage to the test boiler and the facility.

The facility checkout consisted of testing each component prior to and after installation during the construction phase. Visual inspections of the piping revealed that a residue of drawing oil was not removed from the piping during manufacture. A mixture of hexane and alcohol was used to clean the pipe to remove the residue. All welds were radiographed and the piping was helium leak checked as it was installed to facilitate the location of possible leaks. Thus, at the completion of the facility construction a clean, leak tight system was assured.

After the test boiler was installed and the loop was clean, dry and empty the facility was baked out at 400°F for 24 hours. A vacuum system with a liquid nitrogen cooled cold trap was attached to the system. At the end of the 24-hour bake out the system was cooled. With all valves secured and the vacuum pump removed a leak rate of 5 micron liters per hour was observed. This indicated an extremely clean system and the facility was prepared for operation.

The NaK dump tank was filled with 650 lbs NaK with oxide content. The NaK loop was preheated to 400°F and the loop filled. NaK was circulated for 24 hours at 600°F and then drained into the dump tank. The dump tank temperature was then raised to 1200°F for 48 hours at which time a sample of the NaK was taken and analyzed for oxide. The results of the analysis (12 ppm) was well within the 20 ppm required for facility operation.

The NaK loop was again filled and operation commenced with a series of heat loss and calibration runs. The thermocouple calibration runs were made at 800°F, 1100°F and 1300°F at high flow and minimum NaK ΔT across the boiler and served to check the previously installed shell thermocouples against the calibrated thermocouples. A typical calibration run is shown in Figure 30. The heat loss runs were made at a low enough flow to give a NaK ΔT across the boiler of 10°F to 15°F and served to determine the heat loss in the boiler. During these tests the

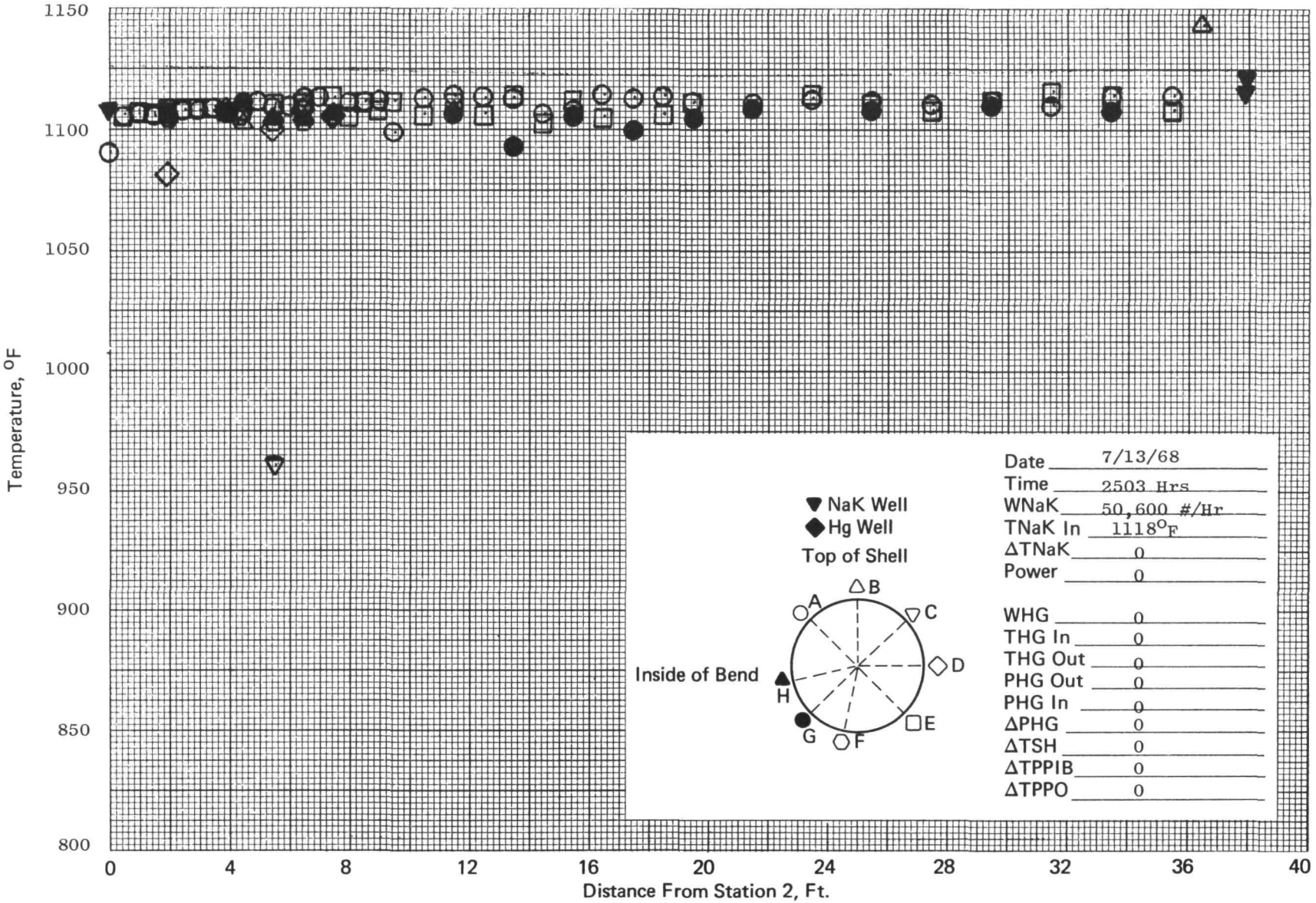

Figure 30. SNAP-8 refractory boiler temperature profile showing thermocouple calibration run.

mercury side was evacuated to minimize heat transfer by convection. The results of these testa are shown in Figure 31 and shows the heat loss to be in the order of 10%. The calibration runs and heat loss runs were made after every shutdown which required the boiler insulation to be removed.

Following the boiler calibration and heat loss runs the mercury dump tank was filled with 2200 lbs of triple distilled mercury. A typical analysis of the mercury is as follows, in ppm. Cu .05-.1, Ag .05-.1, Au - ND, trace cadmium, silicon, lead, titanium, bismuth, aluminum, indium, tin and iron.

The filling was accomplished under an argon gas blanket to minimize the influx of oxygen into the system. The mercury system was filled and operated in the liquid phase to determine the liquid pressure drop across the boiler which would assist in the analysis of the data at a later time.

The static NaK system which acts as a barrier between the primary NaK and the secondary mercury passages had a sample removed for analysis. The results (5 ppm oxygen) indicated the NaK was in good condition. Enough NaK was added to the static NaK system to bring the NaK level to the bottom of the expansion tank.

The NaK and mercury loops were evacuated followed by pressurizing the NaK dump tank with argon and forcing the NaK from the dump tank into the NaK loop. The NaK standpipe liquid level indicator signaled when the loop was full. The NaK dump valve was left open during all times to permit volumetric expansion of the NaK into the dump tank. The main function of the dump valve was to act as a barrier between the NaK dump tank and the boiler in the event the boiler had to be repaired. The gas fired heater is activated at this time to prepare the boiler for mercury injection.

The mercury loop was filled until a level was indicated in the condenser drum. With the primary NaK at approximately 600° to 650° F, the mercury injection was accomplished at low flow. The SNAP-8 startup, where mercury was injected into the 1300°F boiler, was not accomplished during this test for the heater controls and the heater were not designed to do this type of test. Since the primary function of the test was long term endurance the boiler NaK temperature was raised to the design condition of 1300° F, 12,500 lbs/hr mercury flow rate at 200 psia boiler exit pressure from the 600° F at a rate of approximately 100° F per hour. This prevented undue thermal strain on any component in the facility.

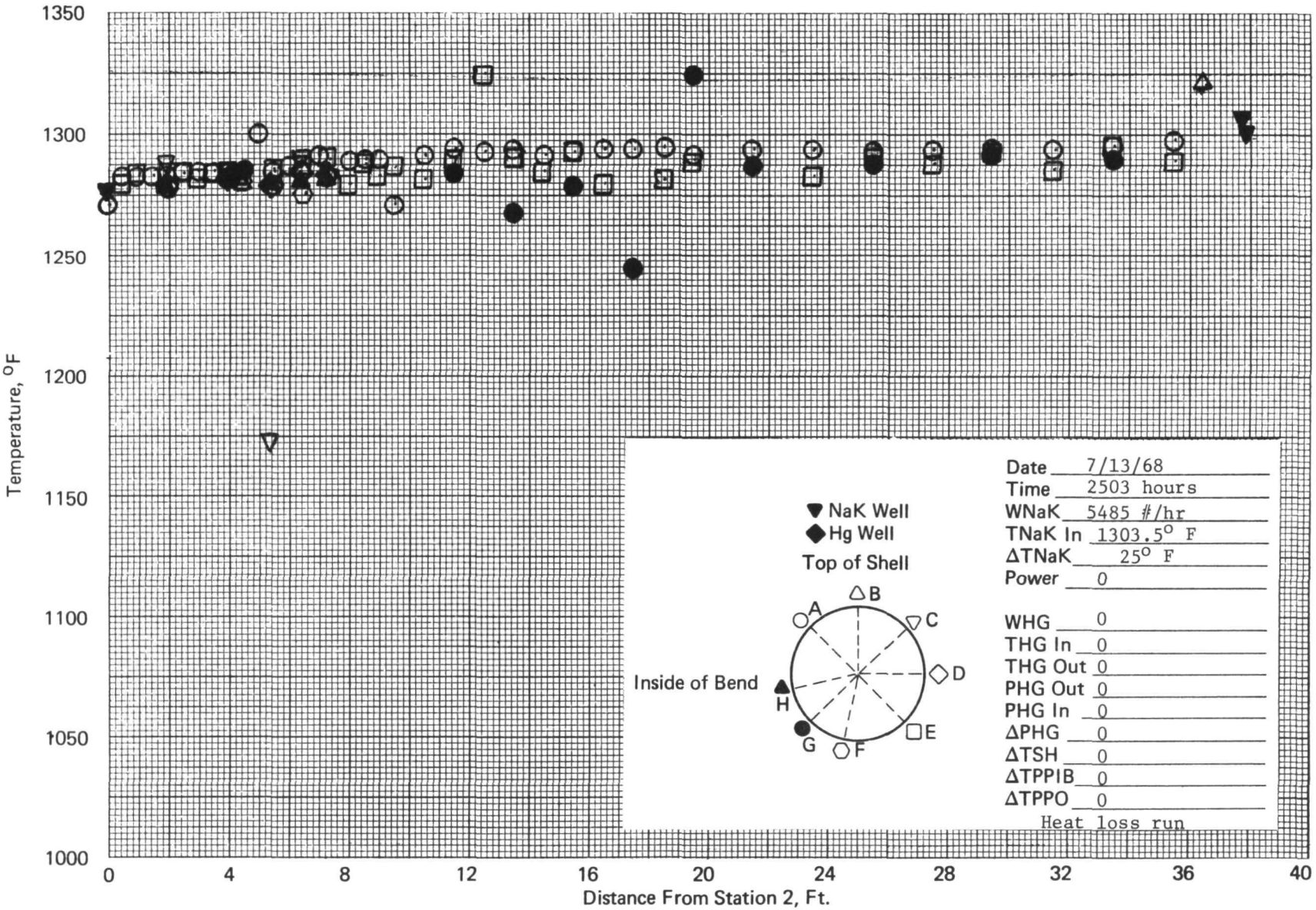

Figure 31. SNAP-8 refractory boiler temperature profile showing typical heat loss run.

When the boiler achieved design conditions, the gas fired heater was set on automatic control and endurance testing commenced. The complete boiler and facility conditions were recorded on a digital printout tape which was monitored by the operator. Each tape was scrutinized for possible boiler or facility problems and one run per week was reduced for submittal to the NASA Project Manager.

The first facility malfunction[5] occurred when a fuse blew on the NaK EM pump. Since this pump is a 3Φ wye connection, the loss of one phase will cause the pump to cease functioning. The fuses were replaced with a special plated fuse to prevent further shutdown and, in addition, a meter relay in conjunction with a current transformer was installed in each current phase of the NaK pump and the mercury pump such that a loss of phase would secure the facility.

One problem that occurred at random times throughout the 2500-hour test phase was the frequent shutdown of the gas fired heater. At the end of the 2500-hour test run the stack was removed and it was found that a steel ring used during the forming of the refractory dome (Figure 32) was not removed and had carburized and broken into pieces, subsequently falling into the heater and covering the flame eye. The ring was removed and subsequent operation verified the fix.

The mercury condenser failed after approximately 2950 hours of operation. The shell of the consenser was removed and it was found that the design of the condenser had assumed that the flow distribution within the condenser would be uniform. Therefore, the hairpins were locked together at the bend preventing the movement of individual tubes. The hairpins were weld repaired and the tubes individually supported to permit the movement of tubes thus accommodating flow maldistribution. At the completion of the condenser repair the operation of the facility was uneventful for the rest of the program.

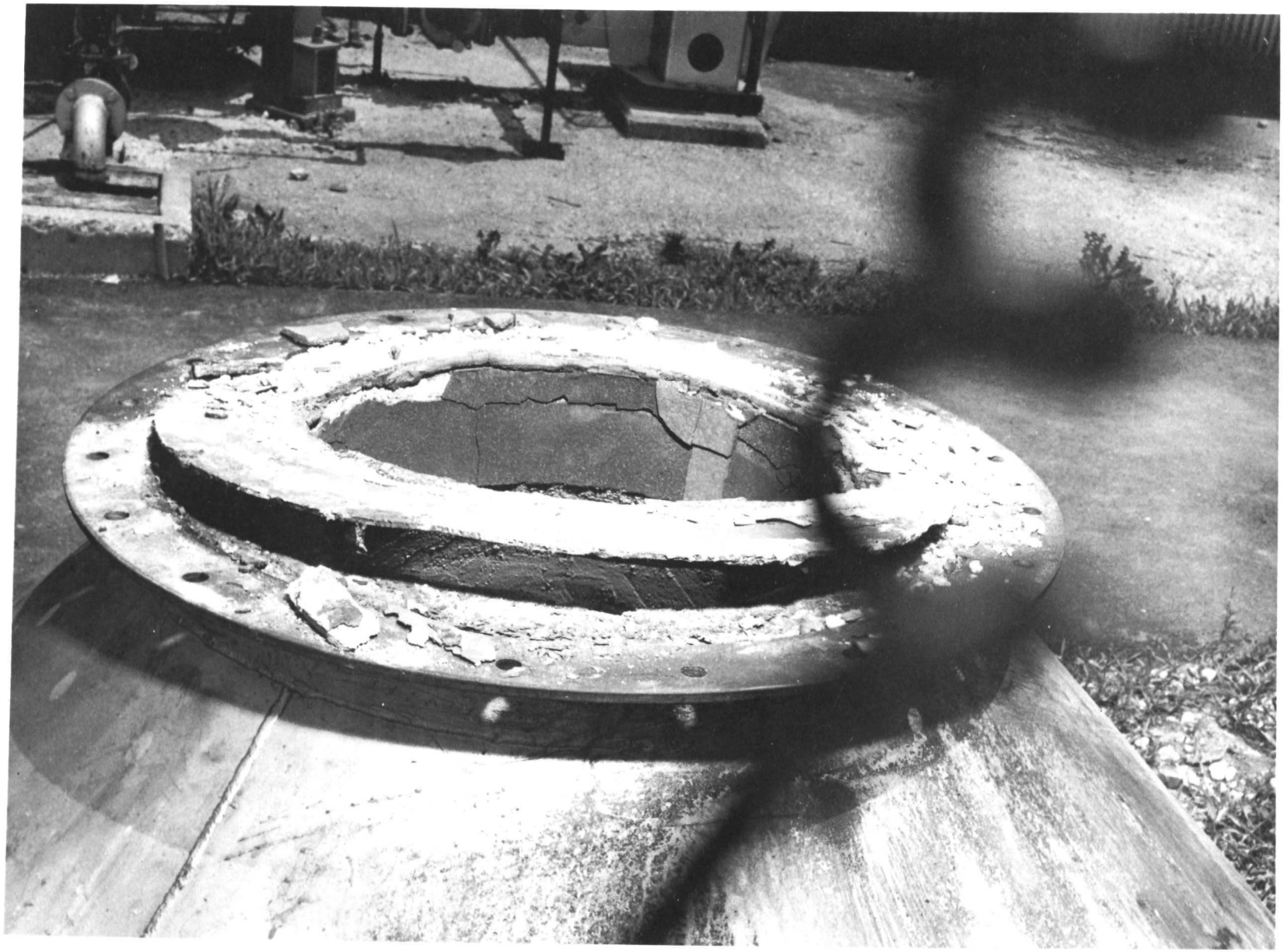

Figure 32. SNAP-8 refractory boiler development facility showing carburized steel ring in NaK, gas fired heater stack.

IV. BOILER HISTORY

The NASA boiler was received in good condition from the Lewis Research Center on December 22, 1967. Work was then initiated to prepare the boiler for installation in the test facility.

The third fluid static NaK system was sampled and analyzed for oxygen and mercury in order to determine if a leak between the mercury and the third fluid existed. No evidence of mercury was found and the oxygen level was acceptable.

A sample of mercury that was received with the boiler was apparently contaminated and it was assumed that the boiler might be in a similar condition. The argon gas in the mercury containment portion of the boiler was bled into an analyzing rig and tested for hydrocarbons. The end caps were then removed and an inspection was made of the boiler with a borescope. This inspection showed the boiler to be relatively clean at both the mercury inlet and outlet ends.

Argon gas was purged through the individual tubes in the boiler using a small diameter sample tube fed through a stopper. The inlet plenum was pressurized and each of the seven tubes was tested to determine that flow was established. This test proved that all tubes were open and argon flow rate was similar in all cases.

The boiler was radiographed to determine the relative location of the tube bundle with respect to the shell. The radiographs showed that the orientation of the tubes within the shell was toward the bottom of the shell. A typical cross section through the boiler at about ten feet from the inlet end is shown in Figure 33. These locations were approximated from X-rays taken at 6 o'clock and 9 o'clock. It was also noted that the inlet and exit bellows were somewhat deformed.

The decontamination process of the boiler shell using HgX, a commercial decontaminant, left a residue on the boiler shell. It has been postulated that such residue might cause an undesirable reaction with the boiler shell at elevated temperatures. Therefore, the shell was flushed with distilled water and wire brushed to remove the residue. While checking the shell surface thermocouples by heating, it was found that a level of mercury vapor was obtained from the thermocouple junction caps indicating a degree of contamination.

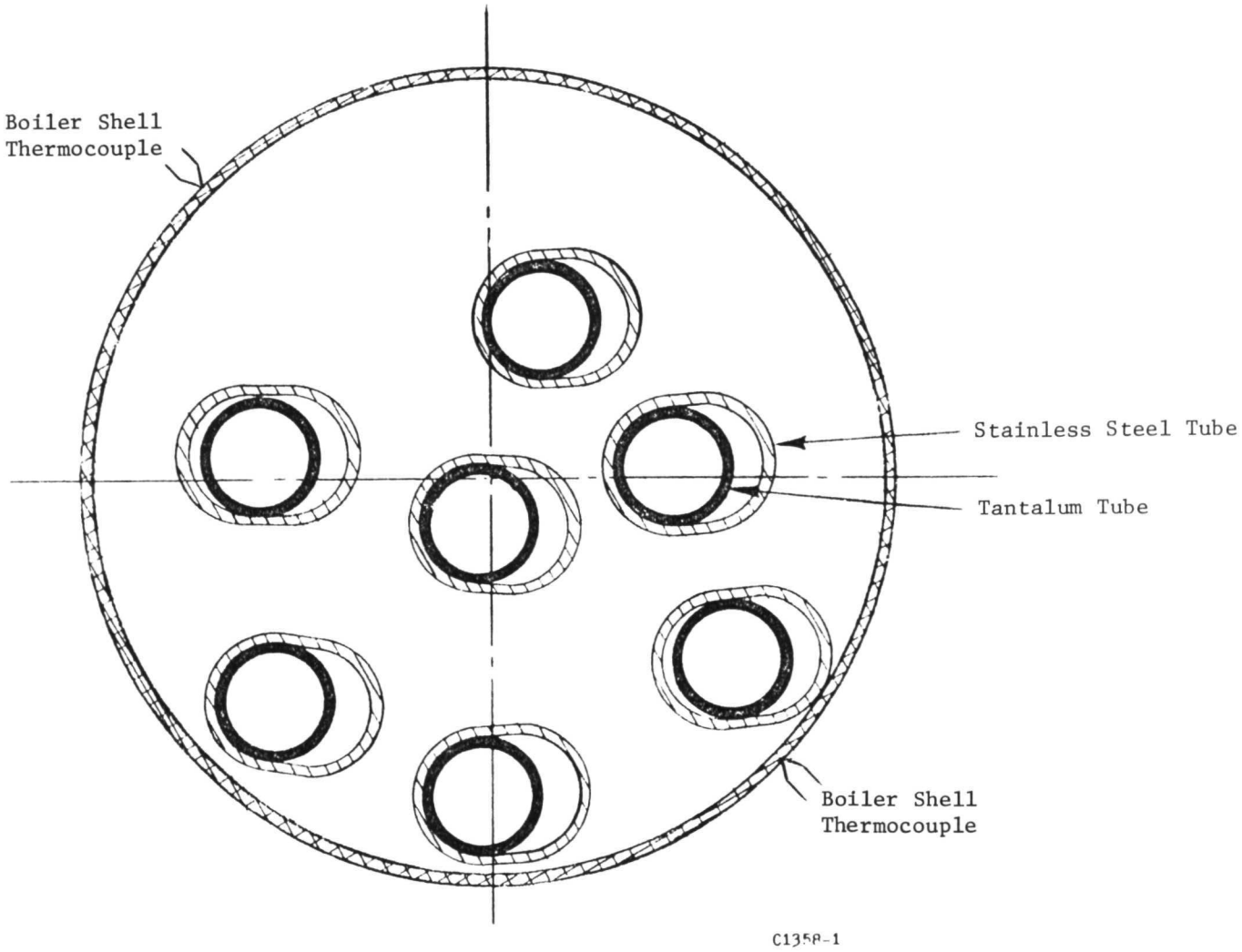

Figure 33. SNAP-8 refractory boiler No. 1. Cross section showing tube location within the shell after 1440 hours of operation.

The boiler was placed into operation at General Electric on February 17, 1968. On February 27, 1968, after 357 hours of operation, a fuse failure in the NaK EM pump created a severe thermal transient on the boiler which in turn caused a separation in the brazed bimetallic joint at the mercury inlet of the boiler[5] due to excess tensile loading. A radiograph of the boiler at the mercury inlet (Figure 34) shows the failure. The boiler was repaired by installing a new bimetallic joint, end cap, bellows and tantalum reducer (Figure 35). This tantalum welding was accomplished in the field by using a converted portable weld chamber (Figure 36). A new section of shell was attached to complete the repair.

At this time, NASA-LeRC decided to attempt to recenter the tube bundle by incorporating 5 new shell spacers into the boiler shell. Segments of the shell were removed to accommodate the spacer installation. A typical spacer installation is shown in Figure 37. The spacer consists of two 180° spacer segments with 4 spacer rods inserted through the tube bundle to maintain tube positions. The rods were welded to the segments and the segments were welded to the shell. Subsequent radiographic inspection indicated an improvement in the tube bundle position.

Discovered during the spacer installation was a heavy deposit on the primary NaK side of the stainless steel tubes. This deposit, shown in Figure 38, was wire brushed off and the tubes cleaned as shown in Figure 39. Figure 39 also shows one of the original spacers which had not been removed along with one of the new spacers. The old spacer indicates some distortion. Following radiographic and mass spectrometer testing to assure boiler integrity, the boiler was placed on test.

The mercury loop inventory which contained NaK due to the above failure was replaced with a new charge to reduce the NaK concentration in the mercury loop from 1.2 to less than 0.1%. The boiler was put into operation on March 11, 1968 and comparative performance before and after the repair is shown in Figure 40.

The difference in temperature between the top and bottom was much improved with the 15^{o} to 20^{o} F temperature variation at the inlet attributed to the incomplete cleaning of the NaK side tube deposit in that region. The much improved heat transfer in the plug region resulted in a higher exit quality from the plug and a major increase in pressure drop of the boiler (171 psi as compared to 112 psi). The pressure drop of the boiler was 202 psi (at the design condition of 11,800 lbs/hr with an NaK inlet temperature of 1305^{o} F and a mercury outlet pressure of 255 psia) as compared to a design value of 80 psi.

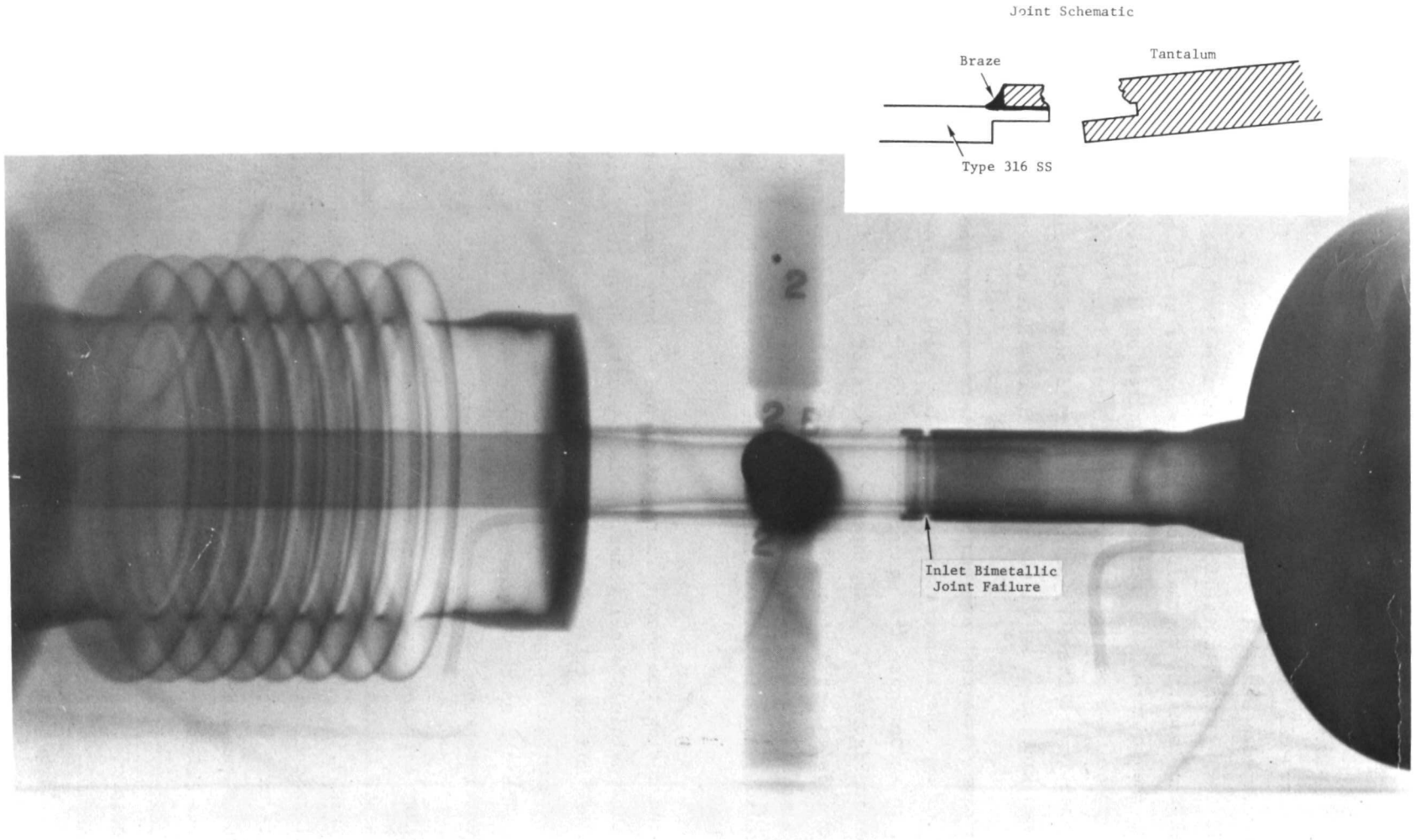

Figure 34. Radiograph of mercury inlet, SNAP-8 refractory boiler SN-1.

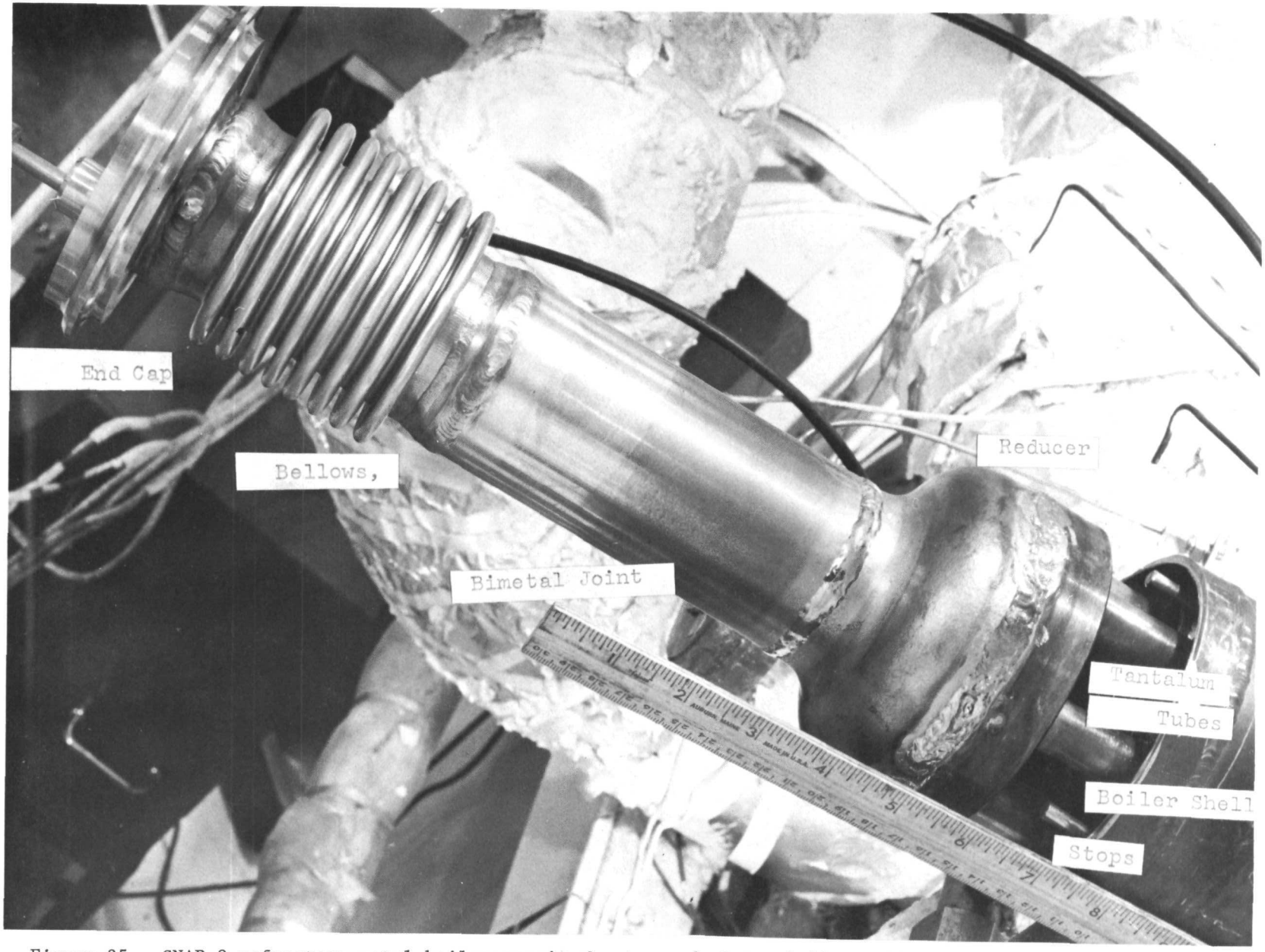

Figure 35. SNAP-8 refractory metal boiler repair showing end plate, bellows, bimetal joint, tantalum reducer installed.

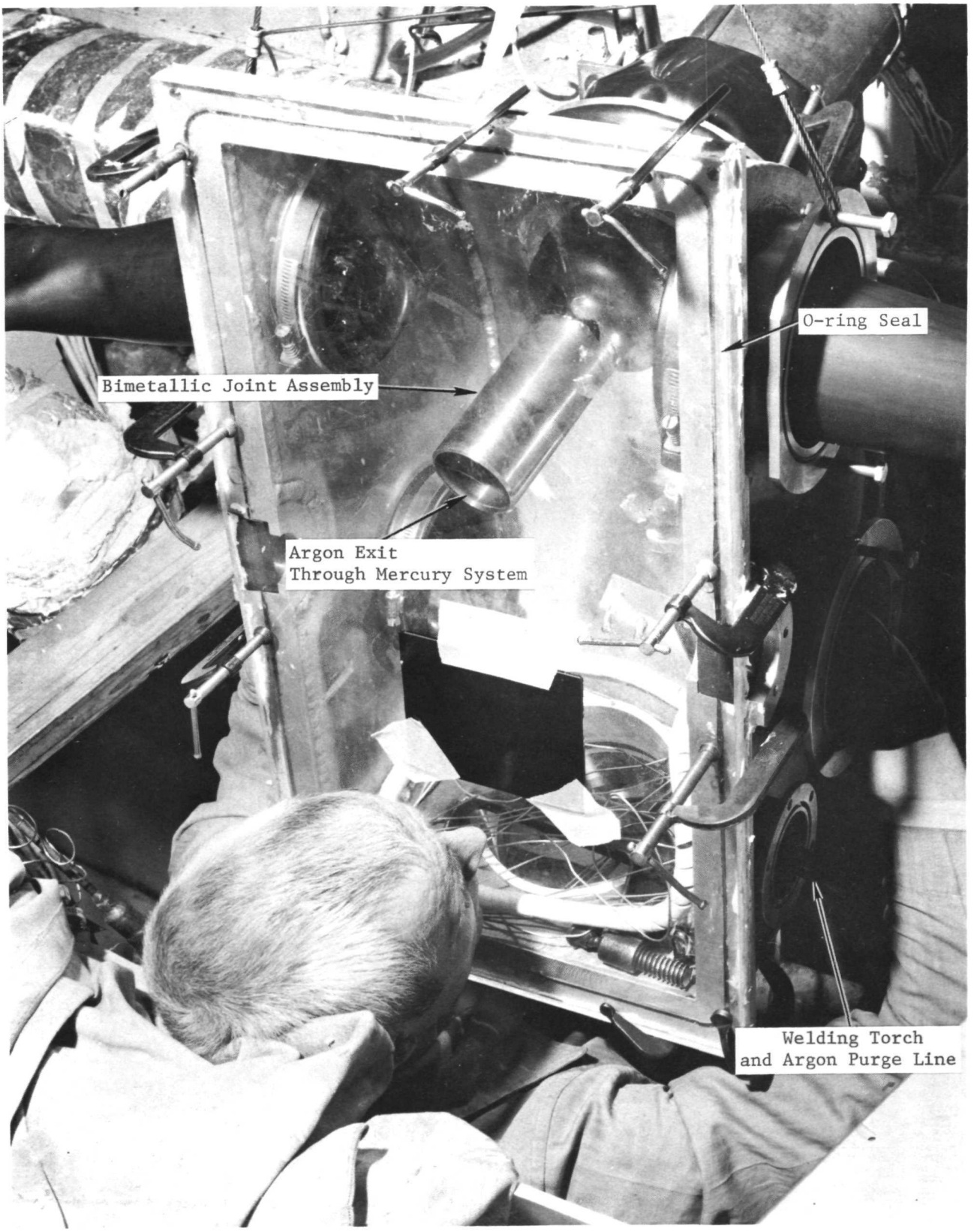

Figure 36. Portable welding chamber used for tantalum welding.

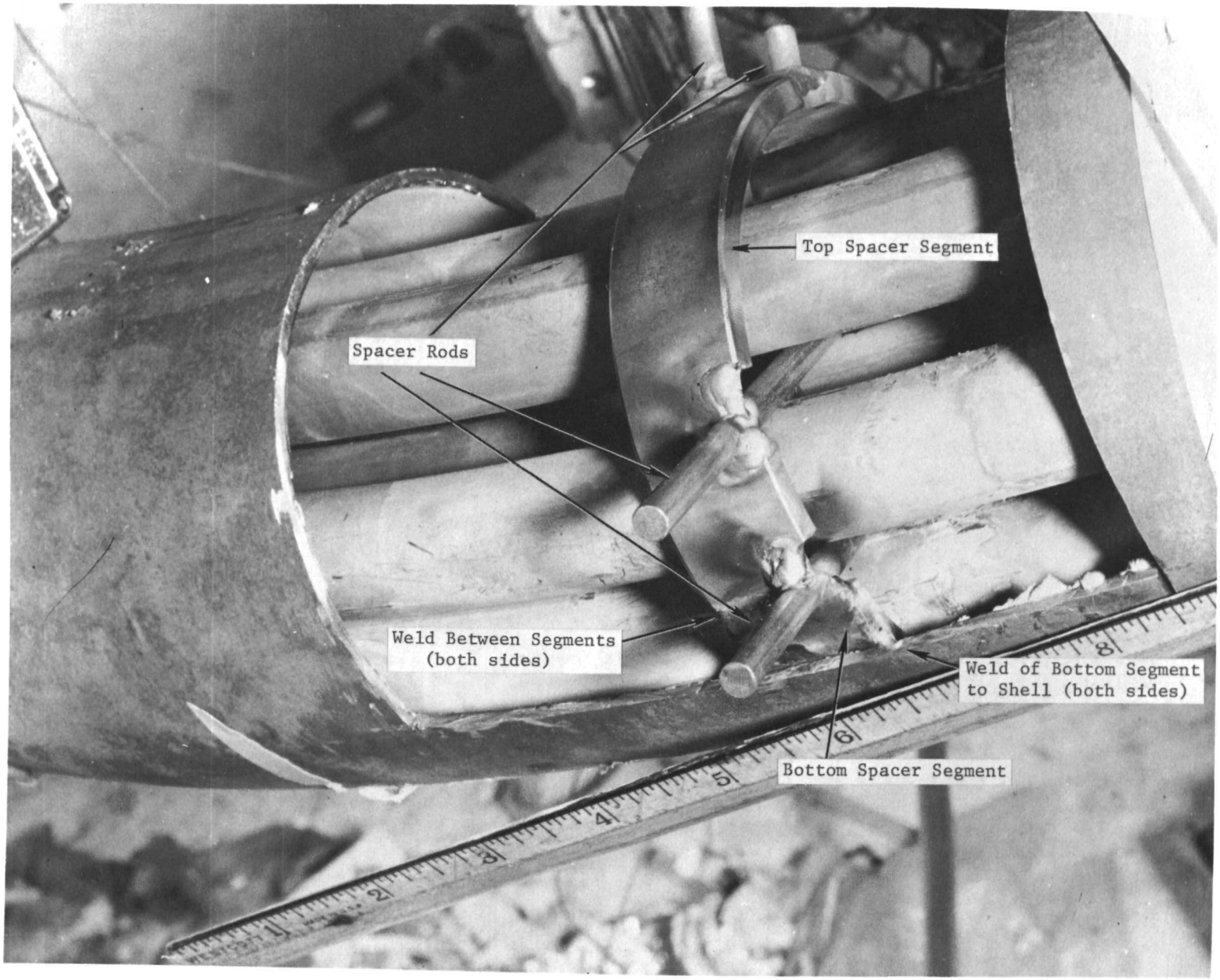

Figure 37. SNAP-8 boiler - typical shell side spacer installation.

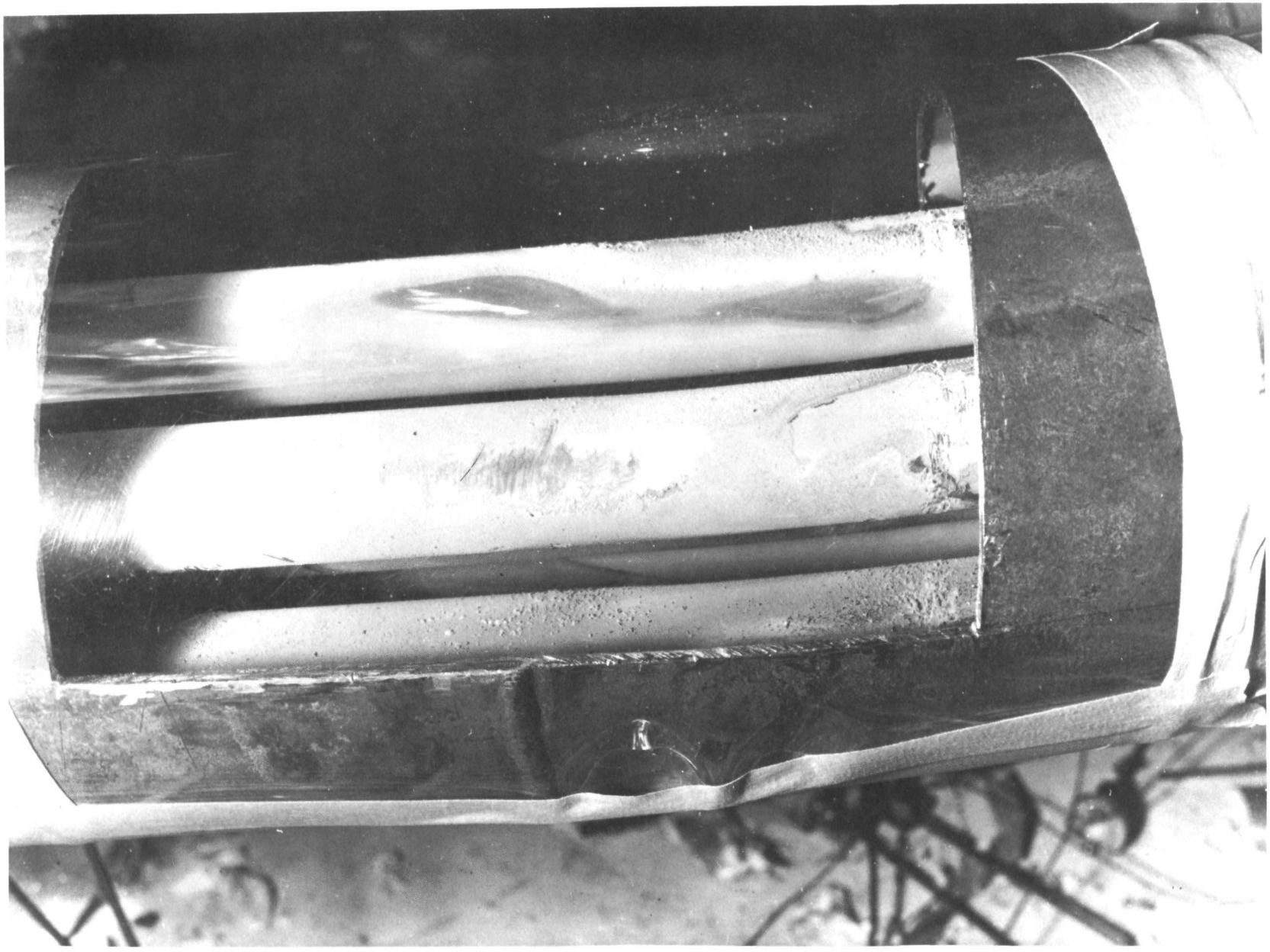

Figure 38. SNAP-8 refractory boiler SN-1 with shell open showing oxide deposits in the plug region.

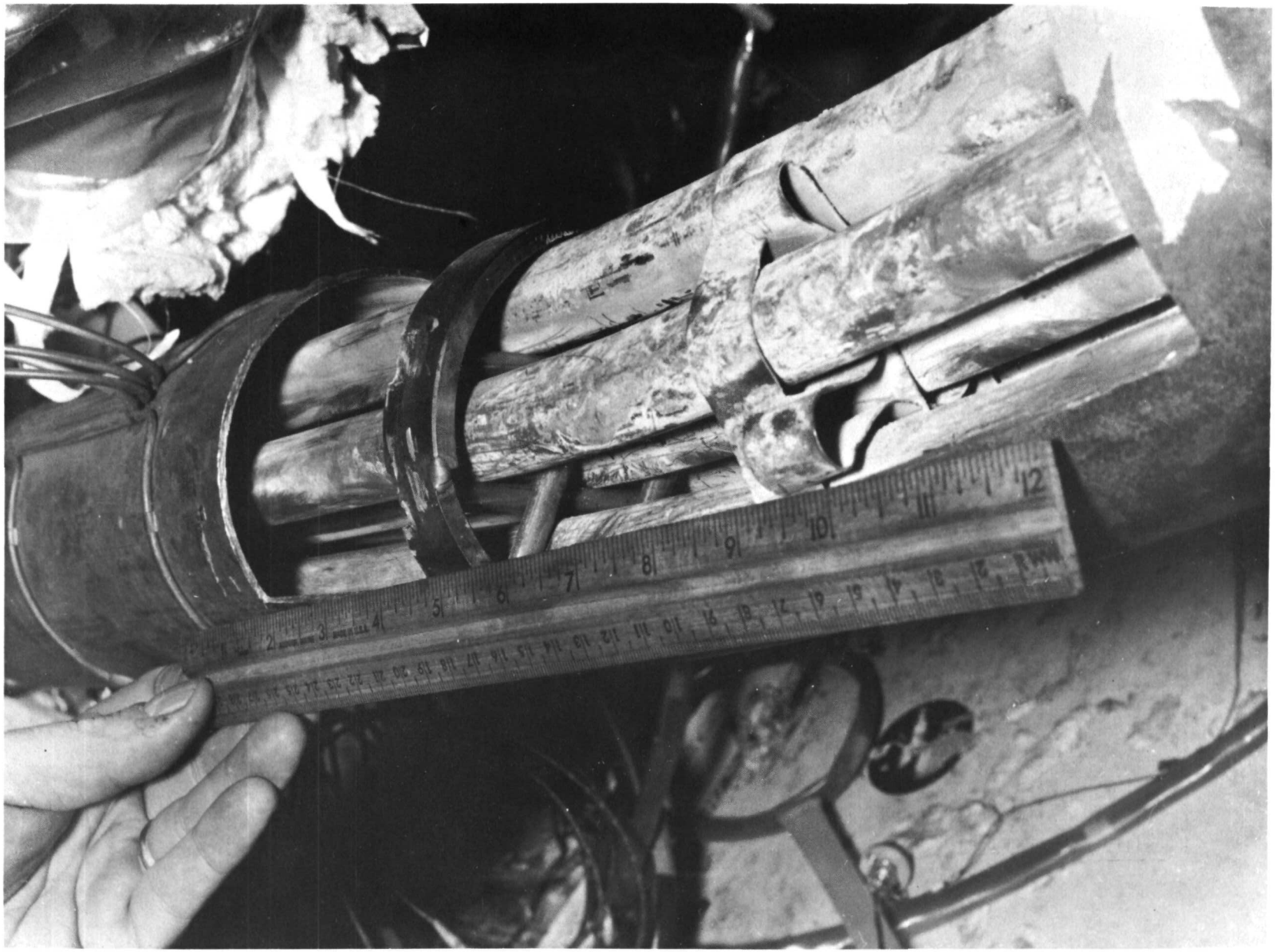

Figure 39. SNAP-8 refractory boiler SN-1 with deposits removed and new tube supports installed.

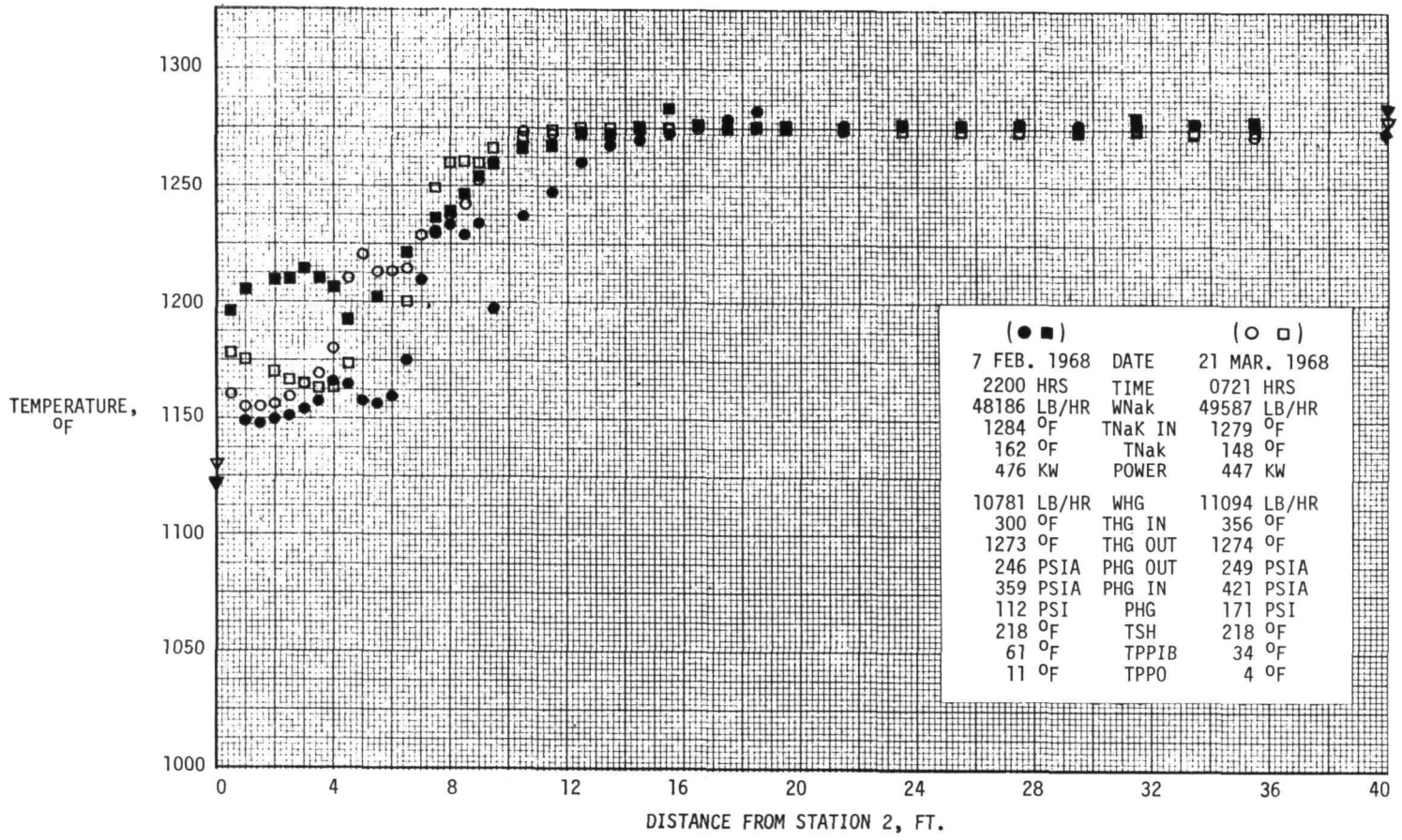

Figure 40. SNAP-8 refractory boiler SN-1 temperature profile.

The shell side NaK pressure drop was increased from about 0.85 psi to about 1.75 psi at a NaK flow rate of 47,700 lbs/hr. This indicates that the combined effect of re-centering the tube bundle and using the new spacer design was to increase the shell side flow coefficient by a factor of about 2.06. However, the pressure drop was still well within the allowable value of 3 psi.

In addition to increasing the shell side pressure drop, the mercury boiler exit pressure and flow rate showed some increase in both the frequency and amplitude of the oscillations associated with these variables.

On May 31, 1968, after 2268 hours of continuous operation, a leak occurred near the NaK exit of the boiler[6]. The facility was secured and the insulation removed from the boiler in the area of the leak. Visual inspection proved inadequate to detect the leak site but with subsequent pressurization of the primary NaK system and the utilization of a soap solution, a very minute leak was detected. The leak area was removed from the boiler (Figures 41 and 42) for metallographic examination. The results of this examination indicated the failure was mechanically or low cycle fatigue induced. The conclusion was based on (1) the absence of any significant internal defects or inclusions which might have grossly weakened the alloy, (2) the lack of any gross deformation in the failed area, (3) the presence of local fissures at the inside surface of the shell near the crack, and (4) the transgranular nature of the crack.

A patch was made from a spare section of shell and welded into place. Nondestructive testing by radiographic, dye penetrant, and mass spectrometer testing demonstrated the integrity of the repair as well as the rest of the boiler. Testing of the boiler resumed.

On June 11, 1968, at the completion of 2500 hours of test, the facility was secured in good working order to inspect the boiler prior to conducting further tests. Radiographic examination of the boiler indicated that the mercury exit bellows (Figure 43) was excessively deformed while the inlet bellows (Figure 44) showed some deformation. In addition, it was discovered that the tantalum tubes had shifted within the stainless steel containment tubes.

The boiler was modified, as shown in Figure 45 , by eliminating the mercury exit bellows and redesigning the mercury inlet such that the bellows service pressure would be that of the static NaK system, namely, 25 psig rather than the high 400 psig

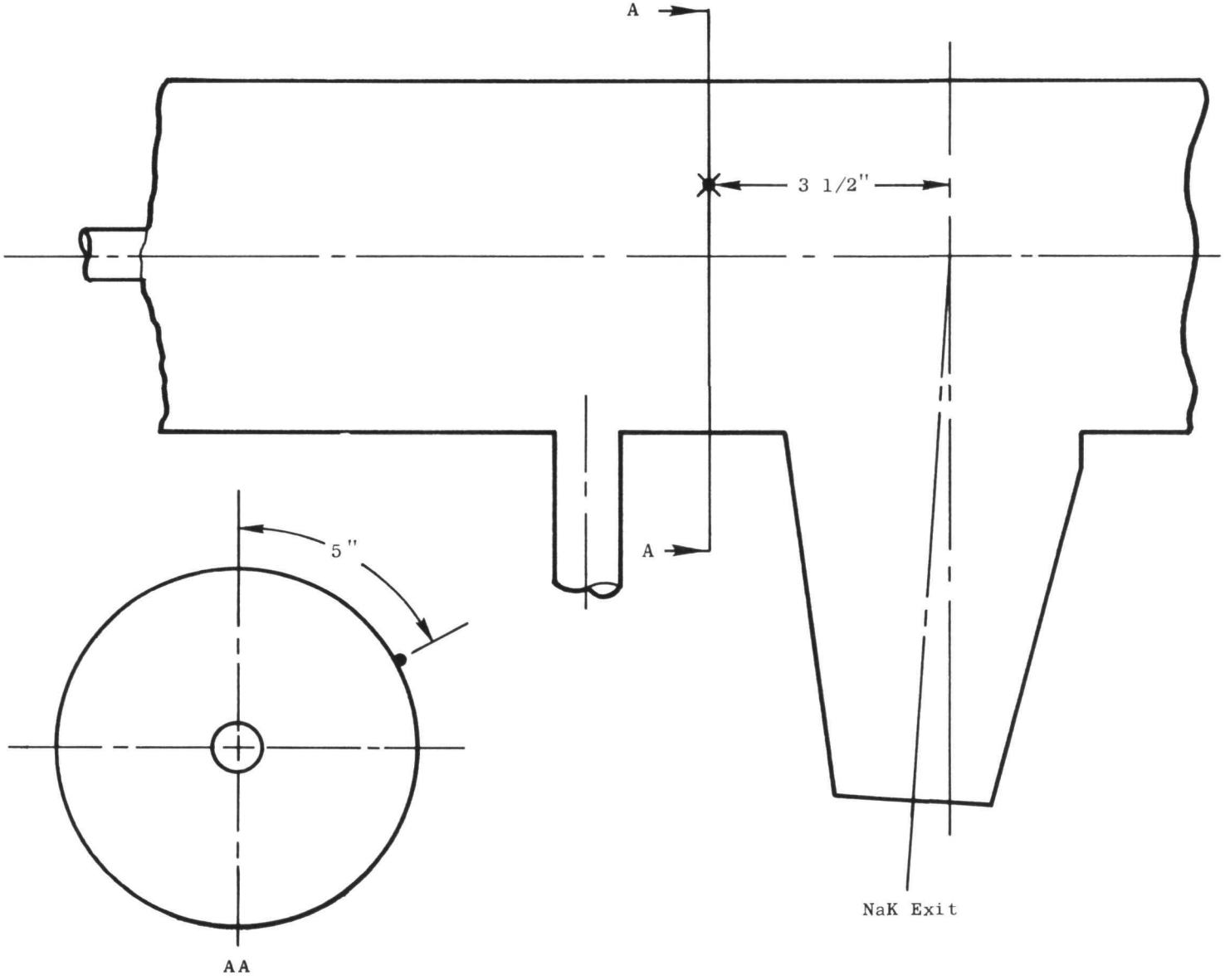

Figure 41. Leak site, SNAP-8 refractory boiler SN-1.

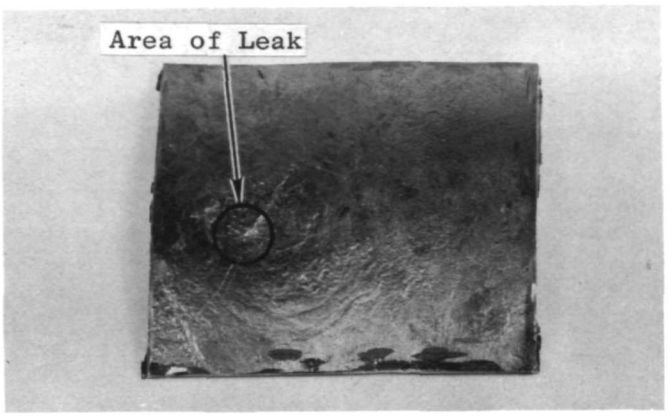

Exterior Surface

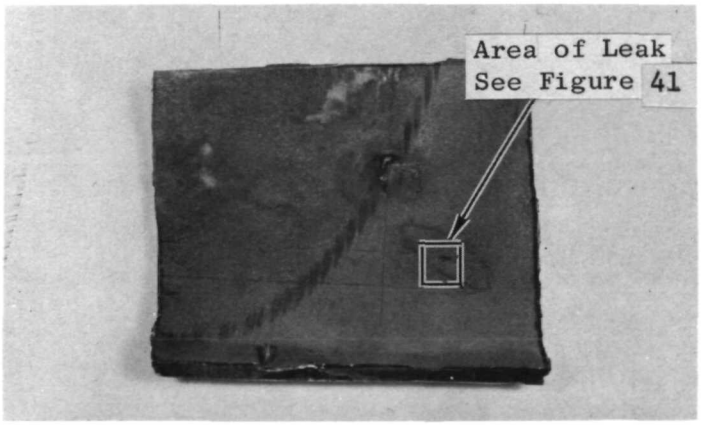

Interior Surface

Figure 42. Interior and exterior surfaces of leak site (full size).

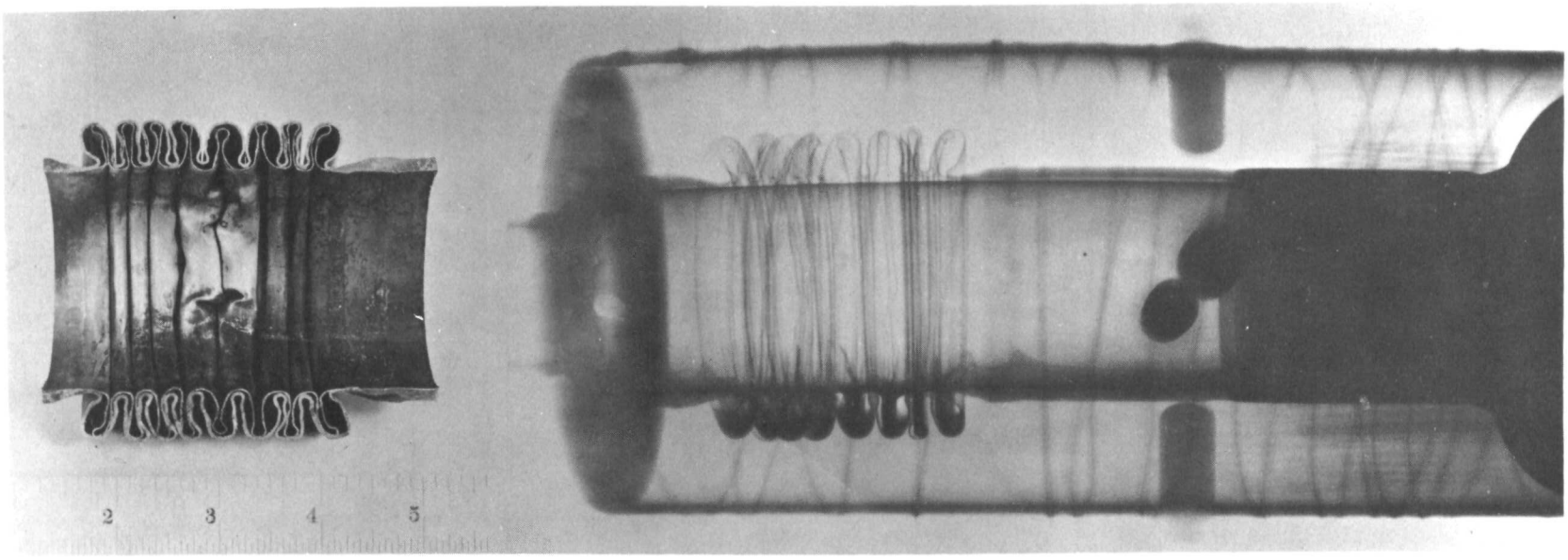

Figure 43. SNAP-8 refractory metal boiler showing radiograph of exit bellows and proposed repair.

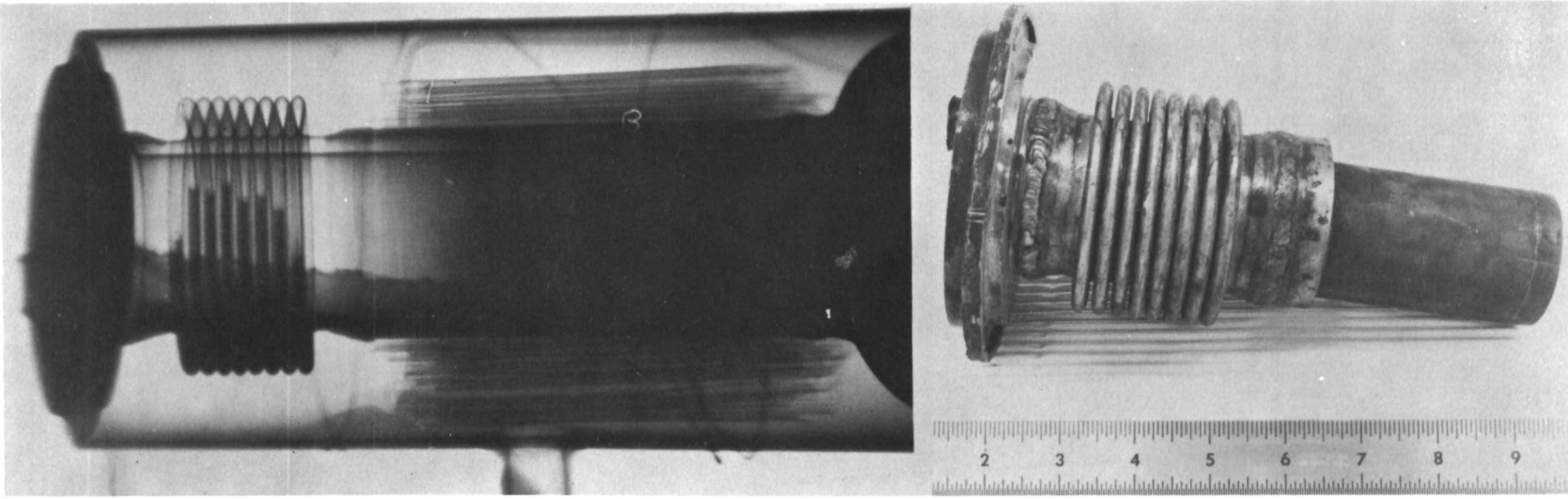

X-RAY OF BELLOWS

BELLOWS AFTER REMOVAL FROM BOILER

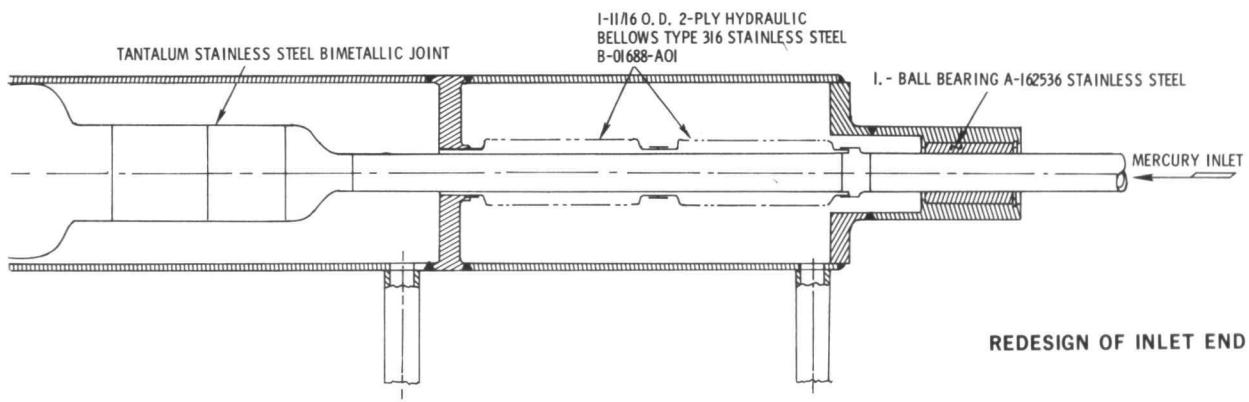

REDESIGN OF INLET END

Figure 44. SNAP-8 refractory metal boiler showing boiler inlet bellows radiograph and proposed repair.

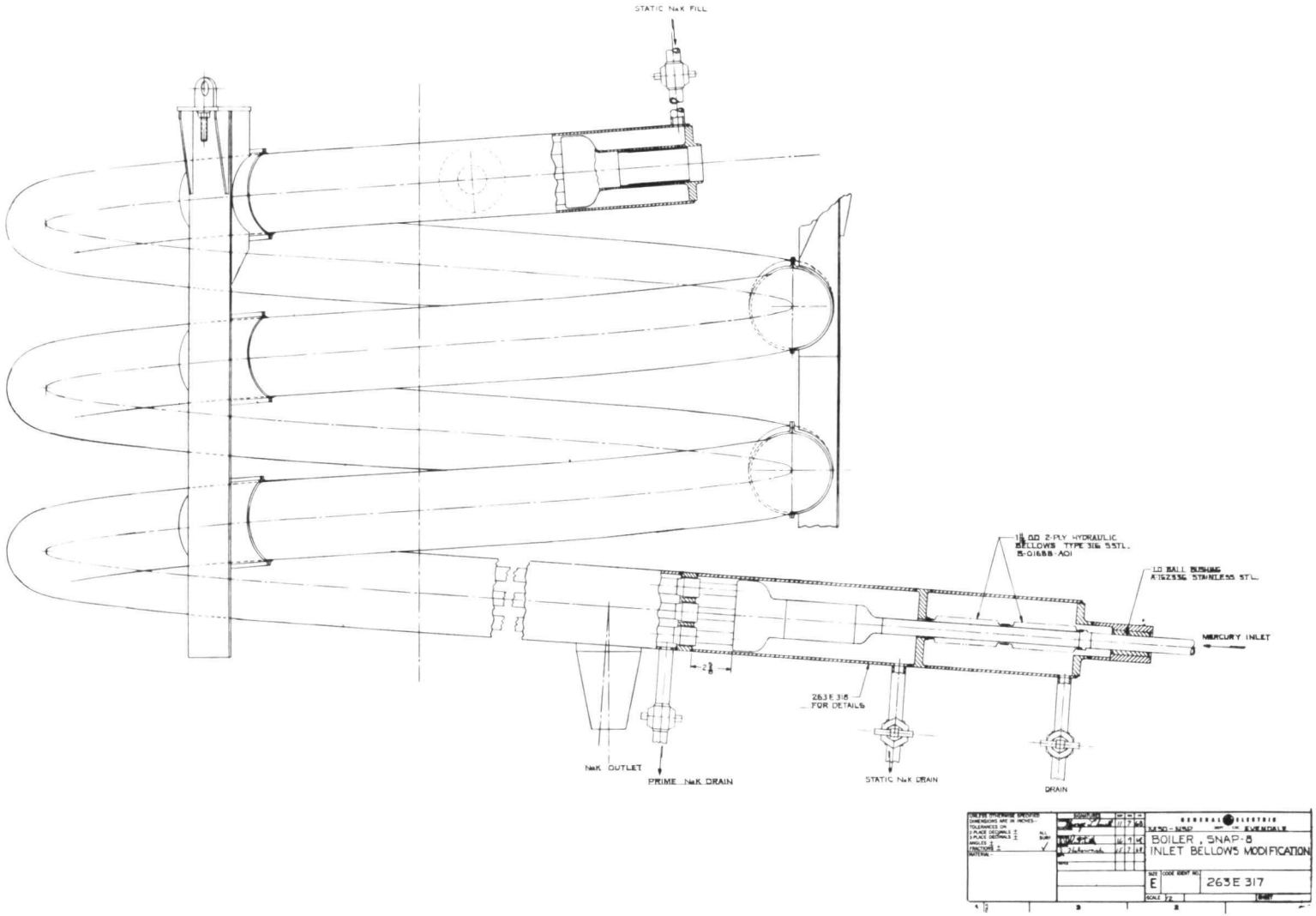

Figure 45. Boiler, SNAP-8 inlet bellows modification.

pressure of the mercury loop. The tantalum tubes were shifted back into the stainless steel containment tubes as shown in Figure 46. Removal of the bellows (Figures 47 and 48) confirmed the deformation of the bellows and subsequent examination concluded that the inner ply of the mercury exit bellows had failed. The gross deformation is shown in Figure 49.

Prior to the rebuild of the boiler the mercury exit bimetallic joint was examined and found to be free of visual defects. The entire exit end of the boiler was cleaned with alcohol to eliminate possible residue that could contaminate the closure welds. A new section of 2-inch outside diameter stainless steel tube was butt welded to the 2-inch OD tube remaining after the bellows removal. A new header was welded to the 2-inch OD tube. After successful radiographic examination and mass spectrometer testing of the mercury containment welds, the tantalum tubes were shifted back into the stainless steel containment tubes. A new hot trap of convoluted zirconium was wrapped around the exit end and a new section of shell was butt welded to the boiler shell and fillet welded to the header. Finally, the static NaK expansion tank was mounted to the boiler shell and the exit mercury vapor connection made to the facility followed by radiographic and mass spectrometer testing.

In the redesigned mercury inlet,differential thermal expansion between the tantalum tube bundle and the stainless steel is accommodated by two hydraulically formed stainless steel bellows connected in series. Before installing the bellows the tantalum tube bundle was moved back into the stainless steel containment tubes to provide the maximum relative length of tantalum tubing to stainless steel tubing in the cold condition. This tends to compensate for the higher expansion of the stainless steel at design operating conditions. The bellows assembly was welded into the boiler by connecting one end to the static NaK header and extending the bellows approximately 1.1-inches and welding it to the mercury inlet pipe. This particular arrangement was chosen for the differential expansion between the tantalum tube and the stainless steel tends to compress the bellows. This was particularly desirable for there was uncertainty in the exact location and relative movement of the tantalum tube bundle with respect to the stainless steel after a number of thermal cycles. Thus the total available differential expansion would be the rated stroke of the bellows (1.1-inches) plus the preset extension of the bellows (1.1-inches) for a total of 2.2-inches. Furthermore,

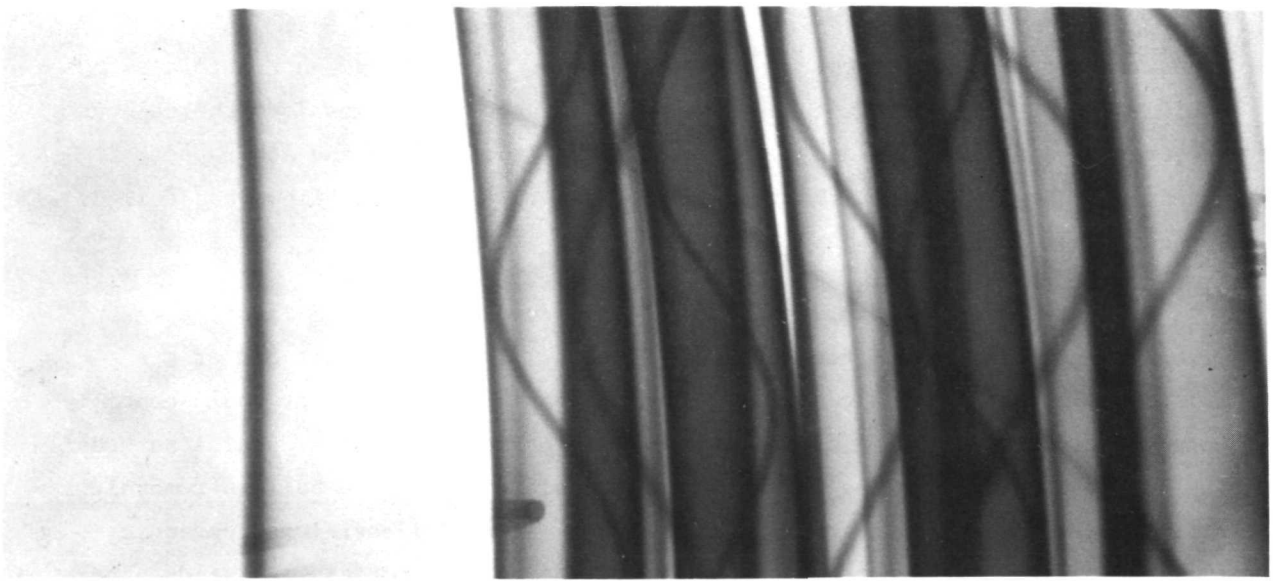

This View is at a Point 90° Down Stream from the Vapor Exit on the Top Coil Looking Vertically Downward.

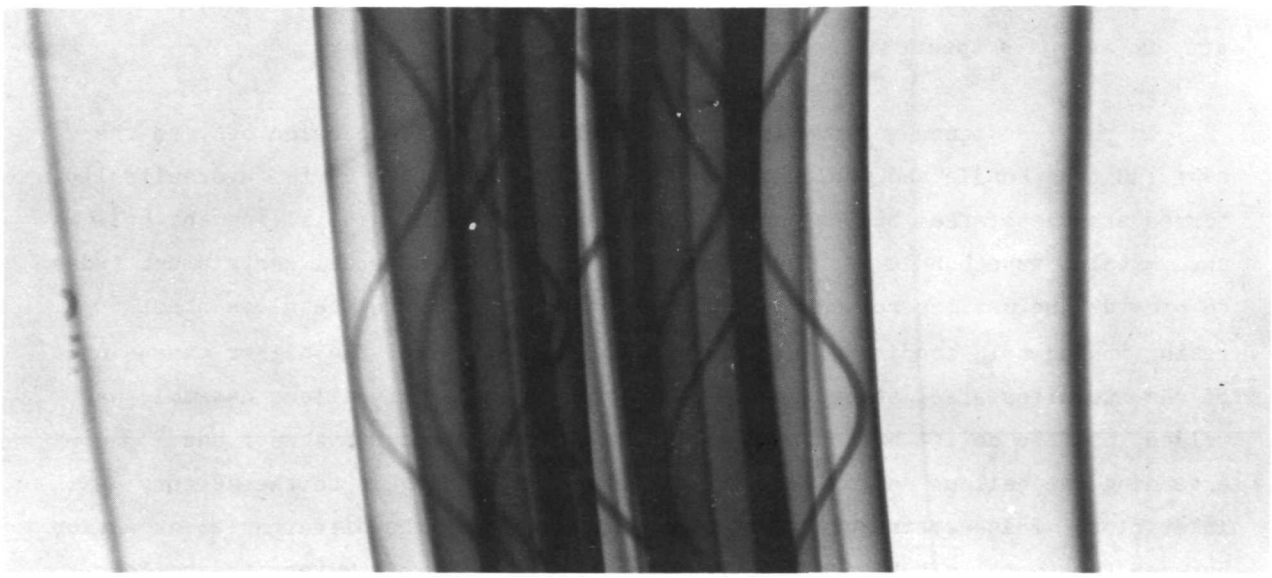

This View is at a Point 90° Up Stream from the End of the Plug Region Looking Vertically Downward.

Figure 46. SNAP-8 refractory metal boiler showing the relative position of the tantalum tubes within the stainless steel tubes and boiler shell.

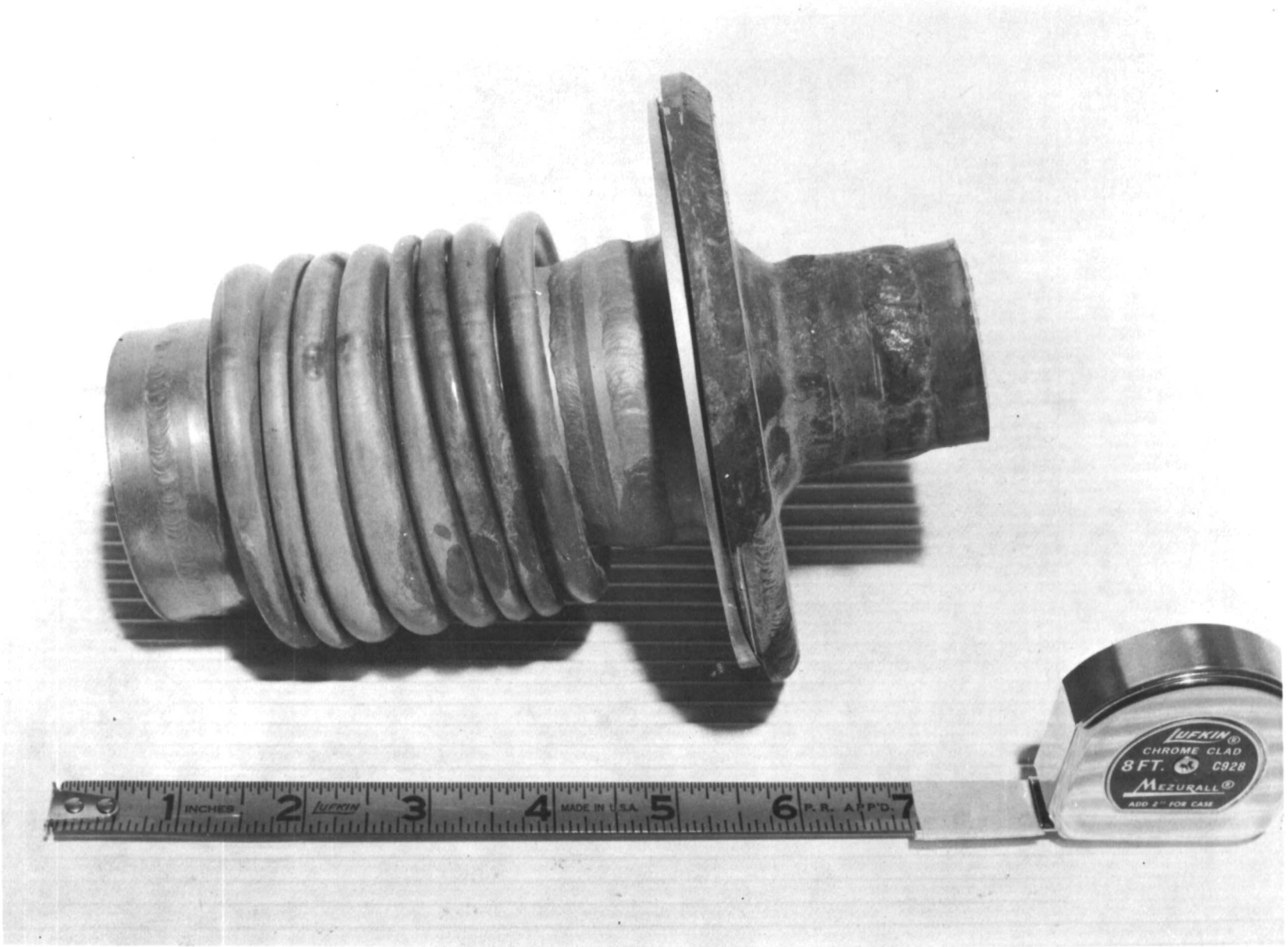

Figure 47. SNAP-8 refractory metal boiler showing exit bellows after removal.

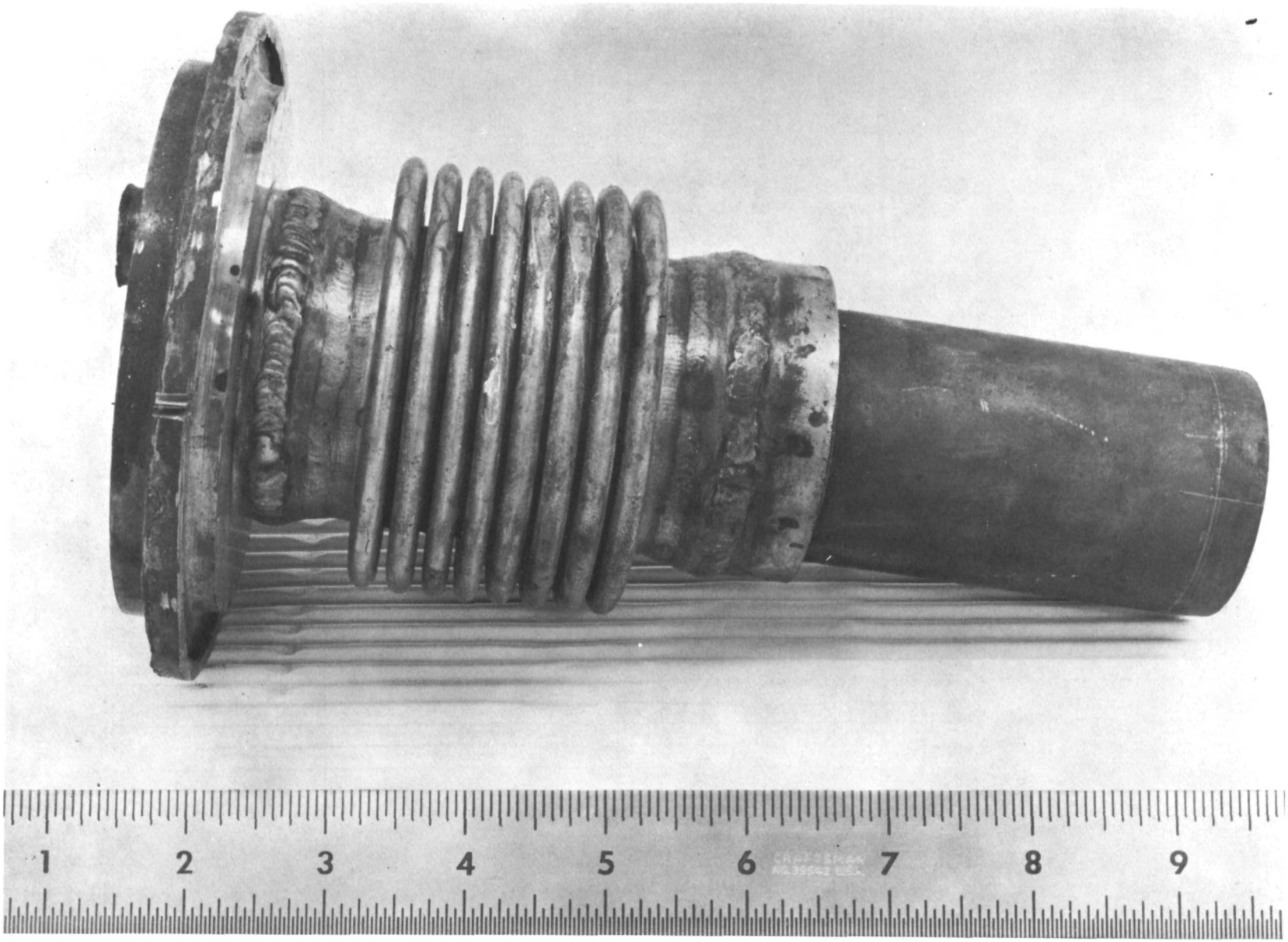

Figure 48. SNAP-8 refractory metal boiler showing inlet bellows after removal.

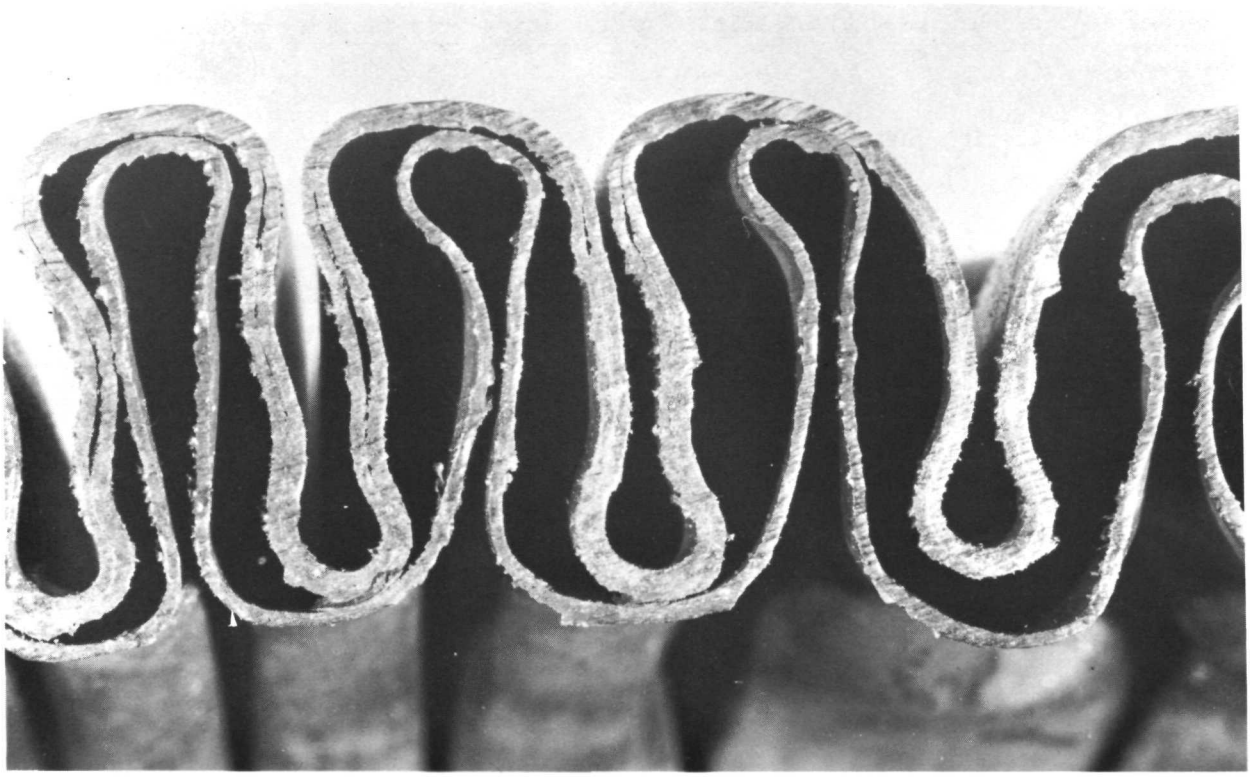

Figure 49. SNAP-8 refractory metal boiler showing gross deformation of the plies.

the bellows assembly is capable of a total compression of 1.8-inches before exceeding the elastic limit.

Finally, a 1.0-inch diameter stainless steel ball bushing was installed. The function of the bushing is to guide the axial movement of the mercury inlet pipe with respect to the boiler shell during operation and to minimize bending stresses in the coextruded bimetallic joint resulting from facility piping movements.

The modification was subjected to helium mass spectrometer testing and radiographic inspection before a section of shell was welded over the entire assembly. The boiler was readied for further testing.

The test boiler was placed in operation on July 12 with a series of isothermal heat loss and thermocouple calibration runs. These runs were made with the mercury loop evacuated and served two purposes. The first was to calibrate the instrumentation and the second was the decontamination of the static NaK system. At the completion of the calibration runs the primary NaK loop was dumped for hot trapping and the static NaK was sampled for analysis to determine whether the static NaK should be drained and recharged. The static NaK analysis showed approximately 10 ppm O_2 and negligible mercury. The analysis of a sample taken from the primary NaK dump tank showed 8 ppm O_2. Thus the system was ready for mercury injection.

Prior to operation, "zero" measurements were taken in order that the relative expansion of the tantalum tube bundle and the stainless shell could be determined. It is interesting to note that the differential expansion during the first thermal cycle was 1/2". During cool-down the tube bundle retracted 1/16". On a subsequent thermal cycle the expansion difference was 3/4" and on the cool-down the retraction was negligible, or 1/16".

Endurance testing commenced on July 12, 1968 and continued until August 20, 1968 and 3155 hours of testing, at which time a leak occurred in the boiler shell at the NaK exit in the same area as the earlier May failure.[7] Removal of the failure area showed a cocked baffle, as shown in Figure 50. The fix of the baffle is shown in Figure 51. This repair was made by moving the two spacers shown in Figure 50 together and welding them to the heavy ring segment. The boiler shell patch was then welded to the boiler, the spacers and the ring segment.

At the completion of repairs, the boiler was mass spectrometer tested and radiographed before being placed on test.

On August 24, 1968 mercury injection was completed and the facility brought to design conditions. Boiler performance appeared to be the same. At this point the boiler endurance continued uneventfully for 10,500 hours. A few shutdowns occurred as a result of power failures and minor loop difficulties, but none were caused by boiler failures. At the completion of the endurance test a series of off-design performance runs was made to determine boiler performance at reactor outlet temperatures specified. This data is plotted in Figures 52 to 56. Unfortunately, the turbine simulator was not sized properly to permit the required boiler exit pressure, thus the test parameters obtainable were severely restricted. The mercury loop was dumped, evacuated, and a series of isothermal heat loss and calibration runs were made. The static NaK system was drained and then the primary NaK loop was drained and evacuated followed by heating with trace heaters for 72 hours to vaporize the NaK residue from the primary loop. Samples of mercury and NaK indicated there had been no communication of mercury-to-Nak or NaK-to-mercury. The boiler was removed for metallurgical examination.

The results of the metallurgical evaluation indicated that (1) there was some loss in the ductility of the boiler shell material, (2) the 321 stainless steel tubing was attacked in the area of the plug region which was coated with a heavy deposit and wire brushed. There was no corrosion observed on the rest of the 321 stainless steel tubing. The tantalum dished head at the mercury boiler inlet showed slight attack, however, this dished head may have been oxygen contaminated during the boiler repair in February 1968. The coextruded and brazed bimetallic joints gave minor indication of defects, however, this defect may have been present since their manufacture. No deleterious effects were observed due to exposure to mercury or NaK.

It is concluded that a design life of 40,000 hours could be expected from this particular boiler.

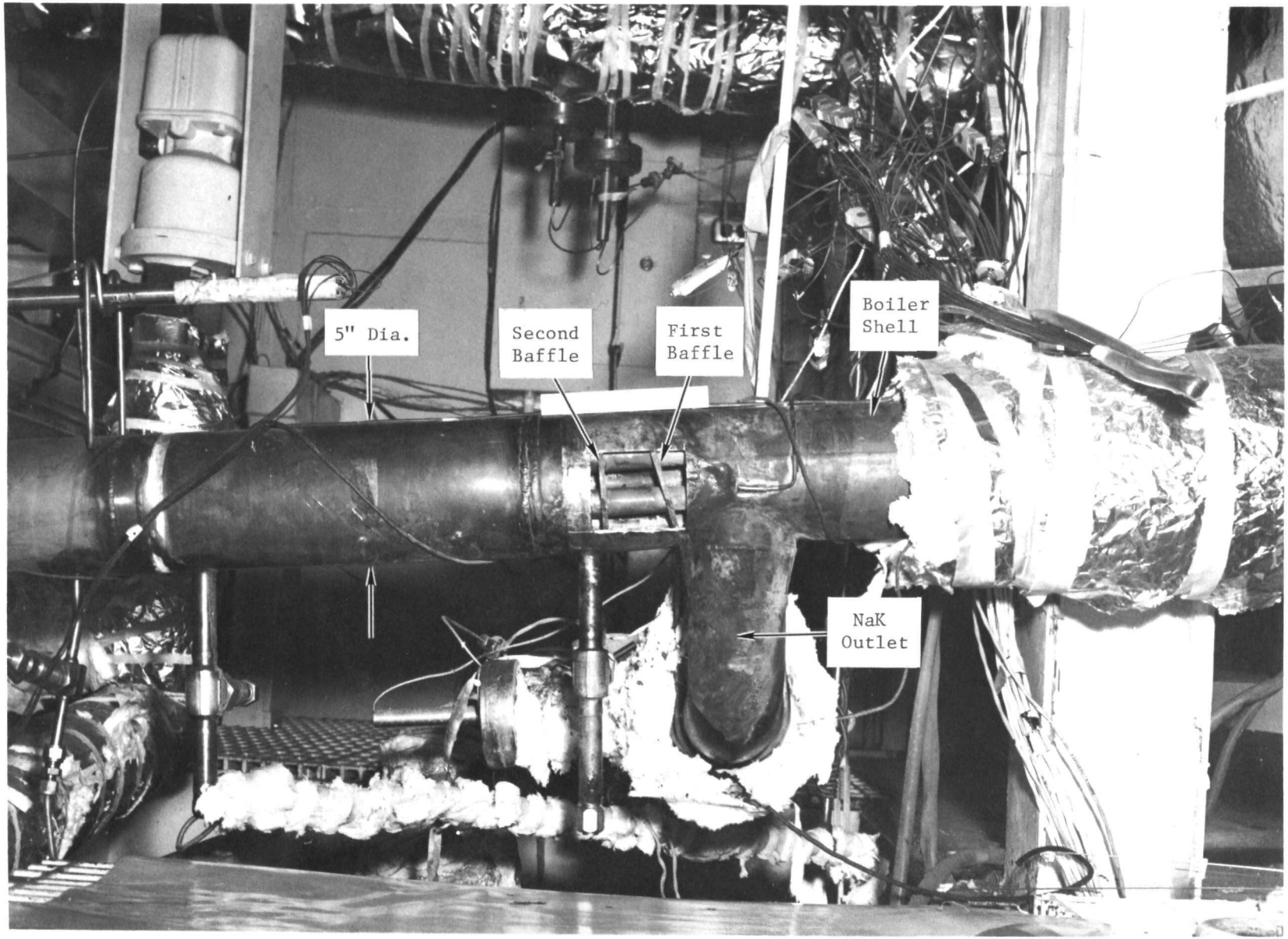

Figure 50. Boiler shell opened to show cocking of the thermal baffles at the NaK outlet region.

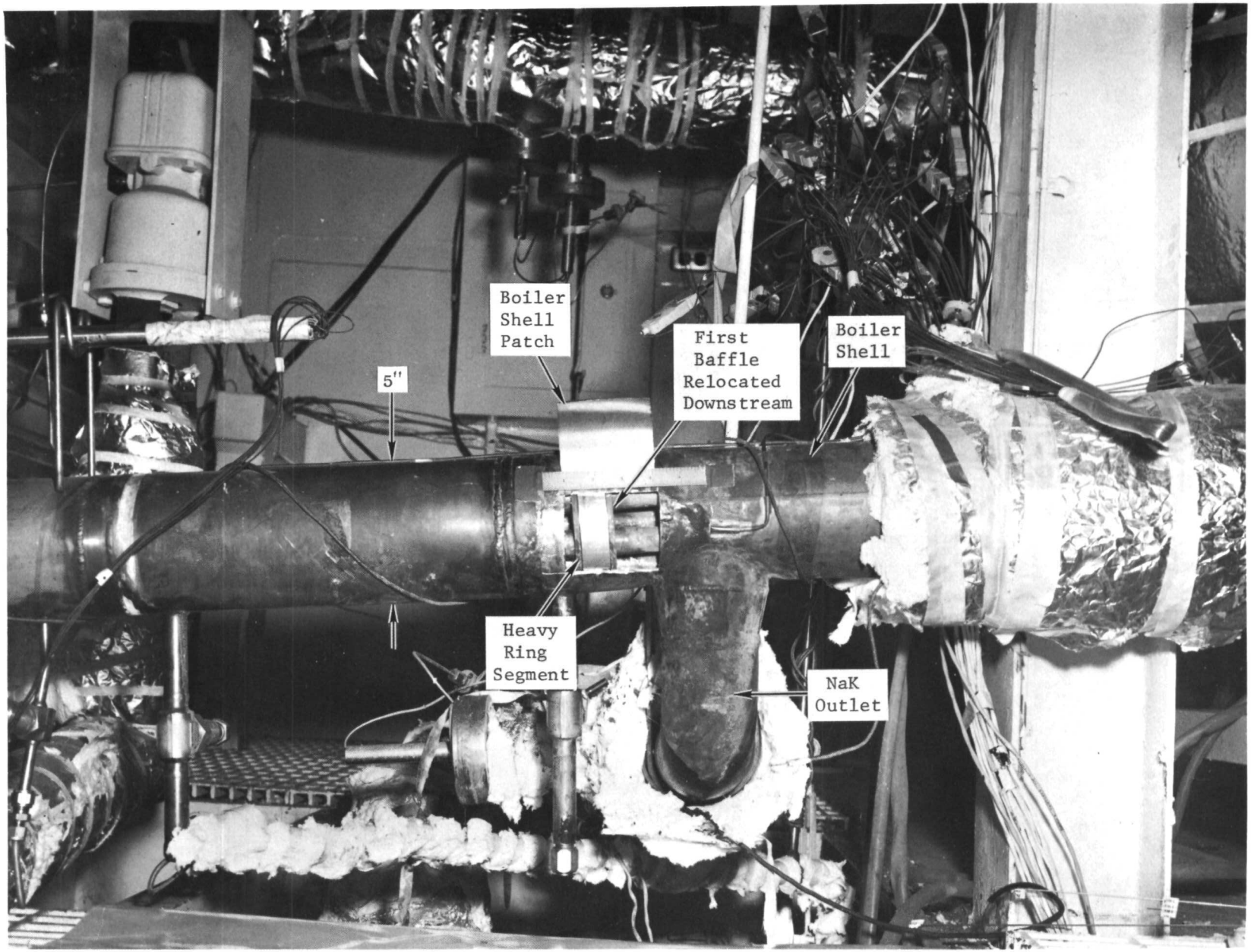

Figure 51. Boiler shell opened to show repair of the thermal baffle at the NaK outlet region.

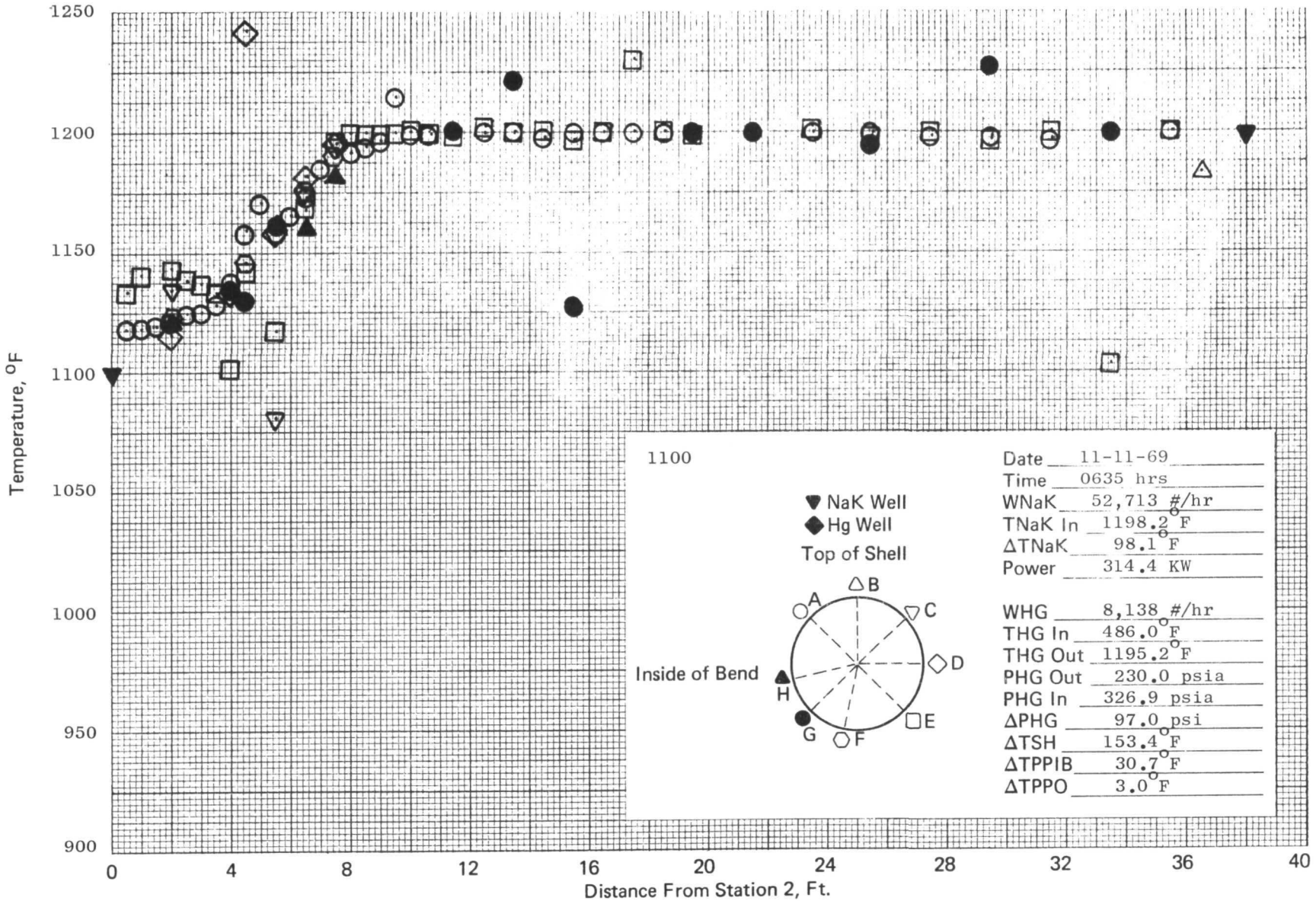

Figure 52. SNAP-8 refractory boiler temperature profile.

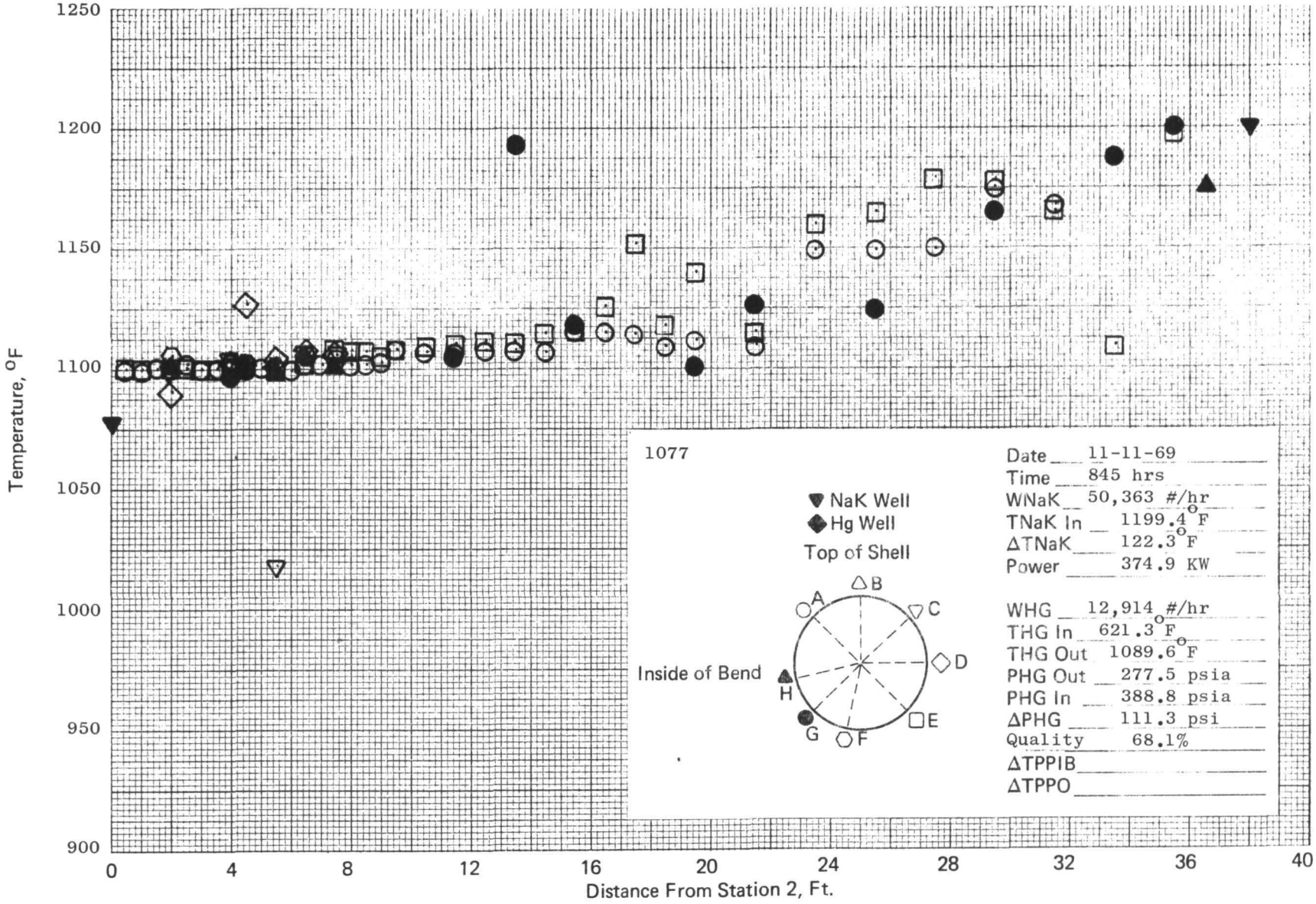

Figure 53. SNAP-8 refractory boiler temperature profile.

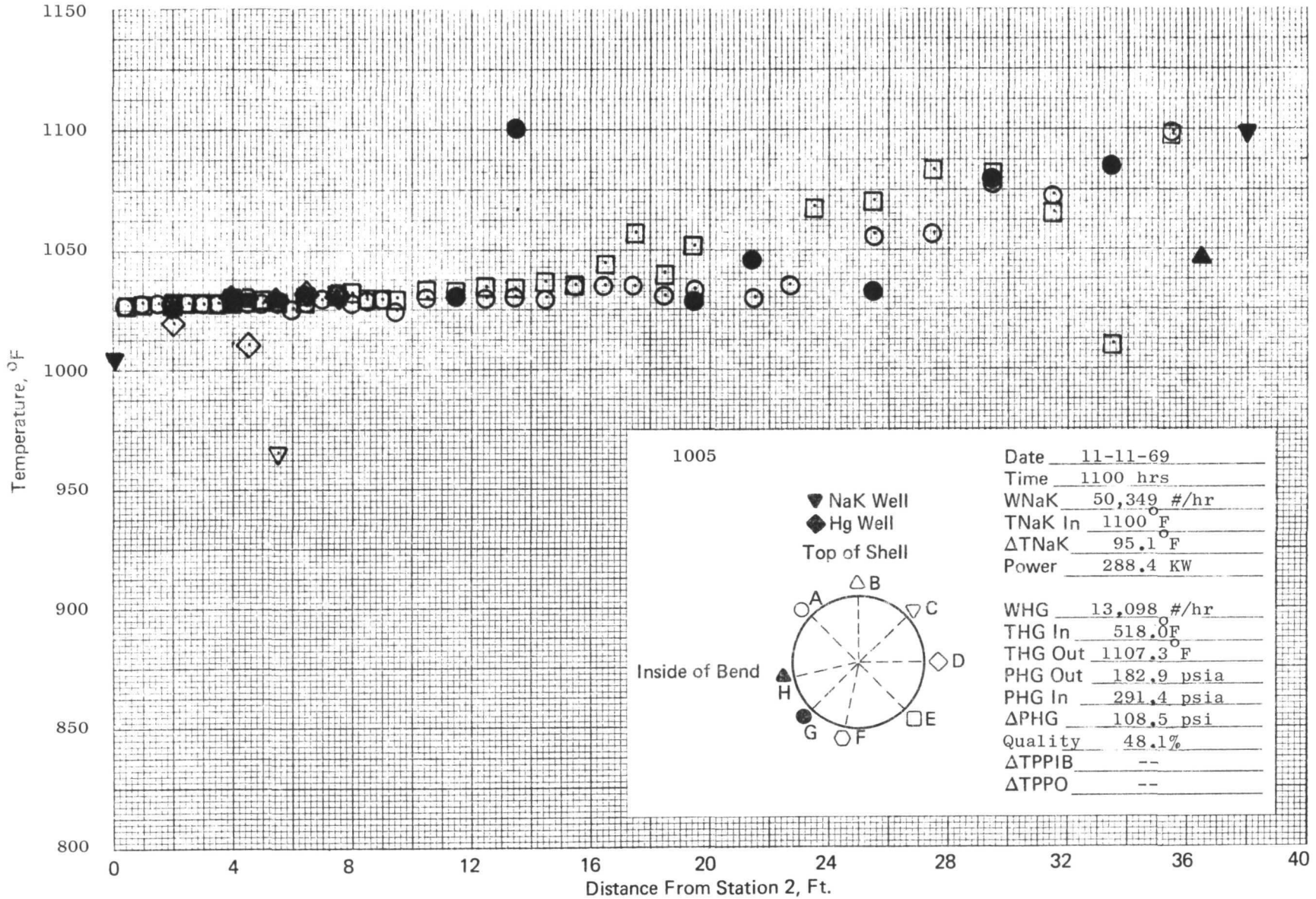

Figure 54. SNAP-8 refractory boiler temperature profile.

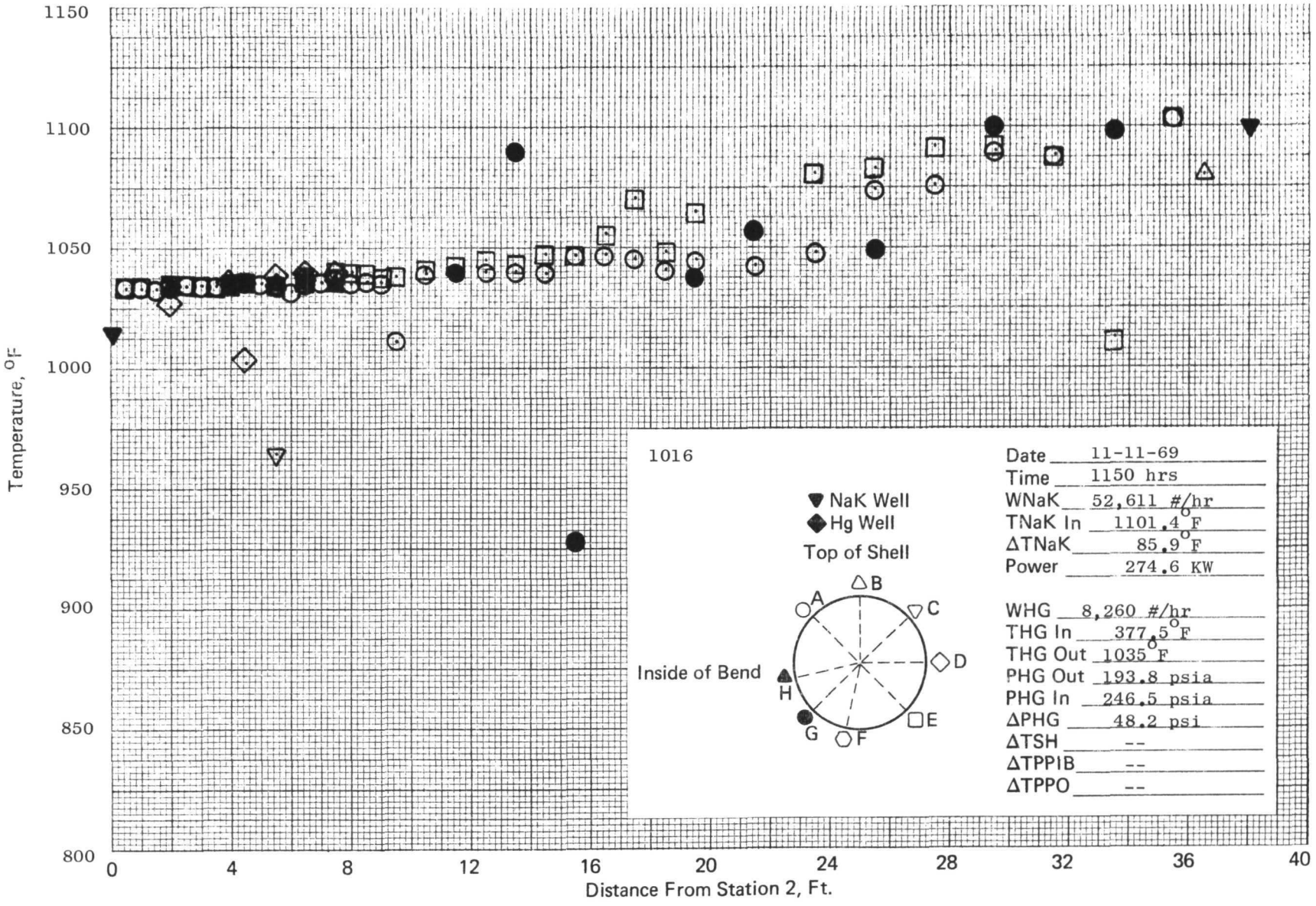

Figure 55. SNAP-8 refractory boiler temperature profile.

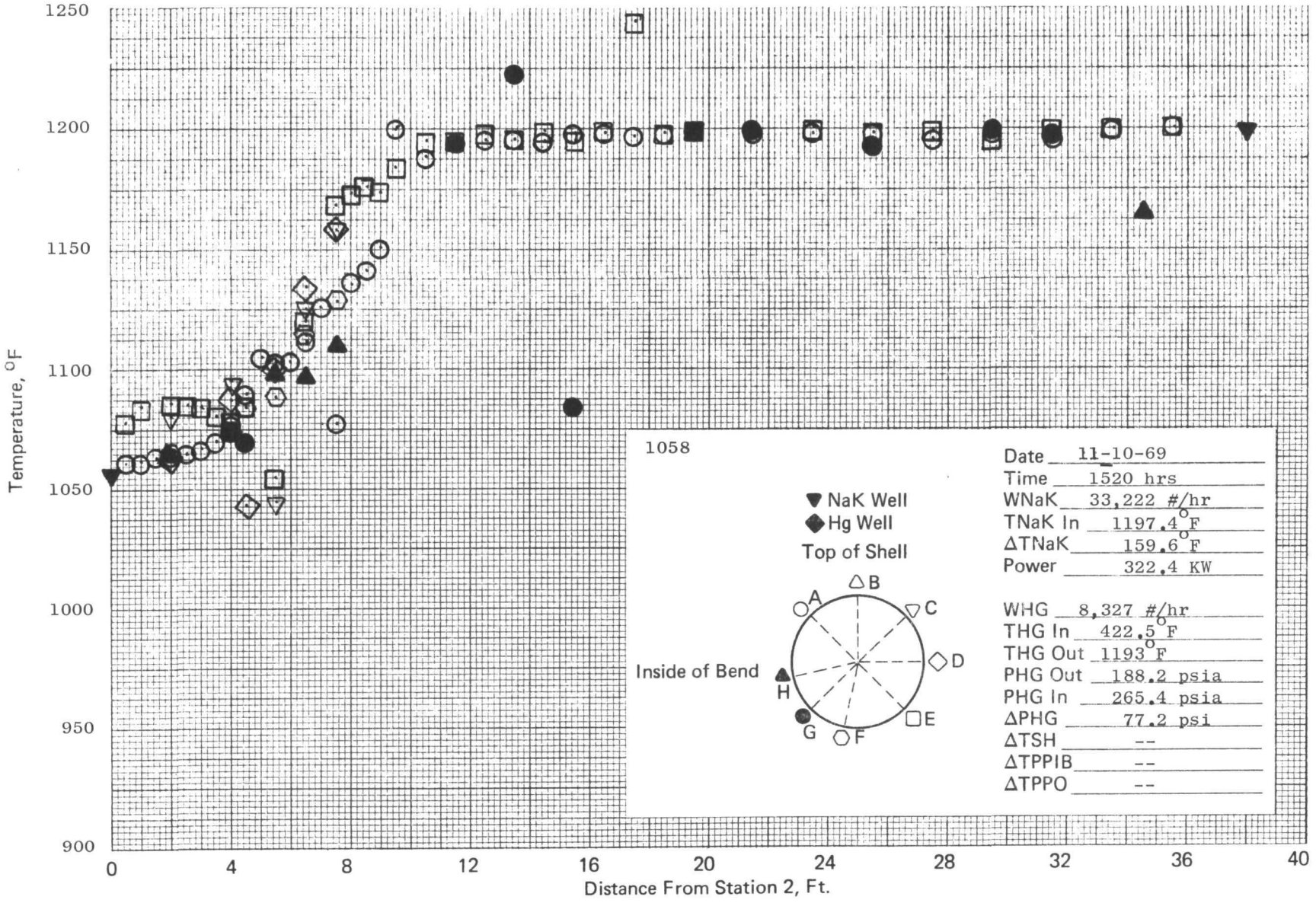

Figure 56. SNAP-8 refractory boiler temperature profile.

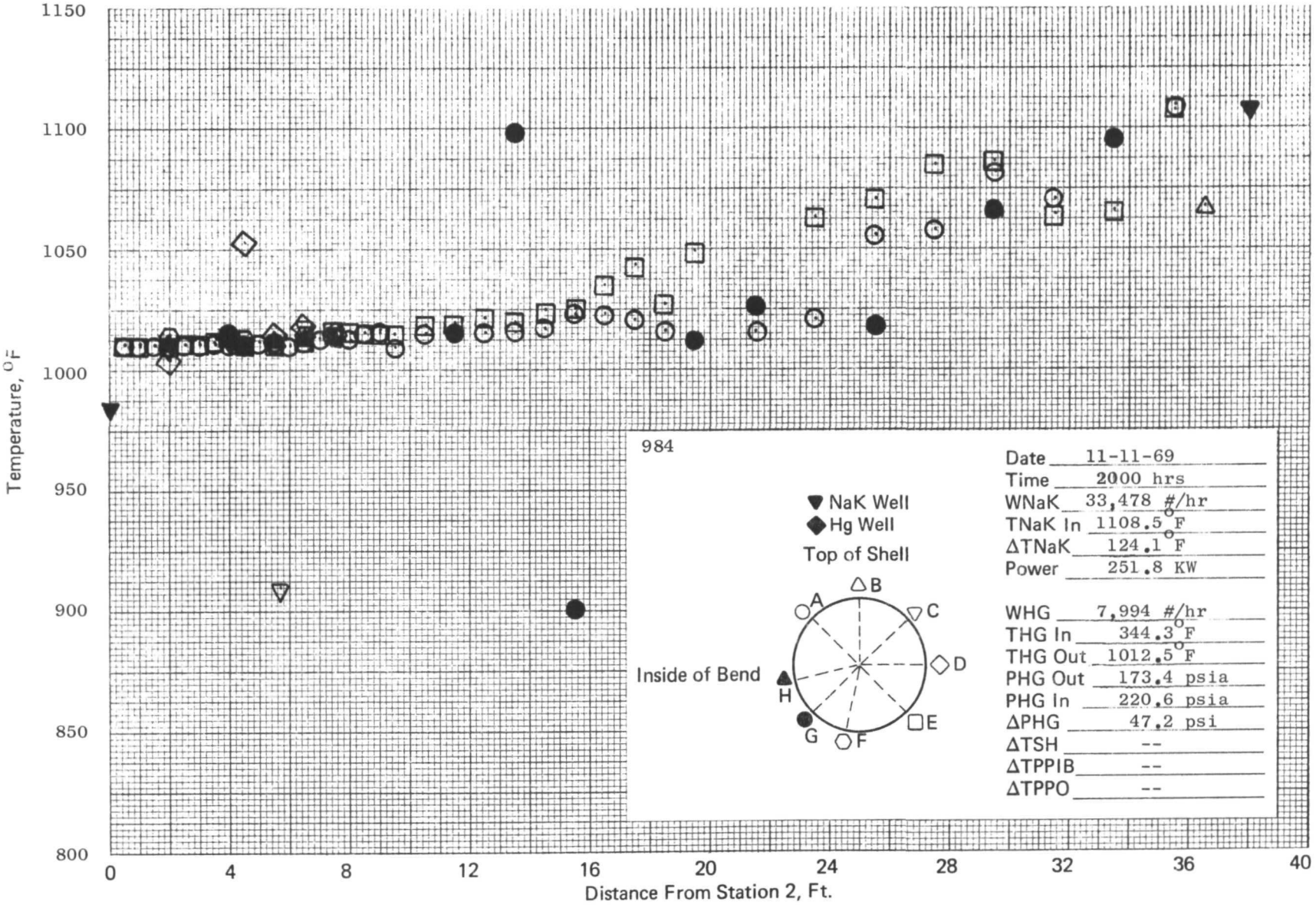

Figure 57. SNAP-8 refractory boiler temperature profile.

V. BOILER PERFORMANCE

The primary purpose of the test data obtained from boiler SN-1 was to determine the change in thermal performance, if any, as a function of test time. Two methods were chosen to provide such detection. The first was the boiler temperature profile wherein the boiler shell thermocouples are plotted as a function of boiler length. One such temperature profile was plotted each week. The second method was the correlation of the overall boiler pressure drop with the pinch point temperature difference at boiling inception.

Figure 58 represents a temperature profile plotted from data obtained during the 1445 hour test at NASA which indicates poor thermal performance. Figure 59 represents the initial critical tests performed at General Electric. When this plot is compared with the previous plots as shown in Figure 60 it indicates that possibly some improvement has occurred.

Figure 61 represents the temperature profile obtained directly after the boiler failure on February 5. This curve compared with the previous data represents an enormous improvement. Also, comparing AGC temperature profile plots (Figure 62) with the post failure plots indicates similarity of performance between SN-1 and SN-2 which was on test at AGC.

Figure 63 represents the initial boiler performance after the May 31 failure and indicates no change in performance.

The temperature profile at start up after the 2500 hour test and rebuild is shown in Figure 64 and the performance has remained the same. A performance matrix, as shown in Table III, was performed in October. The temperature profiles are plotted in Figures 65 through 100. A comparison with Figures 101 through 106 from the May 1968 matrix shows the overall boiler performance has remained constant. A typical plot at the completion of tests in November 1969 is shown in Figure 107 and a comparison of data from right after the February 1968 repair with the November 1969 data also indicates that a performance change has not occurred.

The second method of data analysis was the correlation of the overall pressure drop with the pinch point temperature difference at boiling inception. Since any change in the thermal performance of the boiler is

Table III

SNAP-8 PERFORMANCE MATRIX

No	W_{NaK}	T_{NaKIN}	W_{Hg}
1	49,000 LB/HR	1280 °F	11,000 LB/HR
2			11,500 LB/HR
3			12,000 LB/HR
4			12,500 LB/HR
5		1300°F	11,000 LB/HR
6			11,500 LB/HR
7			12,000 LB/HR
8			12,500 LB/HR
9		1330°F	11,000 LB/HR
10			11,500 LB/HR
11			12,000 LB/HR
12			12,500 LB/HR
13	46,000 LB/HR	1280°F	11,000 LB/HR
14			11,500 LB/HR
15			12,000 LB/HR
16			12,500 LB/HR
17		1300°F	11,000 LB/HR
18			11,500 LB/HR
19			12,000 LB/HR
20			12,500 LB/HR
21		1330°F	11,000 LB/HR
22			11,500 LB/HR
23			12,000 LB/HR
24			12,500 LB/HR
25	52,000 LB/HR	1280°F	11,000 LB/HR
26			11,500 LB/HR
27			12,000 LB/HR
28			12,500 LB/HR
29		1300°F	11,000 LB/HR
30			11,500 LB/HR
31			12,000 LB/HR
32			12,500 LB/HR
33		1330°F	11,000 LB/HR
34			11,500 LB/HR
35			12,000 LB/HR
36			12,500 LB/HR

Tolerances: W_{NaK} ($\pm$ 1000 LB/HR)

T_{NaKIN} ($\pm$ 10 °F)

W_{Hg} ($\pm$ 250 LB/HR)

accompanied by a change in the overall boiler pressure drop, it is possible to detect changes in the thermal performance from changes in the overall boiler pressure drop. For example, when the thermal performance (as measured largely by the heat transfer coefficient in the plug region) is reduced, the overall boiler pressure drop is also reduced.

In order to determine the variables which control the overall boiler pressure drop, a simple theoretical model for the thermal and hydraulic behavior of the boiler was postulated. This model was then analyzed in order to determine the dimensionless groups which govern the boiler performance. The more significant dimensionless groups were then used both to predict and correlate the boiler performance. A brief description of the analytical procedure used, together with the resulting correlations, is given below.

A simple homogeneous model was used to obtain the local pressure gradient, i.e.,

$$\left(\frac{dP}{dL}\right)_{TPF} = \frac{f_H}{D} \quad \frac{W^2}{2g_o N^2 A^2 \rho_H}$$

where

$$\frac{1}{\rho_H} = \frac{1 - x}{\rho_\ell} + \frac{x}{\rho_g}$$

$$f_H = \frac{\text{Constant}}{\left(\frac{4W}{NP_w \mu_H}\right)^n} \quad , \quad P_w = \frac{4A}{D_e}$$

$$\frac{1}{\mu_H} = \frac{1 - x}{\mu_\ell} + \frac{x}{\mu_g}$$

Then

$$\Phi_g = \frac{(dP/dL)}{(dP/dL)_g}_{TPF} = \left(\frac{\rho_g}{\rho_H}\right)\left(\frac{\mu_H}{\mu_g}\right)^n = \frac{x + (1-x)\rho_g/\rho_\ell}{\left[x + (1-x)\mu_g/\mu_\ell\right]^n}$$

For the initial calculation it was assumed that n = o. The local pressure gradient was then integrated assuming a linear variation of quality with length.

$$\Phi_{g_{o-x}} = \frac{\Delta P_{o-x}}{\Delta P_g} = \int_o^x \frac{\Phi_g \, dx}{x}$$

$$\therefore \quad \frac{\Delta P_{o-x}}{\Delta P_g} = \frac{\rho_g}{\rho_\ell} \left(\frac{1-x}{2}\right) + \frac{x}{2} \simeq x/2$$

$$\text{also} \quad \frac{\Delta P_{x-1}}{\Delta P_g} = \frac{\Phi_{o-1} - x\Phi_{o-x}}{1-x} \simeq \frac{1+x}{2}$$

The total mercury boiler pressure drop is given by the expression

$$\Delta P_{TPF} = f_{gP} \frac{L_{TPP}}{D_{eP}} \frac{W^2}{2g_o N^2 A_P^2 \rho_{ge}} \frac{X_{eP}}{2} + f_{gUP} \frac{L_{TPE-UP}}{D_{e-UP}} \frac{W^2}{2g_c N^2 A_{UP}^2} \rho_{gUP} \left(\frac{1 + X_e}{2}\right)$$

$$+ f_{gUP} \frac{L_{SH}}{D_{eUP}} \frac{W^2}{2g_o N^2 A_{uP}^2 \rho_{gUP}}$$

Let

$$\frac{\Delta P_{TPF}}{\frac{W^2}{2g_o N^2 A_{UP}^2 \rho_{ge}}} = K$$

Then

$$K = \overbrace{\left(f_{gUP} \frac{L_{UP}}{D_{eUP}} \frac{\rho_{gE}}{\rho_{gUP}}\right)\left(\frac{L_{SH}}{L_{UP}}\right)}^{K_{SH}} + \overbrace{\left(f_{gUP} \frac{L_{UP}}{D_{eUP}} \frac{\rho_{gE}}{\rho_{gUP}}\right)\left(1 - \frac{L_{SH}}{L_{UP}}\right)\left(\frac{1 + X_e}{2}\right)}^{K_{TPF-UP}}$$

$$+ \underbrace{f_{gP} \frac{L_P}{D_{eP}} + \left(\frac{A_{UP}}{A_P}\right)^2 \frac{\rho_{gE}}{\rho_{gP}} \left(\frac{X_e}{2}\right)\left(1 - \frac{L_{SCP}}{L_P}\right)}_{K_{TPF-P}}$$

Assume

1. Maximum K in Wire Coil Region

2. No Vapor Density Variation $\rho_{gP} = \rho_{gUP} = \rho_{gE}$

$$K = \left(f_{gUP} \frac{L_{UP}}{D_{eUP}}\right) + f_{gP} \frac{L_P}{D_{eP}} \left(\frac{A_{UP}}{A_P}\right)^2 \left(\frac{X_e}{2}\right) \left(1 - \frac{L_{SCP}}{L_P}\right) \quad (1)$$

Where

$$f_{gUP} \simeq 2.6\ f_{gE}$$

$$f_{gP} = 1.06\ f_{ge}$$

Expressions were now required for the plug exit quality and subcooled length. Approximate expression can be obtained by assuming constant overall heat transfer coefficients in the subcooled and two-phase regions of the plug, i.e.,

$$X_{eP} = \left[\frac{W_{NaK}}{W_{Hg}} \quad \frac{C_{NaK}\,\Delta T_{PP}}{h_{fg}}\right] \left\{ \exp\left[\frac{\pi D N L_P U_{TPF-P}}{(WC)_{NaK}} - \frac{\left(\ln \frac{\Delta T_E}{\Delta T_{PP}}\right) \frac{U_{TPF-P}}{U_{SCP}}}{\frac{(WC)_{NaK}}{(WC)_{Hg}} - 1} \right] - 1 \right\} \quad (2)$$

$$\frac{L_{SCP}}{L_P} = \left[\ell n(\Delta T_E/\Delta T_{PP})\right] \Big/ \left[\frac{(WC)_{NaK}}{(WC)_{Hg}} - 1\right] \left[\frac{\pi D N\, U_{SCP} L_P}{(WC)_{NaK}}\right] \quad (3)$$

The dimensionless groups (excluding geometry faction) are as follows:

$$\pi_1 = K = \frac{\Delta P_{TPF}}{\frac{W^2}{2 g_o N^2 A_{UP}^2 \rho_{gE}}} \qquad \pi_5 = \frac{U_{TPF-P}}{U_{SCP}} \rightarrow 1$$

$$\pi_2 = \left(\frac{W_{NaK}}{W_{Hg}} \quad \frac{C_{NaK}\,\Delta T_{PP}}{h_{fg}}\right) \qquad \pi_6 = \frac{(WC)_{NaK}}{(WC)_{Hg}} \rightarrow \text{Constant}$$

$$\pi_3 = \frac{\pi D N L_P U_{TPF-P}}{(WC)_{NaK}} \qquad \pi_7 = \Delta T_{E}/\Delta T_{PP} \text{ (For } \Delta T_{PP} > 10^{\circ} \text{ Solution is not sensitive to } \pi_7)$$

$$\pi_4 = \frac{\rho_{gE}}{\rho_{gP}} \rightarrow 1 \qquad \pi_8 = f_{gP},\ f_{gUP} \rightarrow \text{Constant}$$

The correlation considers π_1, π_2, and π_3 and yields an approximate relationship between these groups. Improved correlations would consider:

1. A more realistic pressure drop model
2. The effective heat transfer area in plug (i.e., the effect of swaging, etc.)
3. Variation of heat transfer coefficient in plug
4. Vapor density variations
5. Effect of π_7 for small ΔT_{pp}
6. Variation of K in wire cool region
7. The effect of coiling the tubes on the pressure drop in the wire coil region.

Equations 1, 2, and 3 were used to construct Figure 108. This figure shows the approximate relationship between π π_2 and π_3. Note that any increase in the heat transfer coefficient in the plug region (U_{TPP}) shifts the resulting curve upward (i.e., to a higher ΔP_{TPF} for the same ΔT_{pp}) due to the higher plug exit quality.

Figure 109 shows the resulting correlation for some of the data taken on the SN-1 boiler at General Electric.

Point No. 1 was taken on 2-3-68 after 21 hours of boiler operation at General Electric. Point No. 2 was taken on 2-5-68 after 65 hours of loop operation, and point No. 3 was taken on 2-7-68 after 121 hours of loop operation. The remaining points designated by triangles were all taken between 2-8-68 and 2-13-68 (150 to 357 hours) and show no trend with time. It may be concluded, therefore, that during the first 150 hours of loop operation the thermal performance of the boiler increased somewhat and then remained essentially constant until the first shutdown.

During the first shutdown several modifications to the boiler were carried out. As a result of these modifications the boiler performance shifted, as may be seen by comparing the circles (after the 1st shutdown) and the triangles (before the first shutdown) in Figure 109. This marked increase in boiler thermal performance was accompanied by a corresponding increase in boiler ΔP and was probably due to the removal of the thick deposits from the shell side of the boiler tubes.

The early history of the SN-1 boiler during operation at NASA-Lewis is shown in Figure 110. Note that the early NASA runs (CADDE RUNS 161-423) agree with the General Electric data taken after the first 150 hours of operation. CADDE RUNS 383, 410, and 423 show a shift to the right and downward indicating a decrease in thermal performance just prior to the A-4 shutdown. Subsequent to the A-4 shutdown the boiler was apparently somewhat "deconditioned". The performance agrees with the early results obtained at General Electric.

In view of the results shown in Figures 109 and 110 it may be concluded that the crud deposition on the boiler shell side occurred early in the life of the SN-1 boiler at NASA-Lewis. Additional contamination on the tube side occurred about the time of the A-4 shutdown. Operation of the boiler at General Electric for about 150 hours removed the tube side contamination. Subsequent mechanical removal of the shell side deposits further increased the thermal performance of the boiler at the cost of a higher boiler ΔP.

The entire plot of weekly points is shown in Figure 111 which indicates performance remained about constant during the course of the endurance test.

V. NOMENCLATURE

A	Tube cross sectional flow area, ft^2
C	constant pressure specific heat, Btu/lb ^oF
D_e	equivalent diameter
f	fluid friction factor, dimensionless
g_c	gravitational constant, ft/sec^2
h_{fg}	latent heat of vaporization, Btu/lb
K	discharge coefficient, dimensionless
L	length, ft
N	number of tubes
n	friction factor (0 for rough tubes, 0.2 for smooth tubes)
P	pressure, lb/ft^2
P_w	wetted perimeter, ft
T	temperature, ^oF
U	overall heat transfer coefficient, $Btu/hr\text{-}ft^2\text{-}^oF$
W	flow rate, lb/sec
X	vapor quality, %
μ	fluid viscosity, lb/sec-ft
ρ	fluid density, lb/ft^3
Φ	two-phase pressure drop multiplier, dimensionless

Subscripts:

E	boiler tube exit
e	plug exit
g	gas vapor
H	homogeneous mixture
Hg	mercury
l	liquid
NaK	sodium-potassium

P	plug region
PP	pinch point (NaK-Hg temperature at Hg liquid vapor interface)
SCP	subcooled plug region
SH	superheated vapor region
TPF	two phase flow
UP	unplugged tube region
X	vapor quality
0	zero quality, overall

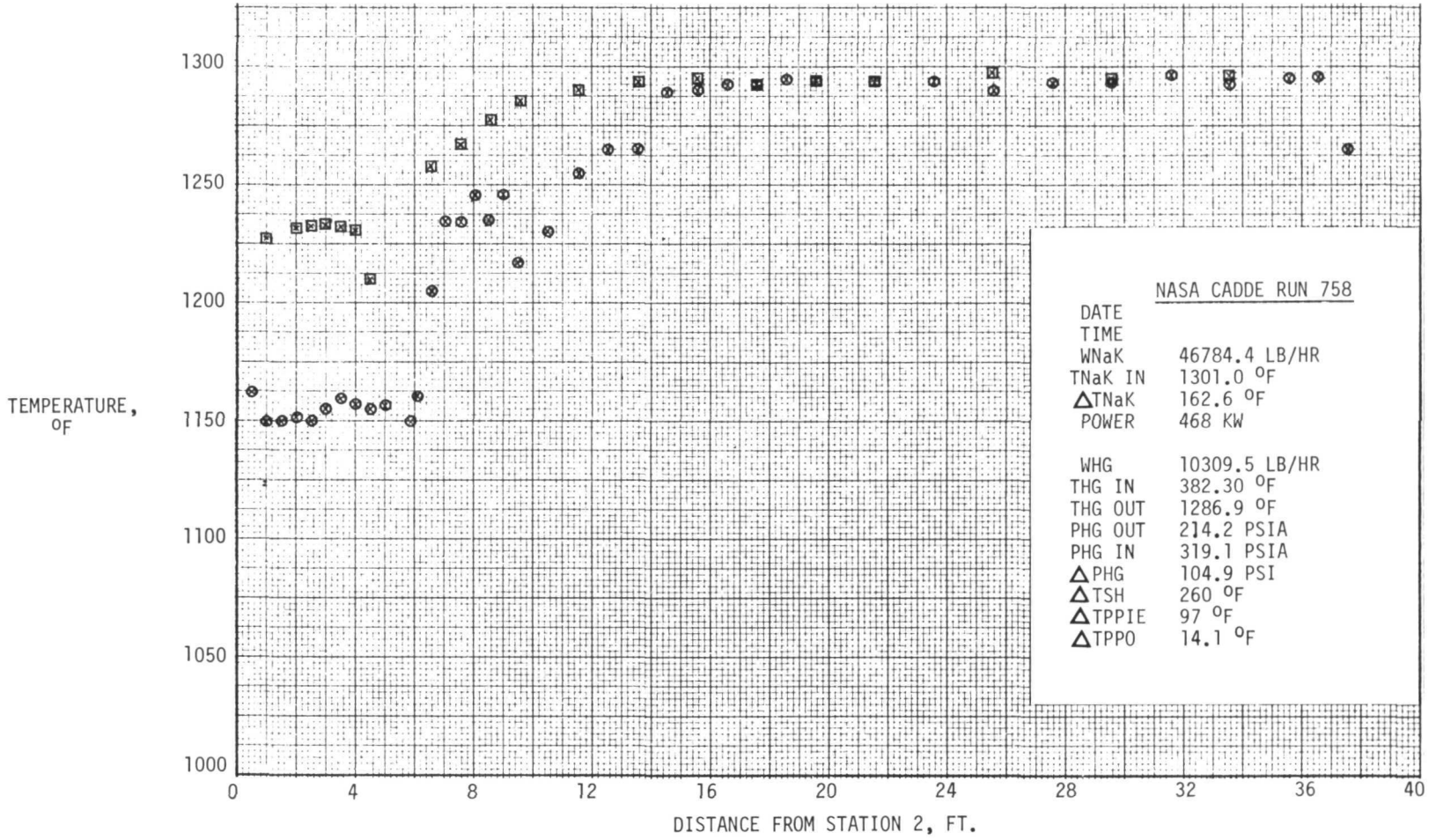

Figure 58. SNAP-8 refractory boiler temperature profile.

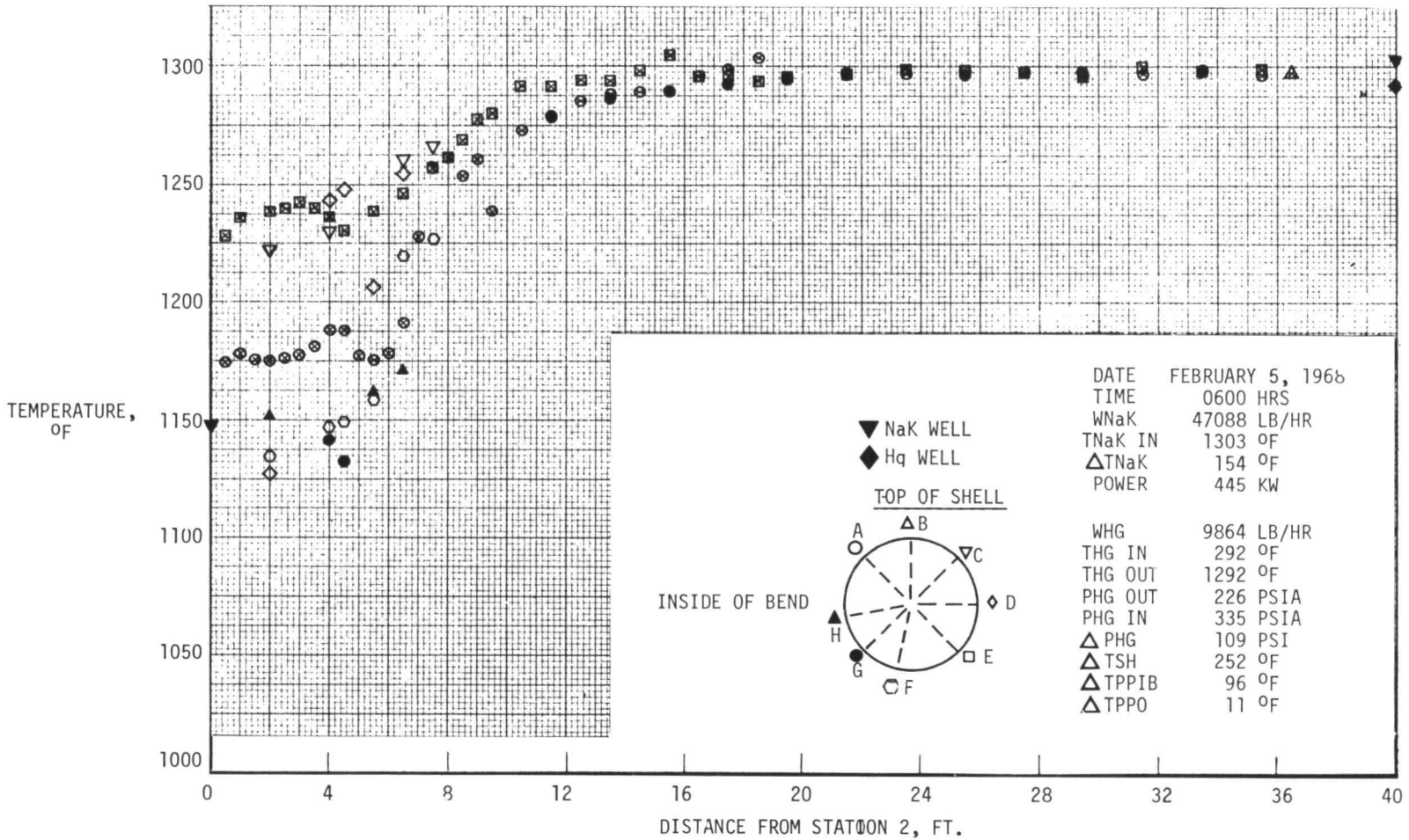

Figure 59. SNAP-8 refractory boiler temperature profile.

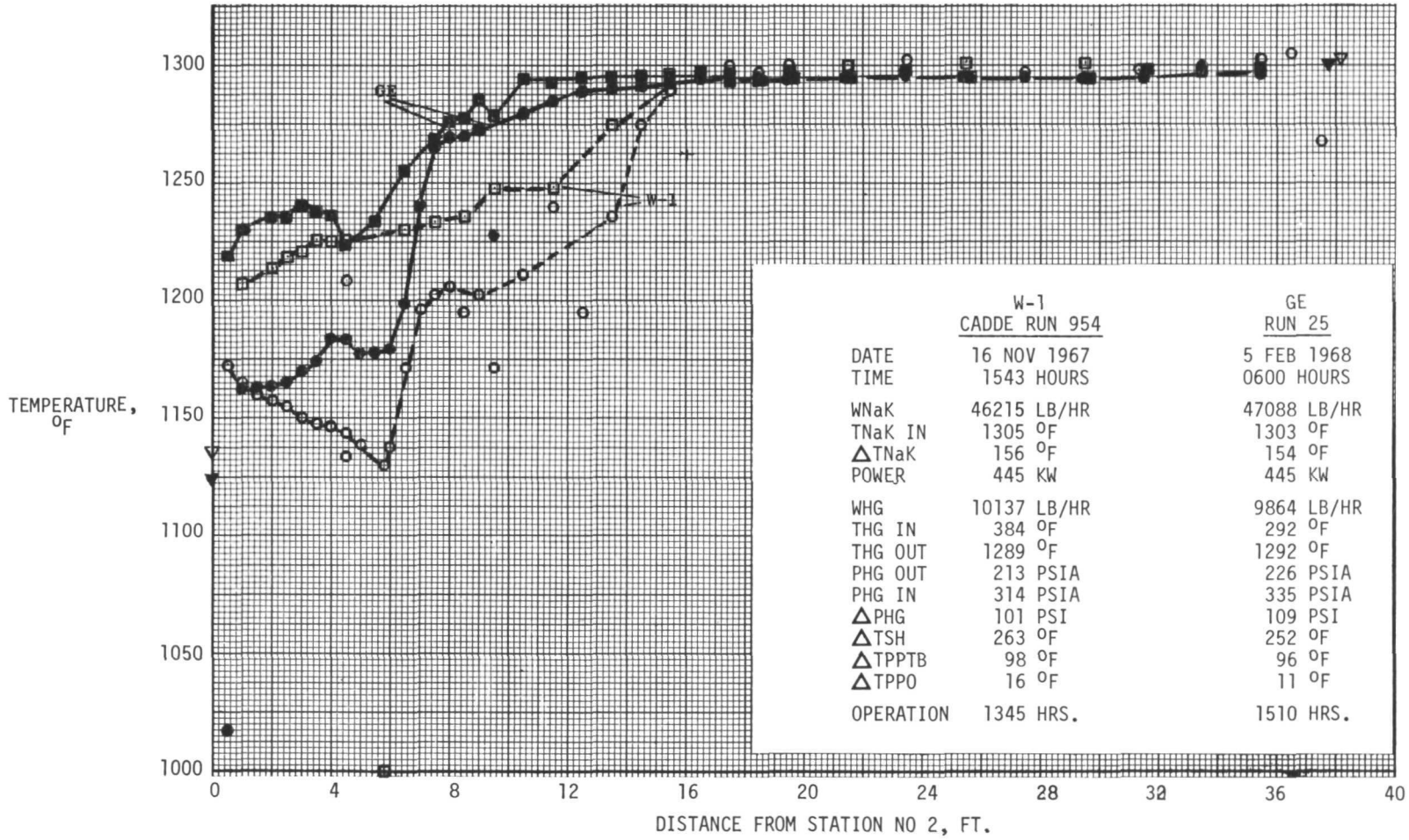

Figure 60. SNAP-8 refractory boiler temperature profile.

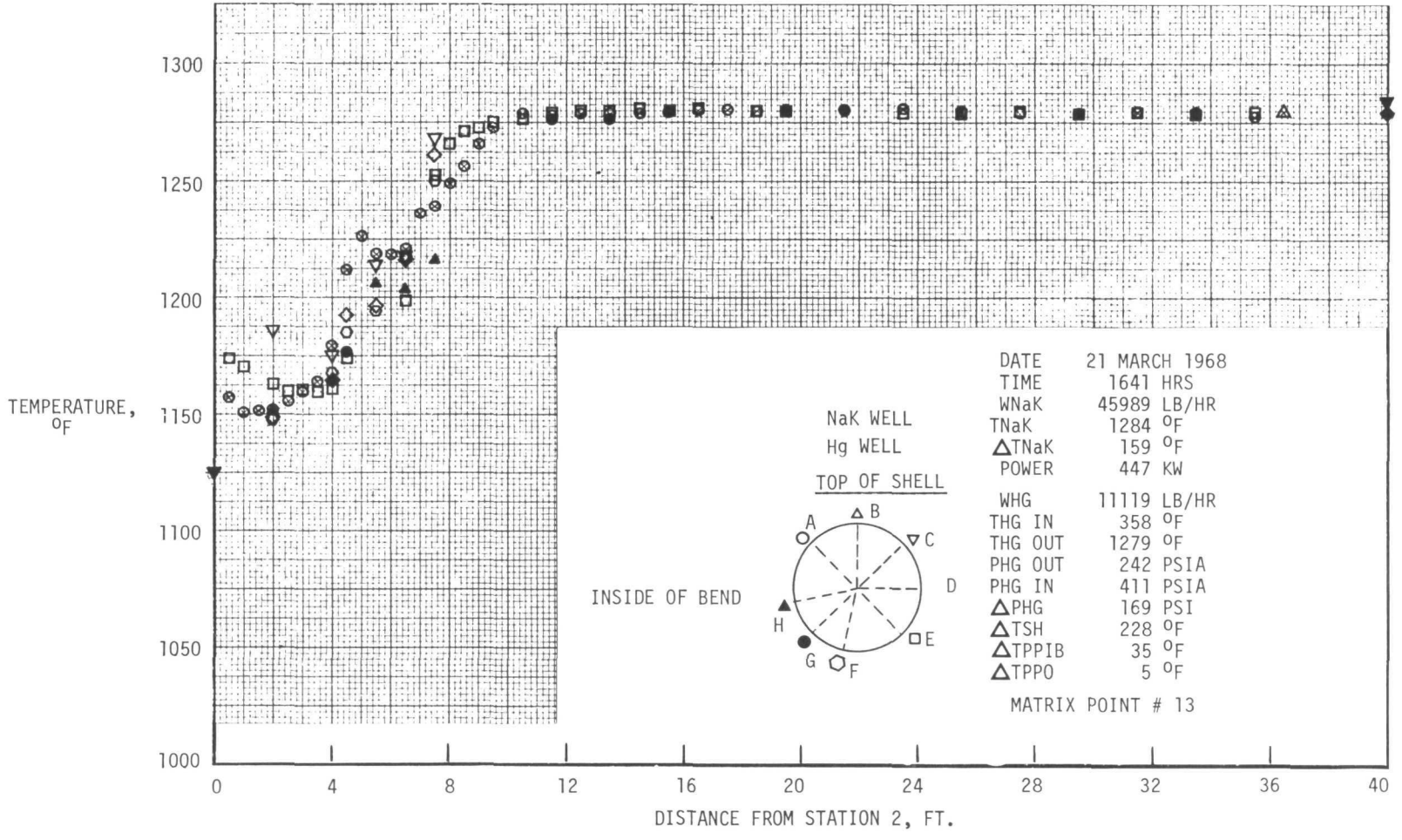

Figure 61. SNAP-8 refractory boiler temperature profile.

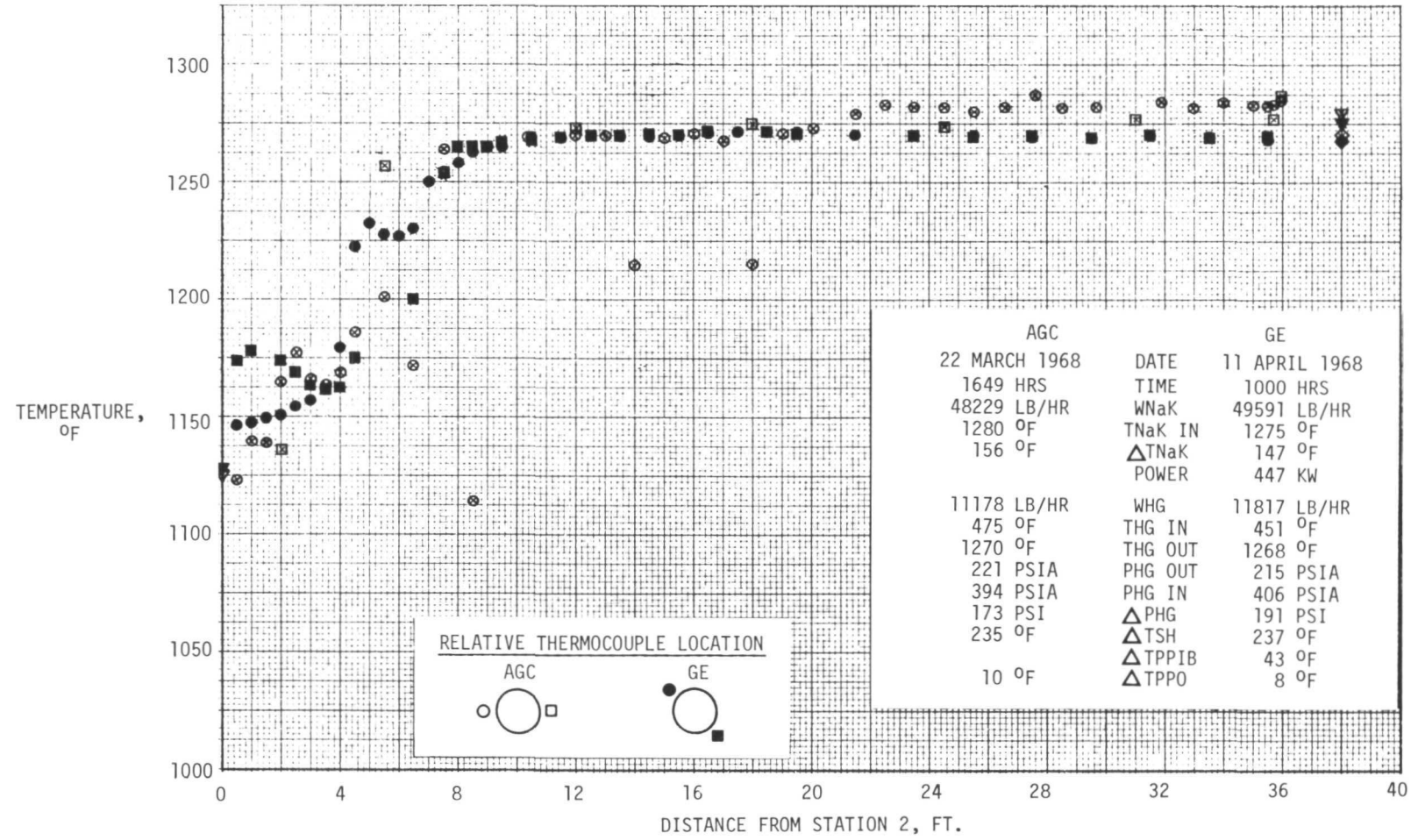

Figure 62. SNAP-8 refractory boiler temperature profile.

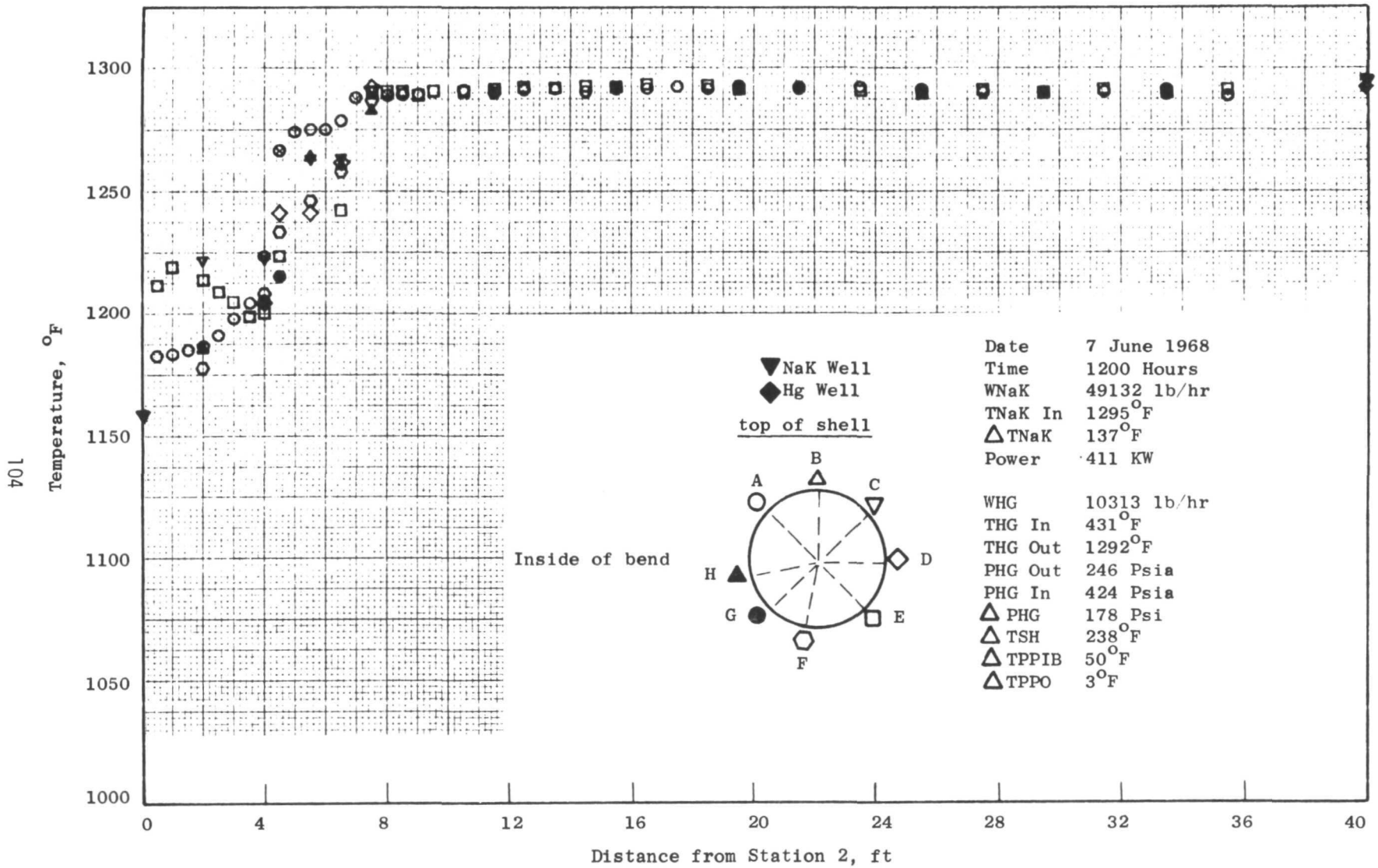

Figure 63. SNAP-8 refractory boiler temperature profile.

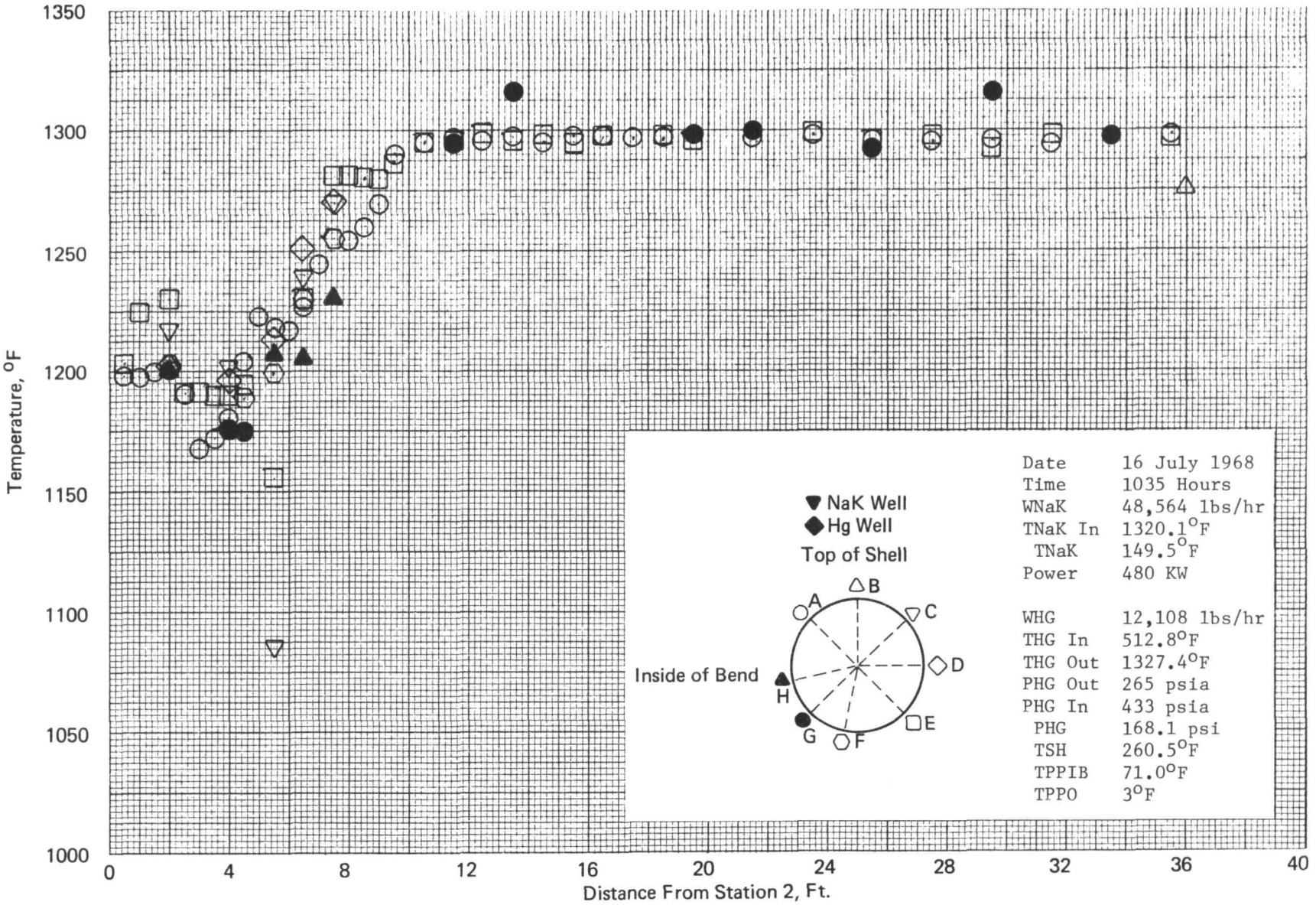

Figure 64. SNAP-8 refractory boiler temperature profile.

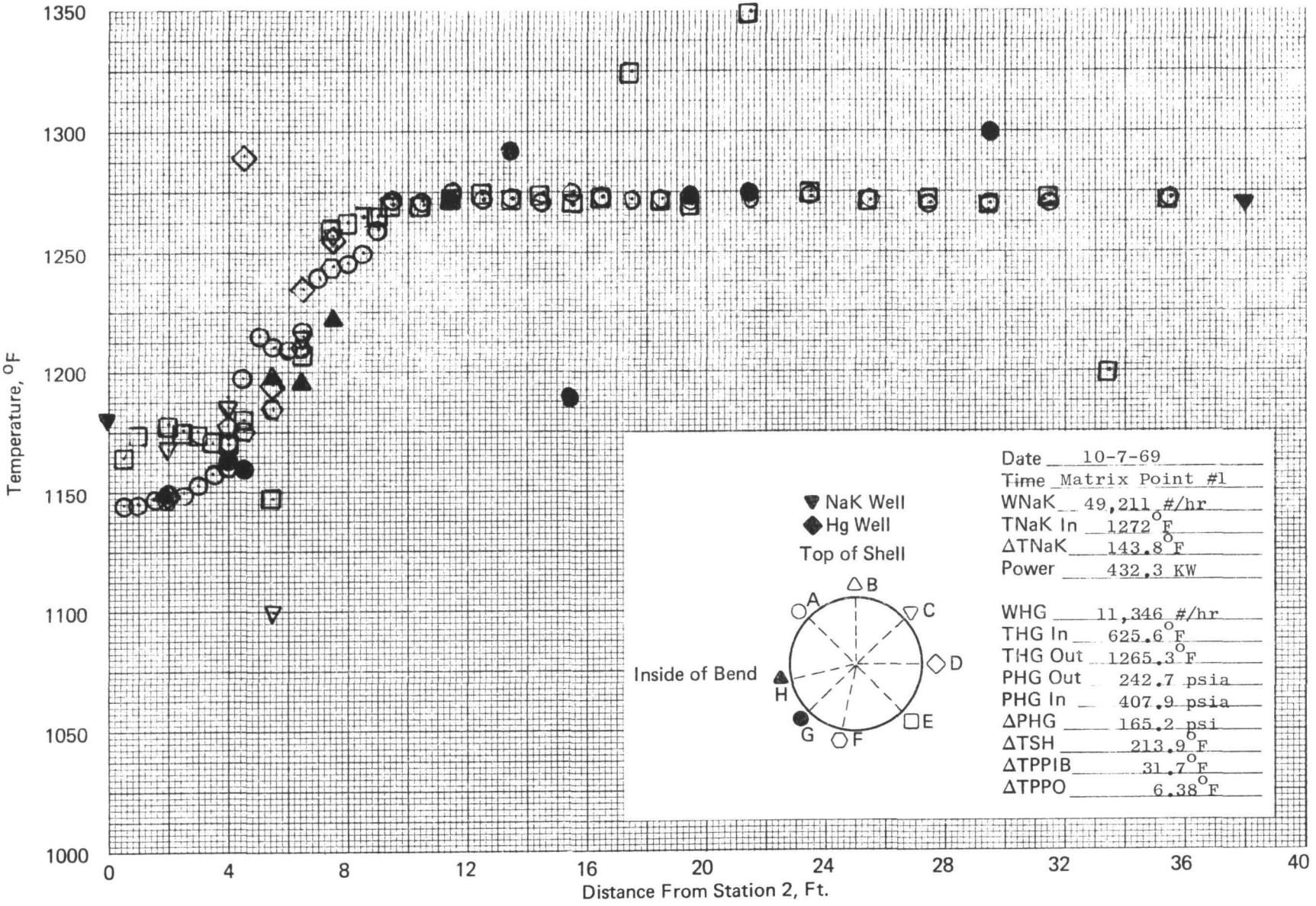

Figure 65. SNAP-8 refractory boiler temperature profile.

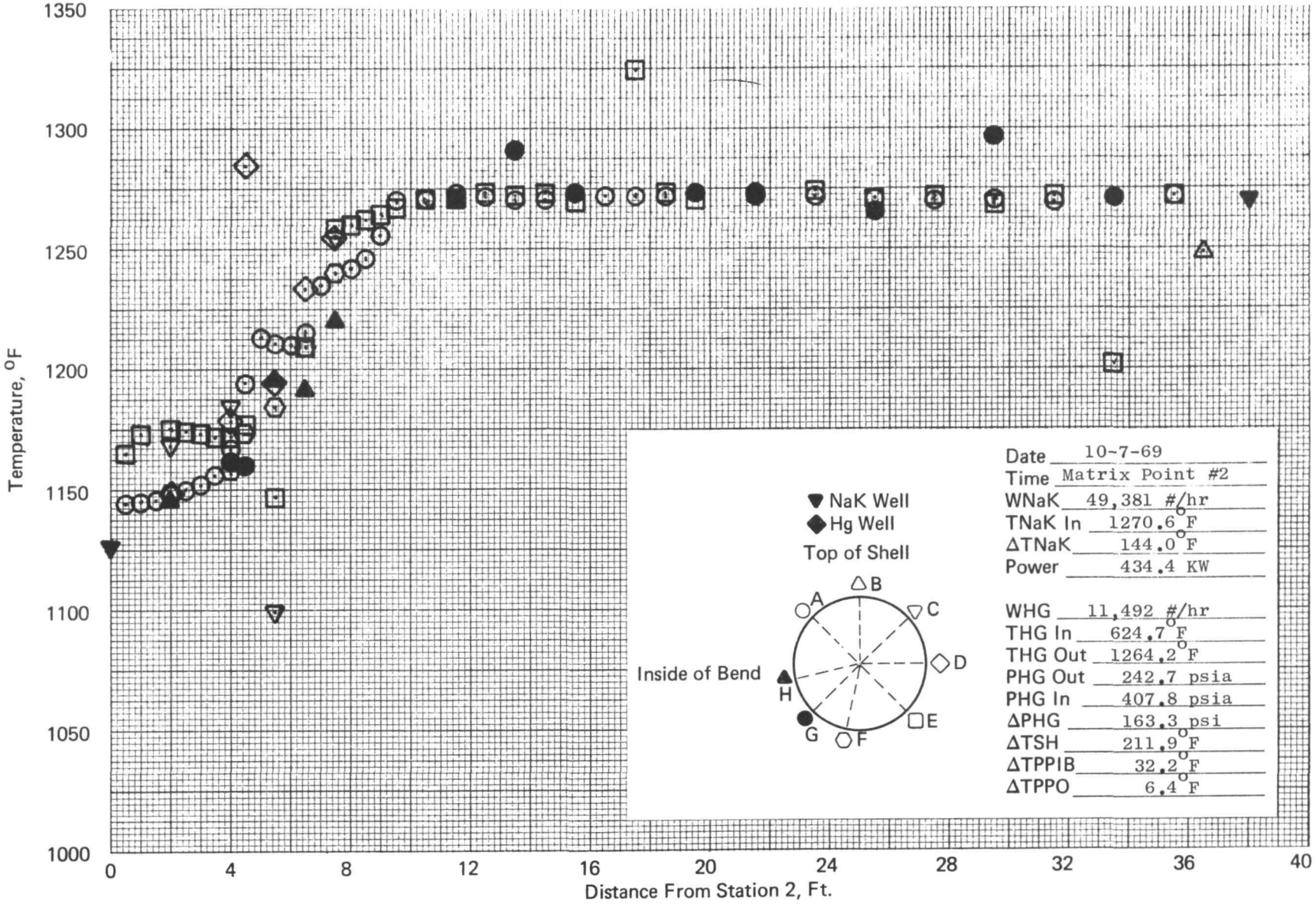

Figure 66. SNAP-8 refractory boiler temperature profile.

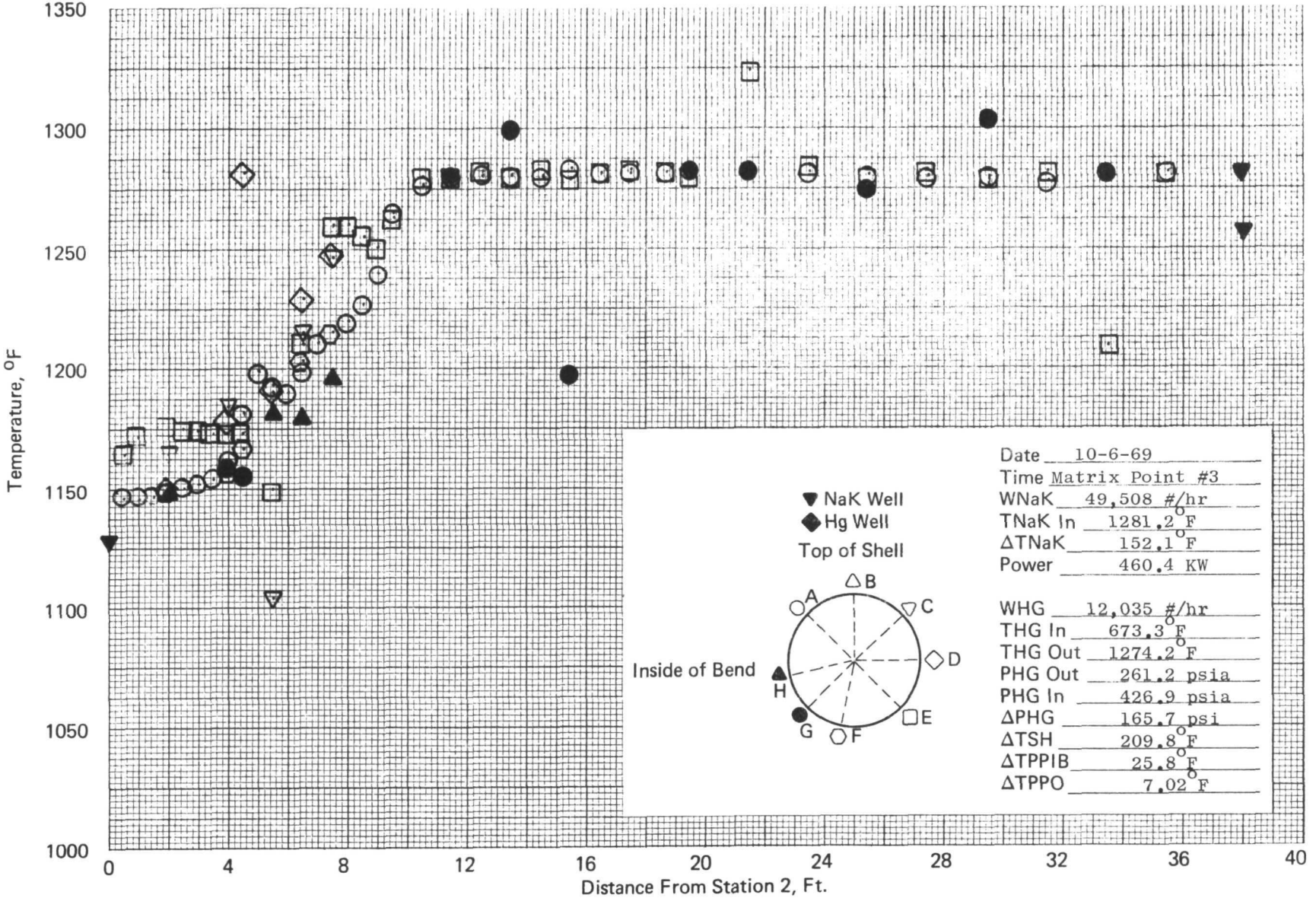

Figure 67. SNAP-8 refractory boiler temperature profile.

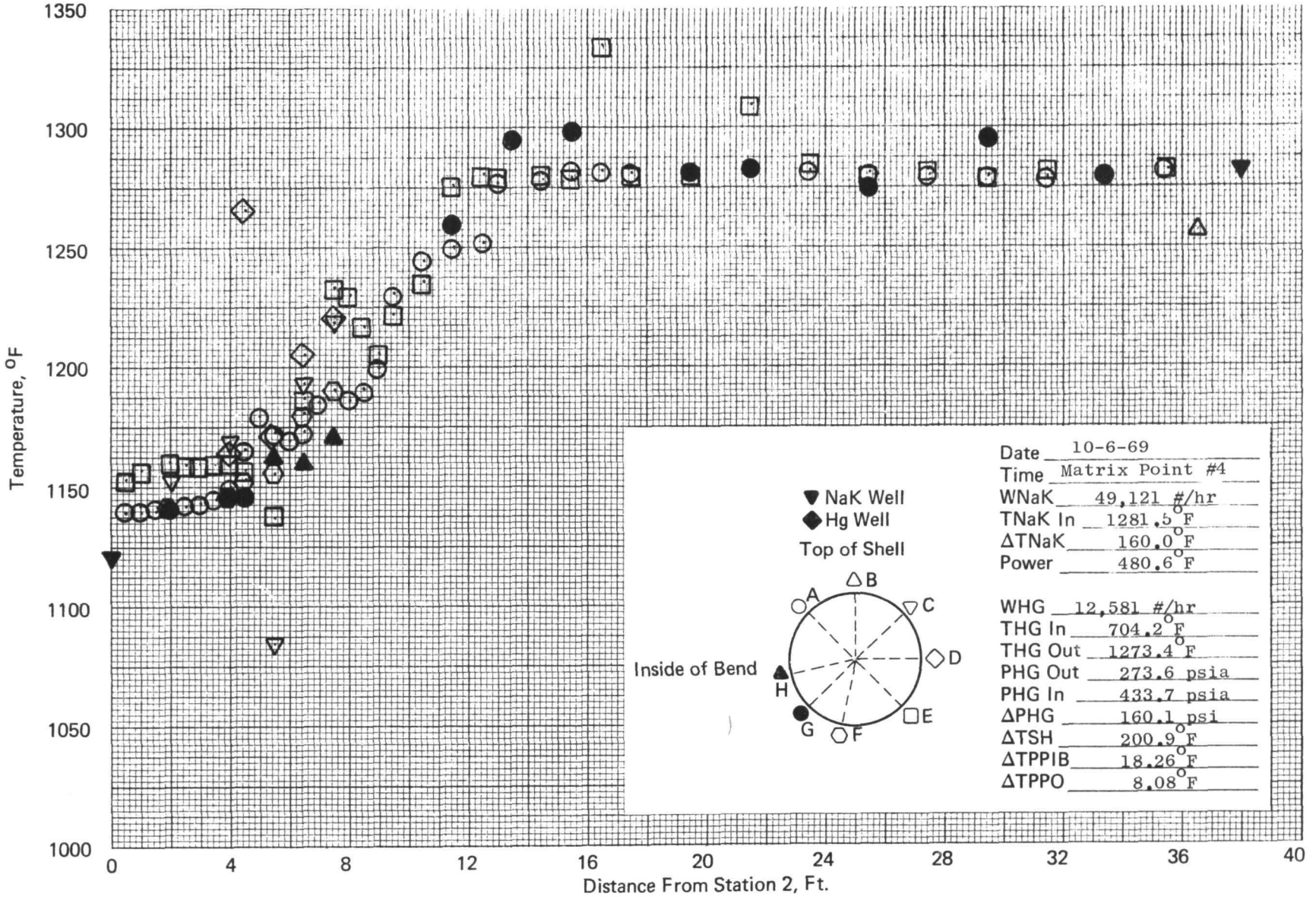

Figure 68. SNAP-8 refractory boiler temperature profile.

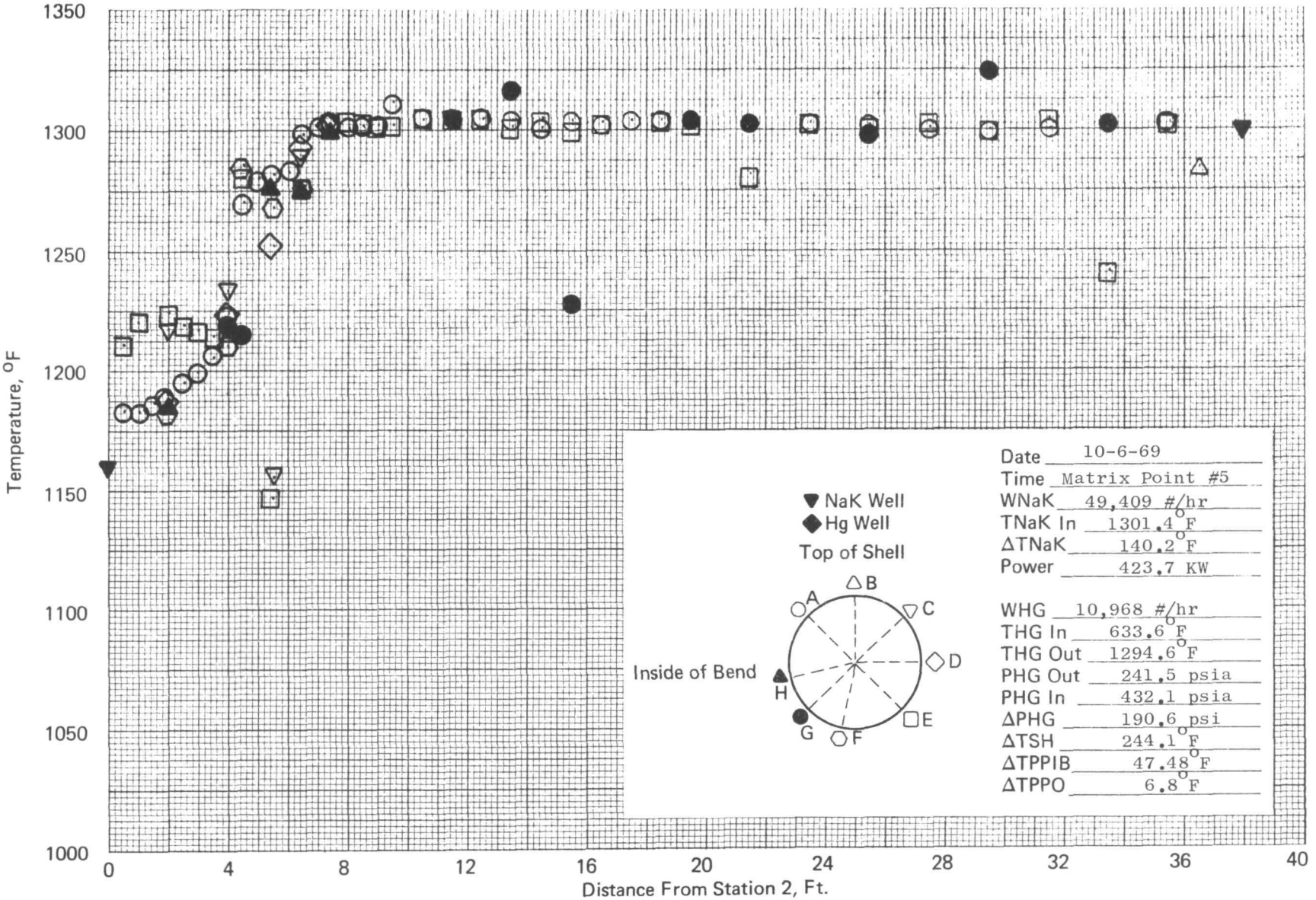

Figure 69. SNAP-8 refractory boiler temperature profile.

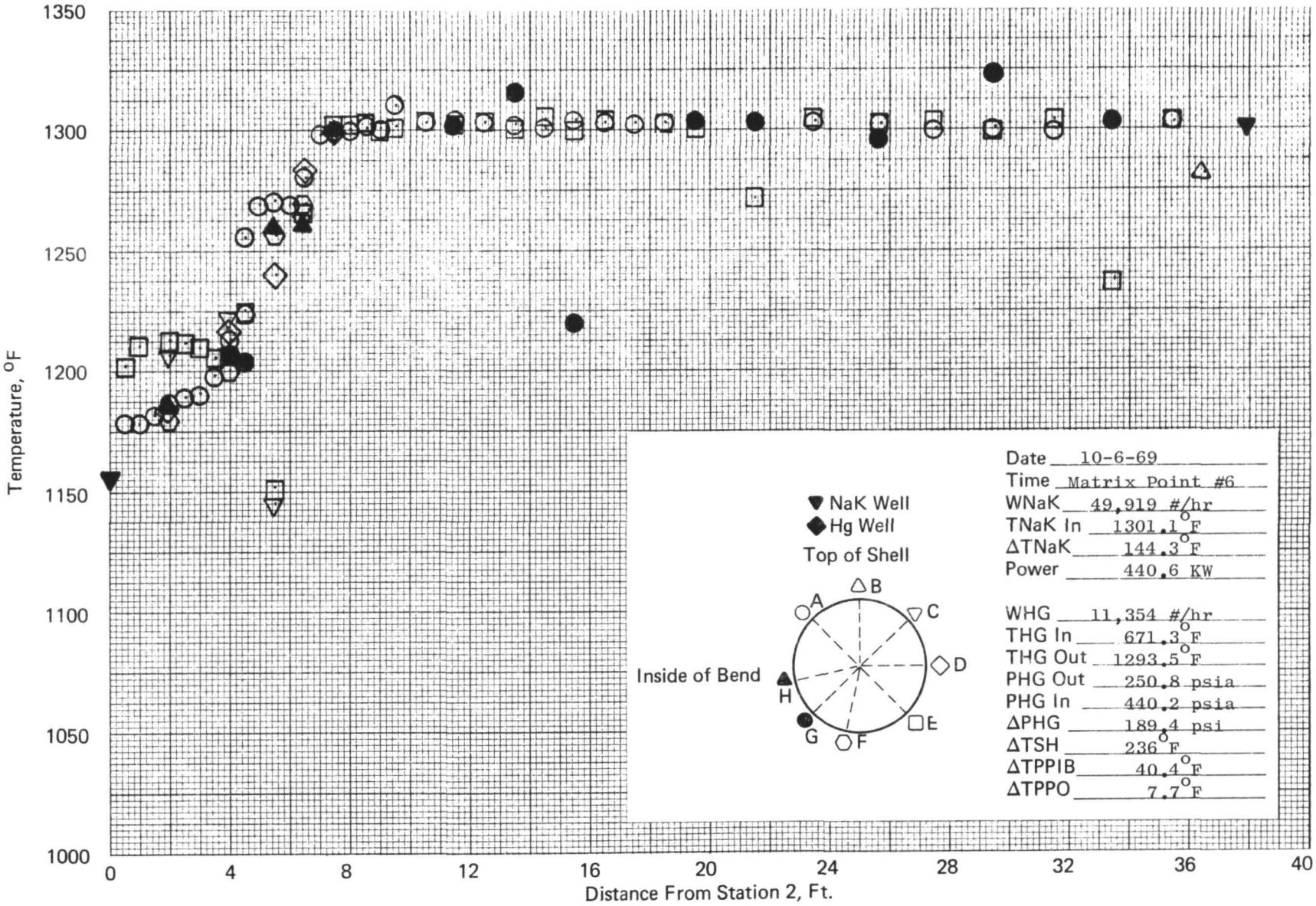

Figure 70. SNAP-8 refractory boiler temperature profile.

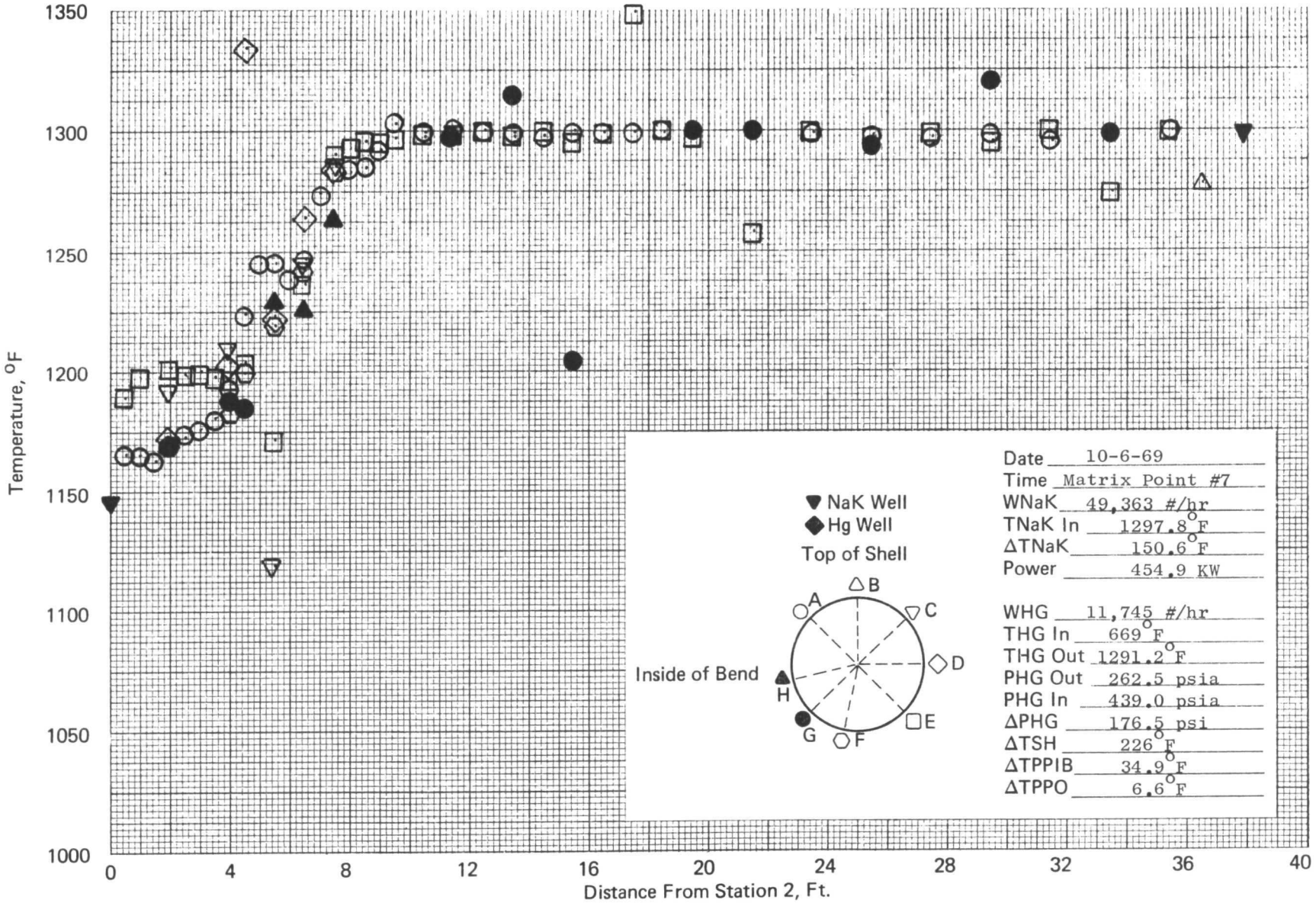

Figure 71. SNAP-8 refractory boiler temperature profile.

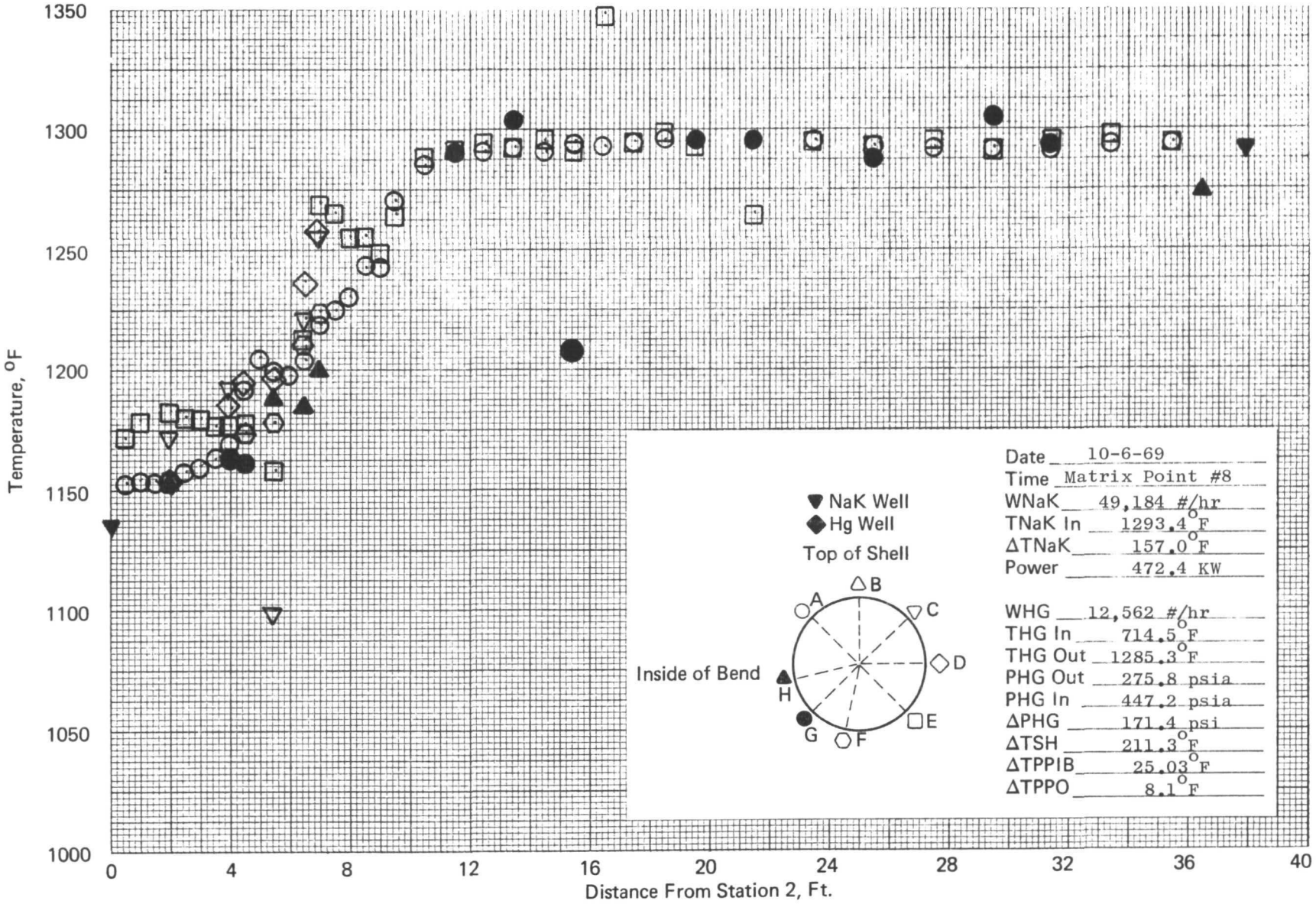

Figure 72. SNAP-8 refractory boiler temperature profile.

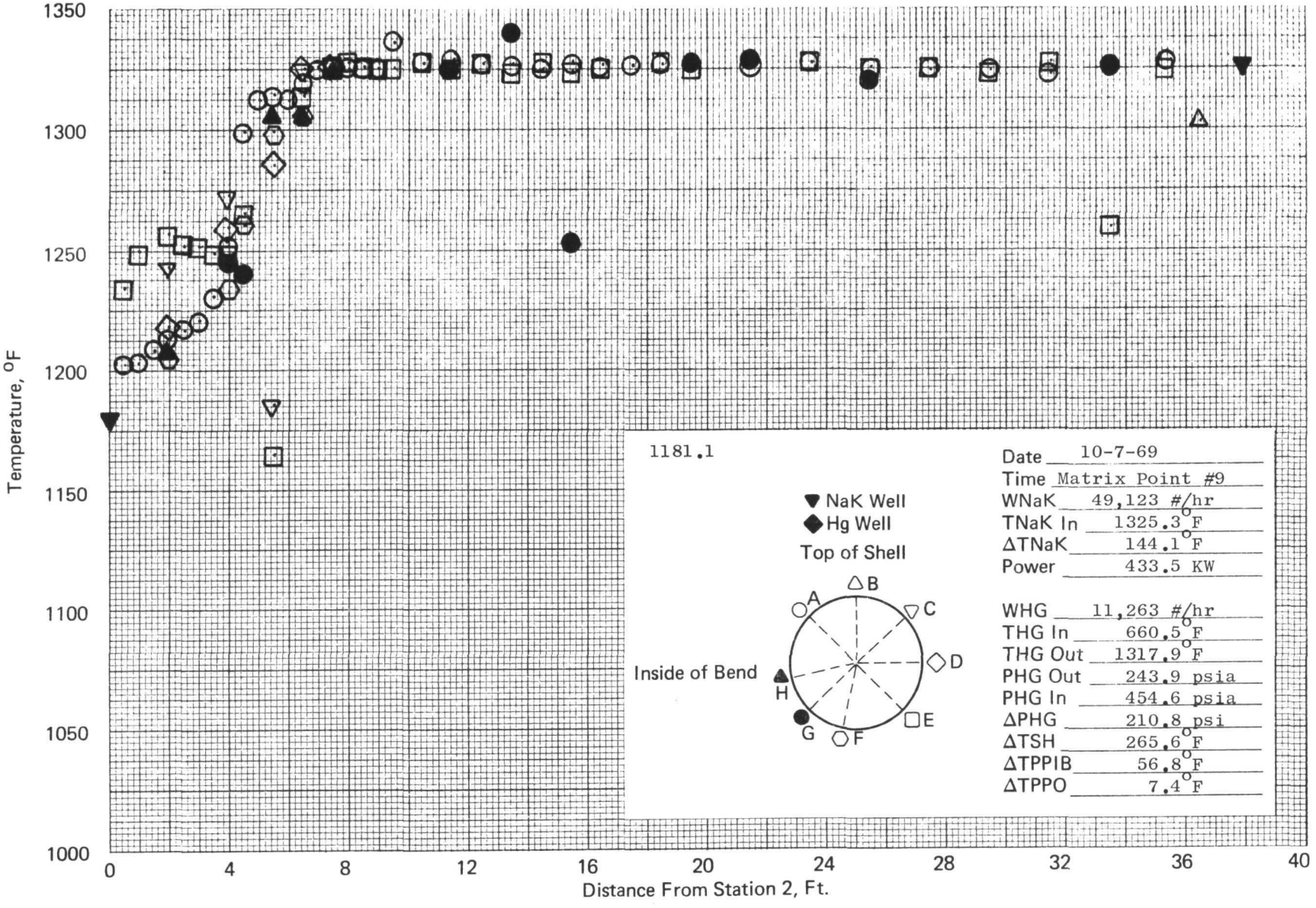

Figure 73. SNAP-8 refractory boiler temperature profile.

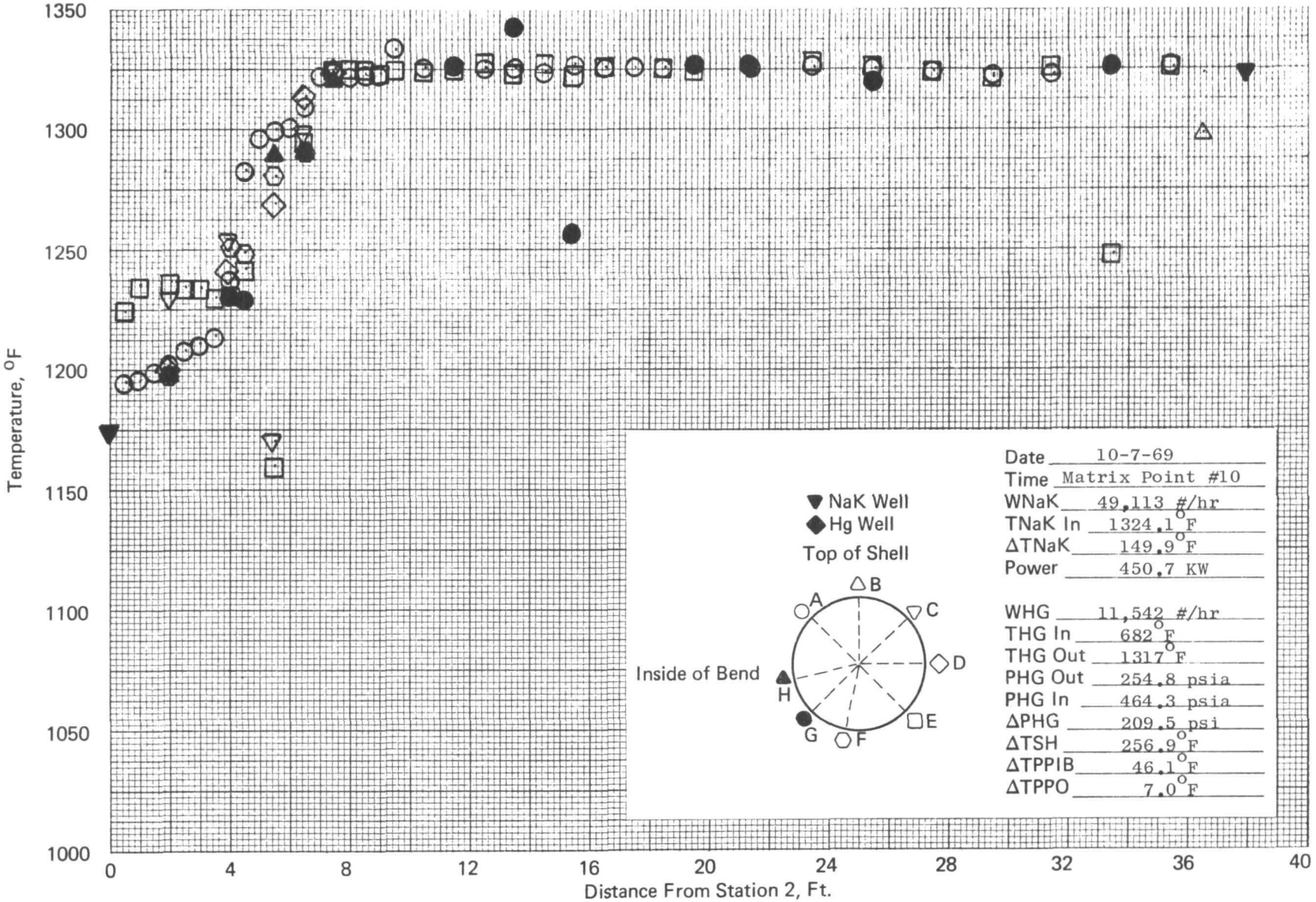

Figure 74. SNAP-8 refractory boiler temperature profile.

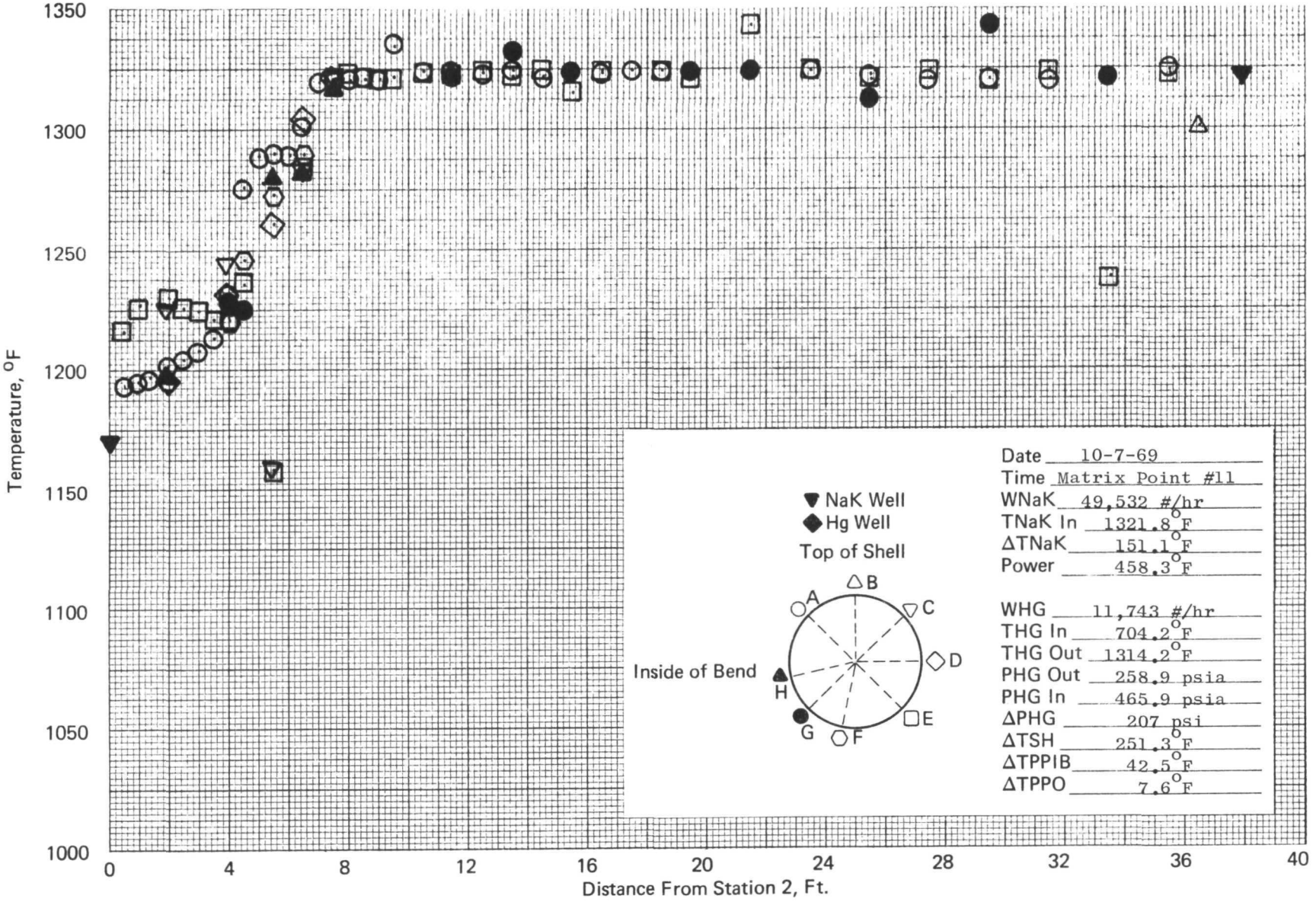

Figure 75. SNAP-8 refractory boiler temperature profile.

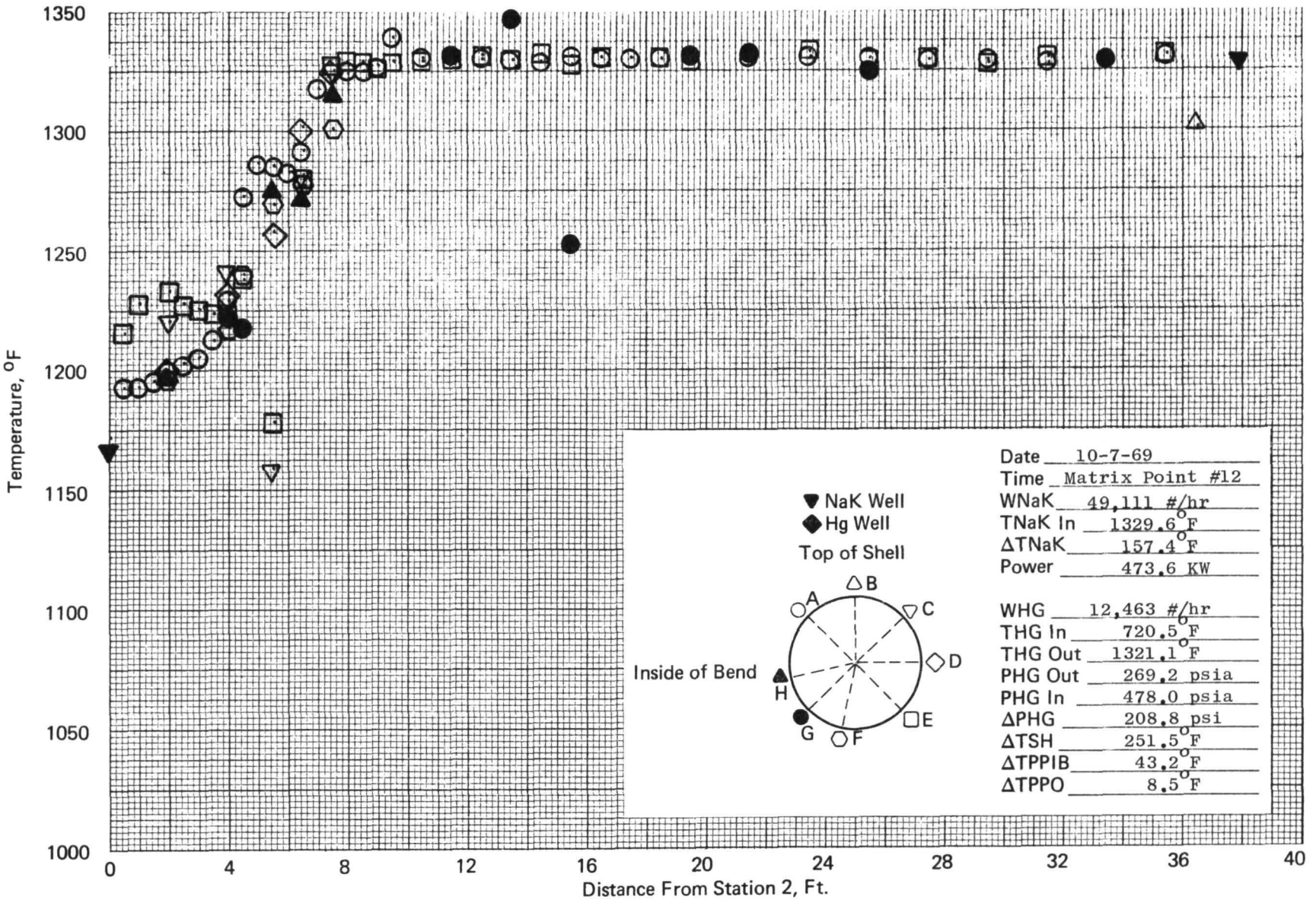

Figure 76. SNAP-8 refractory boiler temperature profile.

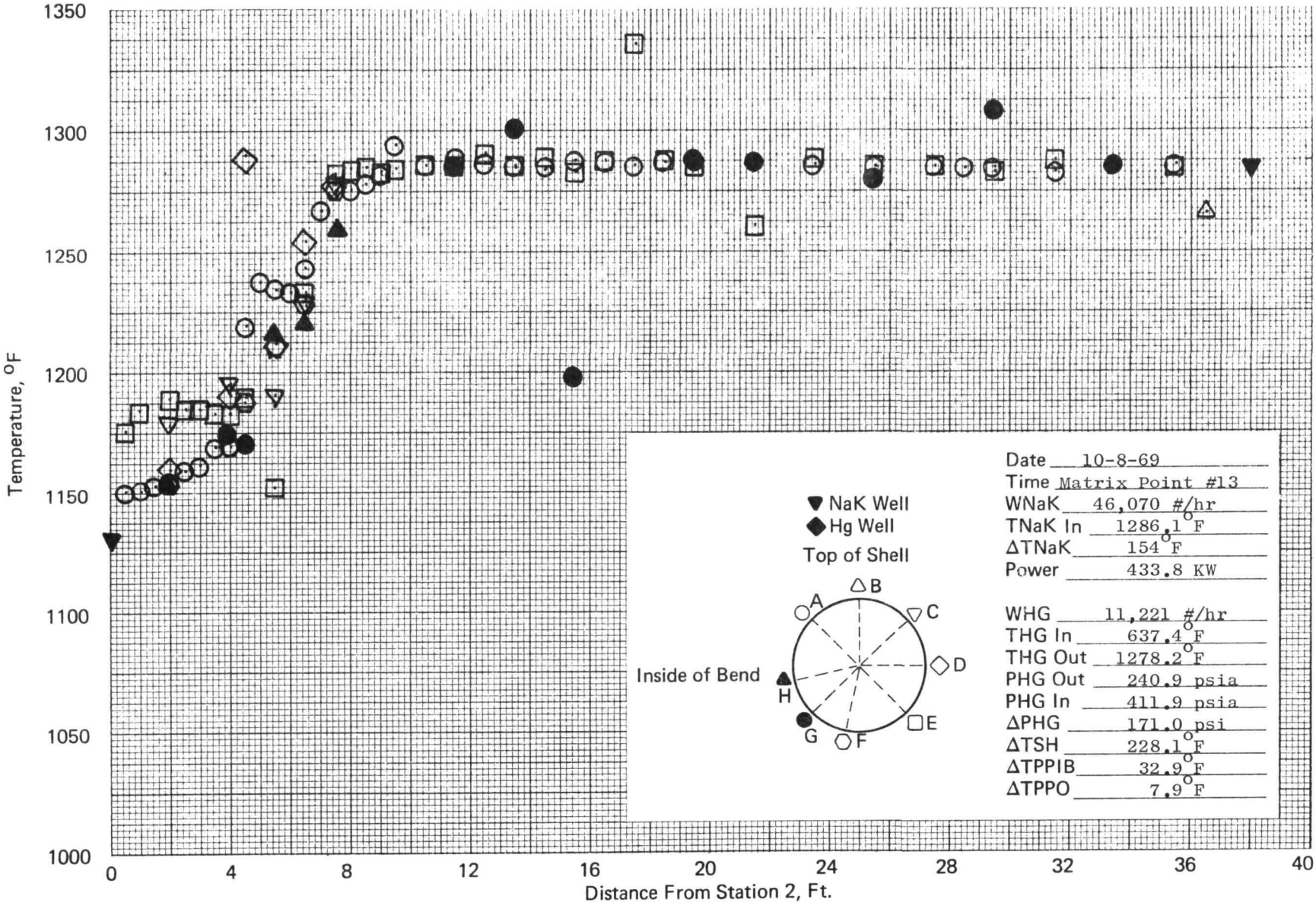

Figure 77. SNAP-8 refractory boiler temperature profile.

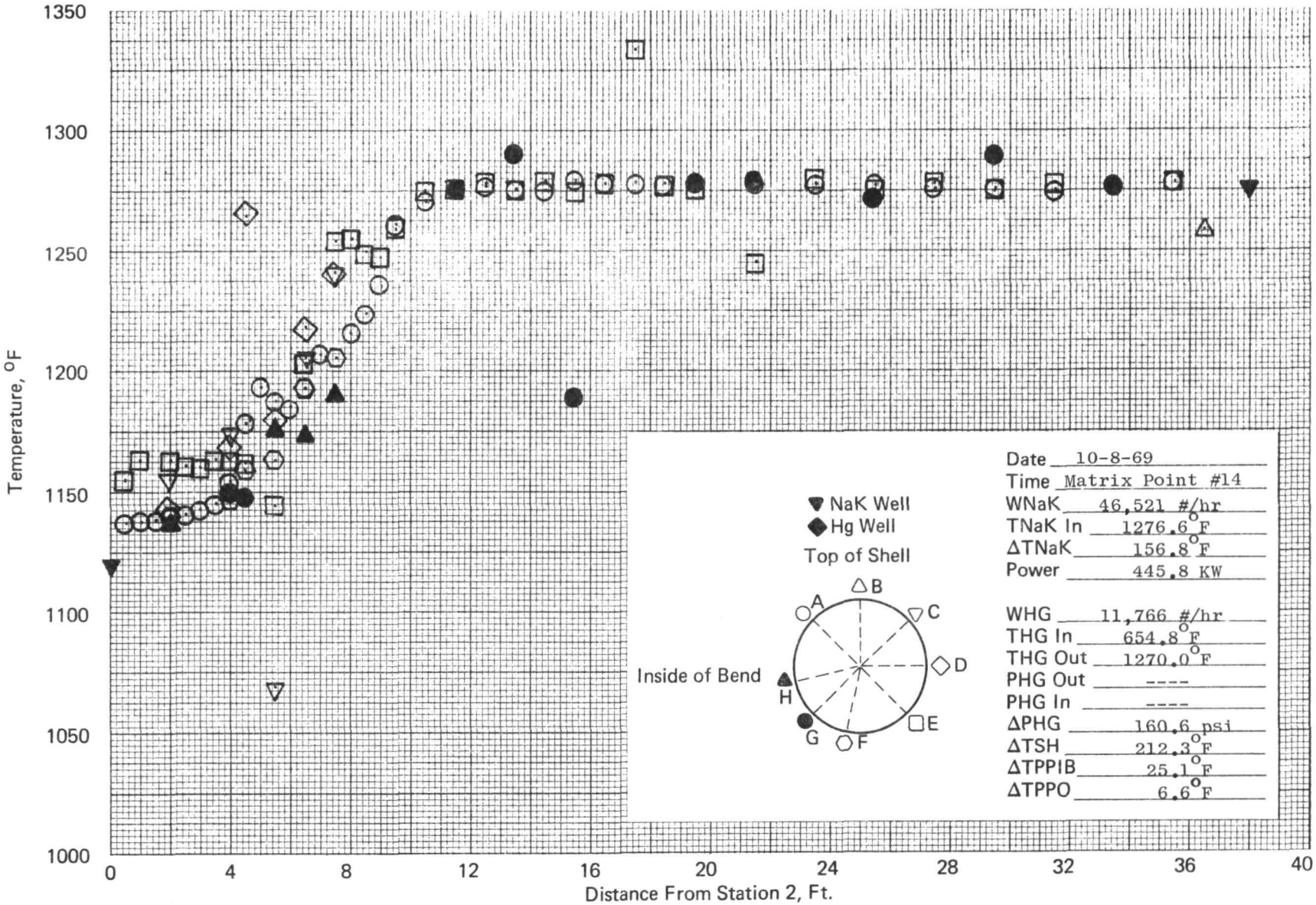

Figure 78. SNAP-8 refractory boiler temperature profile.

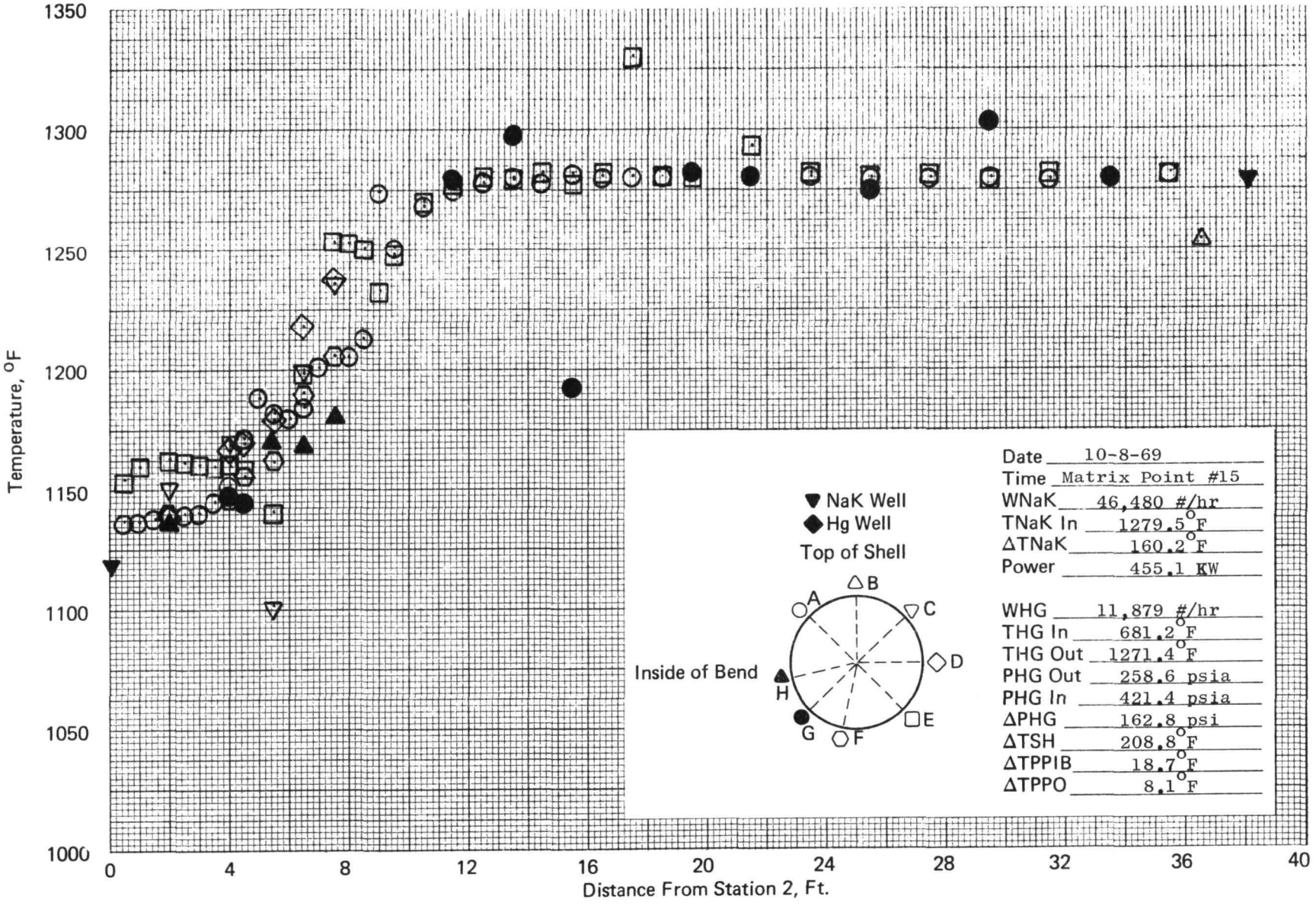

Figure 79. SNAP-8 refractory boiler temperature profile.

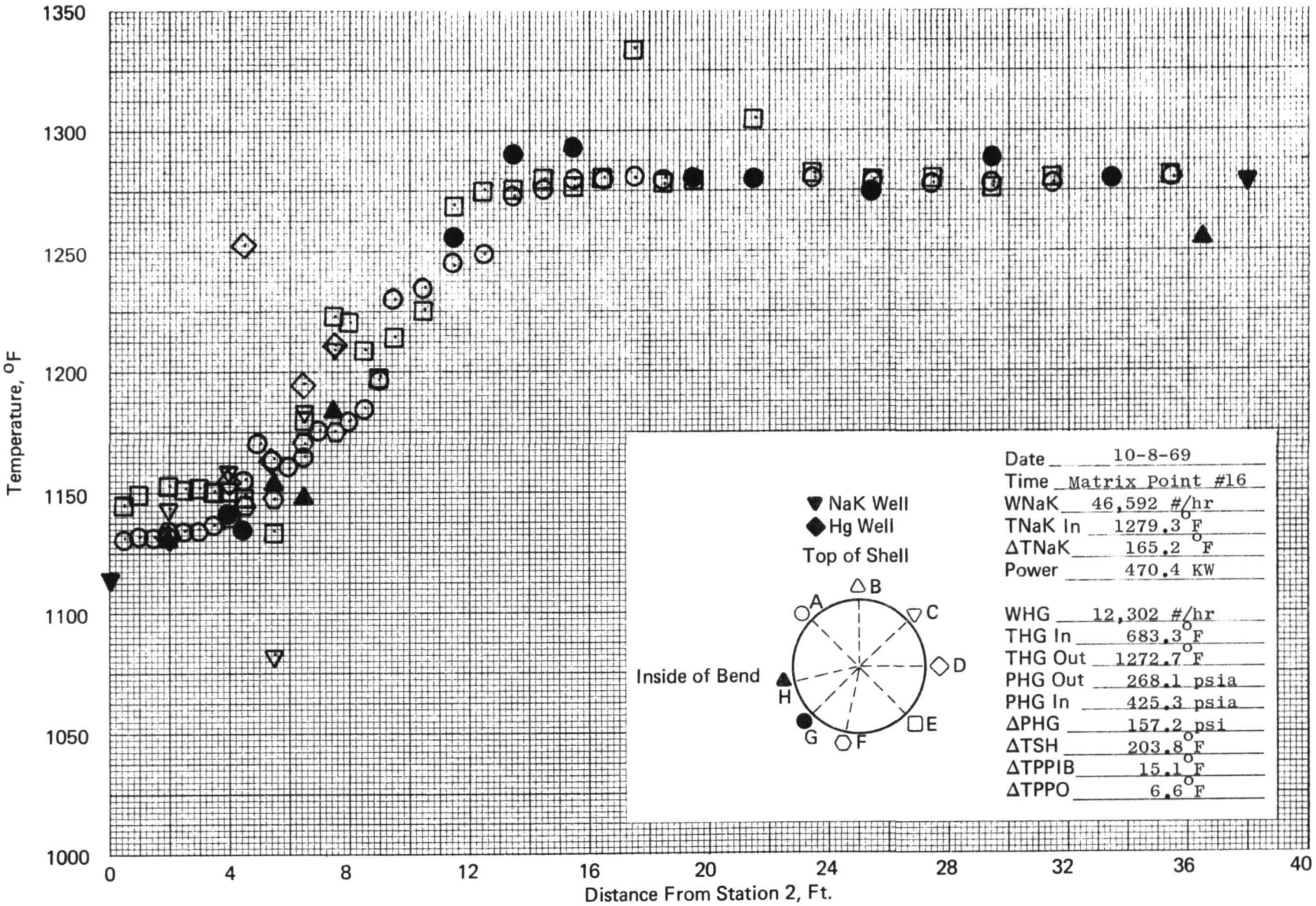

Figure 80. SNAP-8 refractory boiler temperature profile.

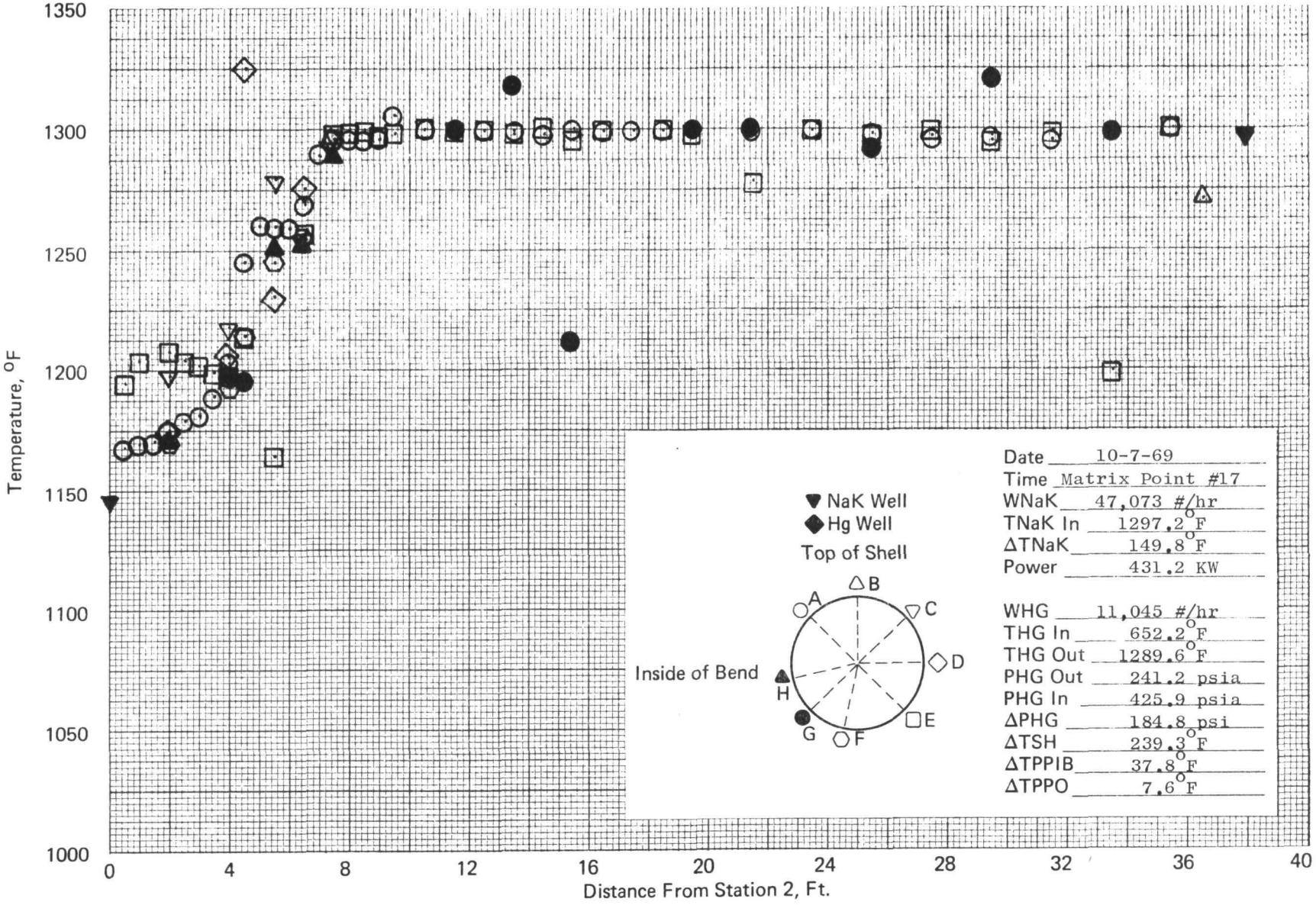

Figure 81. SNAP-8 refractory boiler temperature profile.

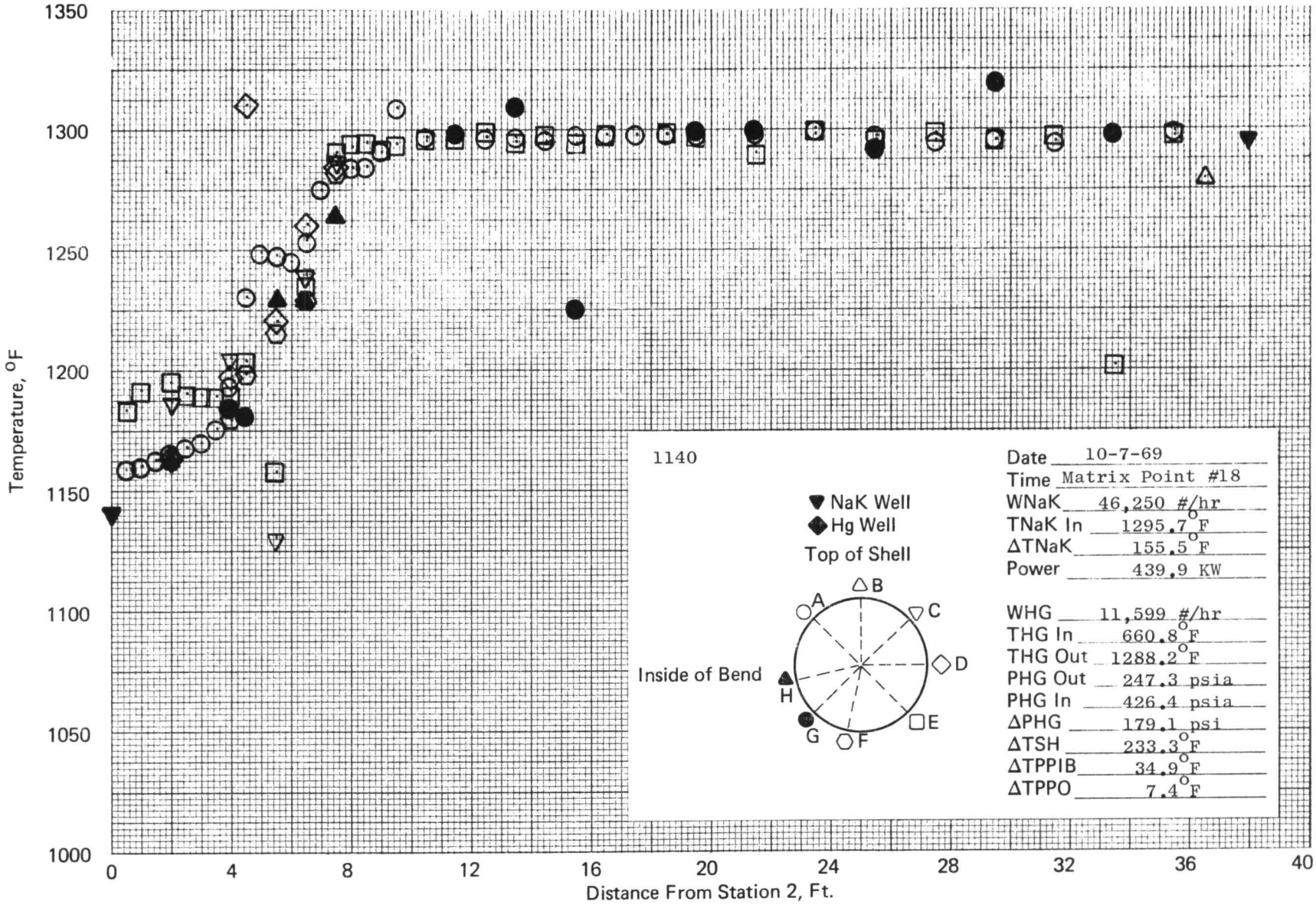

Figure 82. SNAP-8 refractory boiler temperature profile.

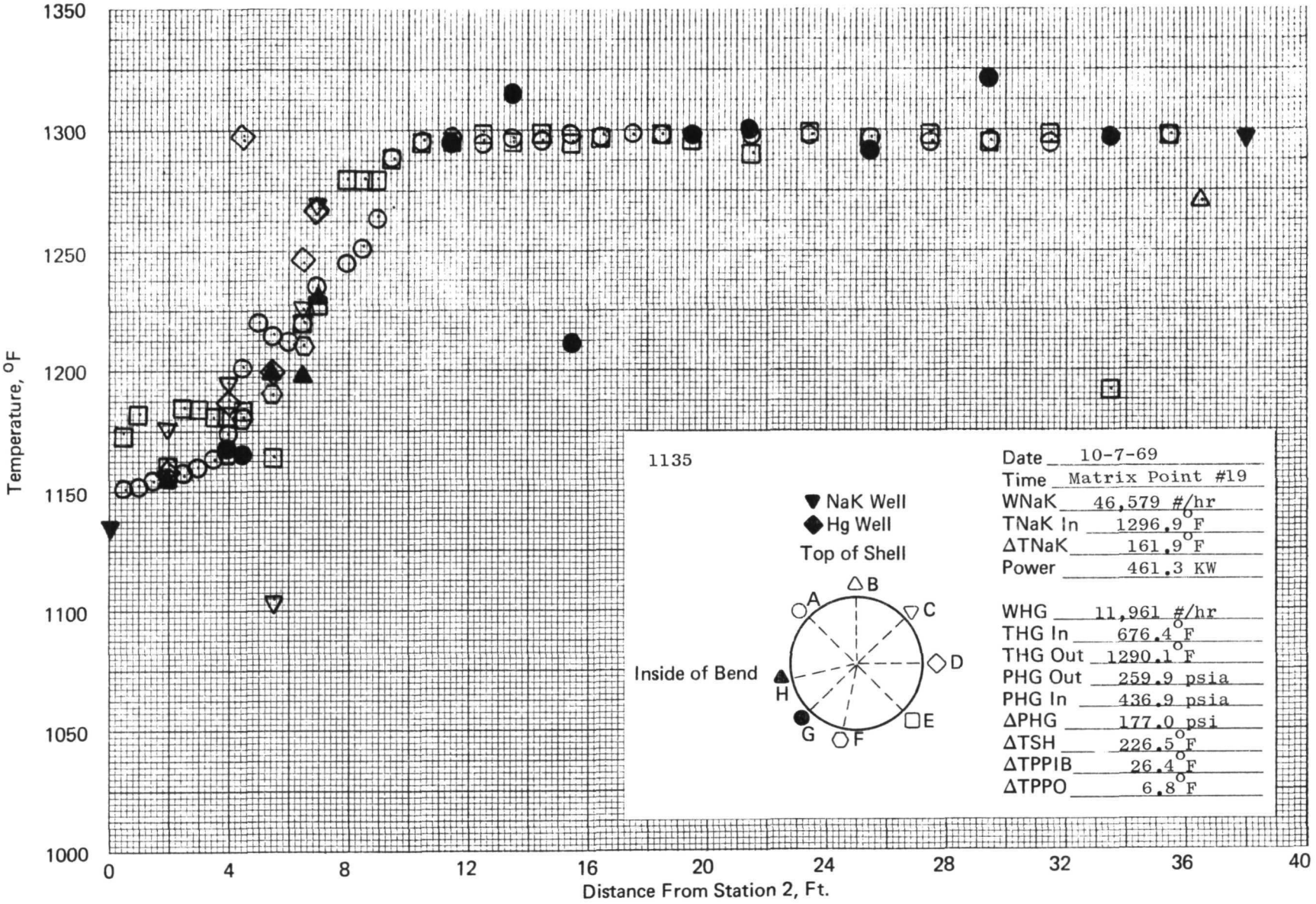

Figure 83. SNAP-8 refractory boiler temperature profile.

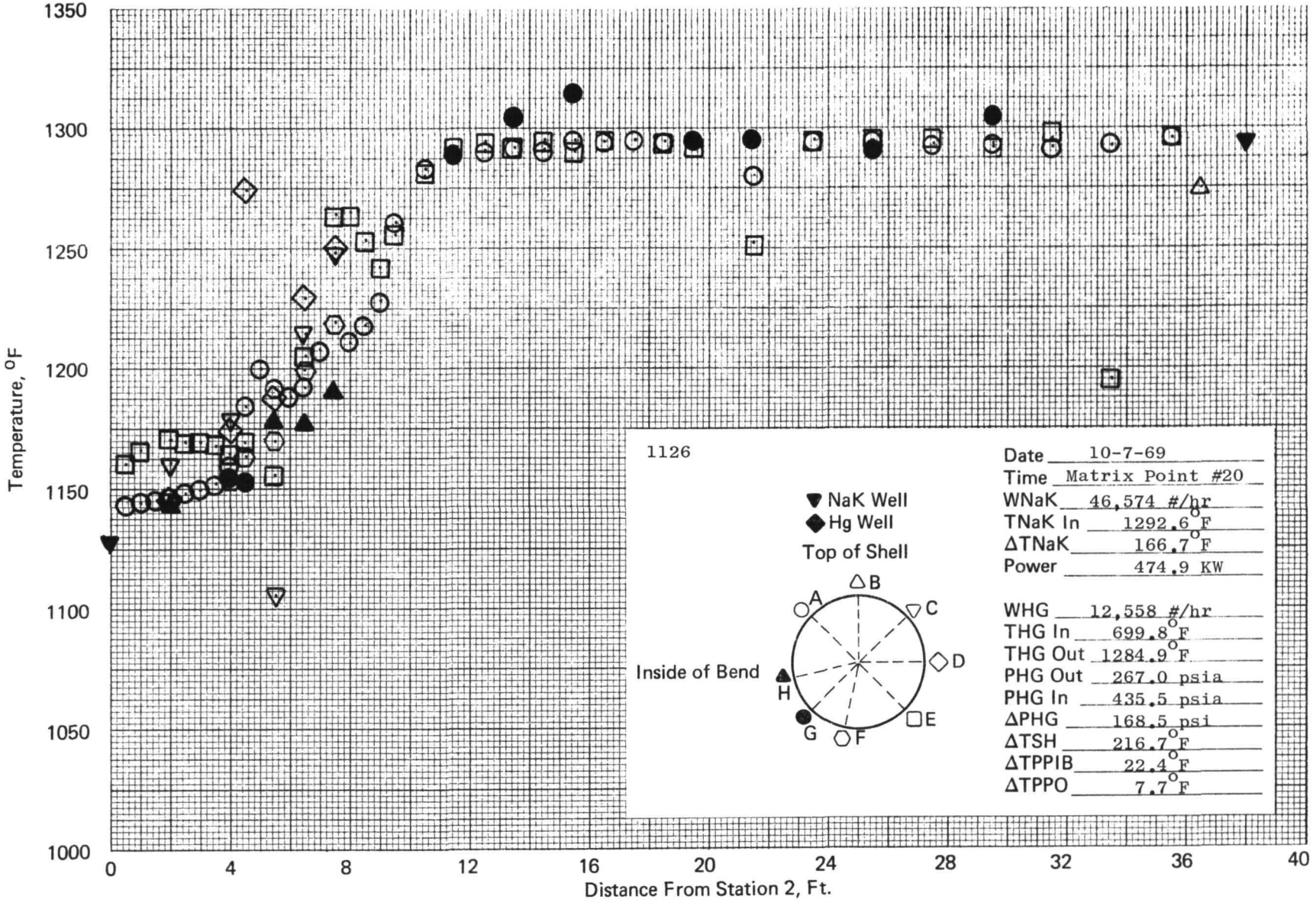

Figure 84. SNAP-8 refractory boiler temperature profile.

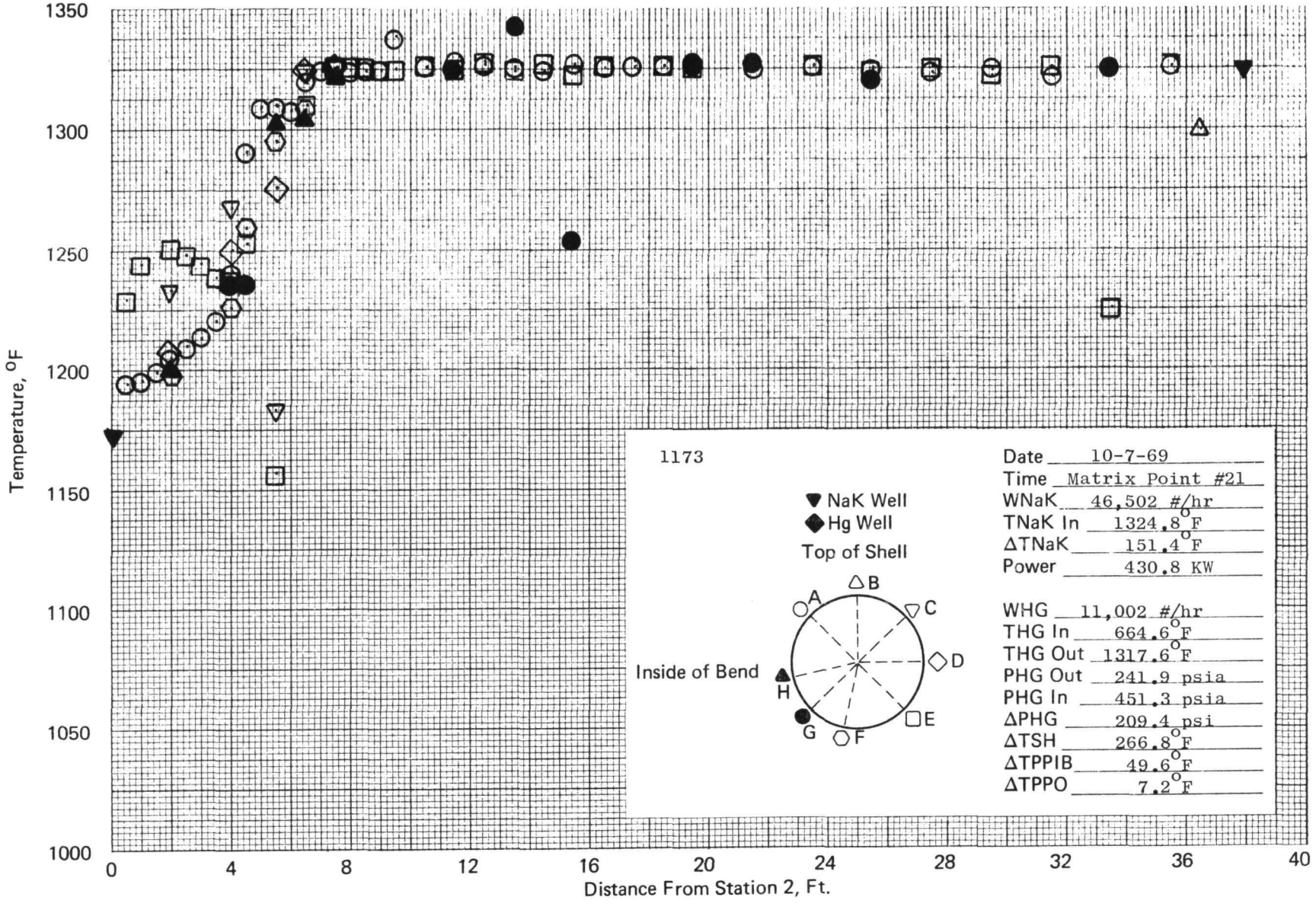

Figure 85. SNAP-8 refractory boiler temperature profile.

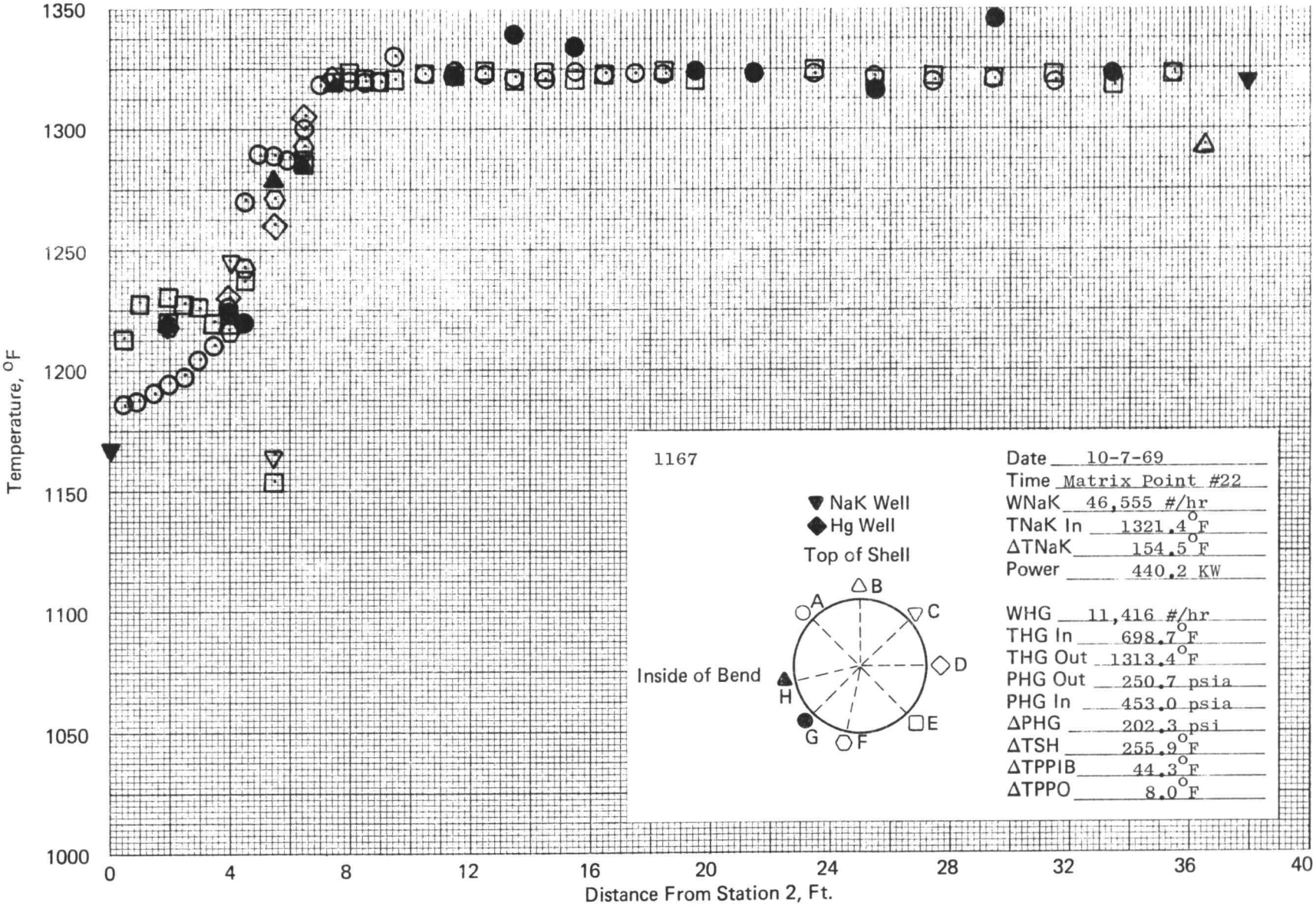

Figure 86. SNAP-8 refractory boiler temperature profile.

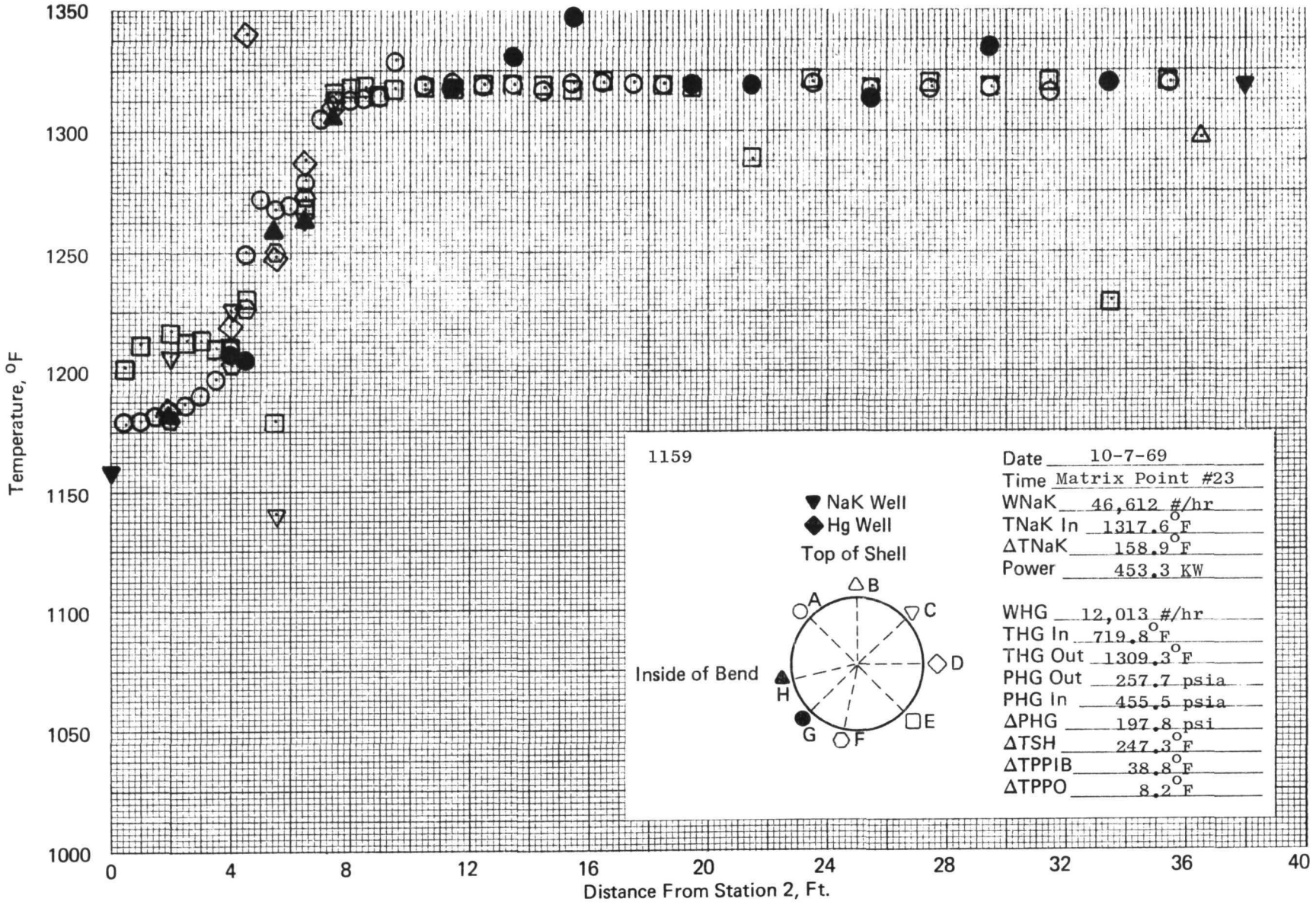

Figure 87. SNAP-8 refractory boiler temperature profile.

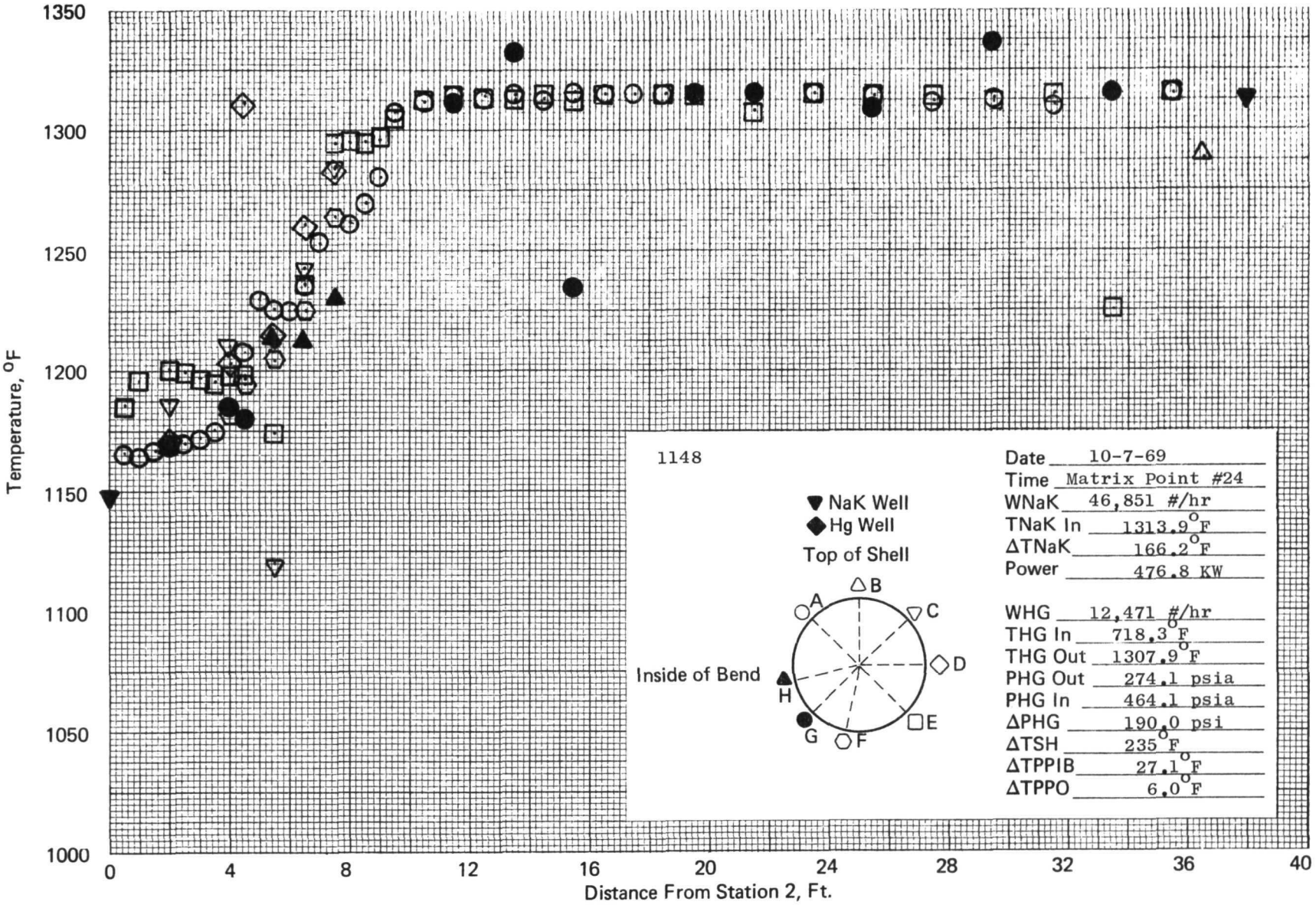

Figure 88. SNAP-8 refractory boiler temperature profile.

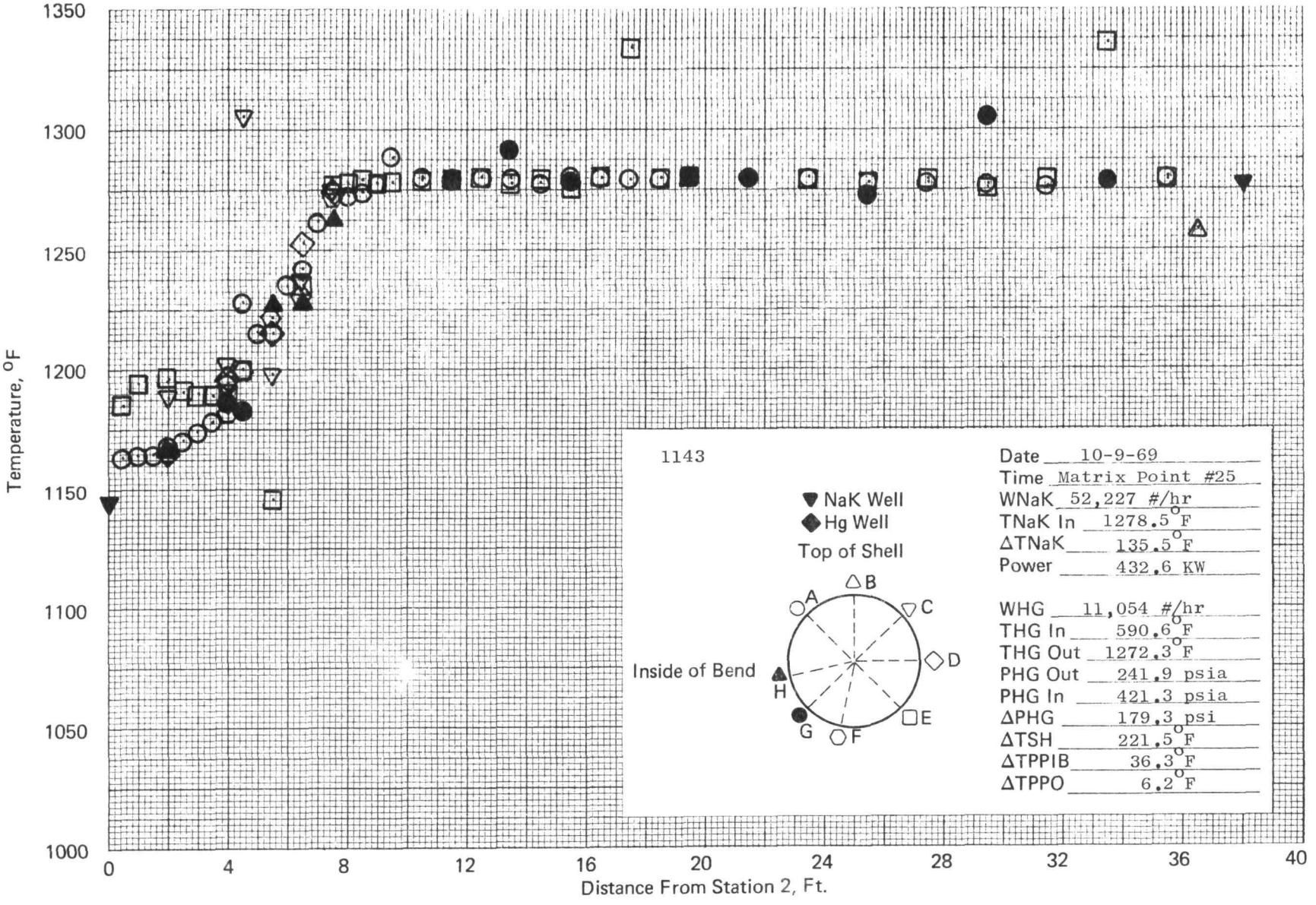

Figure 89. SNAP-8 refractory boiler temperature profile.

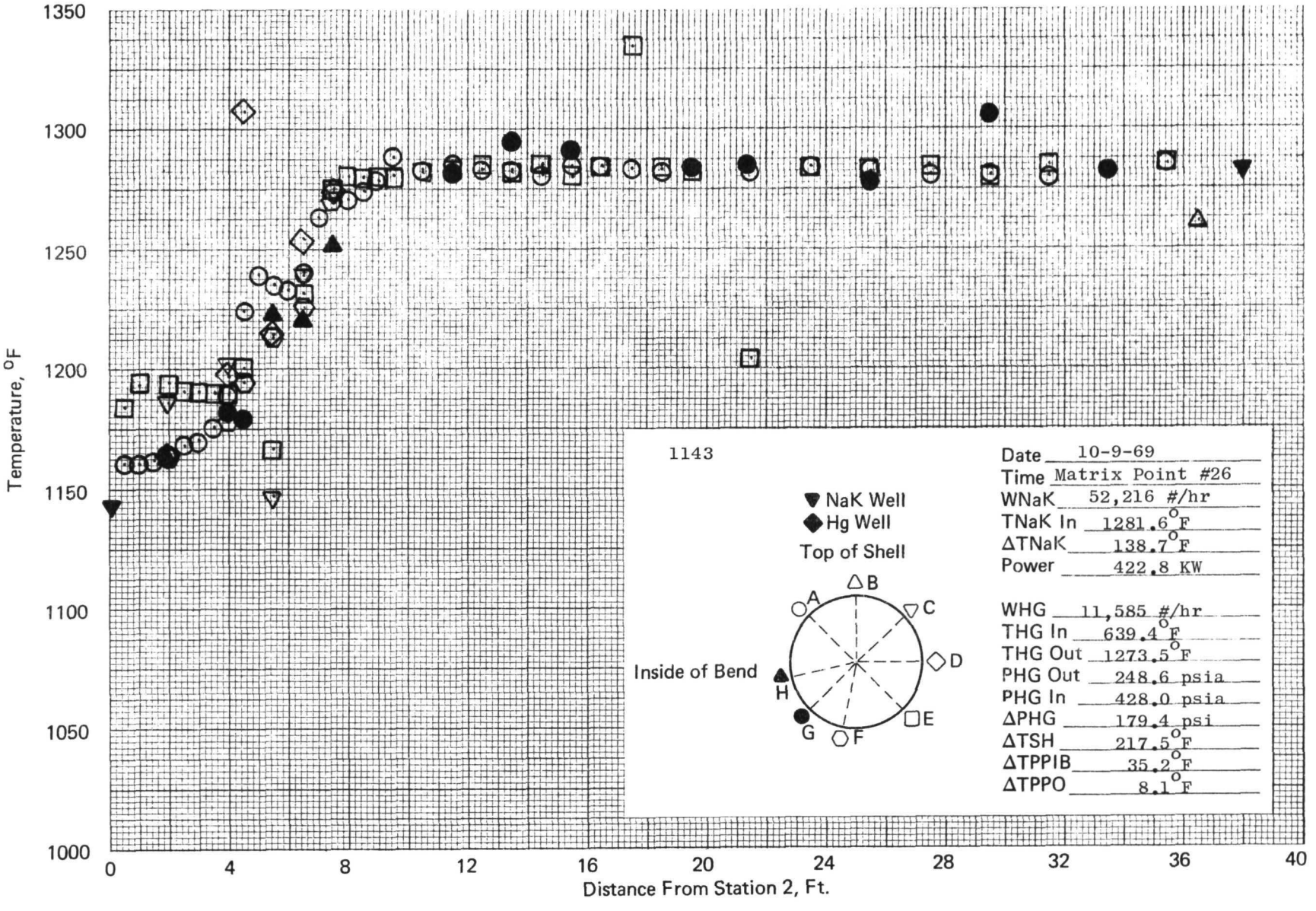

Figure 90. SNAP-8 refractory boiler temperature profile.

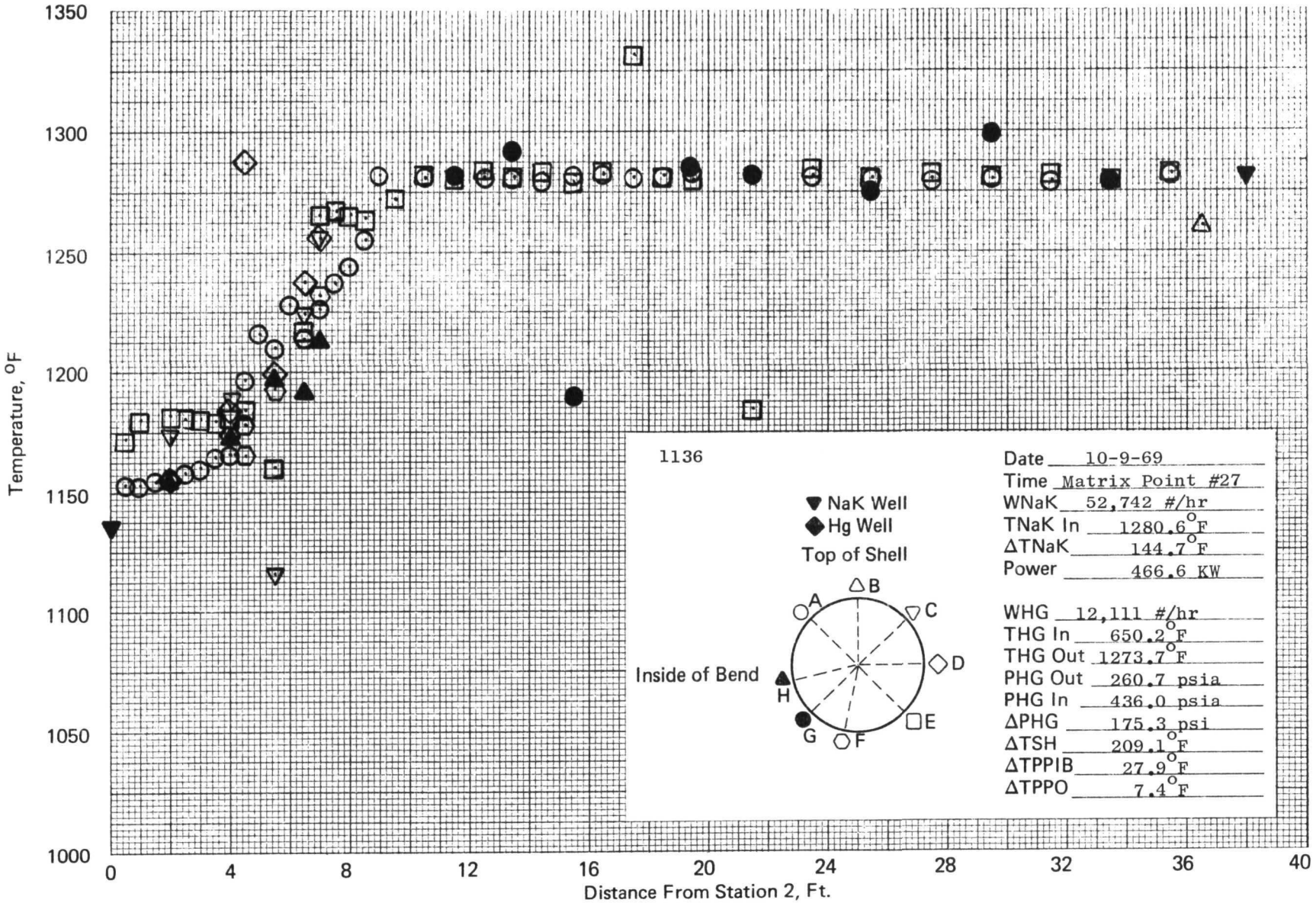

Figure 91. SNAP-8 refractory boiler temperature profile.

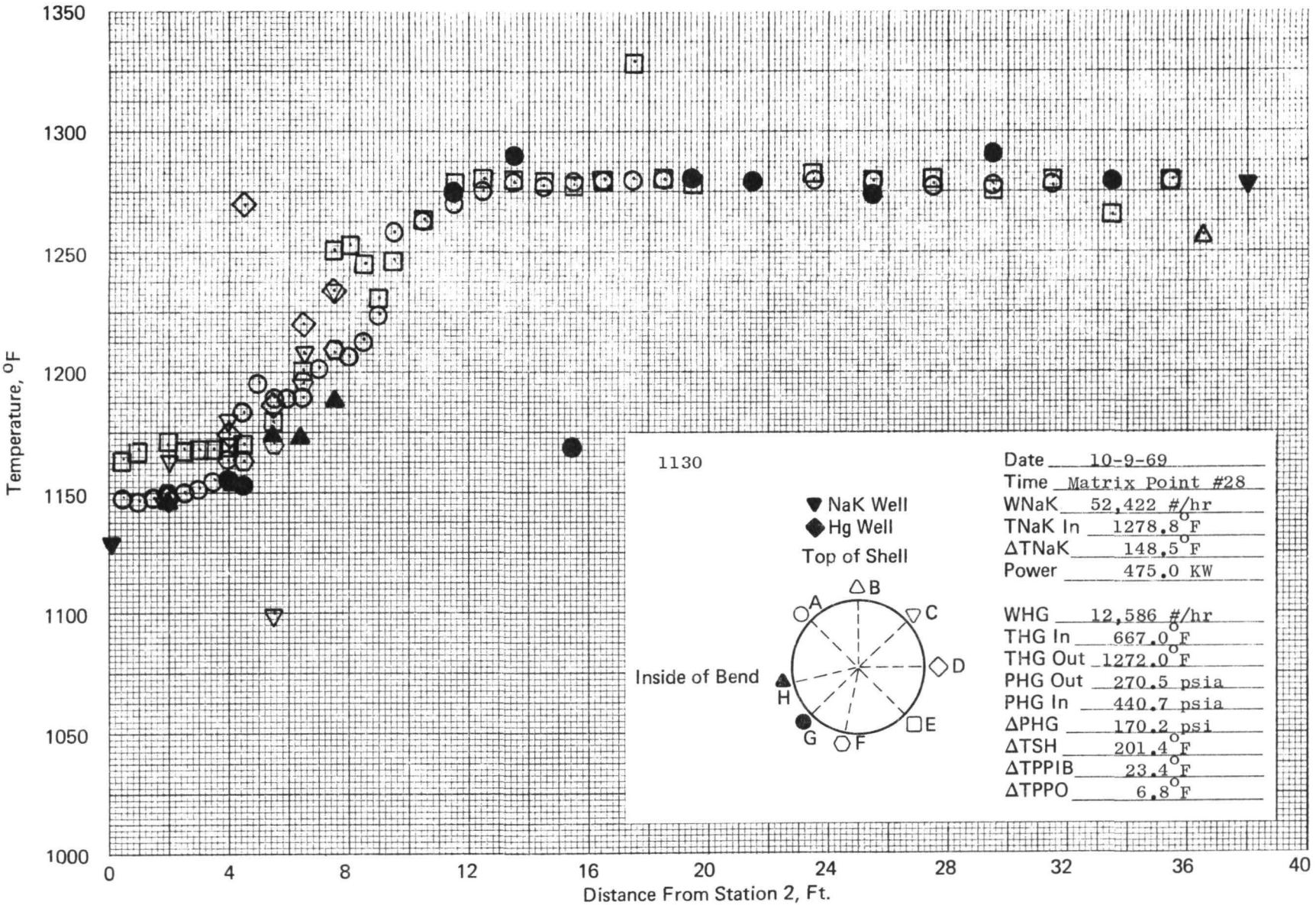

Figure 92. SNAP-8 refractory boiler temperature profile.

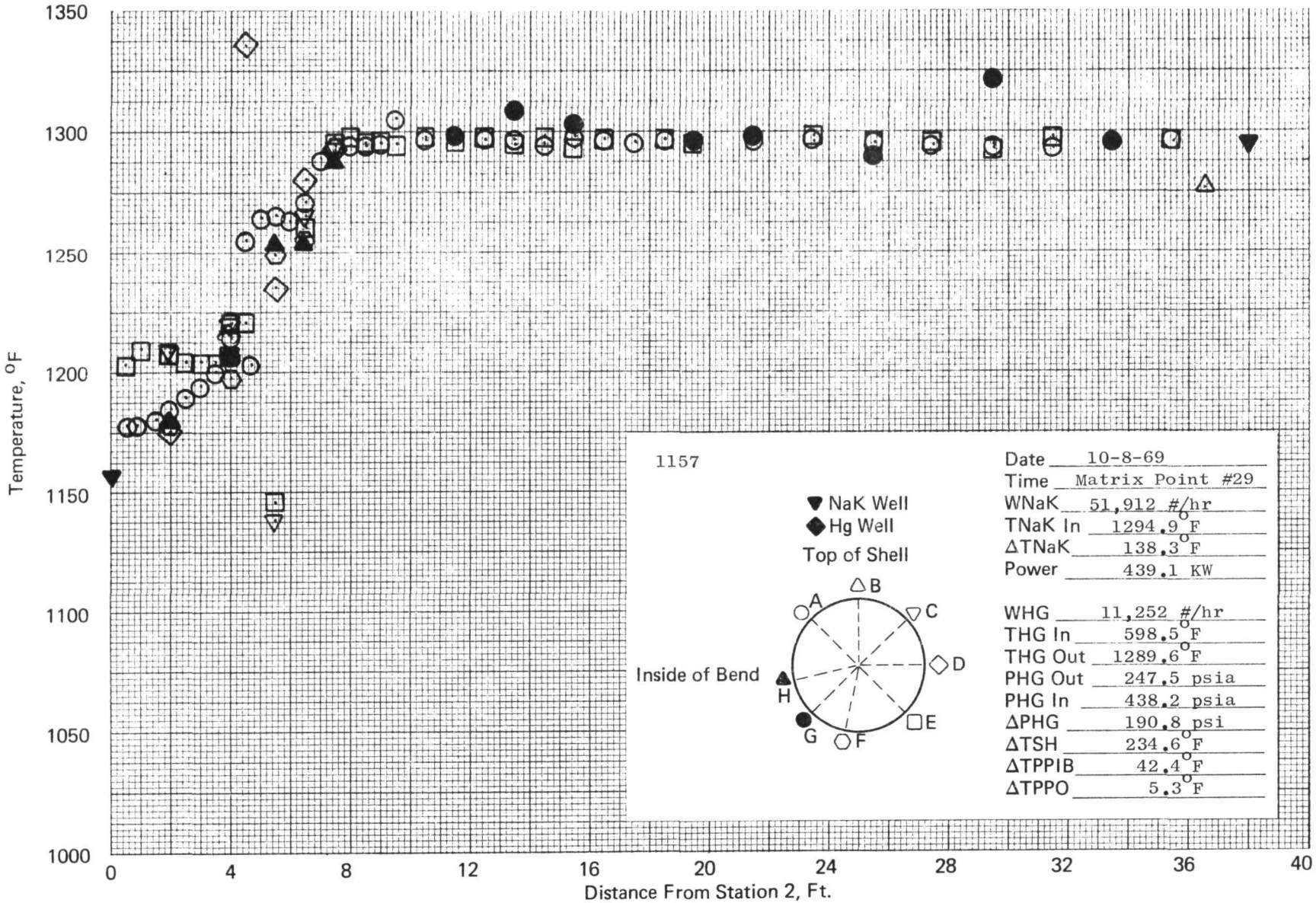

Figure 93. SNAP-8 refractory boiler temperature profile.

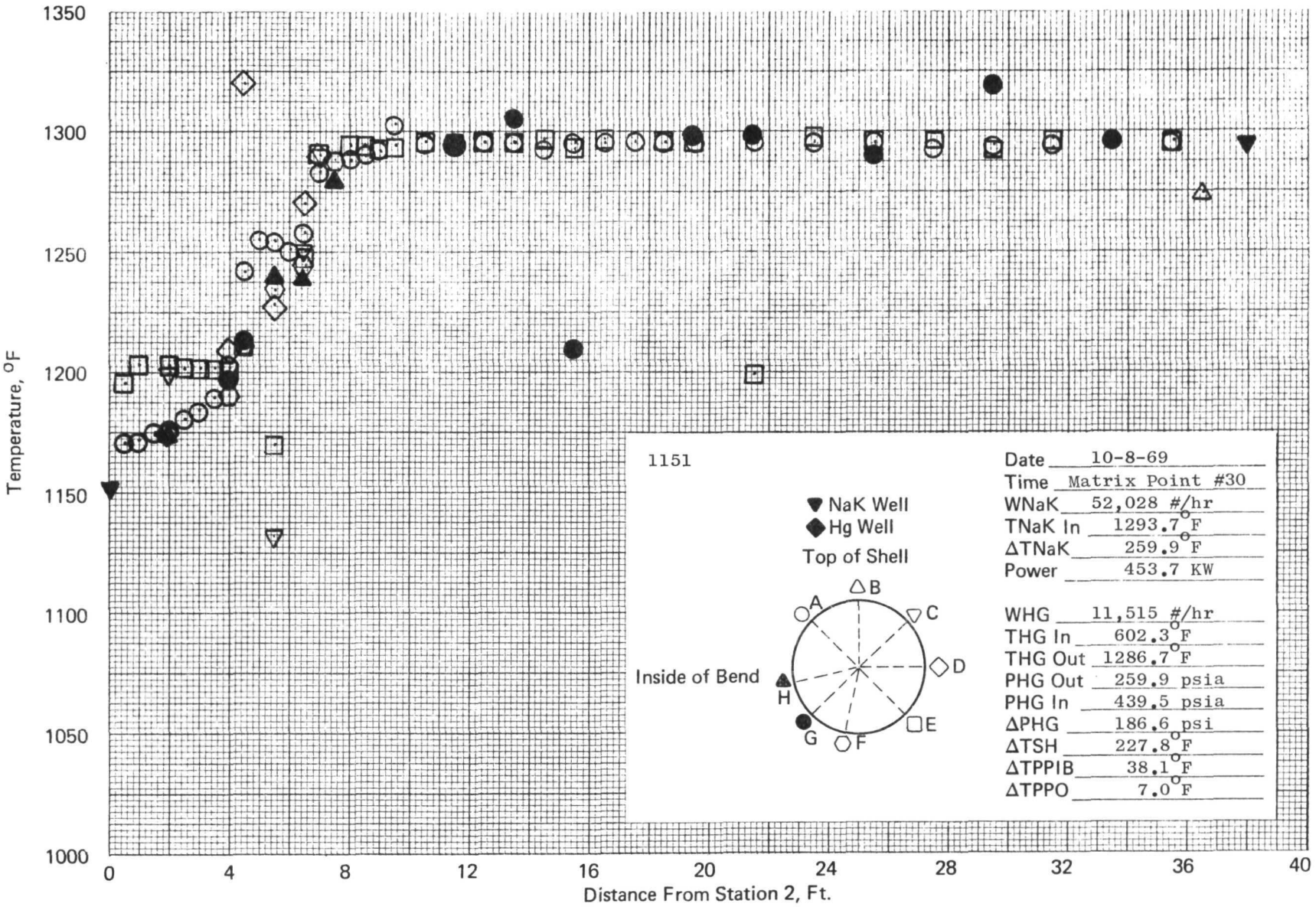

Figure 94. SNAP-8 refractory boiler temperature profile.

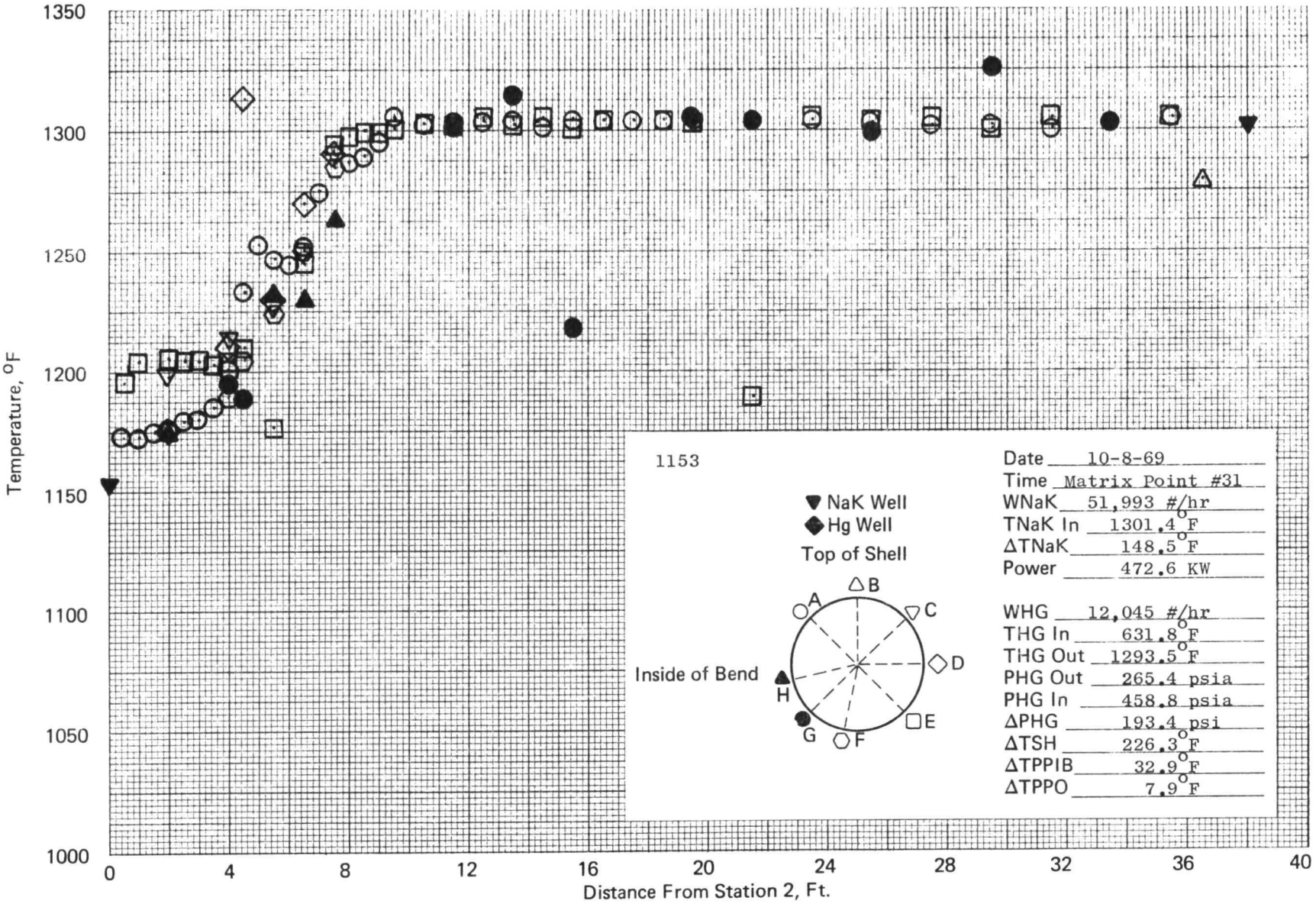

Figure 95. SNAP-8 refractory boiler temperature profile.

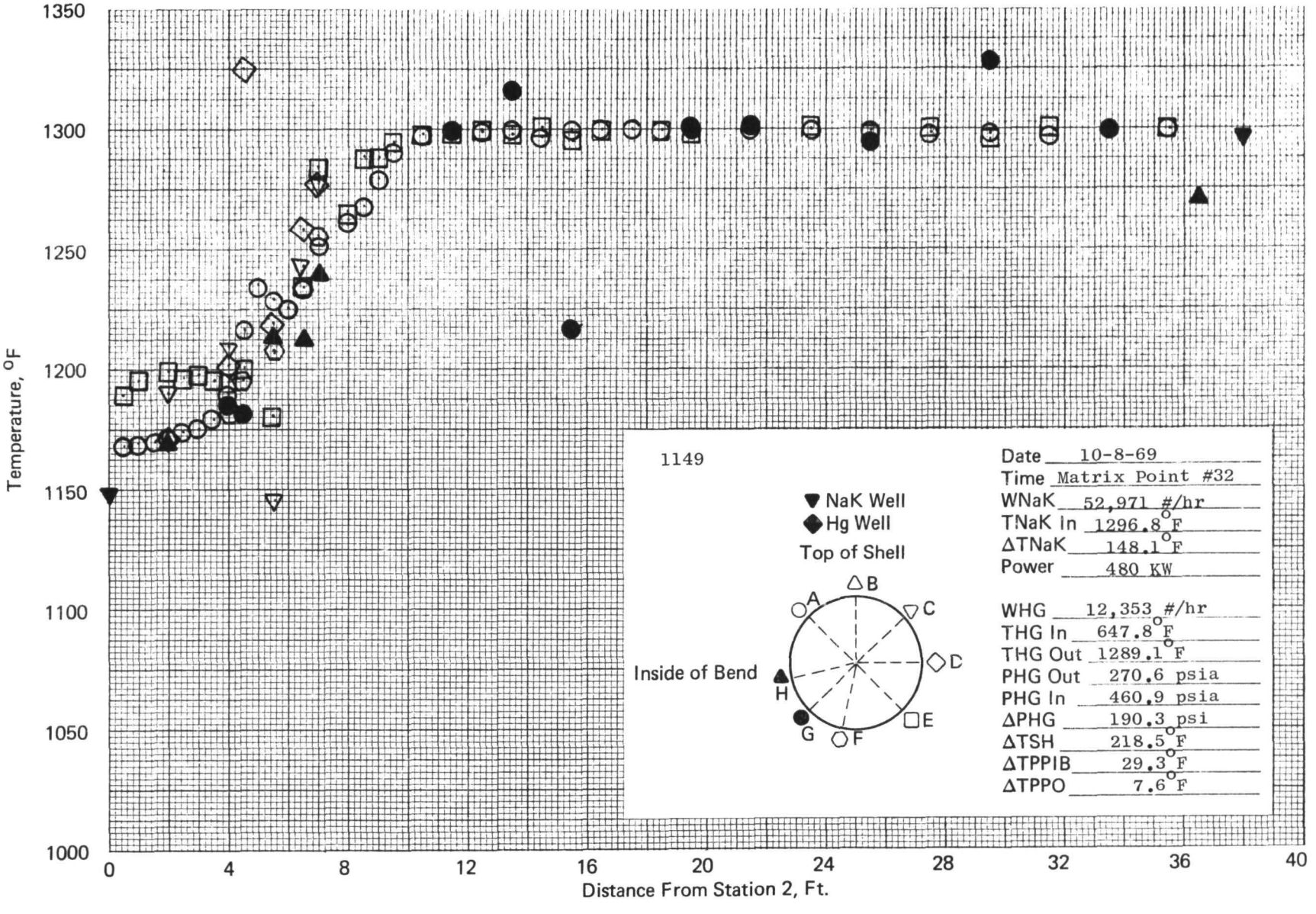

Figure 96. SNAP-8 refractory boiler temperature profile.

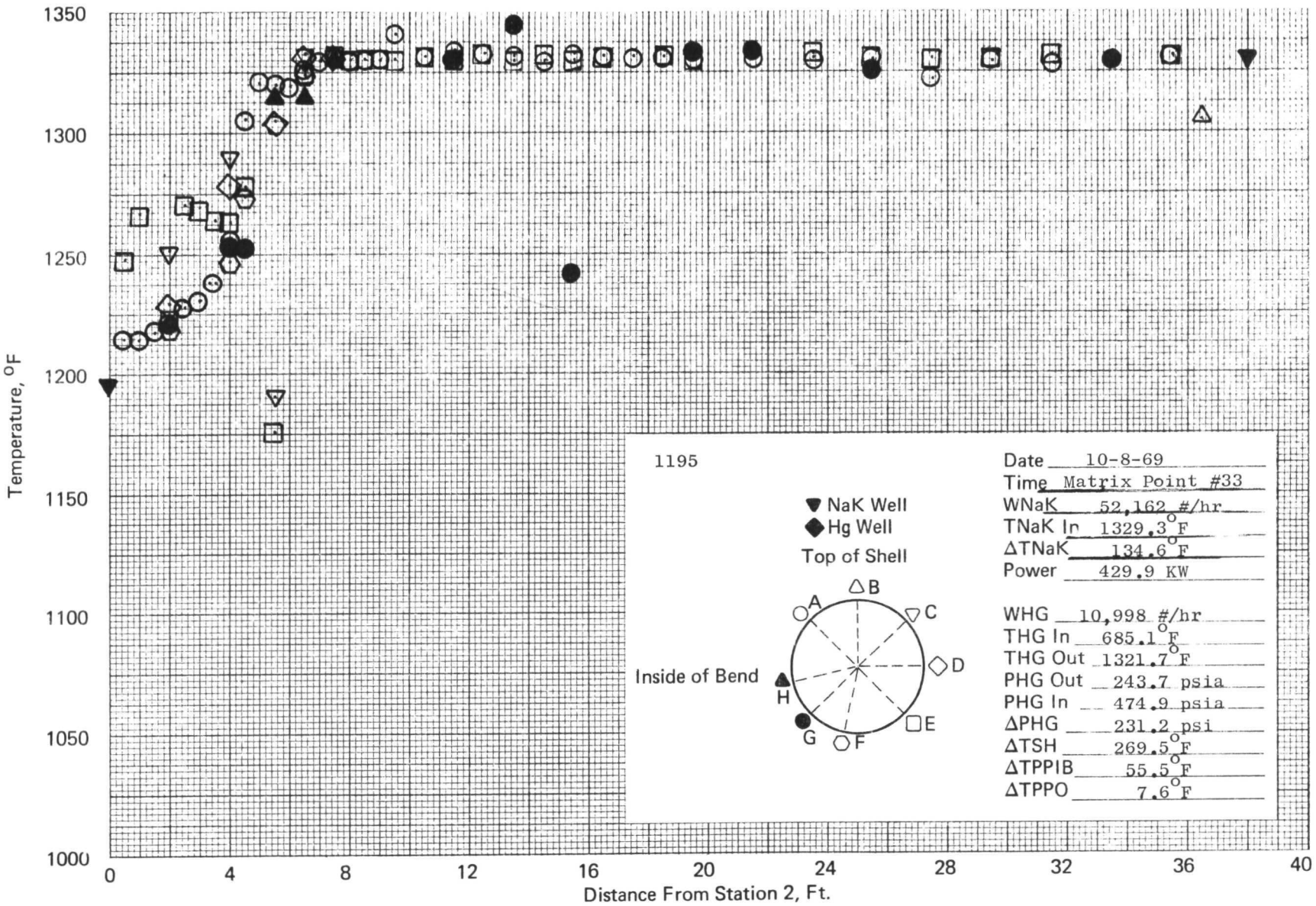

Figure 97. SNAP-8 refractory boiler temperature profile.

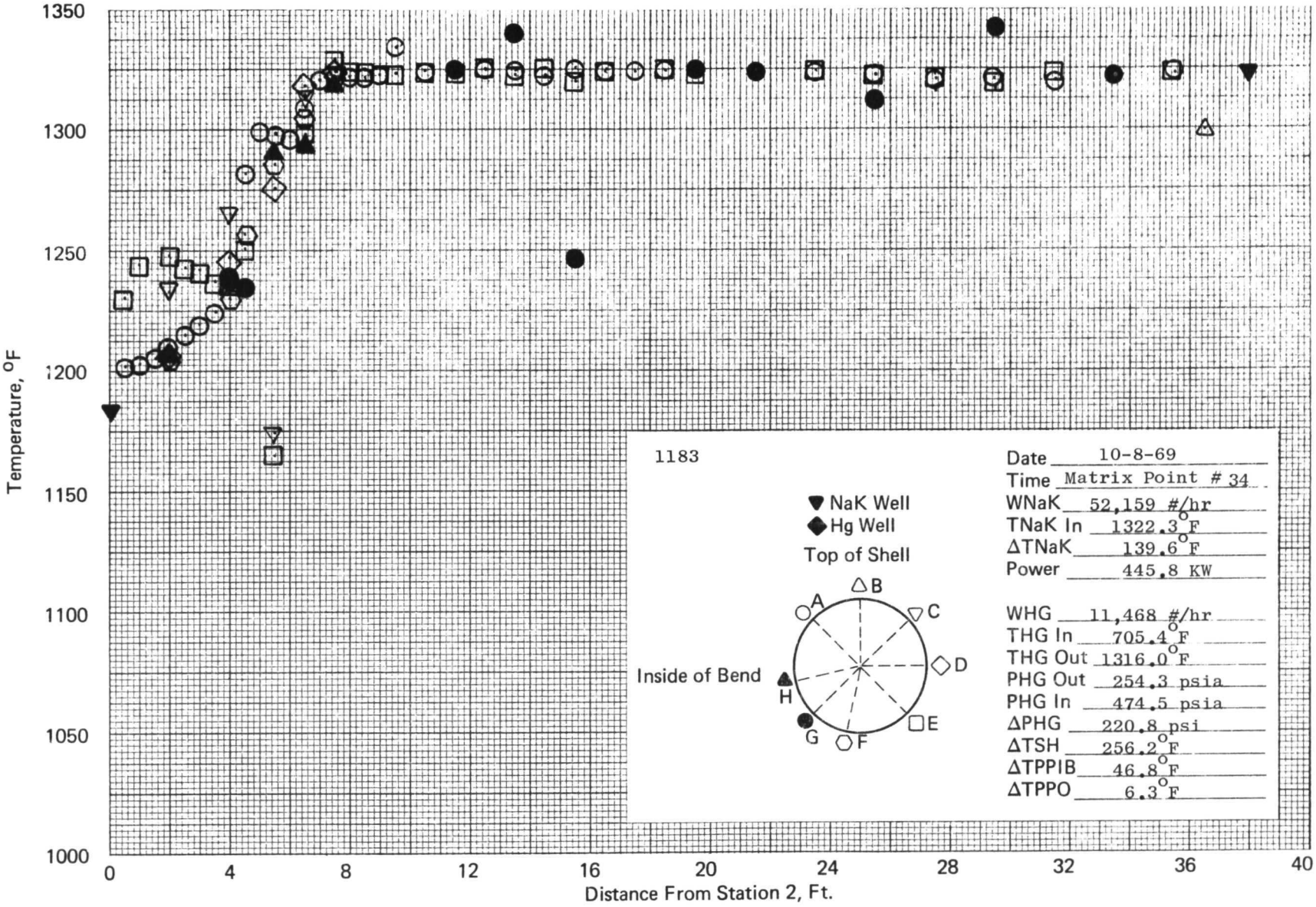

Figure 98. SNAP-8 refractory boiler temperature profile.

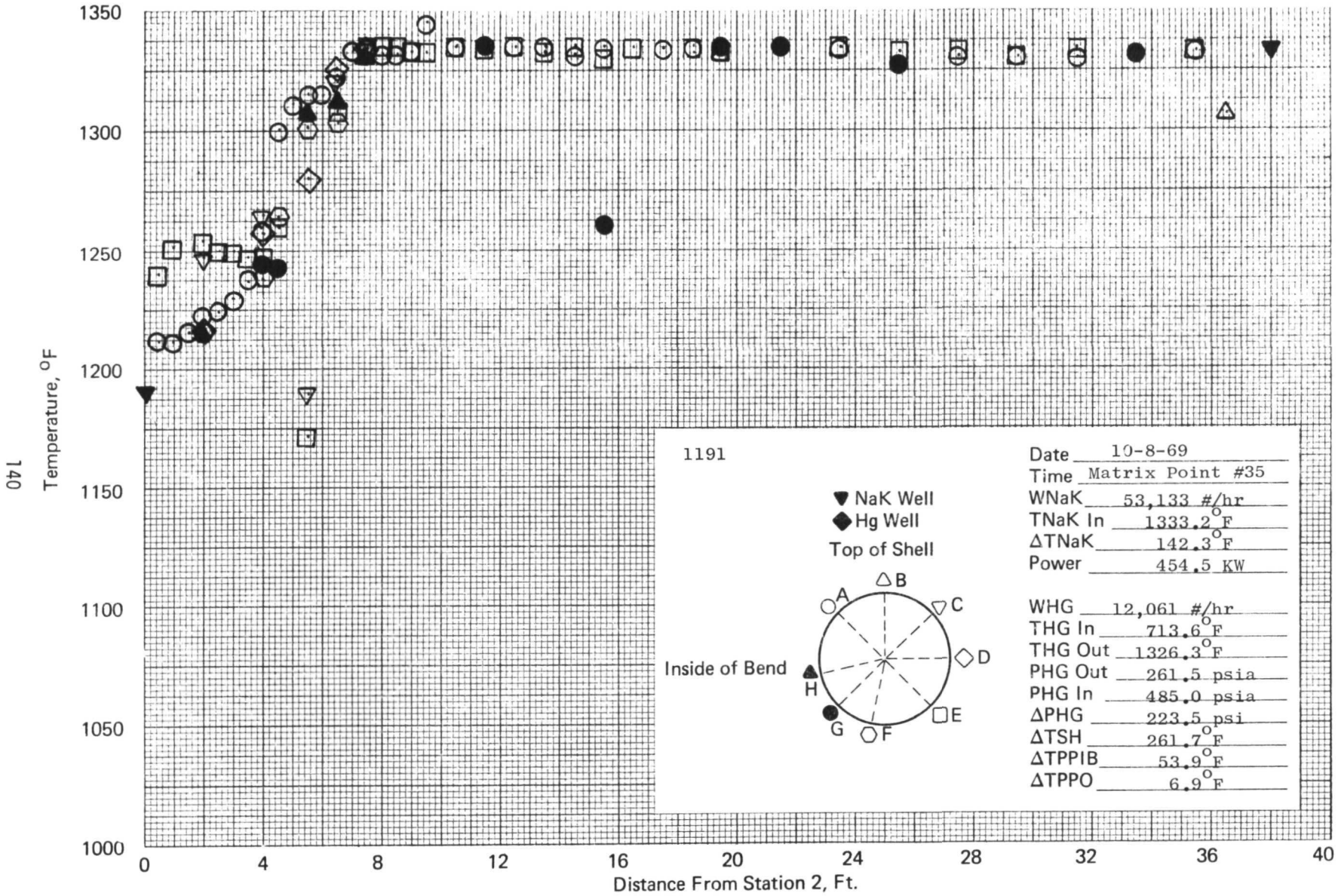

Figure 99. SNAP-8 refractory boiler temperature profile.

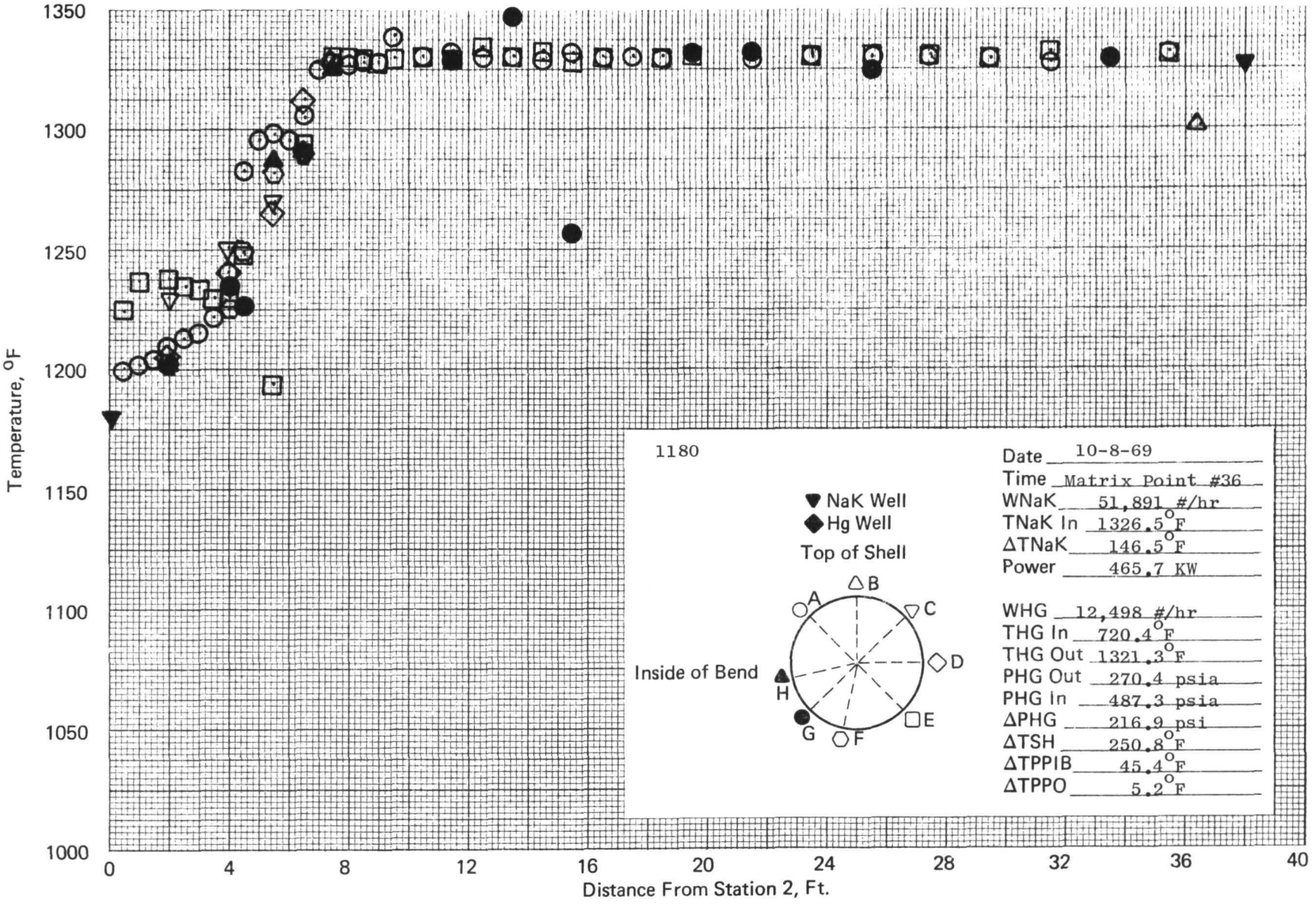

Figure 100. SNAP-8 refractory boiler temperature profile.

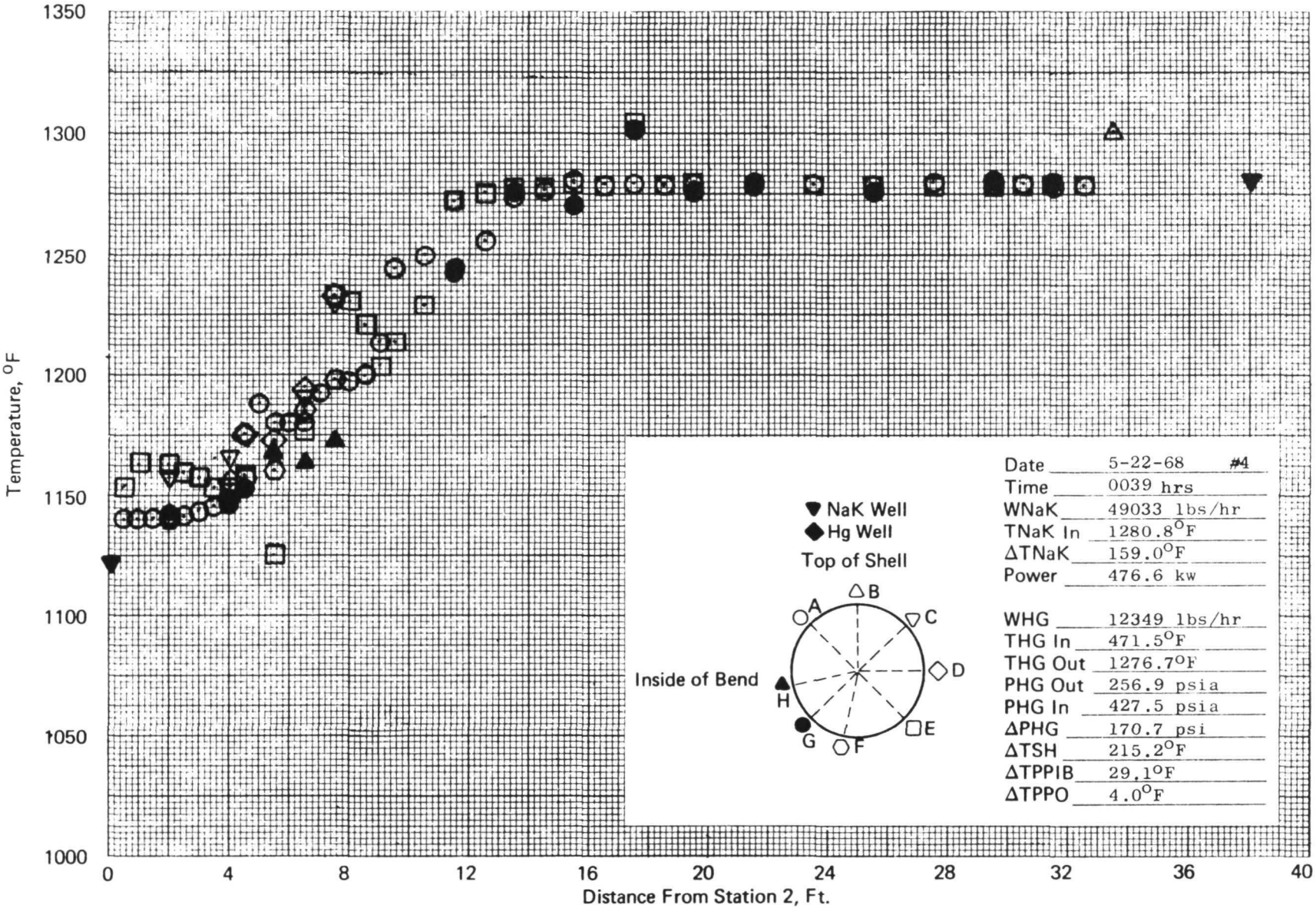

Figure 101. SNAP-8 refractory boiler temperature profile.

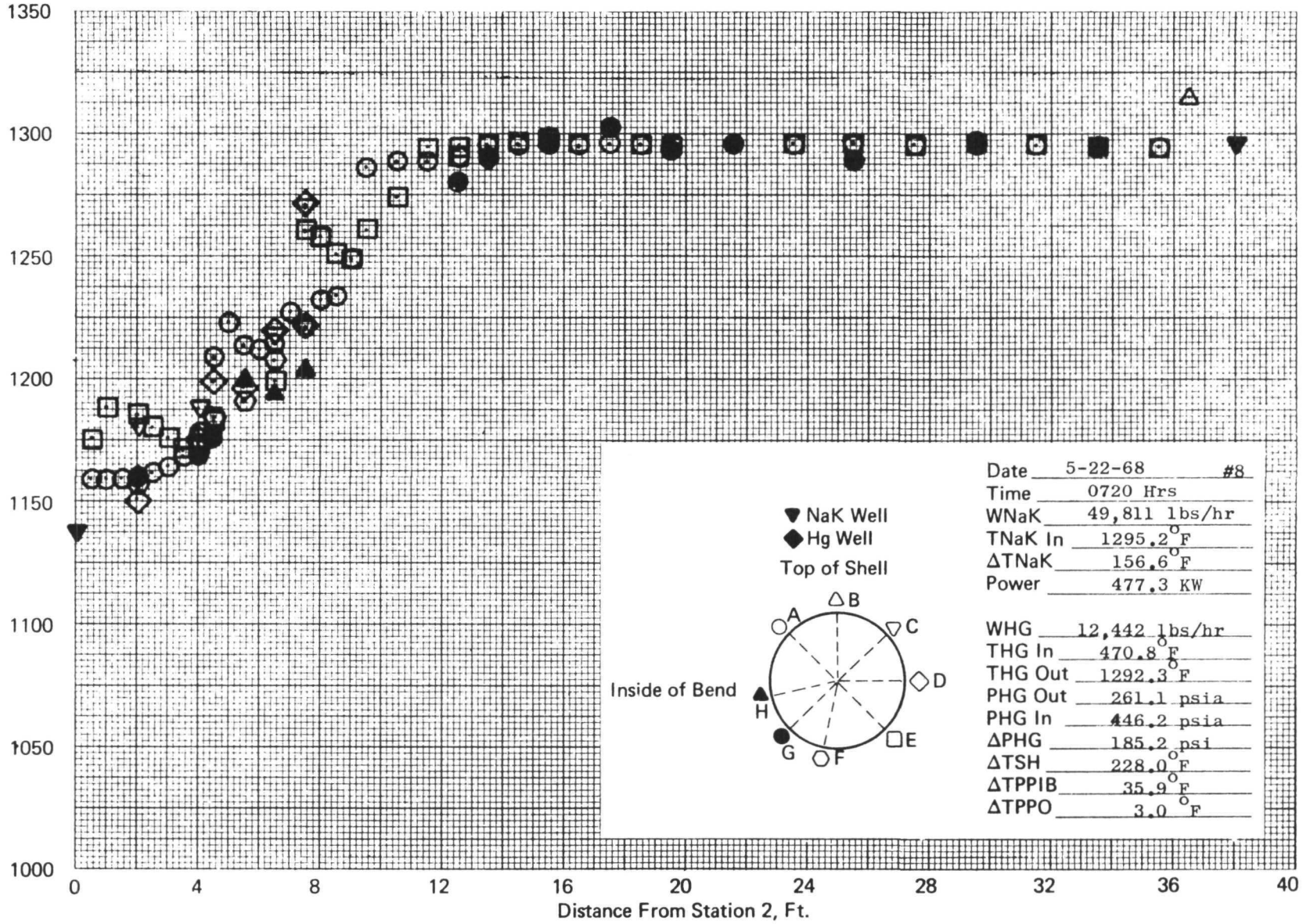

Figure 102. SNAP-8 refractory boiler temperature profile.

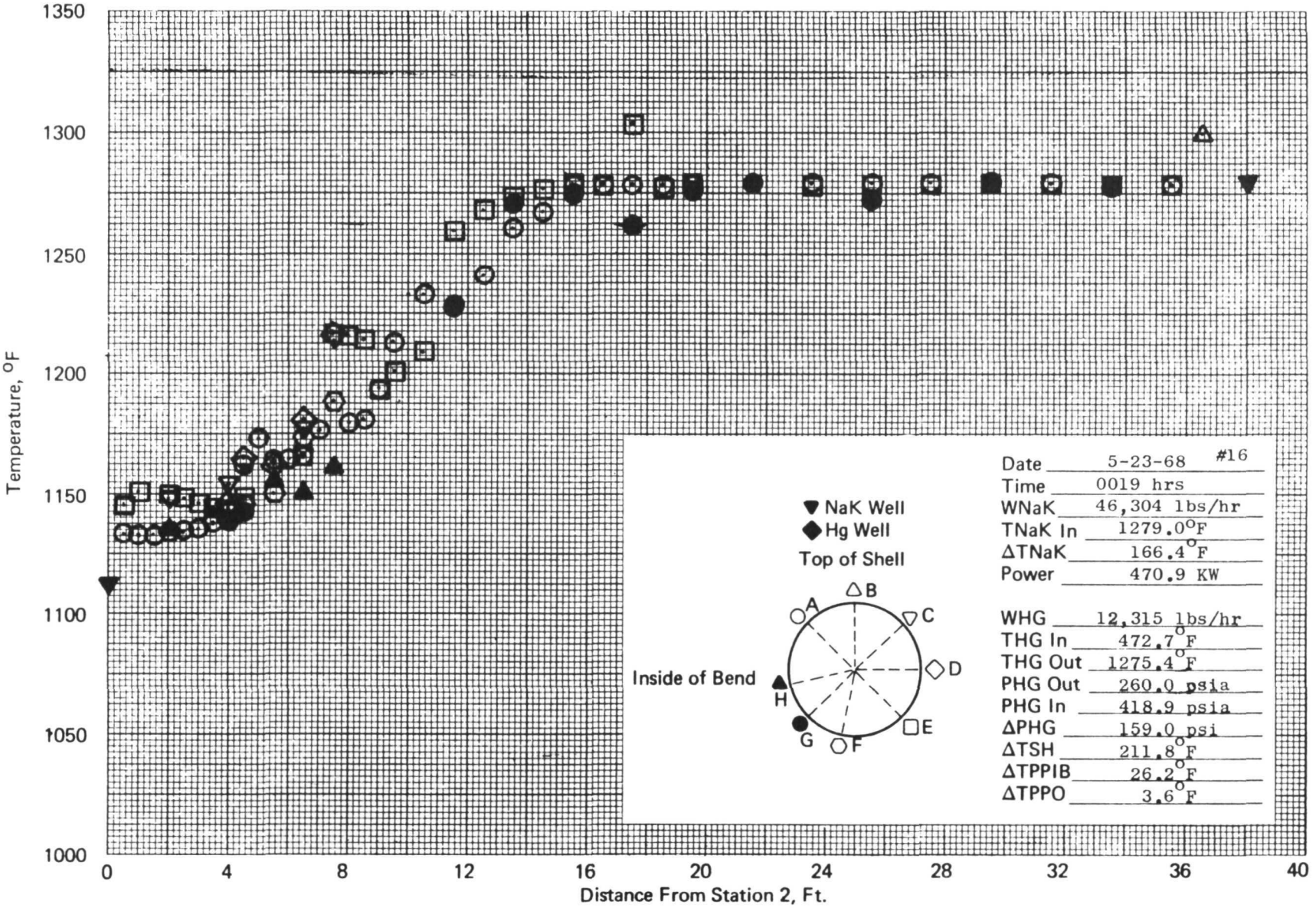

Figure 103. SNAP-8 refractory boiler temperature profile.

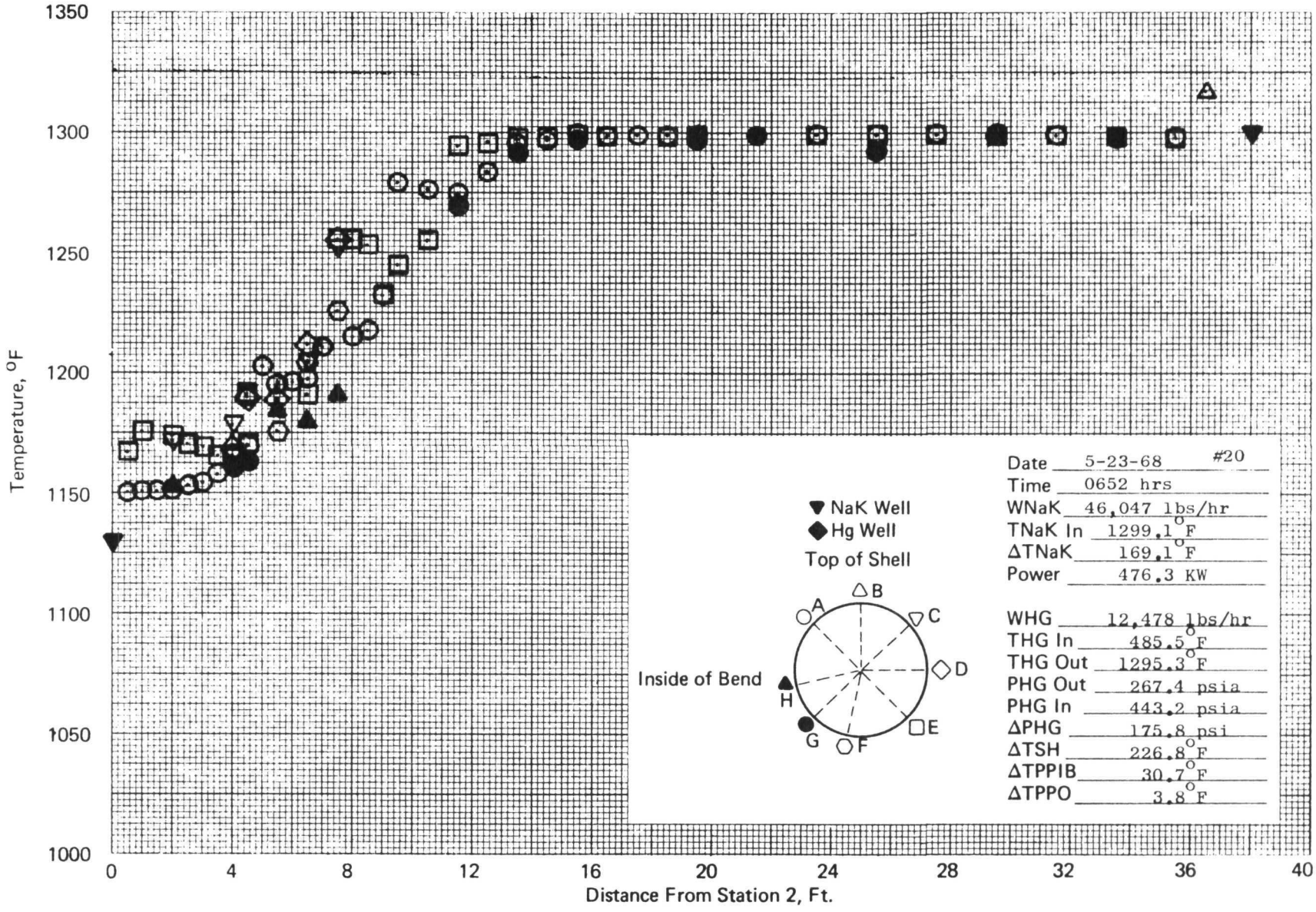

Figure 104. SNAP-8 refractory boiler temperature profile.

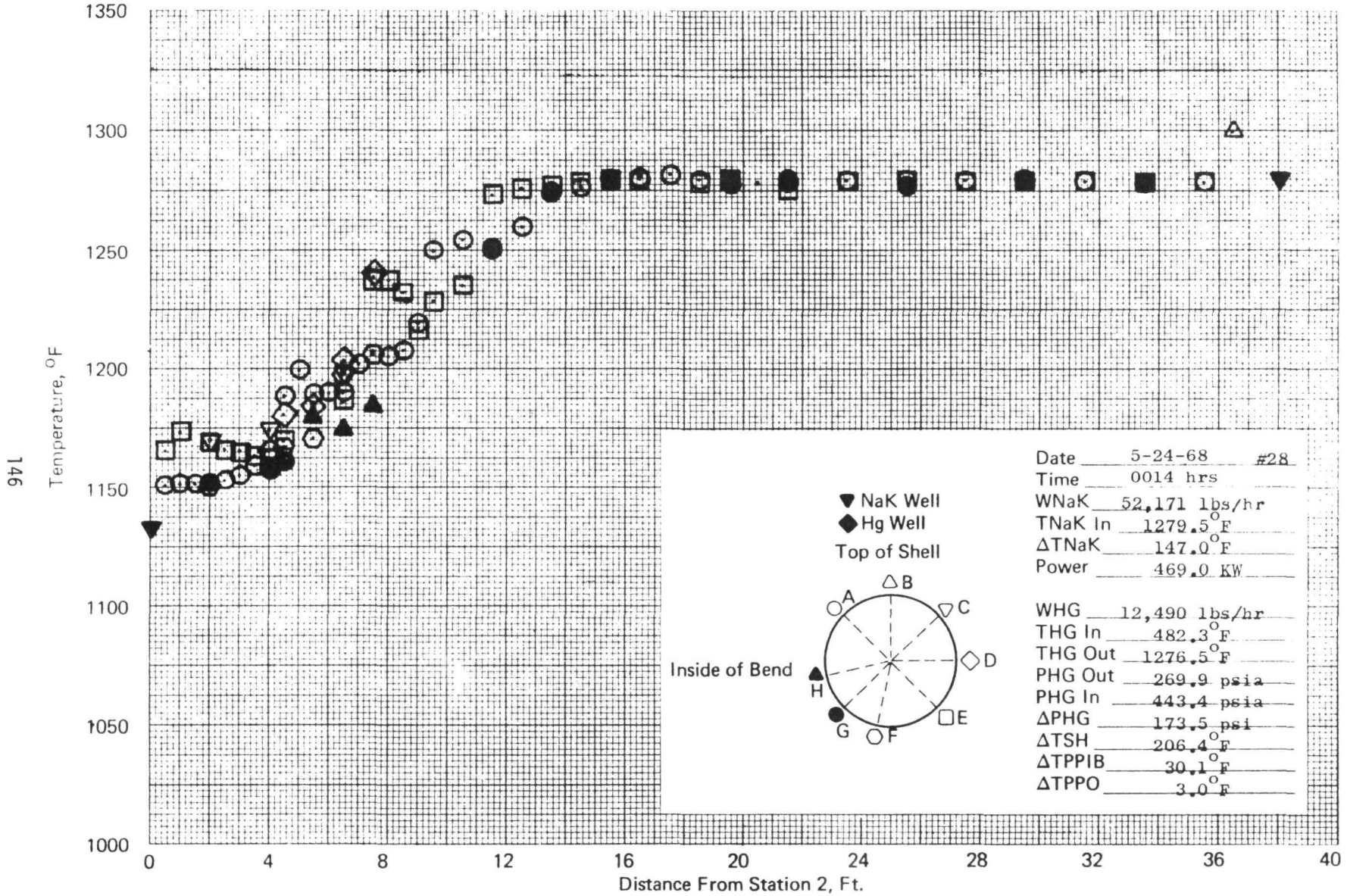

Figure 105. SNAP-8 refractory boiler temperature profile.

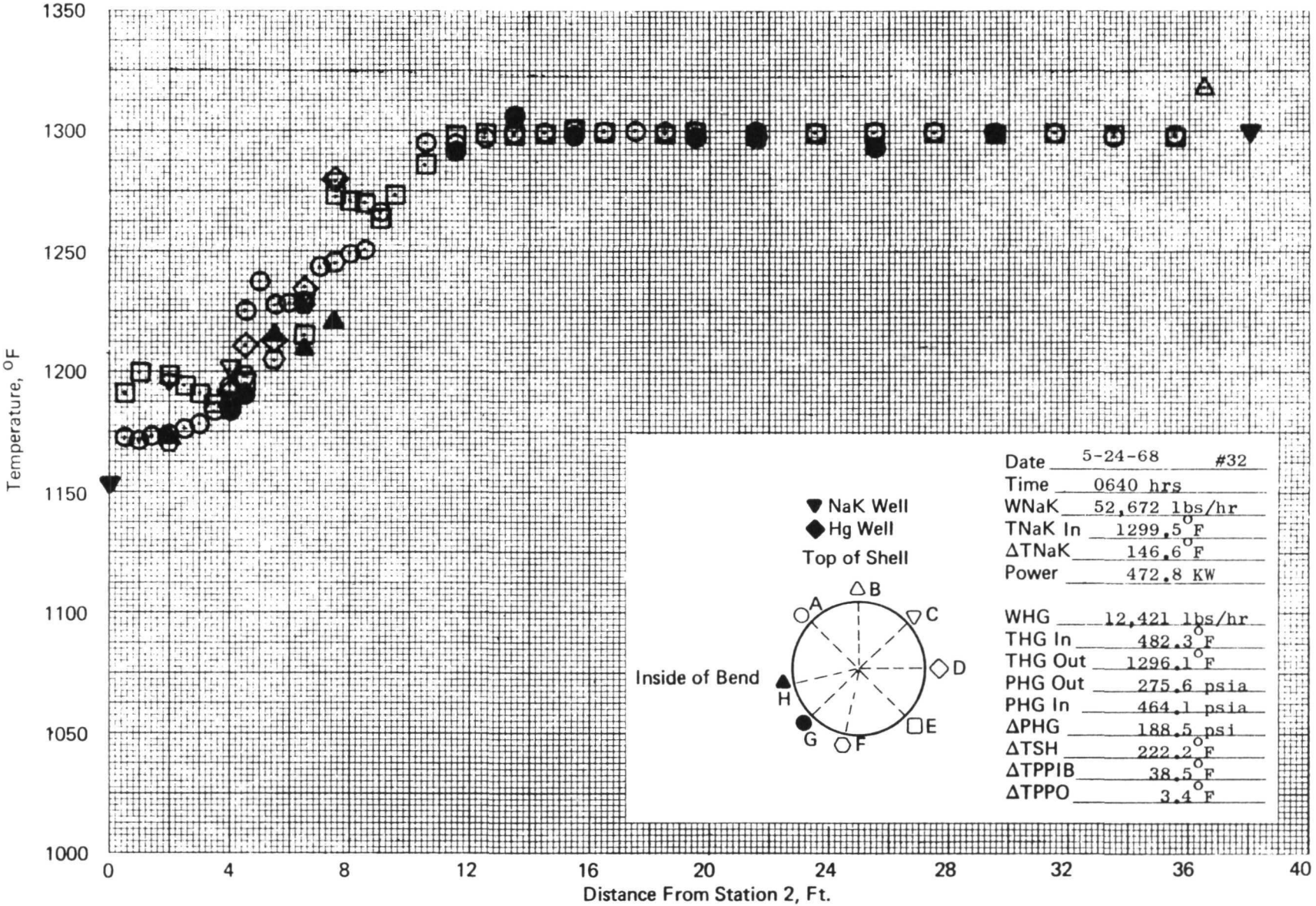

Figure 106. SNAP-8 refractory boiler temperature profile.

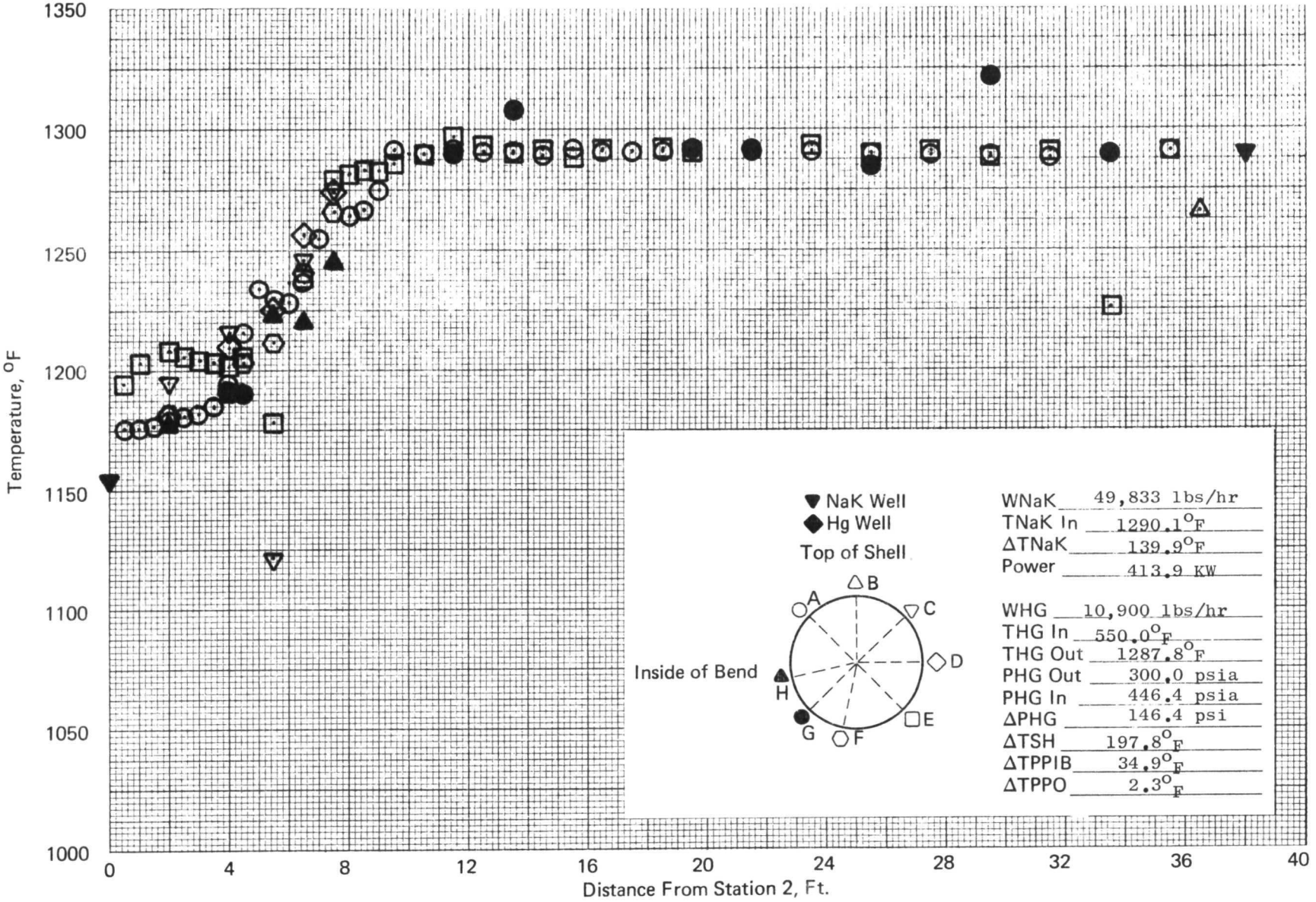

Figure 107. SNAP-8 refractory boiler temperature profile.

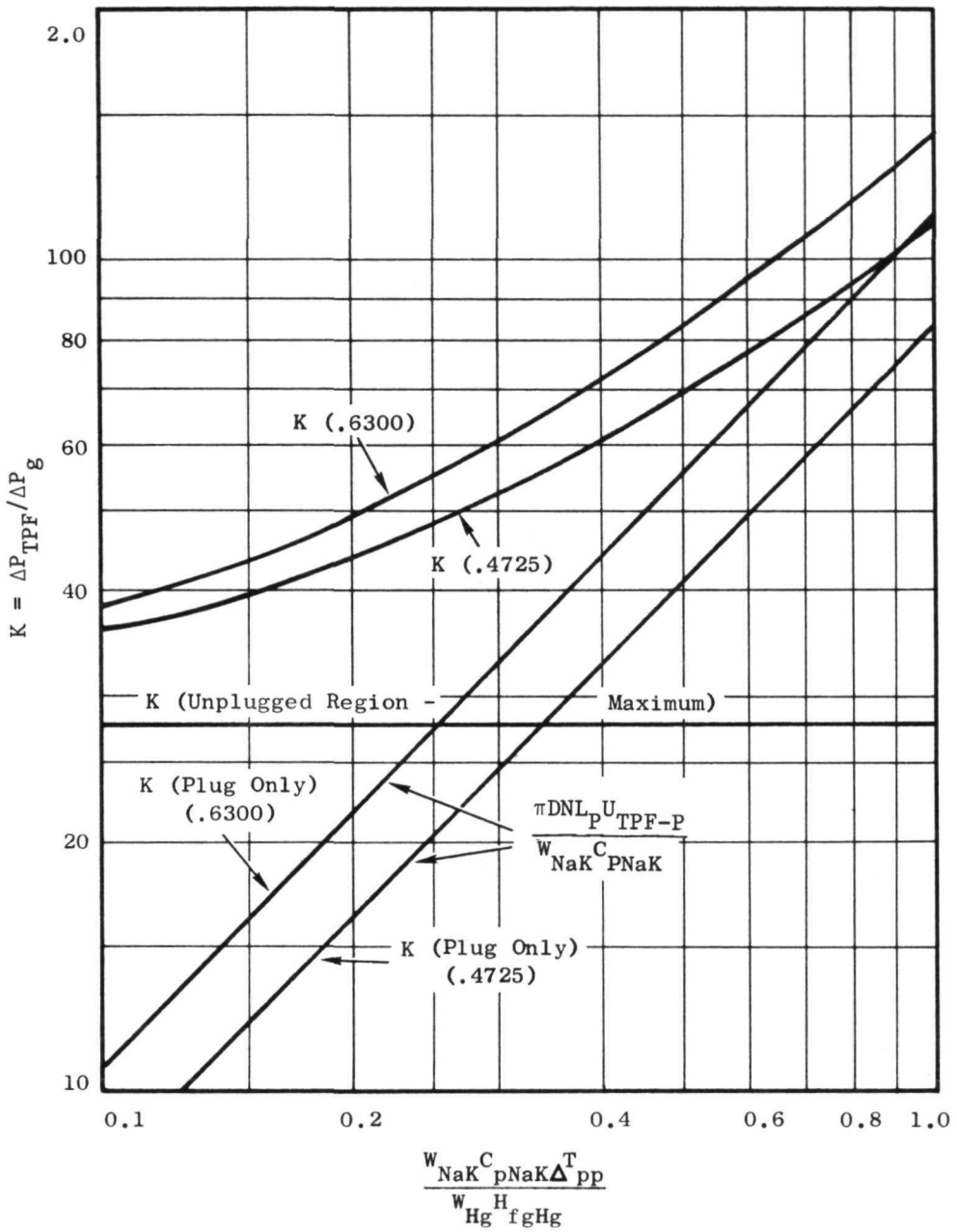

Figure 108. SNAP-8 refractory boiler SN-1 dimensionless boiler pressure drop.

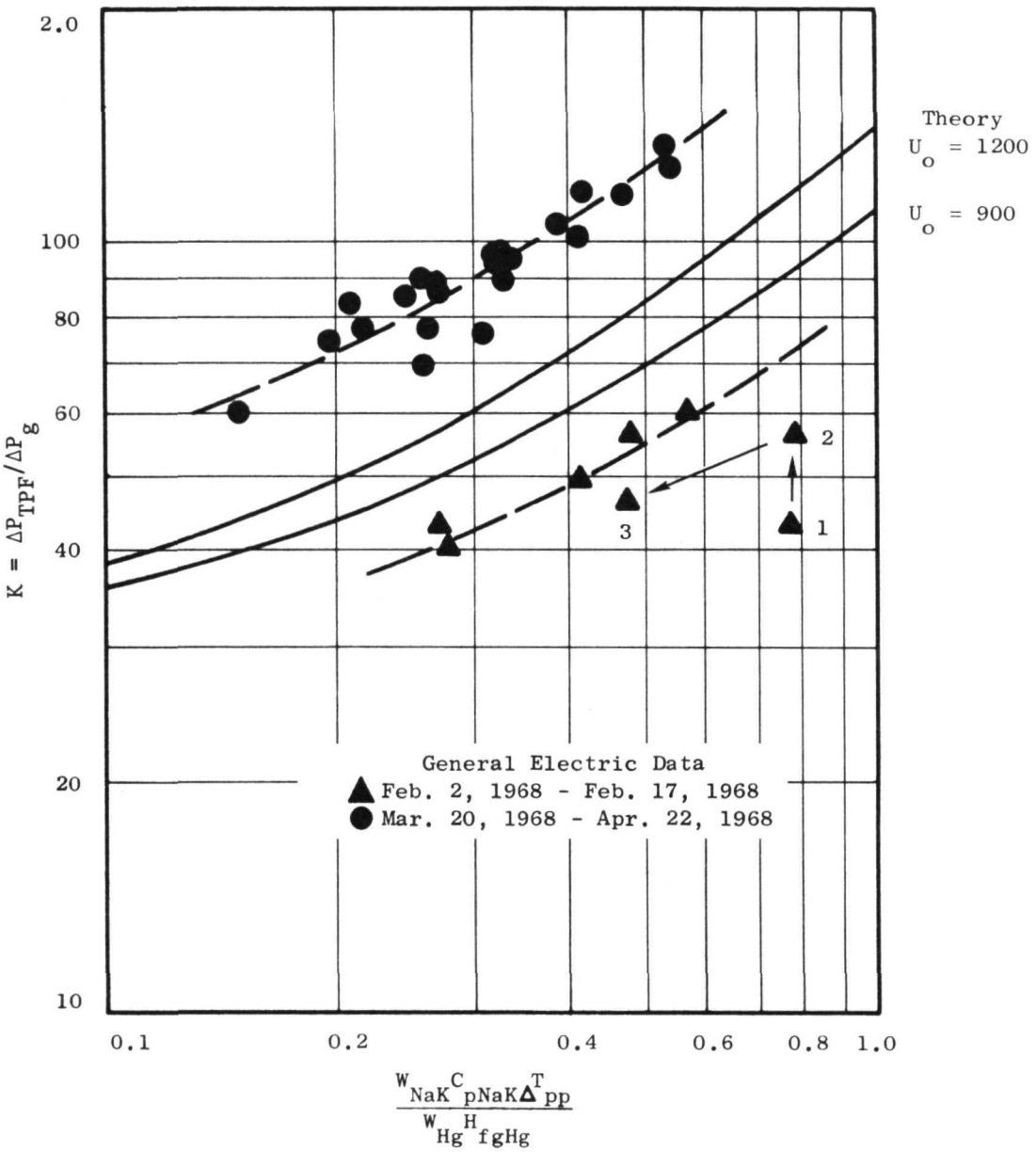

Figure 109. SNAP-8 refractory boiler SN-1 dimensionless boiler pressure drop correlation.

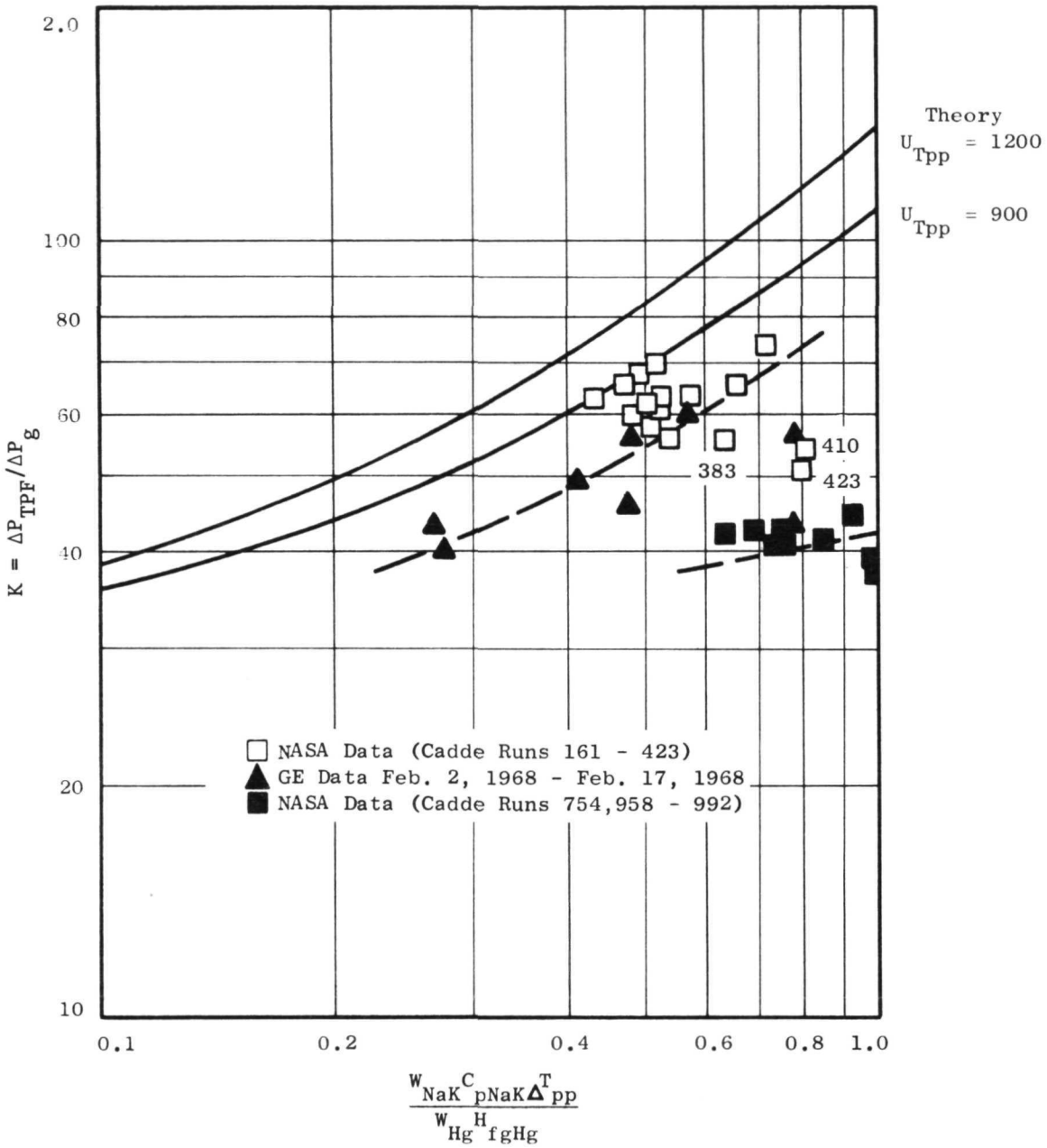

Figure 110. SNAP-8 refractory boiler SN-1 theoretical dimensionless boiler pressure drop correlation.

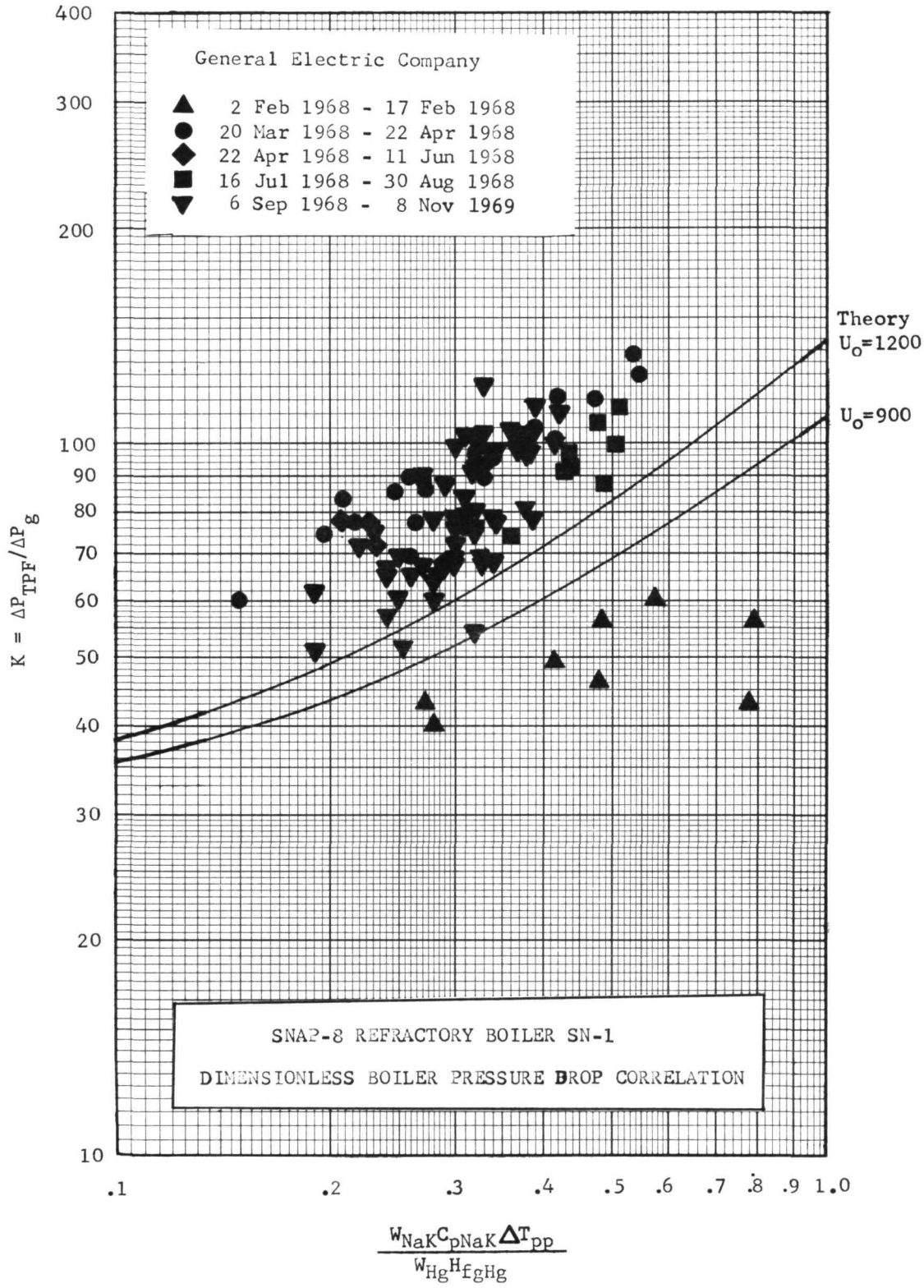

Figure 111. SNAP-8 refractory boiler SN-1 dimensionless boiler pressure drop correlation.

VI. THE CORROSION OF OXYGEN CONTAMINATED TANTALUM IN NaK [8]

Tantalum specimens with homogeneous oxygen concentrations ranging from 50-500 ppm were prepared by contamination at low pressure and subsequently exposed to NaK at 1350°F for 1000 hours to determine the threshold oxygen concentration for corrosion.

Oxygen contaminated specimens were prepared in a high vacuum system (Figure 112). The specimens, measuring 1-inch wide by 22 inches long by 0.040-inches thick were heated by direct resistance. The vacuum chamber was initially evacuated and baked out to achieve a cold wall pressure of 1.5×10^{-9} torr. The specimens were heated to 2400°F and held at a 1×10^{-6} torr pressure maintained by leaking oxygen into the vacuum chamber. The results of this contamination are shown in Table IV. The contaminated specimens for exposure to NaK were suspended from a tantalum wire holder in a tantalum capsule as shown in Figure 113 . The capsules were filled in an electron beam welder at a pressure of 2.5×10^{-5} torr and electron beam welded closed. A total of 28 specimens, as listed in Table V, were exposed to NaK in the tantalum capsules. The specimens were removed from the capsules in a helium environment and cleaned with liquid ammonia.

All the specimens lost weight but the results indicated the higher the initial oxygen concentration of the specimens, the greater the weight loss.

The specimens were bent 120° using a 0.0625-inch radius anvil. The results are shown in Figure 114 . All specimens exhibited ductile behavior. Cracks were noted in the heat affected zone and weld areas of the NaK exposed specimens containing 520 ppm oxygen.

Transverse sections of the NaK exposed tantalum were examined in the as polished and etched conditions and compared to similar specimens which had not been exposed to NaK. Evidence of corrosion was found in tantalum specimens containing 520 ppm and 270 ppm oxygen respectively.

Microhardness traverses were made on specimens before and after exposure to NaK. The hardness and oxygen concentration are summarized in Table VI. The hardness and oxygen concentration of the unwelded specimens was reduced to approximately the same level after exposure to NaK for 1000 hours at 1350°F.

This reduction in oxygen concentration occurred without corrosion in specimens containing less than 270 ppm oxygen before exposure to NaK.

Reductions in the weld and heat affected zone area of welded specimens after NaK exposure were less than for the unwelded specimens.

During NaK exposure of tantalum specimens containing over 270 ppm oxygen, oxygen dissolution and corrosion along the grain boundaries and crystallographic planes would occur. At high temperature, oxygen diffusion and dissolution may occur fast enough to reduce the oxygen concentration in the tantalum region ahead of the advancing corrosion to a value below that necessary for corrosion to occur, thereby preventing corrosion from penetrating very deeply into the specimen.

Results of the tantalum-NaK capsule tests show that oxygen dissolution will occur at the tantalum-NaK interface without corrosion if the oxygen concentration is below 270 ppm.

TABLE IV. OXYGEN CONTAMINATION OF PURE TANTALUM AT 2400°F IN A 1 x 10^{-6} TORR PRESSURE MAINTAINED BY AN OXYGEN LEAK

OXYGEN PARTIAL PRESSURE, TORR	EXPOSURE TIME, HOURS	OXYGEN CONCENTRATION, ppm IN TANTALUM	
		PICKUP	TOTAL
5.2 x 10^{-7}	7	51	115
5.8 x 10^{-7}	11	145	220
4.8 x 10^{-7}	21	220	270
5.2 x 10^{-7}	39	445	520

Average contamination rate 5.4 mg cm^{-2} sec^{-1} $torr^{-1}$

TABLE V. CORROSION OF OXYGEN CONTAMINATED TANTALUM SPECIMENS EXPOSED TO NaK IN TANTALUM CAPSULES

Specimen Condition	Oxygen Concentration, ppm	Welding Atmosphere	NaK Exposure Temperature, °F	NaK Exposure Time, Hrs	Depth of Attack, mils[a]	Weight Loss mg[b]
As-Received	55	Not Welded	1350	1000	No Attack	1.5
As-Received	55	He	1350	1000	No Attack	1.9
As-Received	55	He + 50 ppm Air	1200	100	No Attack	-
As-Received	55	He + 50 ppm Air	1350	1000	No Attack	2.6
As-Received	55	He + 250 ppm Air	1200	100	No Attack	-
As-Received	55	He + 250 ppm Air	1350	1000	No Attack	2.1
Oxygen Contaminated	115	Not Welded	1350	1000	No Attack	3.6
Oxygen Contaminated	115	He	1350	1000	No Attack	5.0
Oxygen Contaminated	115	He + 50 ppm Air	1200	100	No Attack	-
Oxygen Contaminated	115	He + 50 ppm Air	1350	1000	No Attack	4.8
Oxygen Contaminated	115	He + 250 ppm Air	1200	100	No Attack	-
Oxygen Contaminated	115	He + 250 ppm Air	1350	1000	No Attack	4.7
Oxygen Contaminated	220	Not Welded	1350	1000	No Attack	7.8
Oxygen Contaminated	220	He	1350	1000	No Attack	6.7
Oxygen Contaminated	220	He + 50 ppm Air	1350	1000	No Attack	8.7
Oxygen Contaminated	220	He + 250 ppm Air	1350	1000	No Attack	9.1
Oxygen Contaminated	270	Not Welded	1350	1000	2	9.1
Oxygen Contaminated	270	He	1350	1000	3	8.4
Oxygen Contaminated	270	He + 50 ppm Air	1200	100	4	-
Oxygen Contaminated	270	He + 50 ppm Air	1350	1000	3	11.3
Oxygen Contaminated	270	He + 250 ppm Air	1200	100	4	-
Oxygen Contaminated	270	He + 250 ppm Air	1350	1000	3	11.6
Oxygen Contaminated	520	Not Welded	1350	1000	10	20.5
Oxygen Contaminated	520	He	1350	1000	8	17.6
Oxygen Contaminated	520	He + 50 ppm Air	1200	100	20[c]	-
Oxygen Contaminated	520	He + 50 ppm Air	1350	1000	8	19.4
Oxygen Contaminated	520	He + 250 ppm Air	1200	100	20[c]	-
Oxygen Contaminated	520	He + 250 ppm Air	1350	1000	8	20.0

(a) In the Heat Affected Zone adjacent to the weld nugget
(b) Specimen weights, 10-11 grams
(c) Complete penetration of 0.040-inch thick sheet specimen

TABLE VI. OXYGEN CONCENTRATION AND MICROHARDNESS OF UNWELDED TANTALUM SPECIMENS EXPOSED TO NaK FOR 1000 HOURS AT 1350°F.

Specimen	Oxygen Concentration, ppm[(a)]		Microhardness, DPH[(b)]	
	Before Exposure	After Exposure	Before Exposure	After Exposure
As-received	55	3	111	101
Oxygen Contaminated	115	8	123	102
Oxygen Contaminated	220	9	135	101
Oxygen Contaminated	270	7	142	99
Oxygen Contaminated	520	10	171	100

(a) Vacuum Fusion Analysis.

(b) Average of nine equally spaced impressions across the specimen thickness (0.040-inch). No gradients were indicated. 50 Kg Load 50X Objective.

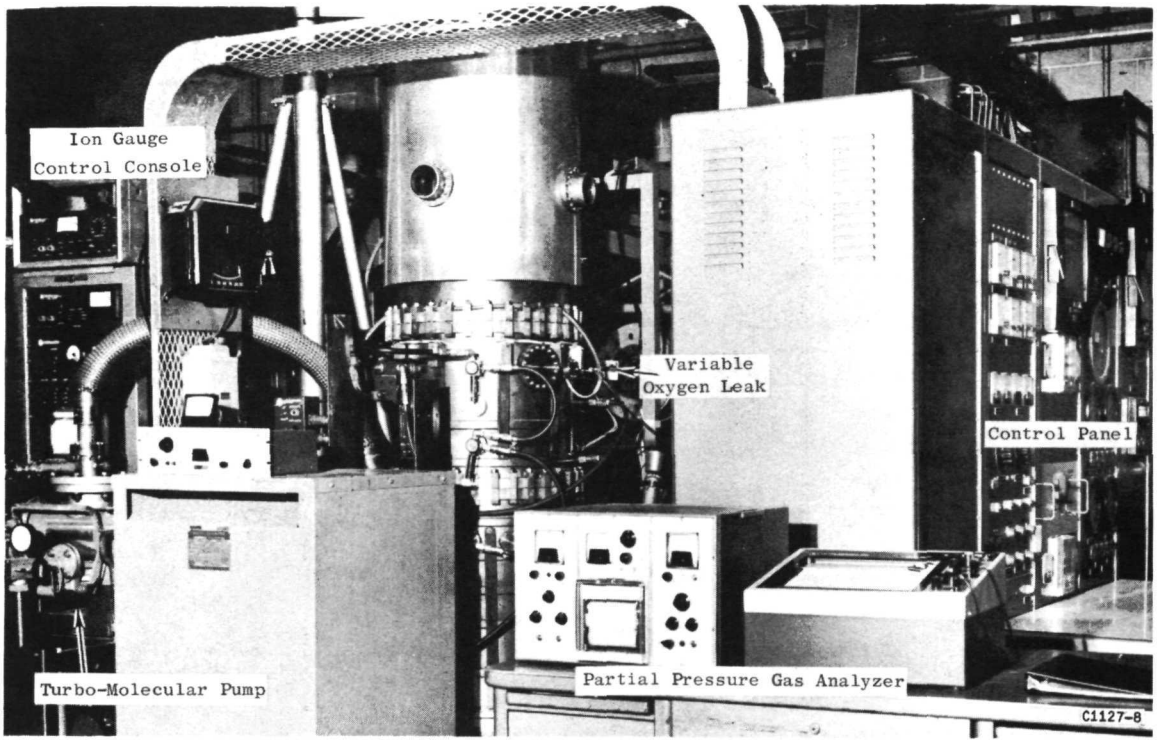

Figure 112. High vacuum (10^{-10} torr range) used for the contamination of tantalum specimens.

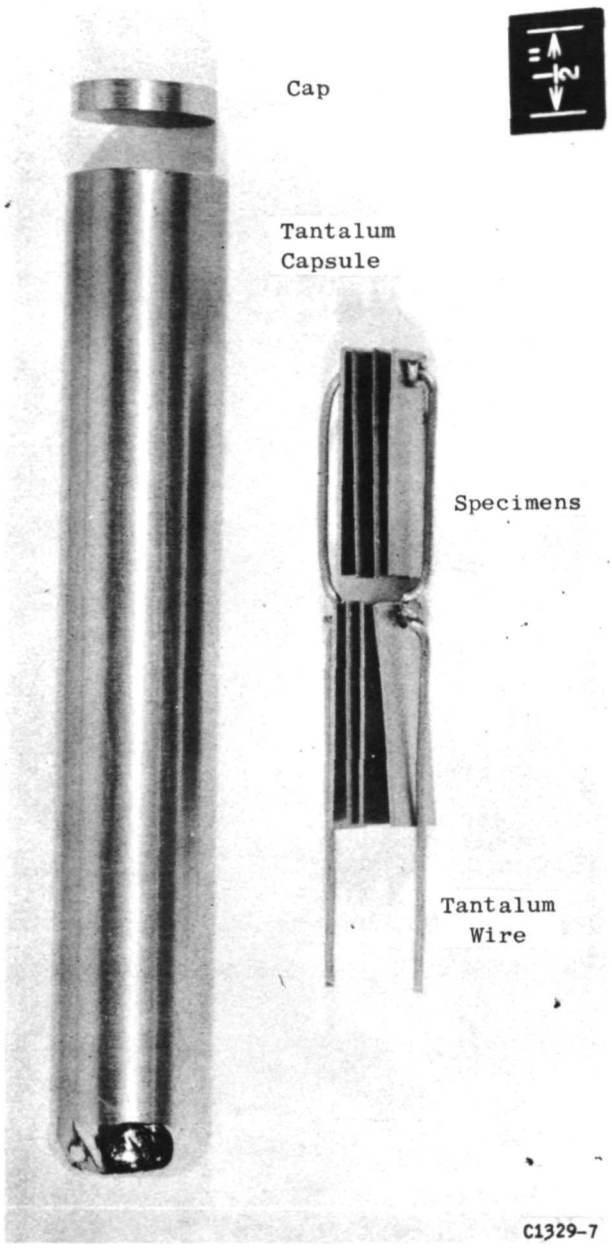

Figure 113. Tantalum capsule and specimens before assembly and filling with NaK.

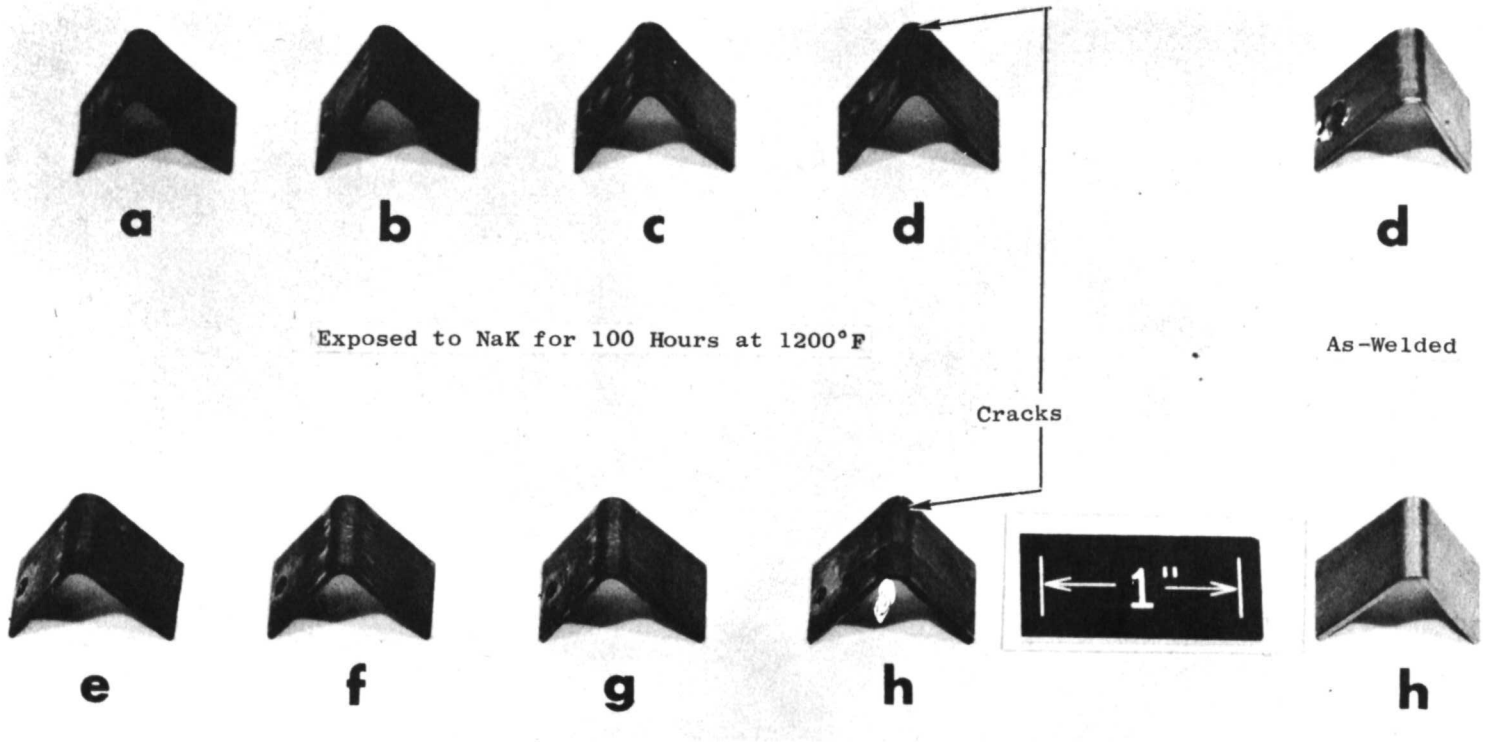

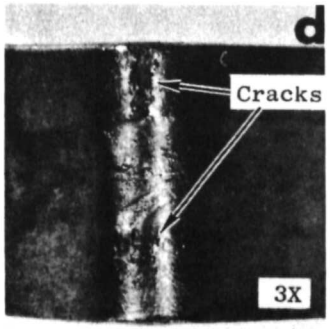

CODE

Specimen	ppm Oxygen in Specimen	ppm Air in Helium Welding Atmosphere
a.	as-recd.	50
b.	115	50
c.	270	50
d.	520	50
e.	as-recd.	250
f.	115	250
g.	270	250
h.	520	250

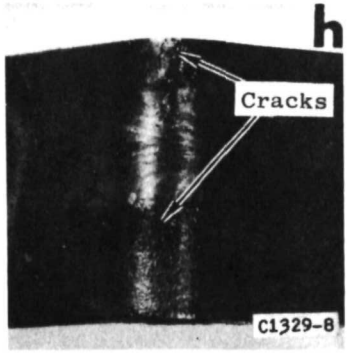

Figure 114. Bend ductility of welded tantalum specimens following exposure to NaK for 100 hours at 1200° F.

VII. THE CORROSION RESISTANCE OF TANTALUM, T-111, and Cb-1Zr TO MERCURY AT 1200°F [9]

Test specimens 0.5-inches wide by 1.0-inch long were sheared from 0.040-inch thick unalloyed tantalum, T-111 alloy (Ta-8W-2Hf) and Cb-1Zr alloy sheet. The specimens were acid cleaned to remove surface contamination. Half of the specimens for each were bent using a 0.406-inch radius ram and a 120° anvil, and the remainder of the specimens were bent with a 0.109-inch radius ram and a 120° anvil to produce strain levels of approximately 5% and 20% as shown in Figure 115. A 5% strain is normally incurred in the bending of tubes for boiler construction.

Part of the bent test specimens was retained in the as bent condition while portions of the remaining specimens were given post bend vacuum anneals. The annealing conditions selected were: 8 hours at 1600°F, 2 hours at 1900°F, and 2 hours at 2200°F. The specimens were encapsulated in a 1.0-inch outside diameter by 0.100-inch wall by 6-inches long seamless tantalum tubing as shown in Figure 116. The capsules were filled with sufficient mercury to cover the specimens at the 1200°F test temperature and the filling was accomplished in a vacuum purged, helium filled, TIG welding chamber. Each tantalum capsule was placed inside a stainless steel capsule and sealed under helium using the identical procedures for the tantalum capsules. Figure 117 shows the capsule test stand.

At the completion of 1000 hours of testing the capsules were sectioned and the residual mercury distilled from the specimens. The cleaned specimens were weighed and no significant weight changes observed. Subsequent fluorescent penetrant inspection revealed the lack of surface cracking. Metallographic examination of the specimens revealed the lack of corrosion or changes in microstructure.

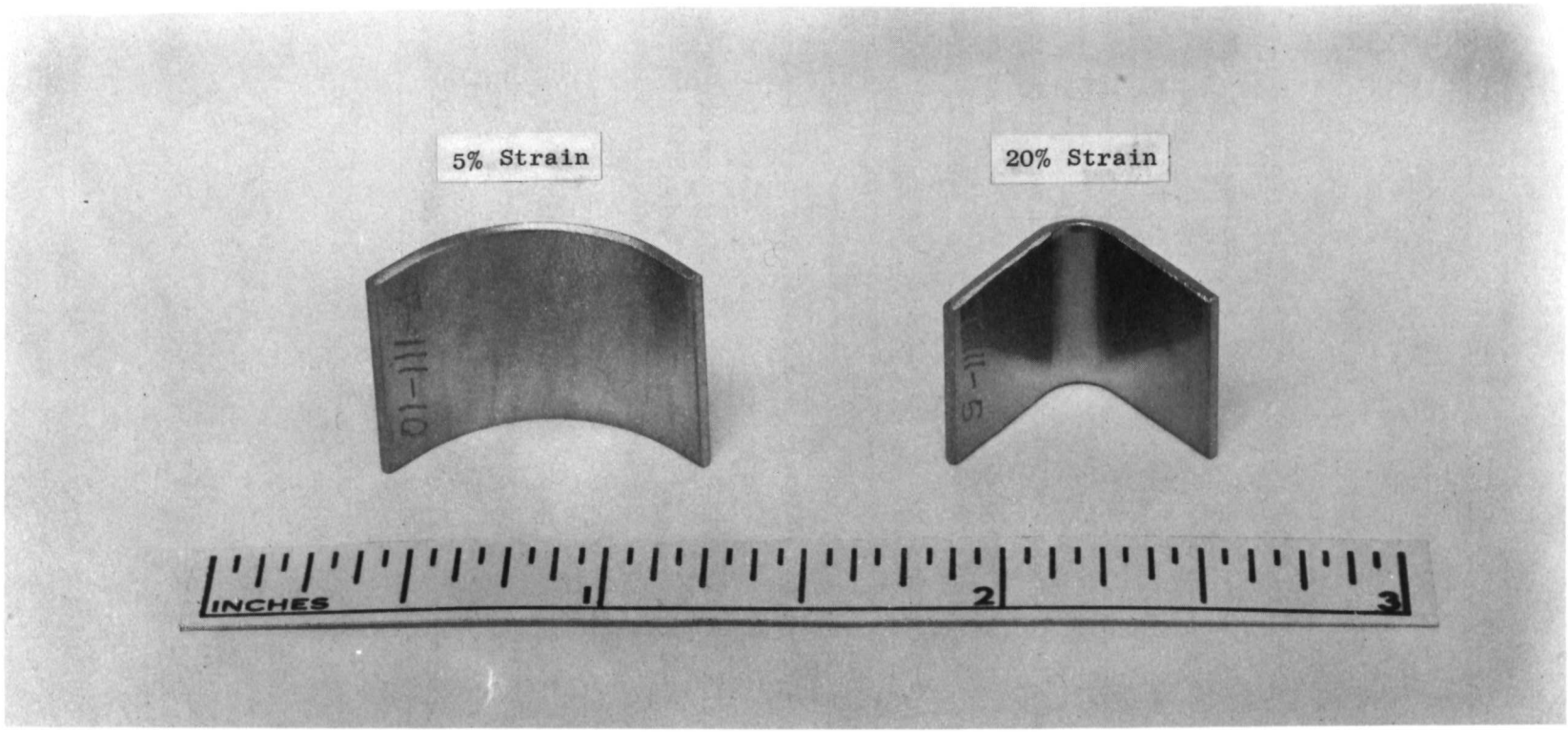

Figure 115. T-111 alloy specimens before exposure to 1200° F mercury.

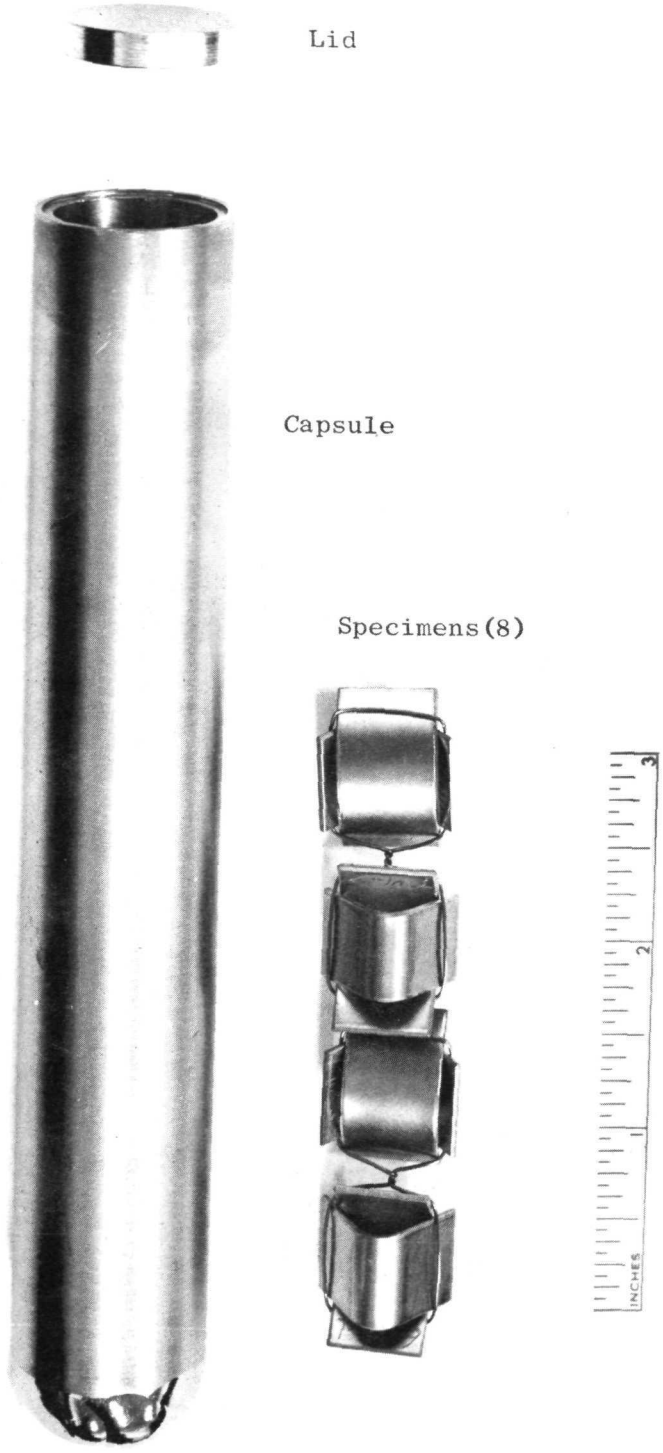

Figure 116. Tantalum capsule and specimens before assembly and filling with mercury.

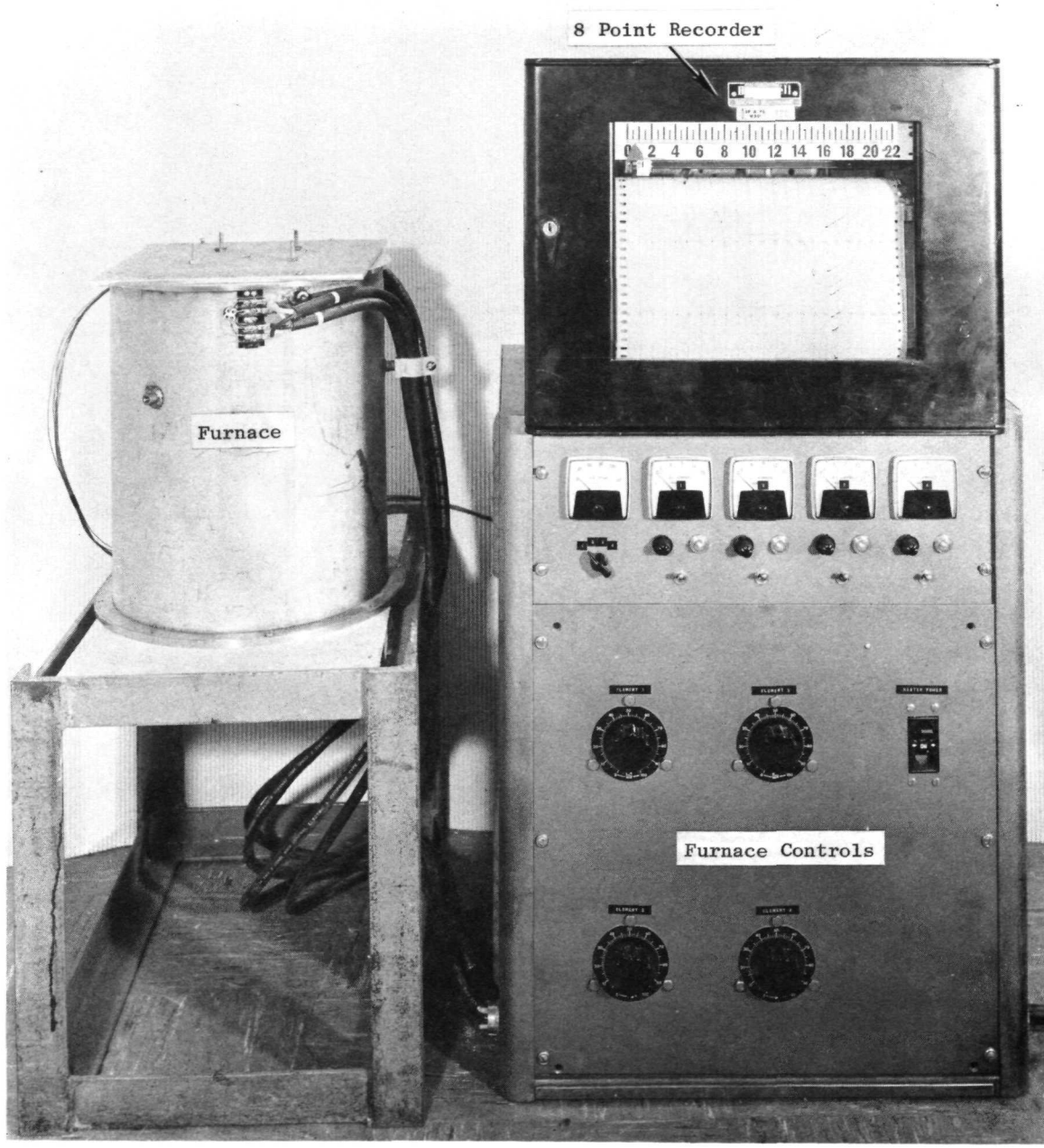

Figure 117. Test facility for isothermal corrosion capsule tests.

VIII. THE EVALUATION OF THE SNAP-8 BOILER[10]

At the completion of the endurance test of the SNAP-8, SN-1 boiler, the facility was secured and the boiler removed for complete non-destructive and destructive evaluation.

The sectioned boiler, shown in Figure 118, was examined visually and found to be in excellent condition. It was observed that after cutting the shell about half way through, the pressure of the tubing cutter would cause the remaining portion of the wall to crack. Metallographic examination of a specimen taken from the outer shell showed an almost continuous grain boundary precipitant as shown in Figure 119 . This precipitate is most likely $M_{23}C_6$ type of carbide phase. Metallographic examination of the OD and ID of the shell revealed little corrosion or oxidation.

A bend specimen of the boiler was bent with the ID in tension over a 1-T anvil and cracked after 100° of bend. There was some loss of ductility of the stainless steel shell material, but it is not detrimental to boiler operation.

The 1-inch OD by 0.035-inch wall Type 321 flattened tubes used to contain the static NaK fluid were found to be covered with NaK oxide in the plug region which was easily removed with a damp cloth. The tubes, except in the plug region, were bright and shiny. The report of the February 17, 1968 boiler failure [5] described a heavy deposit in this region which was mechanically removed. Metallographic examination of this area revealed some attack in the OD of the tubing to a depth of 0.0005-inches as shown in Figure 120. An analysis for interstitial elements in the plug region showed a high oxygen content (201 ppm) and a higher carbon content (279 ppm).

The other stainless parts showed no sign of attack or degradation from either the static or flowing NaK. The inlet section of the boiler, shown in Figure 121, was in good condition and the bellows was not deformed.

Metallographic examination of the tantalum dished head at the boiler inlet showed a minor amount of corrosion on the static NaK side. The attack, shown in Figure 122, penetrates to a depth of 2 mils. The morphology of the corrosion indicates the cause as being a slight contamination of the tantalum surface. The tantalum dished head at the boiler exit showed no sign of attack. The oxygen

oxygen contamination could have occurred during the field repair [5] at which time the dished tantalum head was replaced. Chemical analyses shows the oxygen concentration at the boiler exit to be 10 ppm as compared to 40 ppm at the boiler inlet. Oxygen dissolution as influenced by the higher exit temperature (1300°F) could also explain the difference in oxygen concentration. Figure 122 also shows some surface cracks on the ID of the tantalum orifice. These were probably the result of machining processes and not corrosion.

Metallographic examination of the pretest tantalum tubing used in the fabrication of Boiler SN-1 revealed severe grain boundary attack on both the ID and OD, as shown in Figures 123 and 124. These defects may have resulted from surface contamination during processing and subsequent acid pickling.

Deposits were noted at the exit of the plug on the ID of the tantalum tube as shown in Figure 125. This deposit was water soluble and a spectrographic analysis of the deposit indicated the major constituent to be chromium $>10\%$ with minor amount $<10\%$ of cobalt, iron and nickel. These elements, except for the cobalt, which is a major constituent of L-605, are the major constituents of stainless steel. Stainless steel and L-605 are utilized as piping in the facility.

The tantalum tubes were split longitudinally and removed from the plugs, as shown in Figure 126. Metallographic examination of a section in this area indicated the pretest grain boundary voids but no sign of attack. Liquid metal exposure would tend to accentuate these grain boundary voids; no corrosion was observed.

Both tantalum-316 stainless steel transition joints were evaluated. Helium mass spectrometer testing proved the joints leak tight. Fluorescent penetrant inspection of the joints showed no indication on the brazed joint but one indication on the coextruded joint. Ultrasonic examination of the coextruded joint confirmed the fluorescent penetrant defect and several indications were noted on the brazed joint, particularly in the inner annulus or wide braze section of the joint.

Photomicrographs of the coextruded joint are shown in Figure 127. The separation is 0.016-inches long. A photomicrograph of the worst area of the brazed joint is shown in Figure 128. One void approximately 0.003-inches in diameter is shown and several smaller voids are present.

Post test evaluation of the SN-1 boiler materials following test has indicated the excellent compatibility of the selected materials with NaK and mercury at elevated temperatures. No major corrosion or degradation was observed and all indications point to a 40,000 hour life at observed corrosion rates.

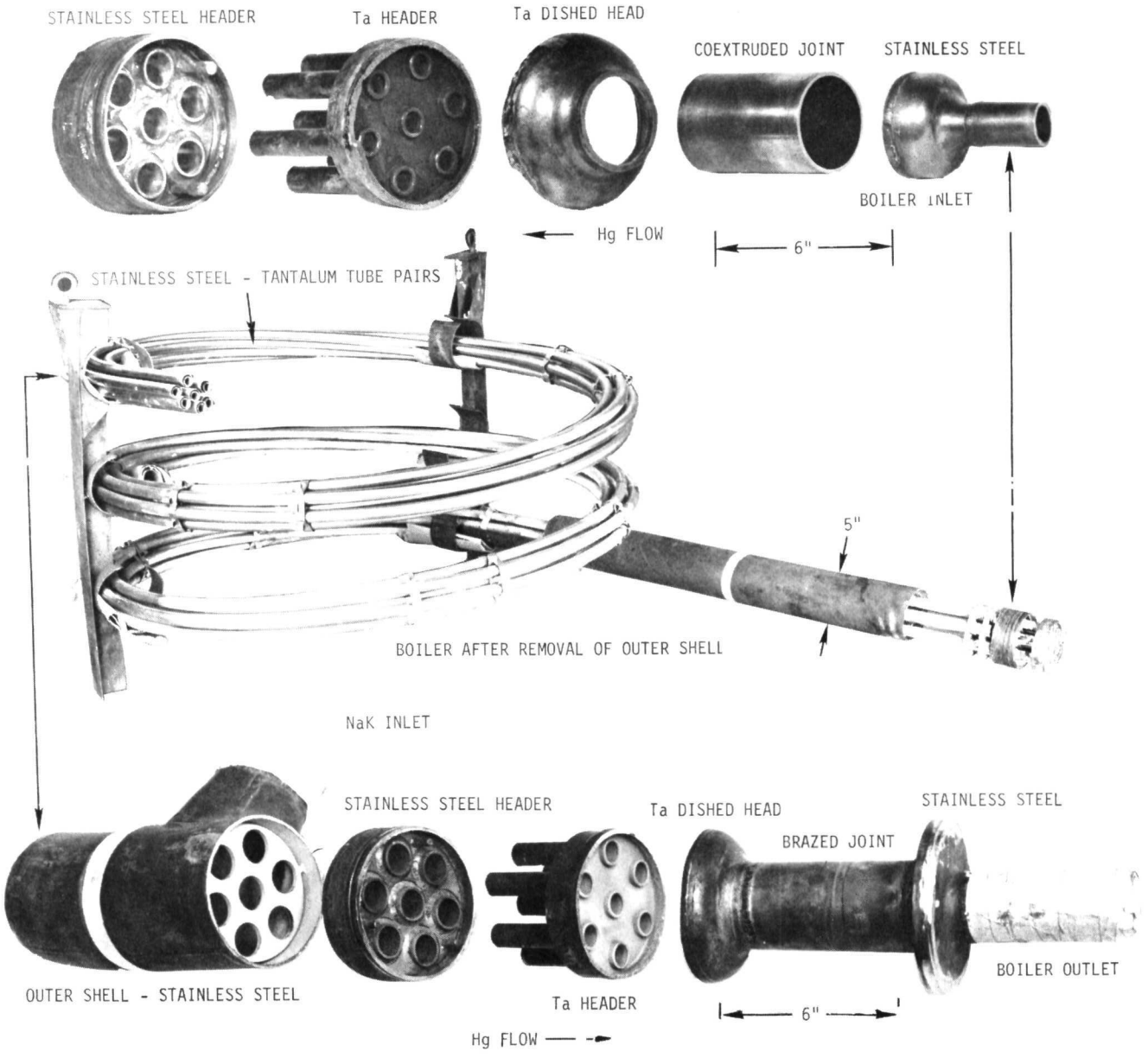

Figure 118. Sectioned SNAP-8 boiler following testing.

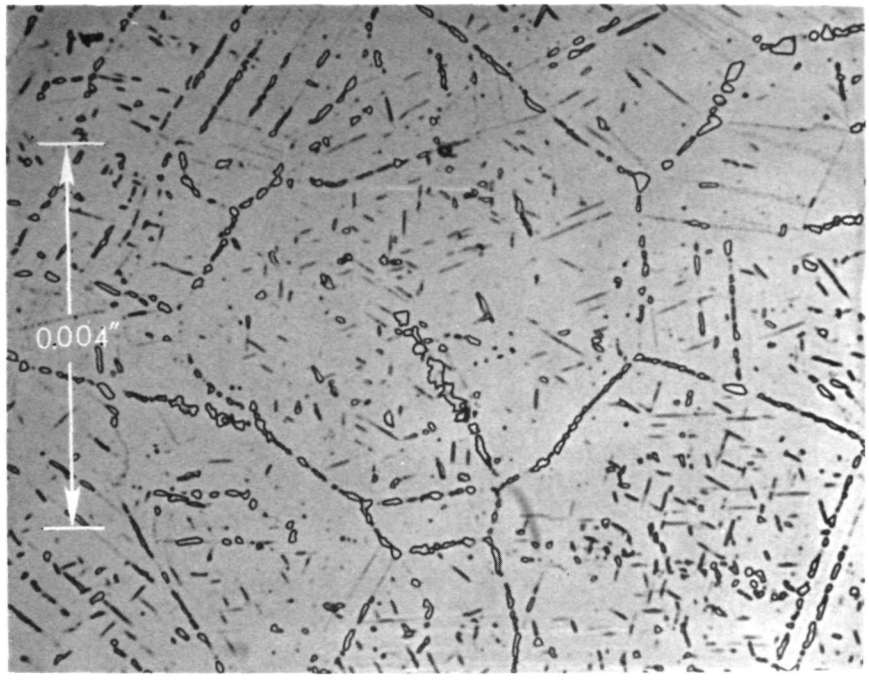

H24041C Etchant: 10% Oxalic

Figure 119. Microstructure of the 316 stainless steel outer tube shell at the NaK inlet of SNAP-8, SN-1 boiler.

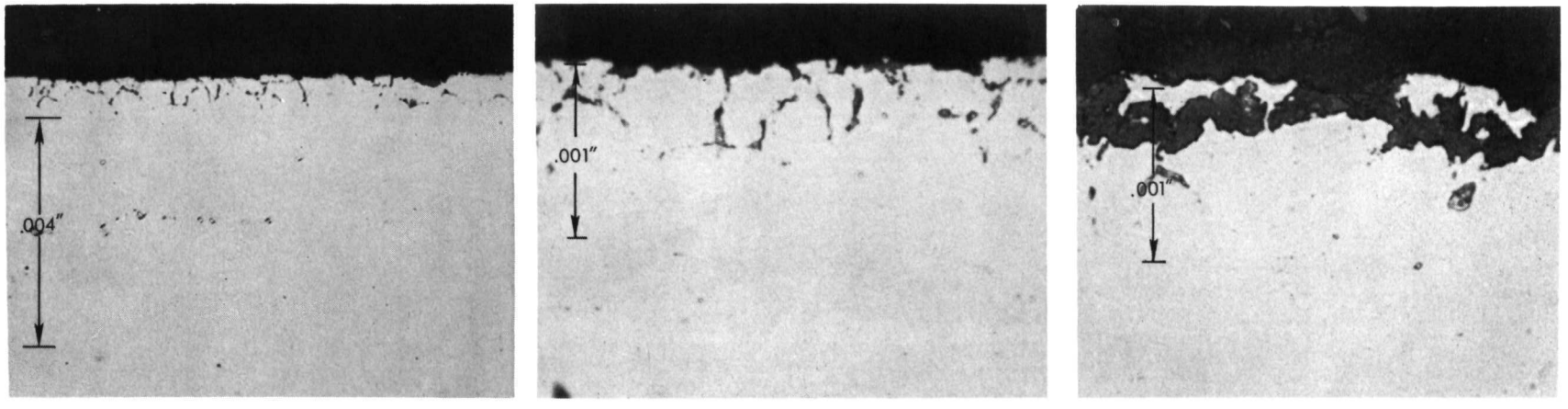

Figure 120. OD of stainless steel tube separating the static and flowing NaK circuits in plug area 2 feet downstream of the header at the boiler inlet.

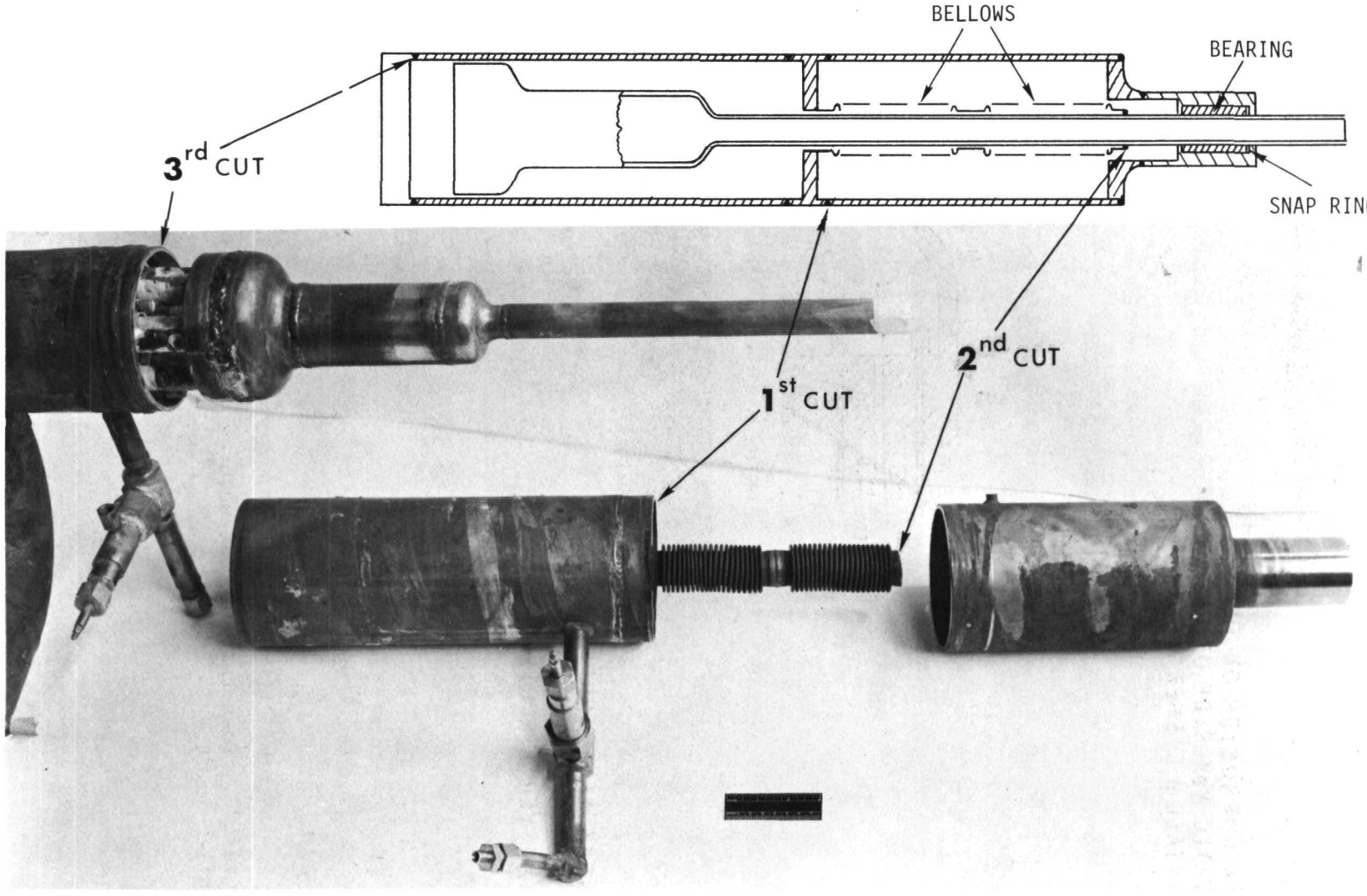

Figure 121. Sectioning of the SNAP-8 boiler for evaluation - removal of the outer stainless steel shell at the boiler inlet.

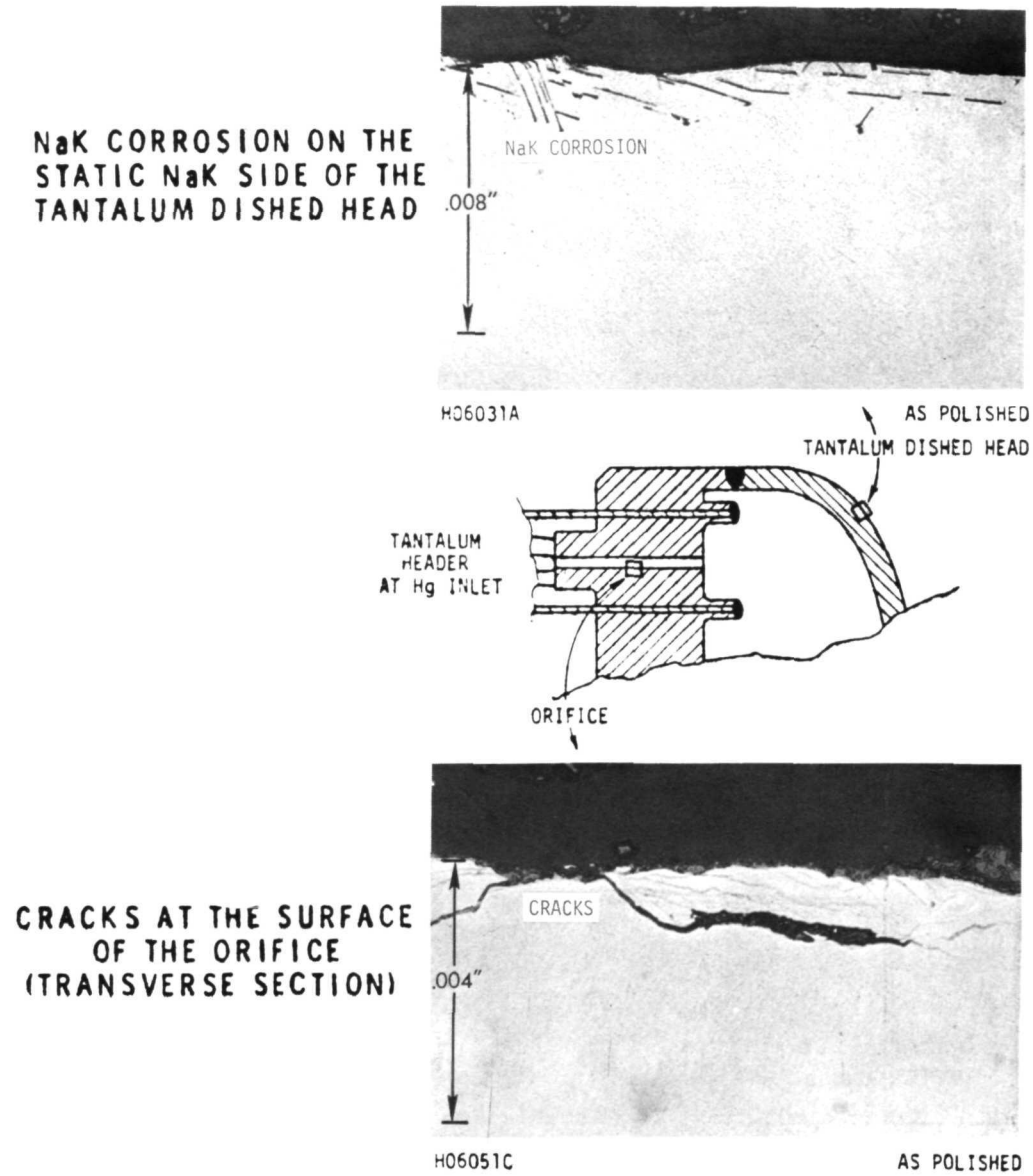

Figure 122. Post-test microstructures of the tantalum at the boiler inlet.

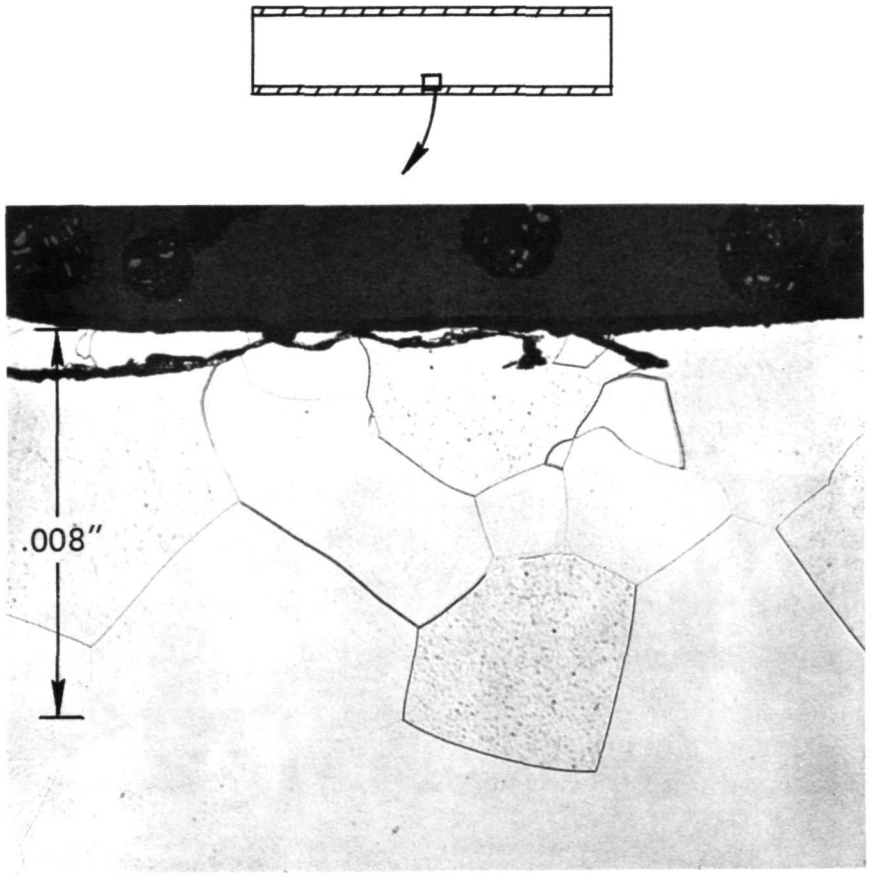

H24021A ETCHANT: $30NH_4F$, $50HNO_3$, $20H_2O$

Figure 123. Tantalum tube - 0.670" ID x 0.040" wall used in the construction of the SNAP-8, SN-1 boiler in the pretest condition.

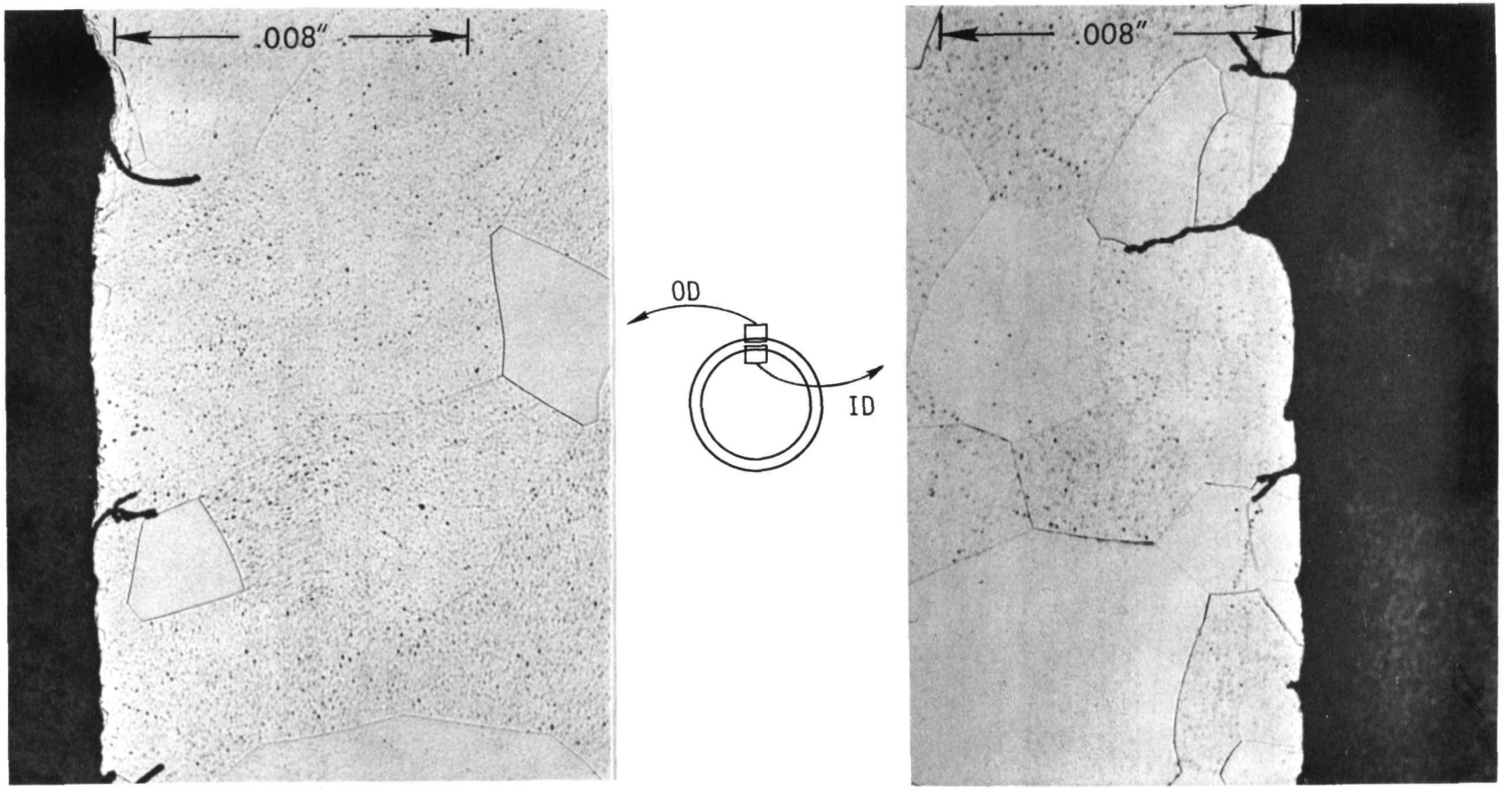

H24021B ETCHANT: $30NH_4F$, $50HNO_3$, $20H_2O$

H24021C ETCHANT: $30NH_4F$, $50HNO_3$, $20H_2O$

Figure 124. Tantalum tube - 0.670" ID x 0.040" wall used in the construction of the SNAP-8, SN-1 boiler in the pretest condition.

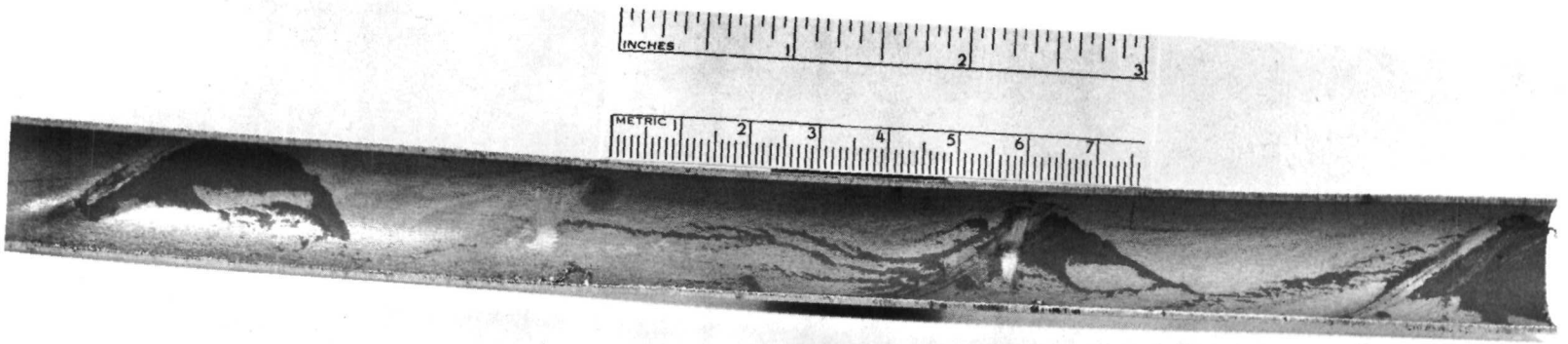

Figure 125. Dark gray deposit on the ID surface of a tantalum boiler tube at the exit of the plug section.

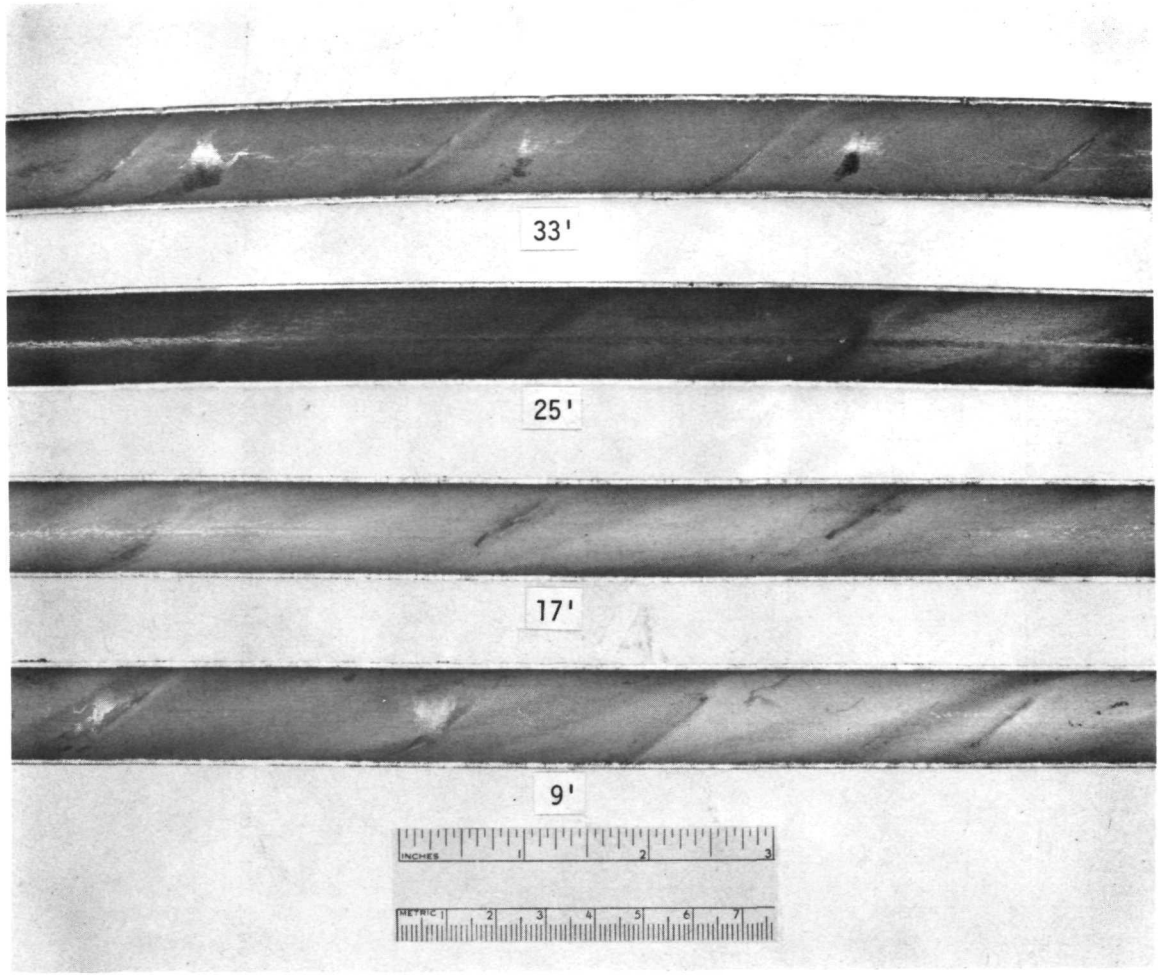

Figure 126. ID of tantalum tube exposed to mercury at distances marked from the header at the boiler inlet.

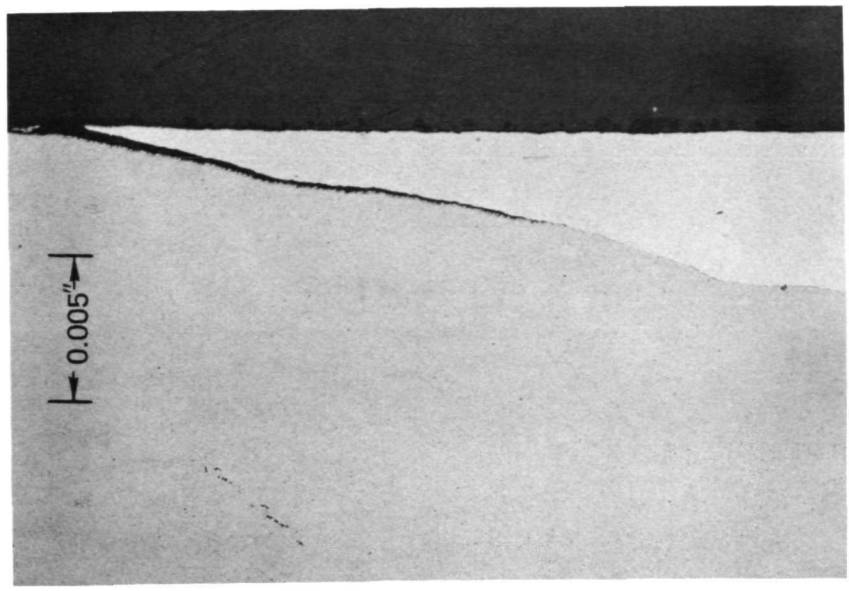

H92021B

ETCHANT: NH_4F
HNO_3
H_2O

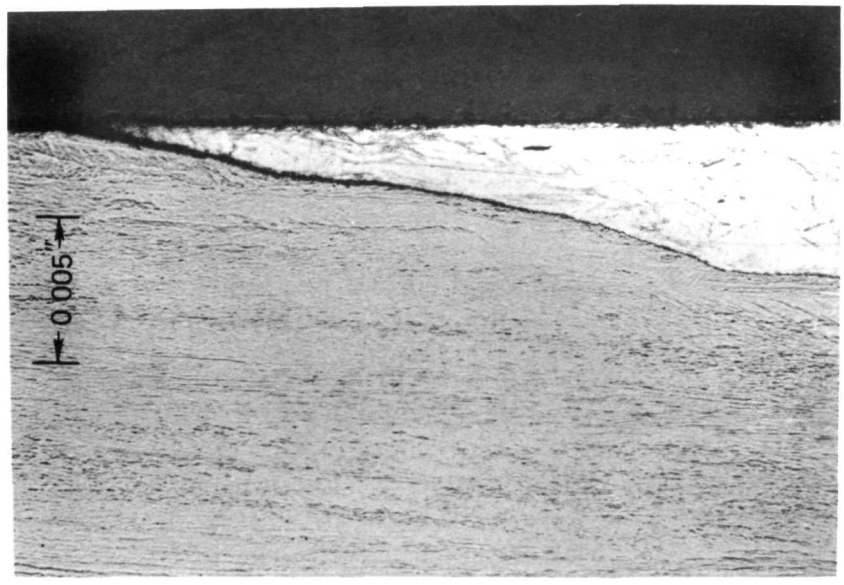

H92021A

AS POLISHED

Figure 127. Separation of 316 stainless steel feather-edge from tantalum on OD of coextruded joint from inlet of SN-1 boiler.

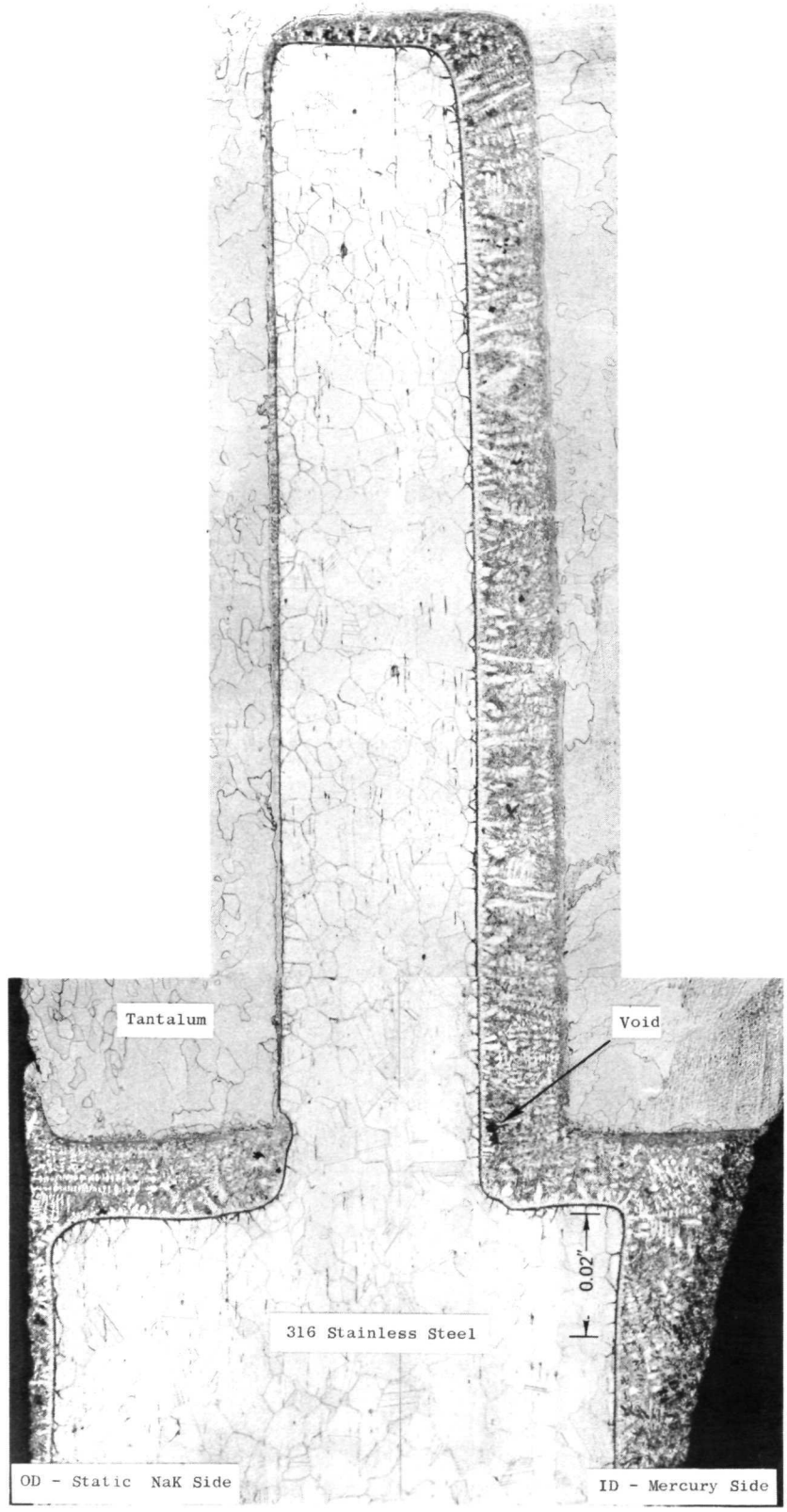

Figure 128. Microstructure of the Ta/316 SS brazed joint from mercury exit of SN-1, SNAP-8 boiler.

IX. MERCURY THERMAL SHOCK TESTING OF 2-1/2 INCH DIAMETER BIMETALLIC JOINTS FOR SNAP-8 APPLICATION [11]

The startup sequence of the SNAP-8 power conversion system subjects the entire boiler to a severe thermal shock when 70°F mercury is injected into the 1300°F boiler. In the present boiler design, 2.50-inch diameter tantalum-316 stainless steel tubular transition joints are required at both the inlet and exit of the boiler. For this reason representative joints utilizing brazing and coextrusion techniques were prepared for thermal shock testing to determine their reliability.

The brazed joint, shown in Figure 129, was vacuum brazed at 2160-2180°F for five minutes using a cobalt base filler alloy. Following brazing, the joint was nondestructively tested utilizing dye penetrant, ultrasonic and mass spectrometer techniques. No rejectionable defect was observed. The coextruded joint was not inspected prior to test.

The test assembly, shown in Figure 130, consisted of welding the brazed joint and the coextruded joint together at the tantalum ends. The coextruded joint was positioned at the test section inlet and an 0.060-inch diameter orifice installed downstream of the two joints to restrict the flow of mercury through the test section and to suppress film boiling of the mercury in the joint areaa. A vacuum jacket surrounds the bimetallic joints to prevent oxygen contamination of the tantalum during test. A bellows is used to couple the vacuum jacket and the test section together in order to accommodate the differential thermal expansion between the vacuum jacket and the test section during cycling. The joints were heated electrically by a ceramic heater which was wrapped around the vacuum jacket. Chromel alumel thermocouples were attached to the stainless steel and tantalum section of each joint. Test temperatures were recorded on a high speed oscillograph which allowed the temperature transient of each joint to be compared.

The thermal shock test facility is shown in Figure 131 and consists of a mercury EM pump, the test section, storage tank and a water cooled heat exchanger. An evacuation and gas pressurization port was used to evacuate the loop before the test and to pressurize the loop with helium for mass spectrometer testing at specified intervals during the test.

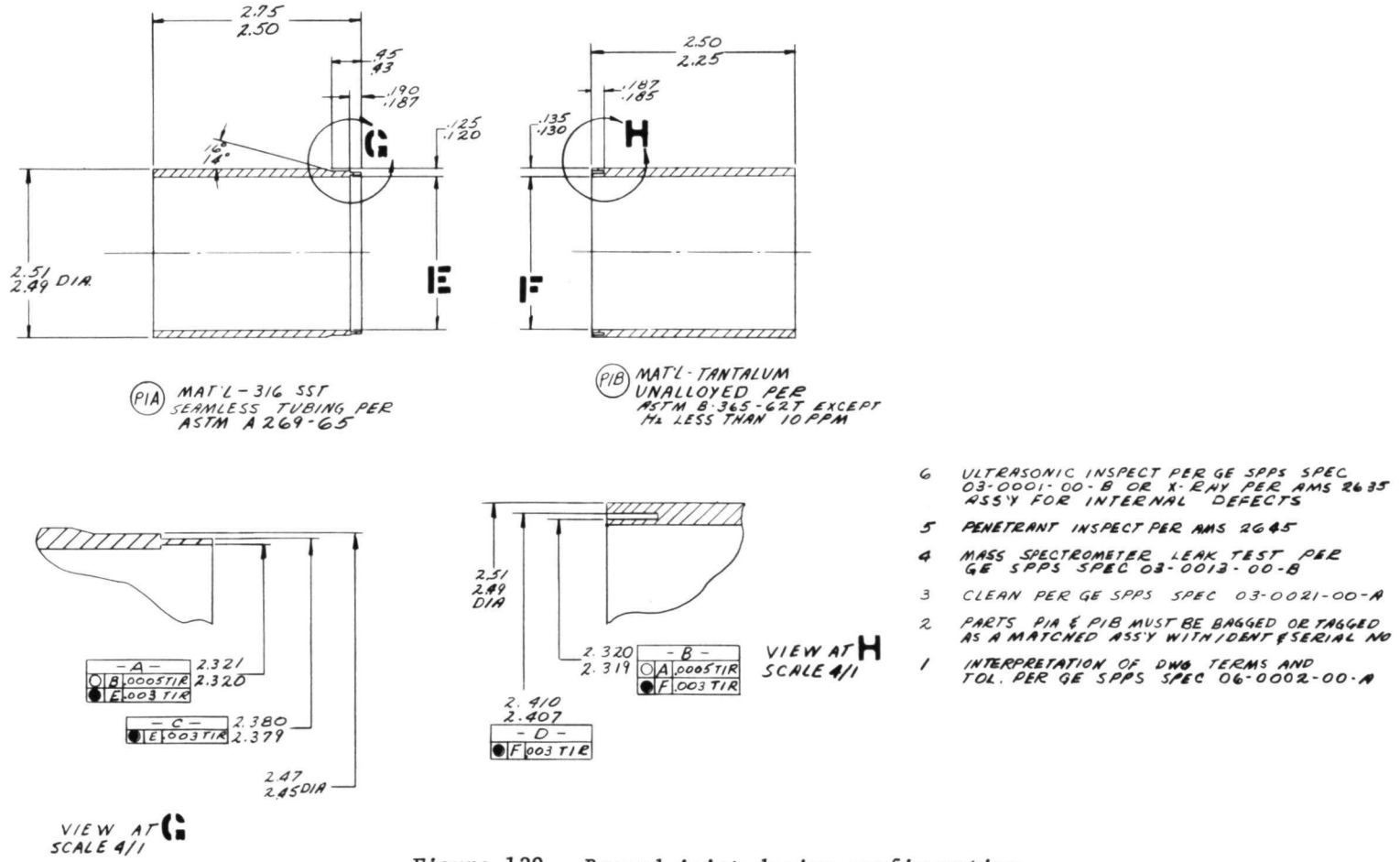

Figure 129. Brazed joint design configuration.

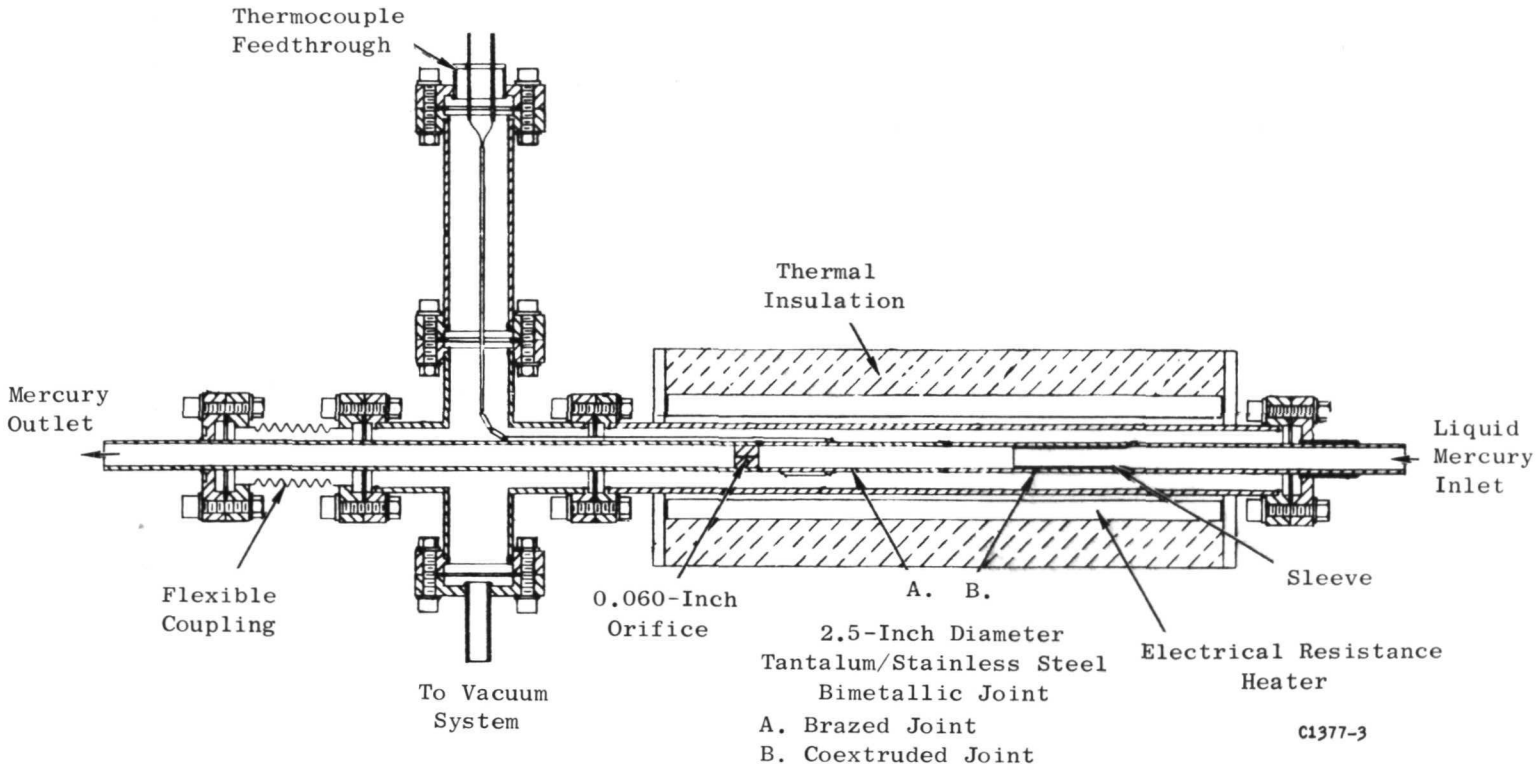

Figure 130. Bimetallic joint thermal shock test section.

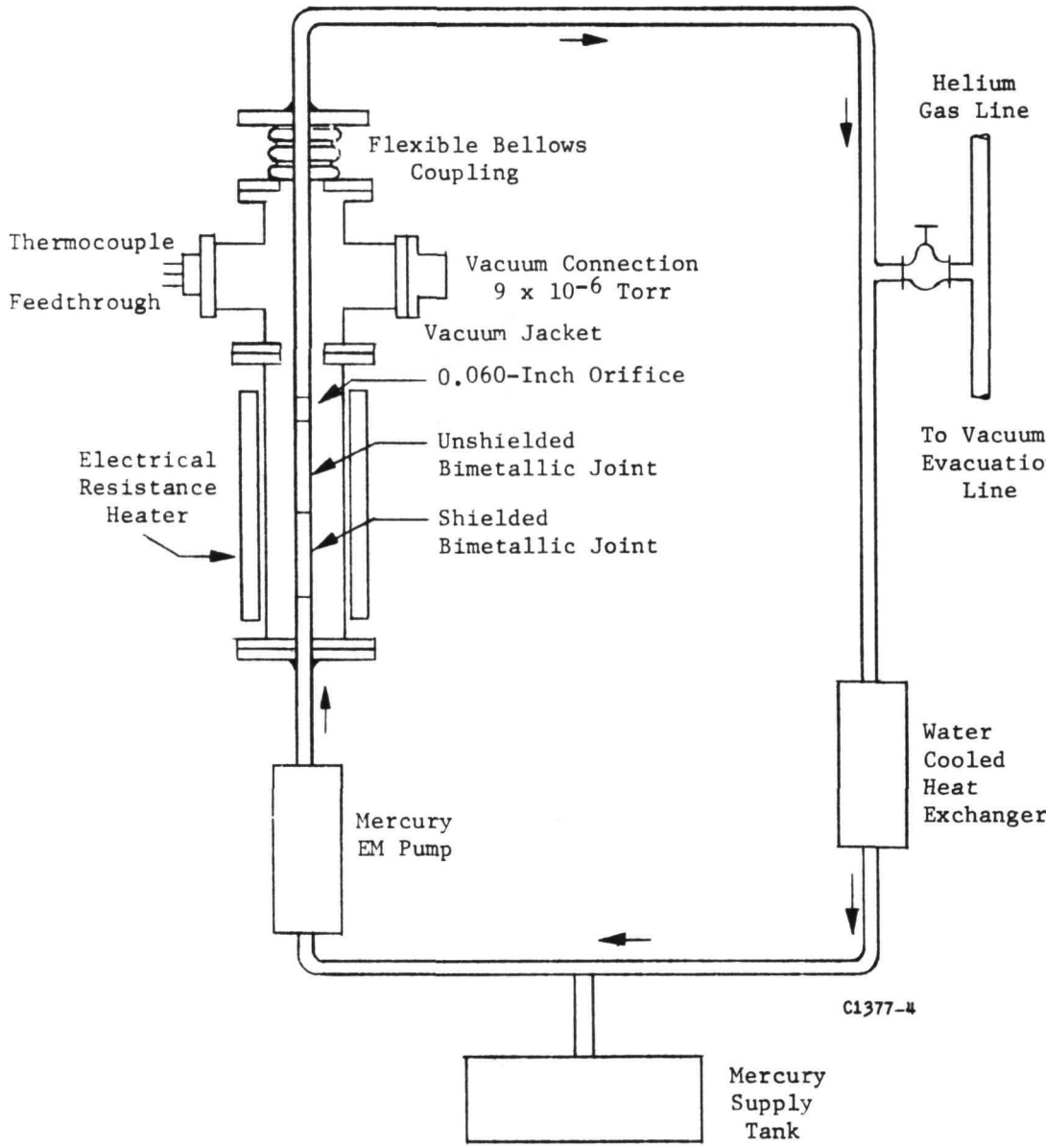

Figure 131. Schematic tantalum/type 316 stainless steel bimetallic joint mercury thermal shock test facility.

A typical thermal shock cycle, shown in Figure 132, consisted of heating the bimetallic joints to 1300°F in 30 minutes and maintaining this temperature for 1 hour. The mercury pump was activated and 300°F mercury at 325 psig was forced into the test section. Mercury flow was maintained for 30 minutes before the pump was secured and the mercury allowed to drain from the test section. Electric heat was constant throughout the program except for mass spectrometer tests.

The test program was to consist of 100 thermal cycles with helium mass spectrometer testing to occur after 5, 10, 25, 50 and 100 cycles. At the completion of the 55th cycle, a pressure rise was noted in the vacuum jacket. Subsequent helium mass spectrometers testing confirmed the leak and the bimetallic joints were removed from the vacuum jacket. The failure was observed to have occurred in the coextruded joint at the interface between the tantalum and the stainless steel. Metallographic examination of the coextruded joint indicated a void in the interface between the stainless steel and the tantalum as shown in Figures 133 and 134.

A typical thermal transient of the test section is shown in Figure 135. The coextruded joint was more severely shocked than the brazed joint which was positioned downstream. The probable reasons for the variation in their cooling rate can be attributed to the fact that the mercury vaporized as it entered the test section and a momentary pulse in mercury is observed. Also, the brazed joint is thicker than the coextruded joint causing a decrease in cooling rate.

The coextruded joint was replaced by a brazed joint and thermal cycling resumed. The first brazed joint was cycled 155 times while the replacement joint was cycled a total of 100 times without failure. Subsequent metallographic examination showed the brazed joints to be in excellent condition. A typical thermal transient is shown in Figure 136 and the difference in temperature decrease is attributed to their respective locations.

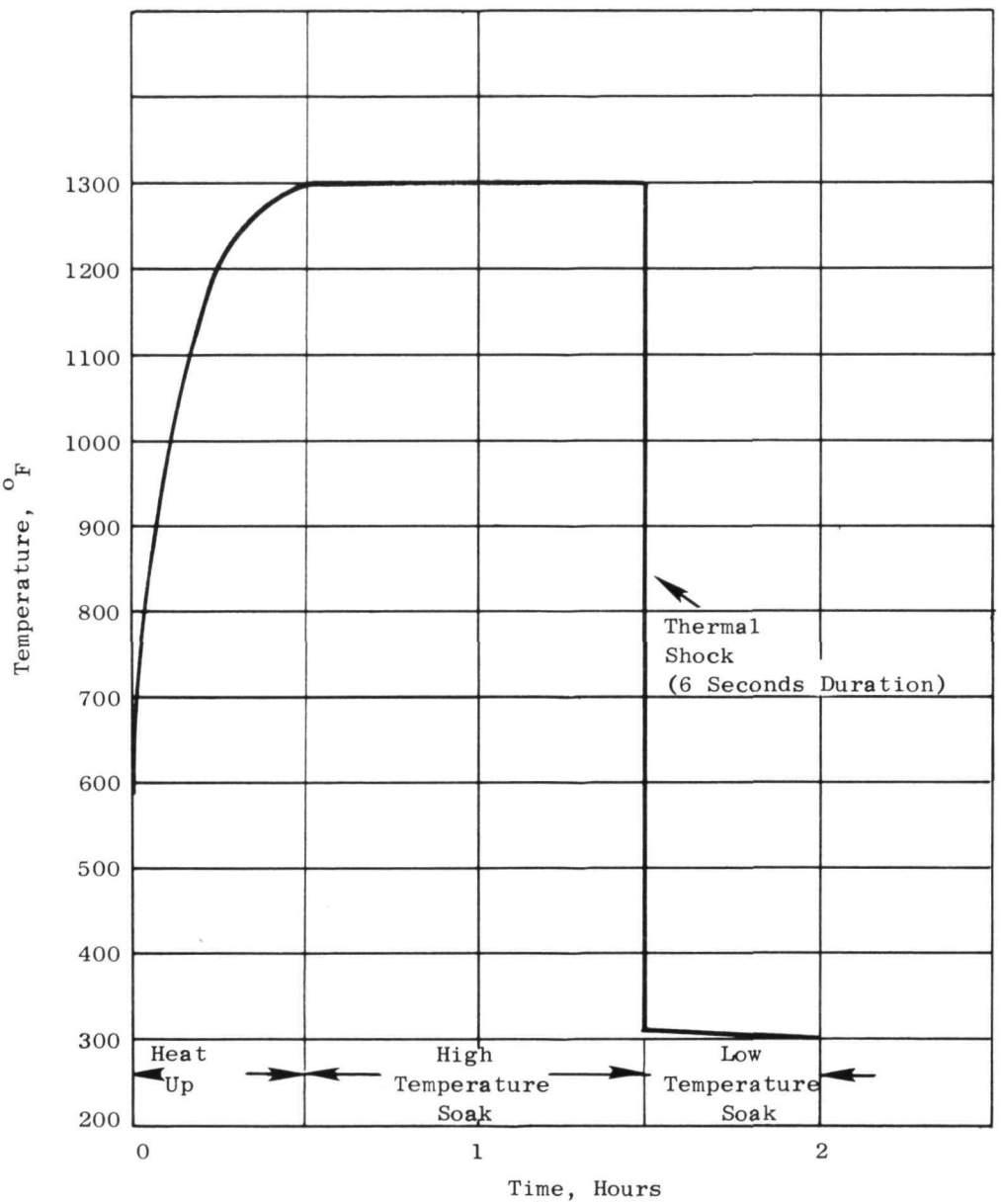

Figure 132. Typical thermal shock cycle of a $2\frac{1}{2}$-inch diameter, SNAP-8 type, tantalum/type 316 stainless steel bimetallic joint.

Transverse Section

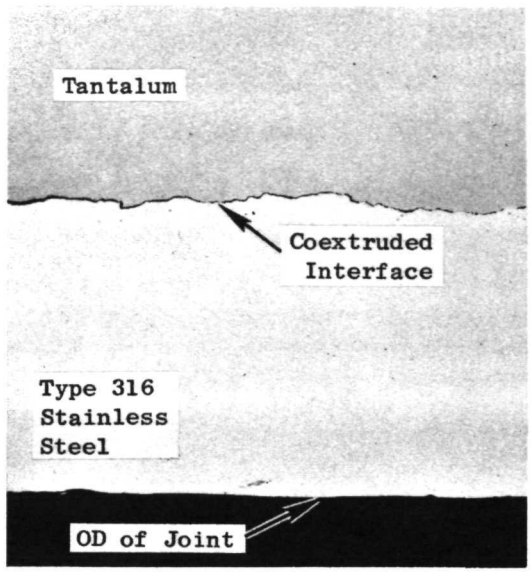

Unetched
F900311

Mag.: 50X

Longitudinal Section

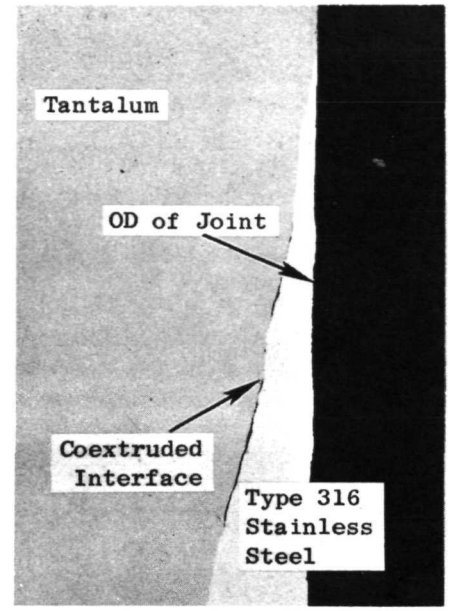

Unetched
F900611

Mag.: 50X

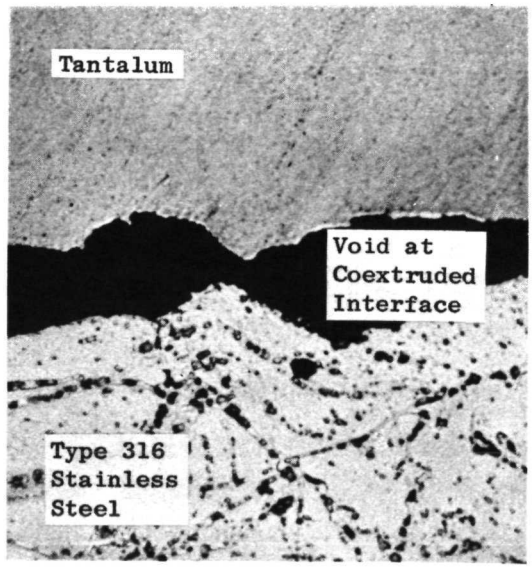

Etchant: 10 Oxalic
100 H_2O
Electrolytic
F900313

Mag.: 1000X

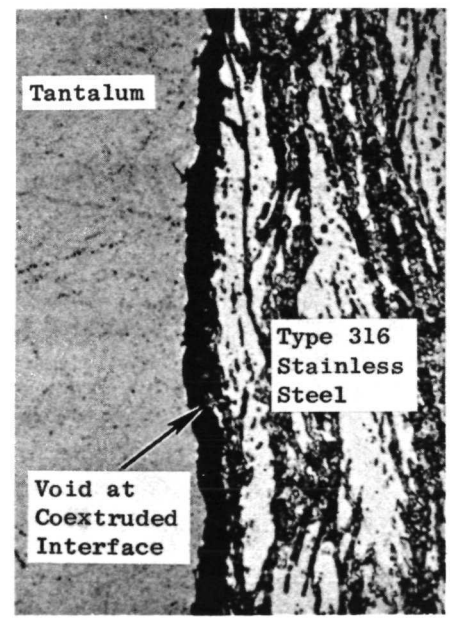

Etchant: 10 Oxalic
100 H_2O
Electrolytic
F900614

Mag.: 1000X

Figure 133. Typical microstructures in joint area coextruded tantalum/ type 316 stainless steel joint after mercury thermal shock test.

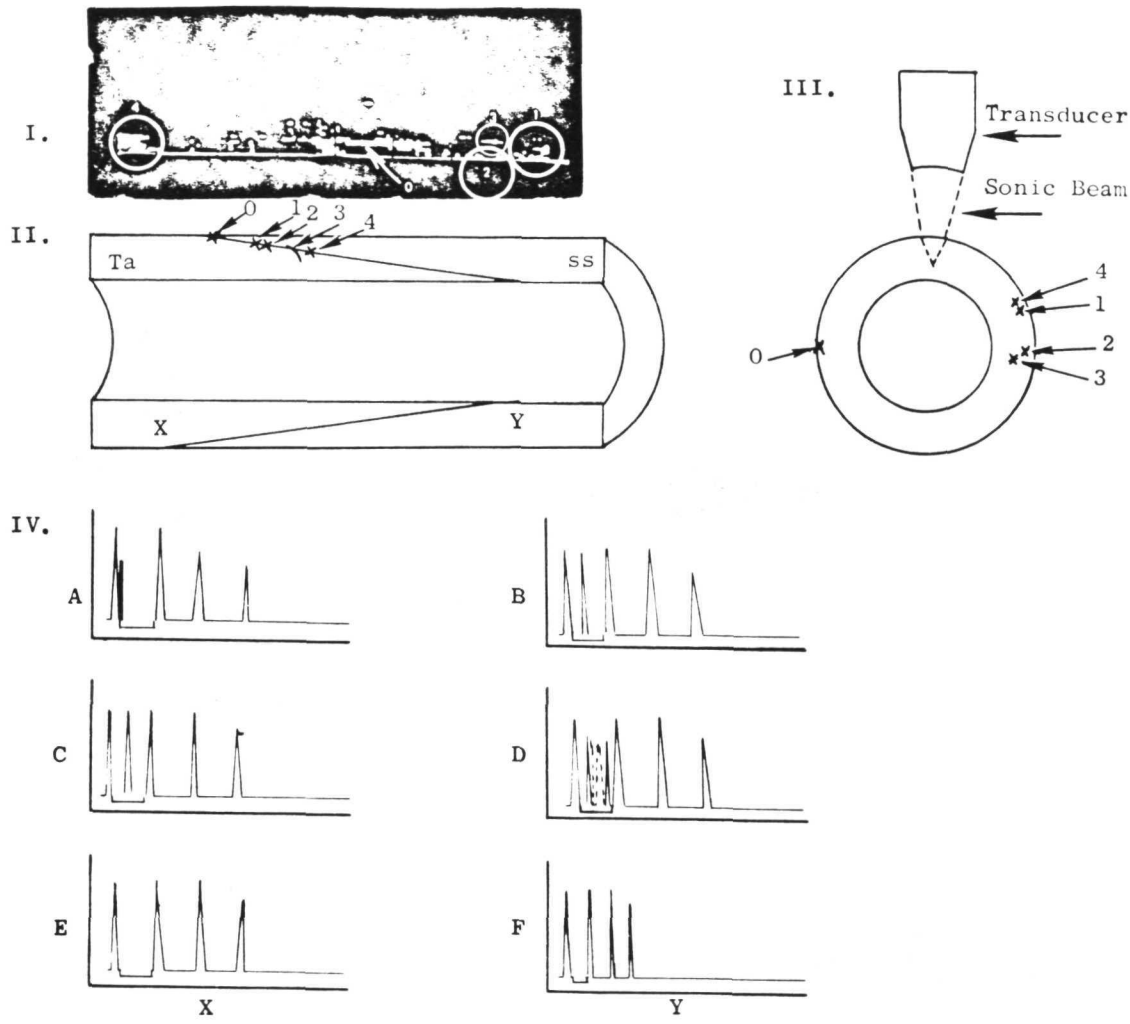

I. C-scan recording depicting areas of interface discontinuity. White indicates response areas.

II. Longitudinal cross section indicating depth of indications relative and wall thickness. Note depth of #3

III. Transverse cross section of joint indicating depth of indication and method of ultrasonic inspection.

IV. A-scan presentation of A. defect #0 near OD B. defect #2 depth C. defect #1 & 4 depth D. defect #3 change of depth E. & F. change of time base due to velocity change created by change of ratio of Cb-1Zr to S.S.

Figure 134. Presentation from ultrasonic inspection of coextruded tantalum/type 316 stainless steel joint after mercury thermal shock test.

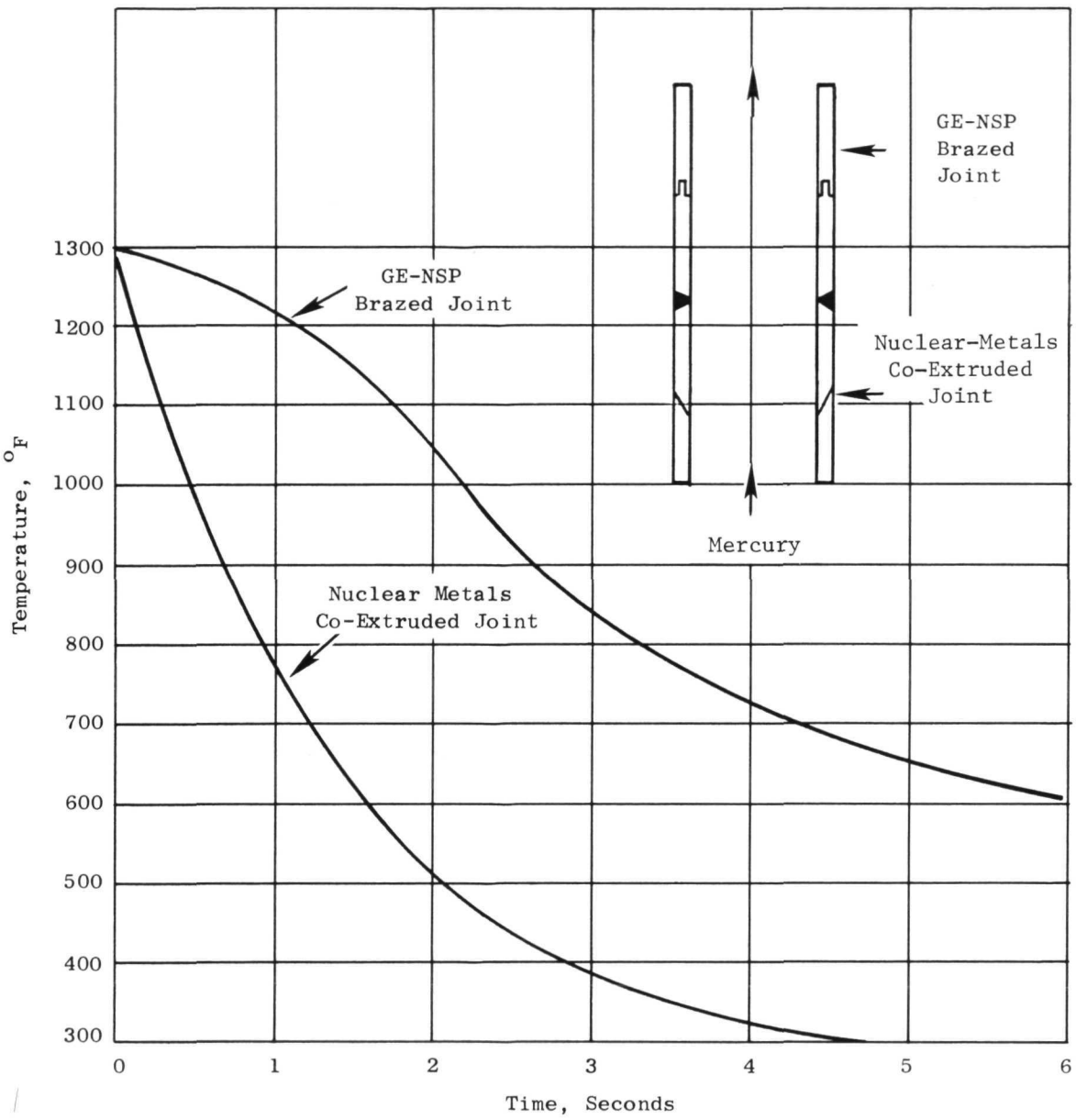

Figure 135. Transient temperatures of $2\frac{1}{2}$-inch diameter tantalum/Type 316 stainless steel coextruded and brazed joints.

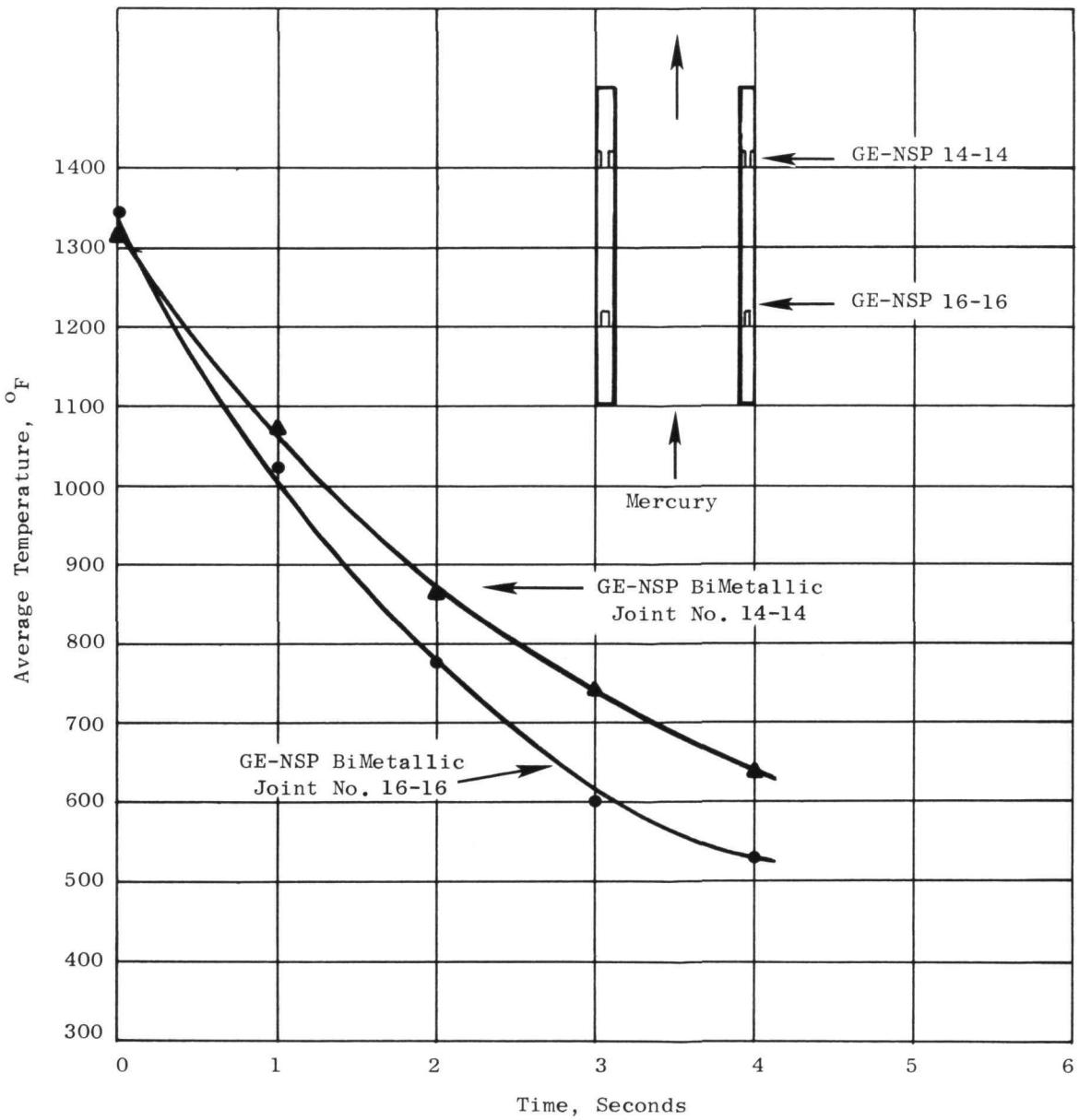

Figure 136. Transient temperature of $2\frac{1}{2}$-inch diameter, tantalum/Type 316 stainless steel brazed joints.

X. THE SHELL SIDE HYDRAULIC TESTS OF A FULL SCALE SNAP-8 MULTIPLE TUBE BOILER[12]

A series of shell side flow studies of a model boiler using water were conducted to evaluate the frictional characteristics of the SNAP-8 boiler. The test model is shown in Figure 137 .

Nine helical wire coils were used for flow studies. The wire coils were used as turbulence promoters by installing them around the tube bundle next to the shell. The various helices were used to determine the mixing versus pressure drop relationship as shown in Figure 138 which shows that a pitch to diameter ratio of about two is a good compromise for minimizing pressure drop and promoting good mixing. Three different geometries of tube supports (Figure 139) were flow tested. The results of these tests are plotted in Figure 140 which shows that spacer #2 has the lowest loss coefficient.

Shown in Figure 141 is an illustration showing the lack of mixing at the NaK exit of the boiler. This poor mixing is a good reason for the poor shell temperature distribution in this area. The temperature distribution from boiler testing is shown in Figure 142. A plexiglass flow model (Figure 143) was constructed to provide a manifold at the exit to promote good mixing. The manifold was tested, and shown in Figure 144 is an illustration of the results showing good mixing.

The results of this test were incorporated in SNAP-8, SN-4.[13] Boiler SN-4 was tested at AGC and it appears that the problems associated with boiler SN-1 namely, poor tube support and the temperature maldistribution in the high heat transfer zone, have been alleviated.

NOMENCLATURE

SECTION X

Symbols	Description	Dimensions
A_F	Net Flow Area	in^2
c	Clearance between the Shell I. D. and Bundle Diameter	inch
d_w	Wire Coil Diameter	inch
D	Diameter	inch
D_e	Equivalent Diameter	inch
D_s	Shell Inside Diameter	inch
K	Loss Coefficient	dimensionless
K*	Loss Coefficient based upon Shell Side Velocity Head	dimensionless
ΔP	Measured Pressure Drop	psi
N_{Re}	Reynolds' Number, $\frac{\rho D_e V}{\mu}$	dimensionless
V	Shell Side Average Velocity	ft/sec
ρ	Density	lb/ft^3
μ	Absolute Viscosity	lb/hr-ft

Subscripts

ax	Axial Flow
sh	Shell Side
sp	Spacer
wc	Wire Coil

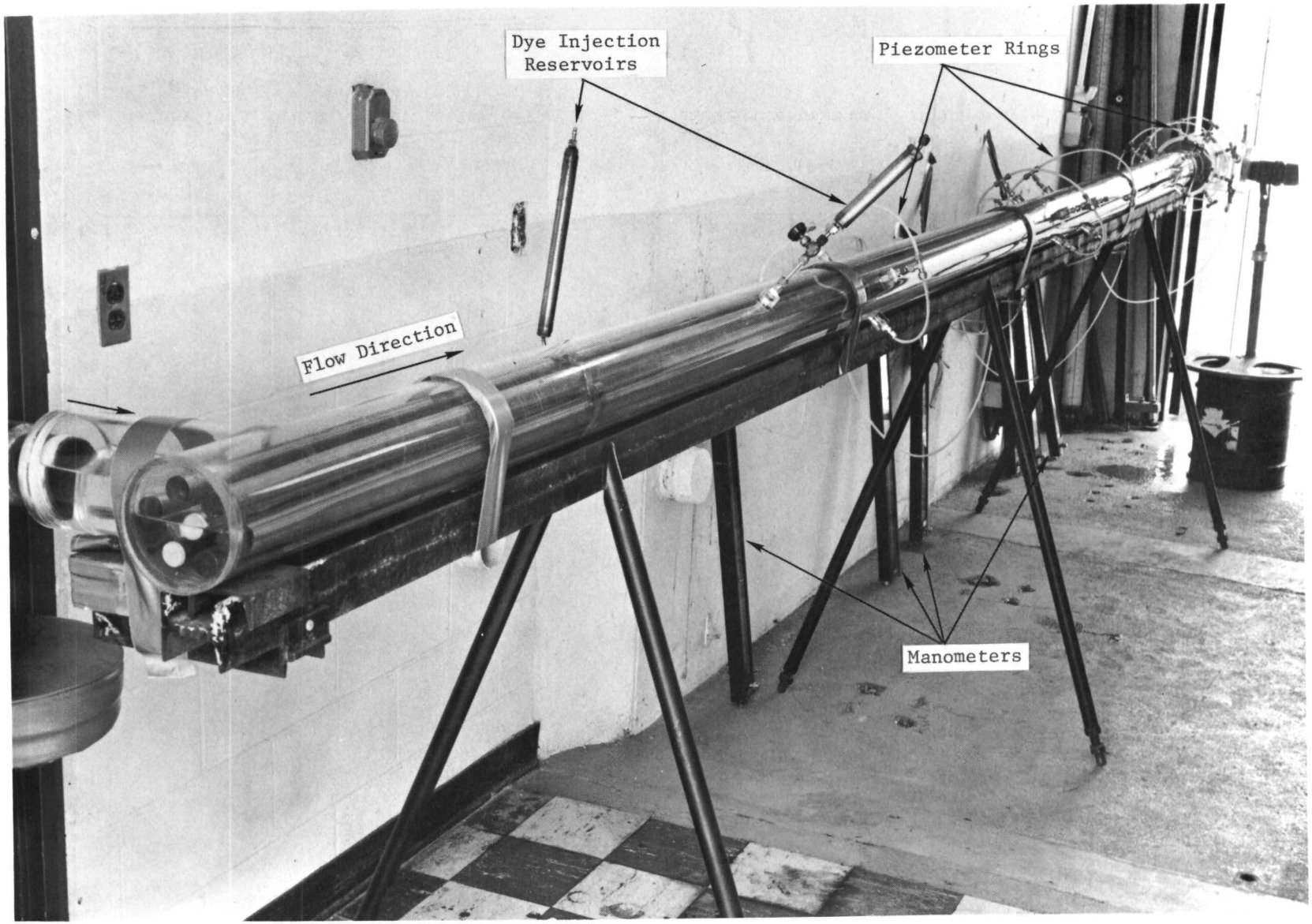

Figure 137. Photographic view of the shell side hydraulic test setup.

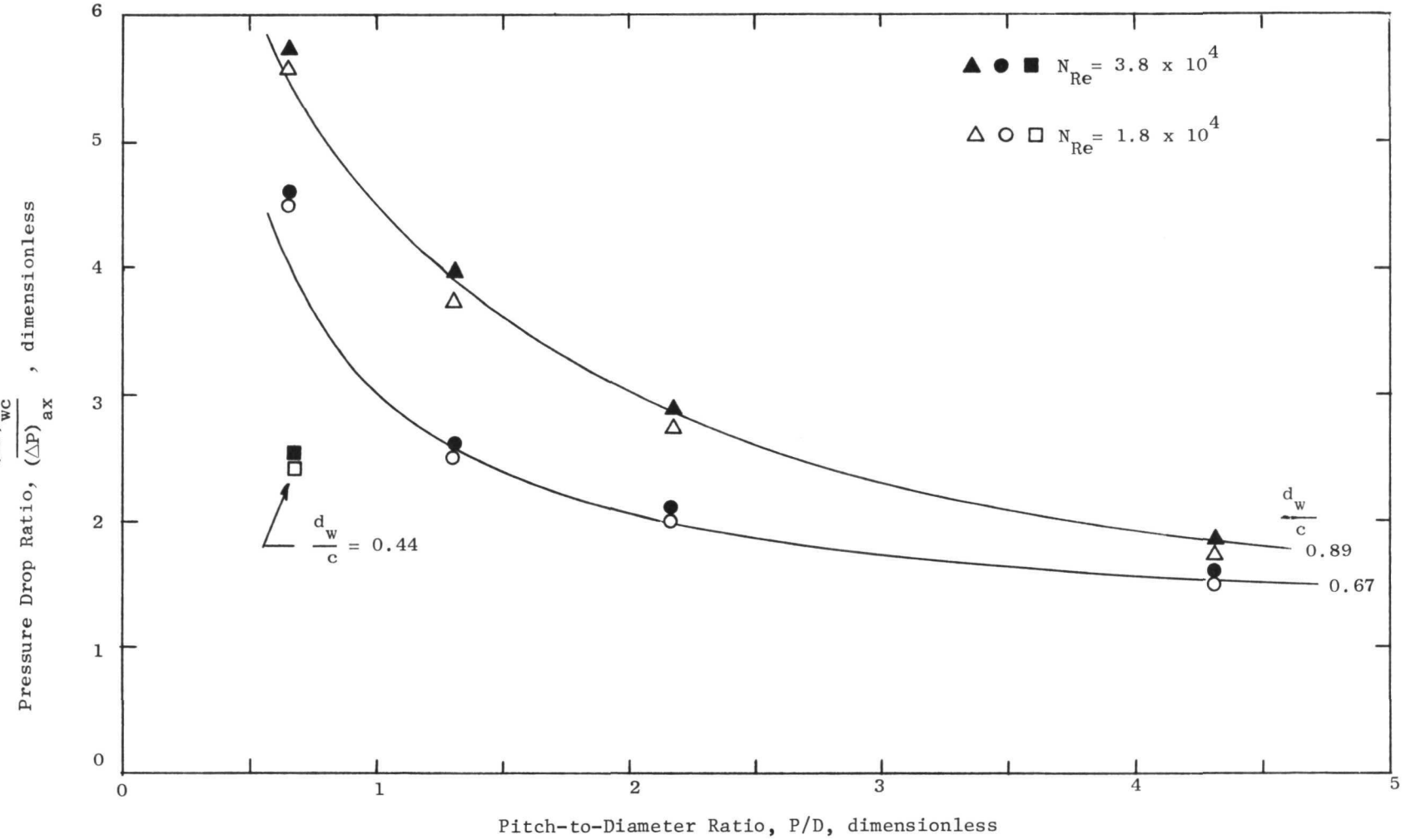

Figure 138. Pressure drop ratio $(\Delta P)_{\omega c}/(\Delta)_{Ax}$ vs turbulence promoter - P/D over a Reynolds number range $1.8\times10^4 \leq N_{RE} \leq 3.8\times10^4$.

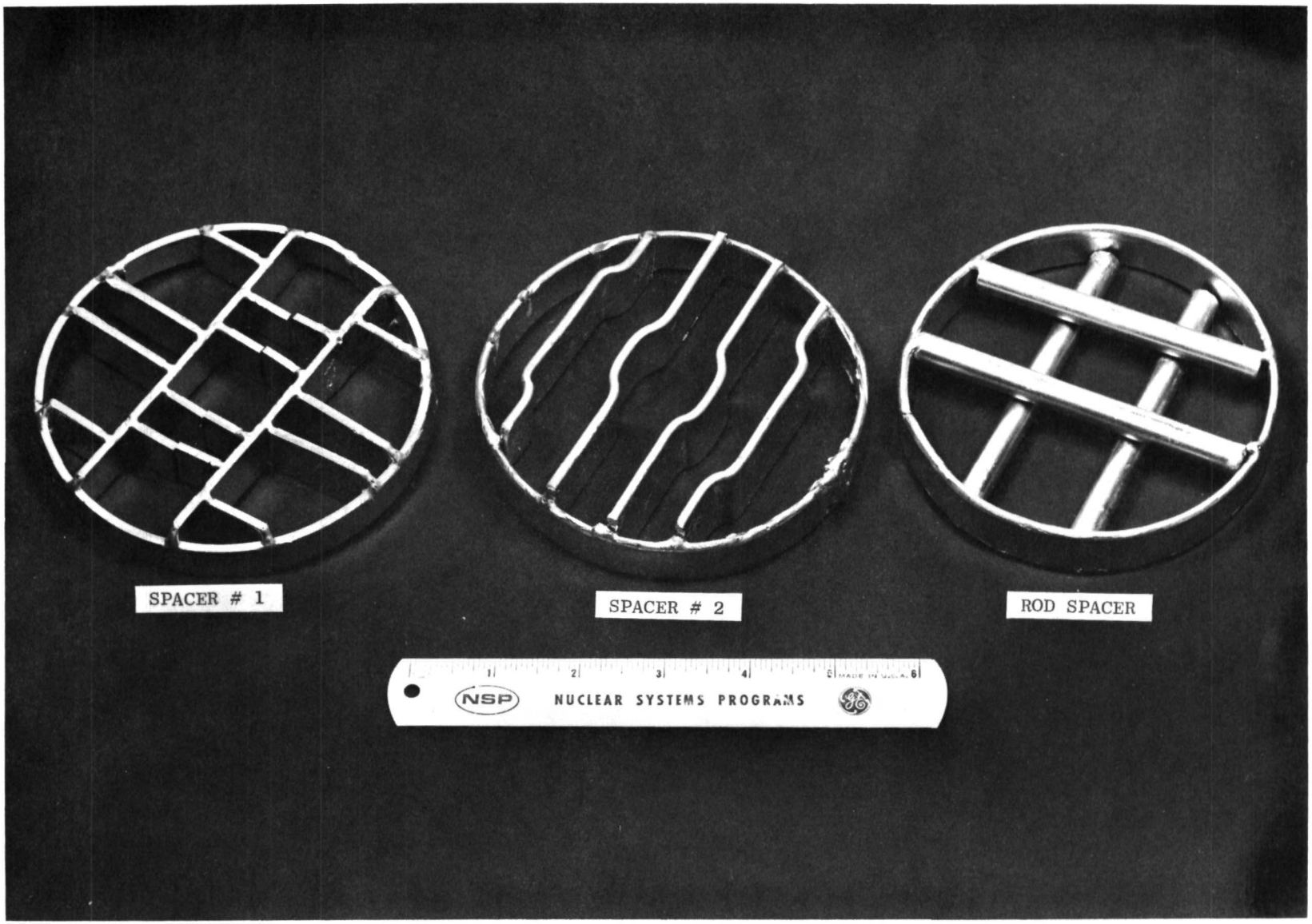

Figure 139. Photographic view of the tube supporting spacers.

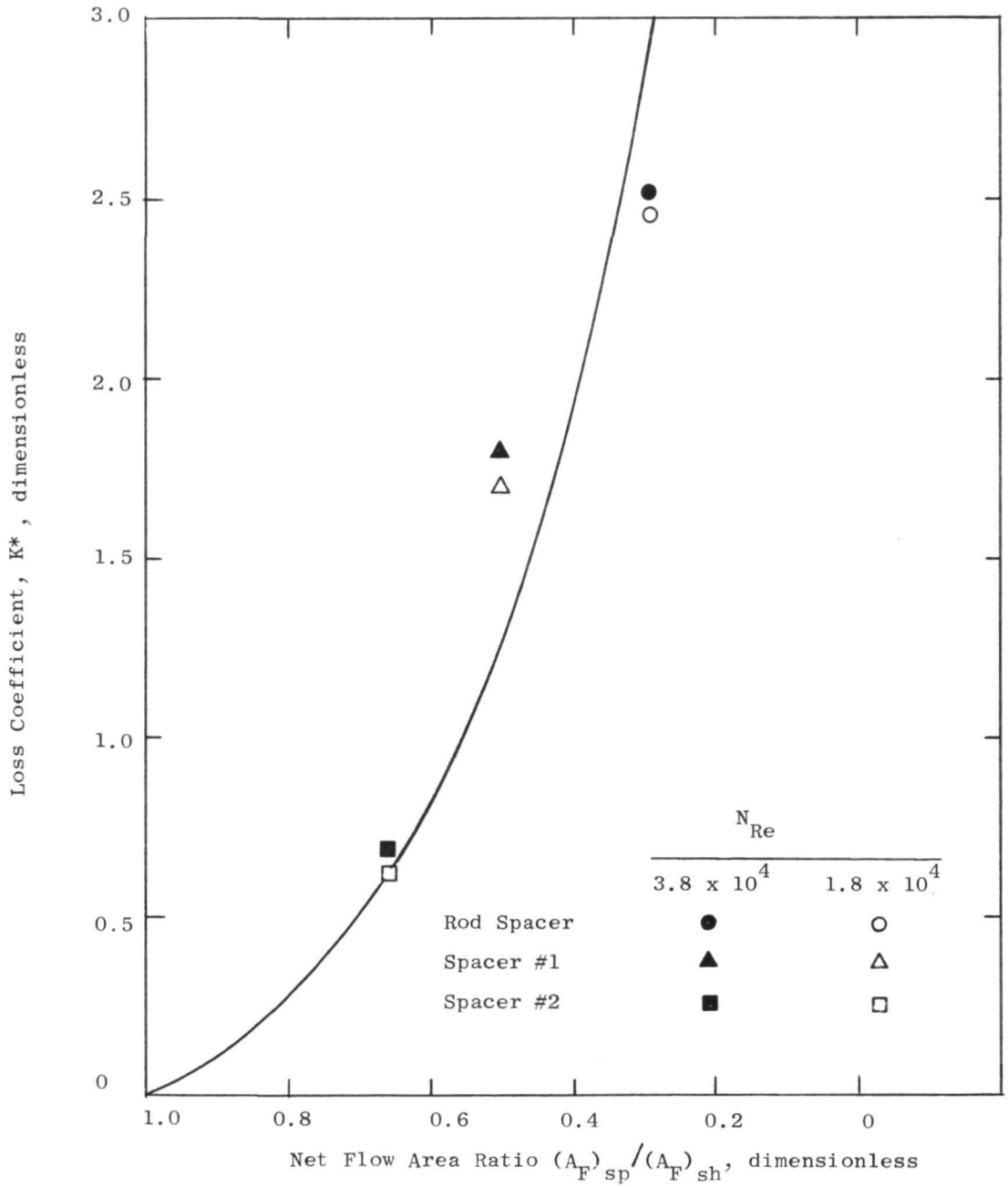

Figure 140. Spacer loss coefficients vs area ratio over a Reynolds number range of $1.8\times10^4 \leq N_{RE} \leq 3.8\times10^4$.

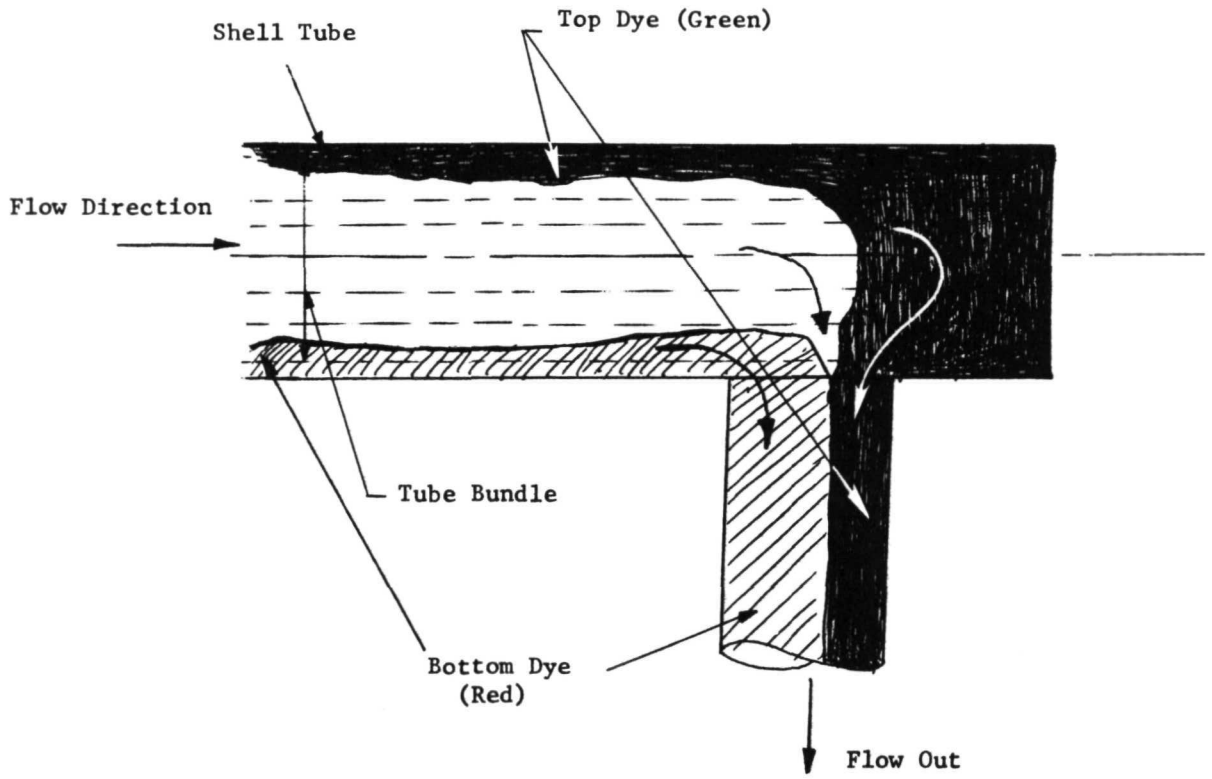

Figure 141. Illustration of poor mixing of shell side flow in the exit region.

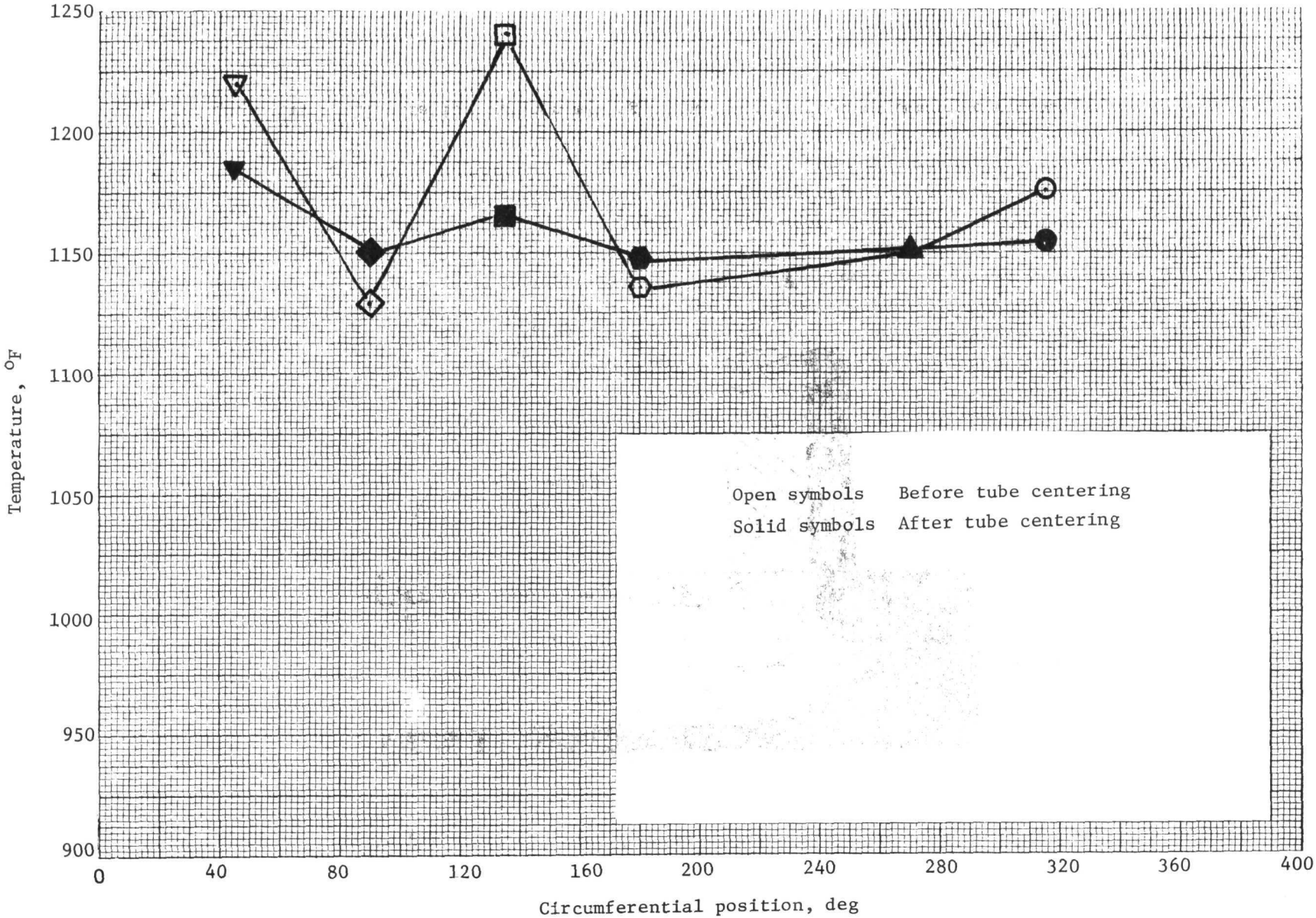

Figure 142. SNAP-8 refractory metal boiler showing temperature distribution at NaK exit.

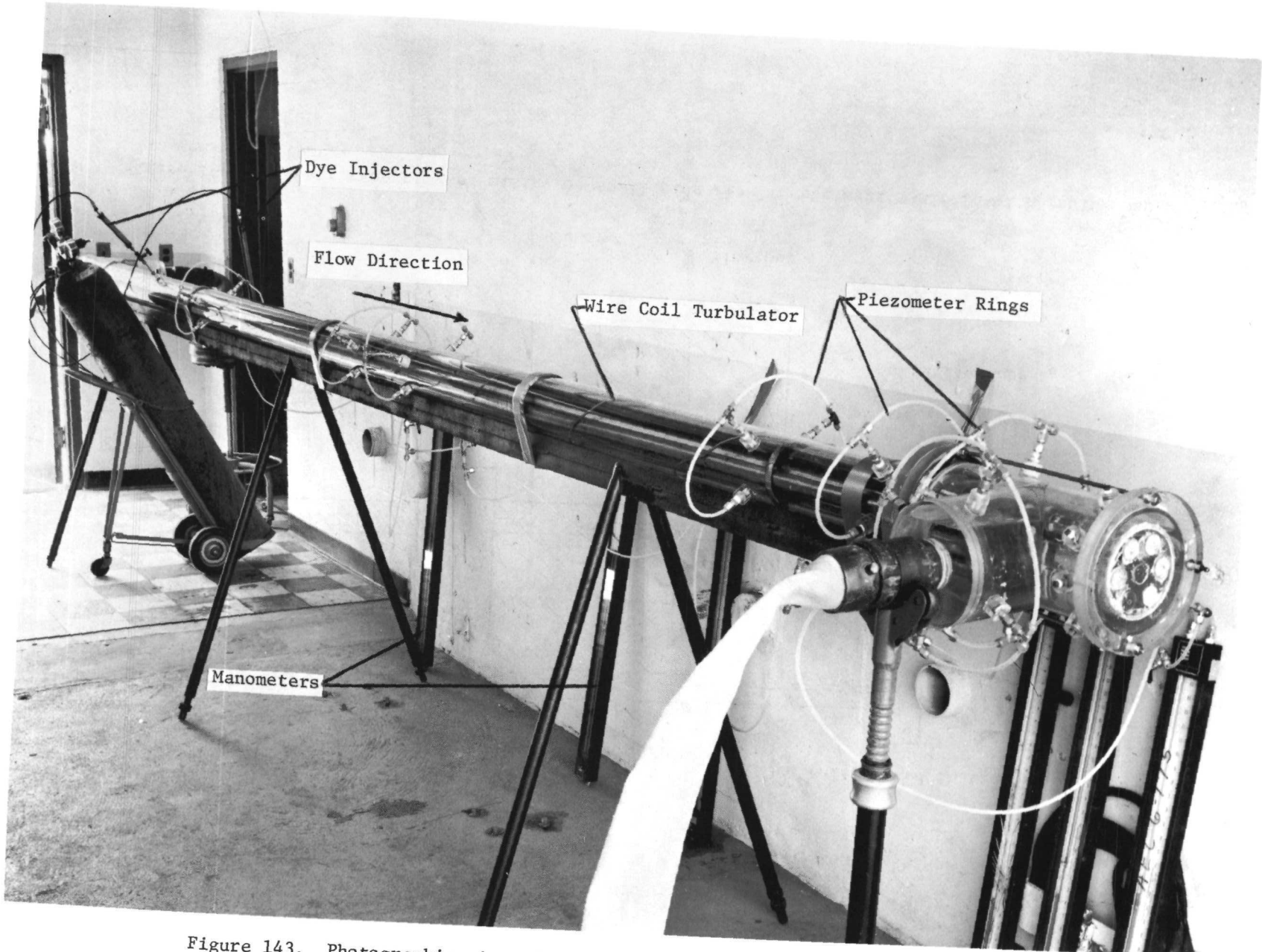

Figure 143. Photographic view of SNAP-8 boiler shell side hydraulic tests.

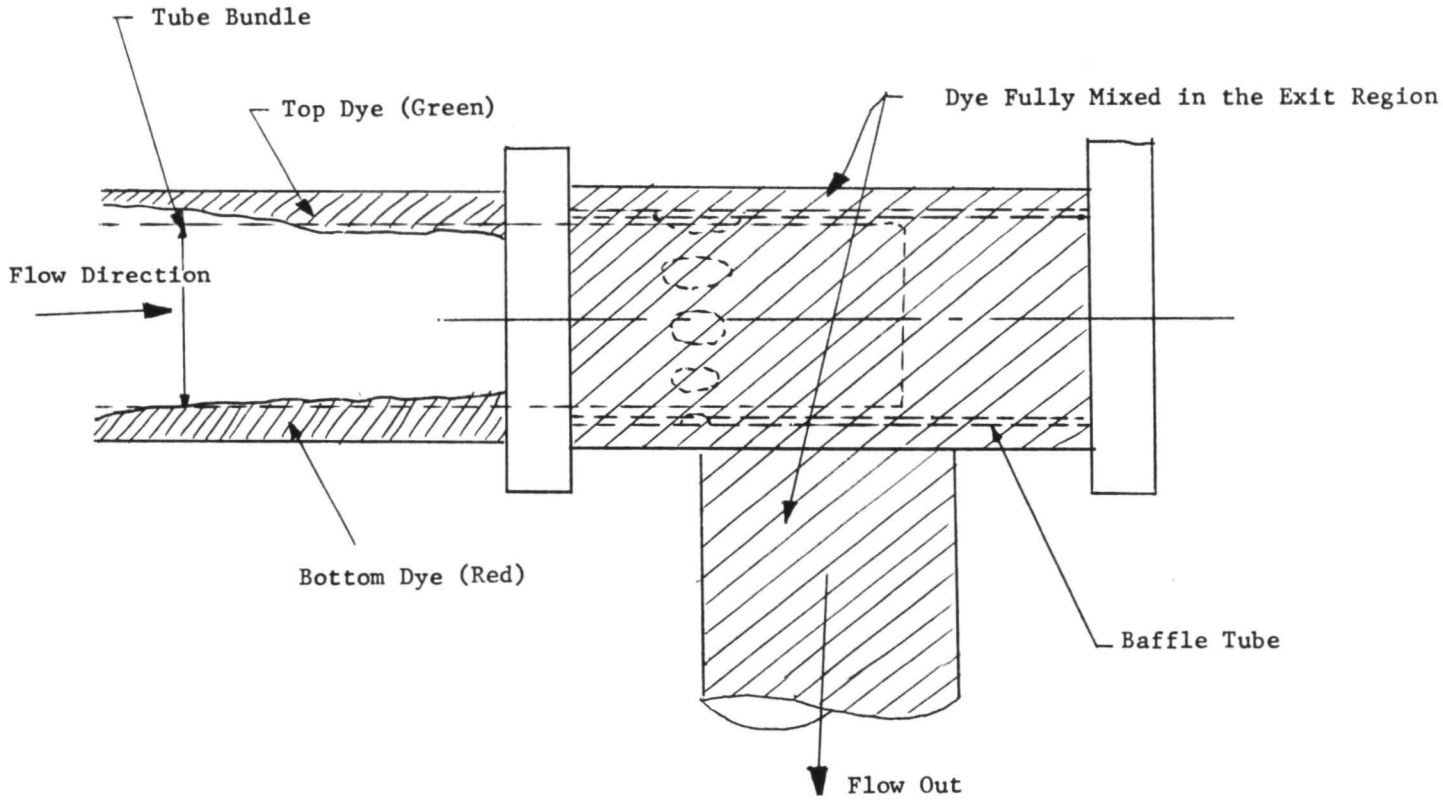

Figure 144. Illustration of good mixing of shell side flow in the exit manifold with radial ports in the shell tube.

XI. THE HIGH TEMPERATURE LOW CYCLE FATIGUE BEHAVIOR OF TANTALUM[14]

An investigation of the low cycle fatigue behavior of unalloyed tantalum was made in the temperature range between room temperature and 1400°F.

Uniaxial cyclic and monotonic tests were performed in a reverse loading machine. Induction heating was used in all experiments and a thermocouple was attached to the specimens for temperature control. The specimens were situated in a purified argon atmosphere. Load versus time (at constant crosshead rate) was recorded for the monotonic tests. For the cyclic tests, dimetral stresses were measured, recorded, and served as the basis for control of the test. An X-Y recorder was used to record hysteresis loops of load and diameter change. Additionally, both load and diameter were recorded as a function of time.

A total of 10 low cycle fatigue tests were completed and the results are included in Table VII. Stress range versus life results are shown in Figures 145, 146 and 147. At 600°F the stress range increases with cycling. The results at 1000°F show no clear trend. There is an increased strength of the material at 1100°F over 600°F for each diametral strain range and, as expected, the increased stress range for increasing levels of strain range. At 1350°F various frequencies and strain ranges are employed and the stress range is seen to decrease with decreasing frequency of strain rate and with decreasing strain range.

The primary purpose of this study was to obtain useful data for design purposes. Thus the procedure for generating equivalent stress amplitude curves for materials in Section III of the ASME Nuclear code were followed. This requires the conversion of the strain range data to equivalent stress amplitude or

$$\sigma_a = \frac{E\Delta\varepsilon_t}{2}$$

and introducing a safety factor of either 2 on stress amplitude or 20 on life, whichever is more conservative. A plot of σ_a versus N'_f (Figure 148) using the factor of 20 on life is shown for the three temperatures of the test.

It should be noted that the high value of equivalent stress does not mean the material is capable of supporting those stresses. Rather, they are the elastic equivalent of strains, which are obtained through elastic thermal stress analyses and apply only for fatigue life prediction.

TABLE VII

SUMMARY OF FATIGUE TEST RESULTS

Test No.	Temp., (°F)	Diametral Strain Amplitude (ε_d)	Plastic Strain Range ($\Delta\varepsilon_p$)	Total Strain Range ($\Delta\varepsilon_t$)	Stress Range ($\Delta\sigma$ psi)	Frequency CPM (ν)	Cycles to Failure (N_f)
4A	600	0.002	0.0069	0.0085	49,000	6.94	10,001
8A	600	0.01	0.0038	0.0409	70,000	.64	273
10A	1100	0.00187	0.0062	0.0083	53,900	3.40	12,230
9A	1100	0.01	0.00382	0.0409	70,400	2.62	487
8B	1100	0.00448	0.0165	0.0189	63,500	1.88	2,355
2B	1350	0.00466	0.0175	0.0195	52,000	9.25	1,912
3B	1350	0.01014	0.0393	0.0413	51,000	6.47	740
5B	1350	0.00194	0.00672	0.0084	43,500	7.34	17,500
6B	1350	0.01	0.0389	0.0407	47,000	0.60	1,177
7B	1350	0.00448	0.0170	0.0185	40,000	1.88	2,387

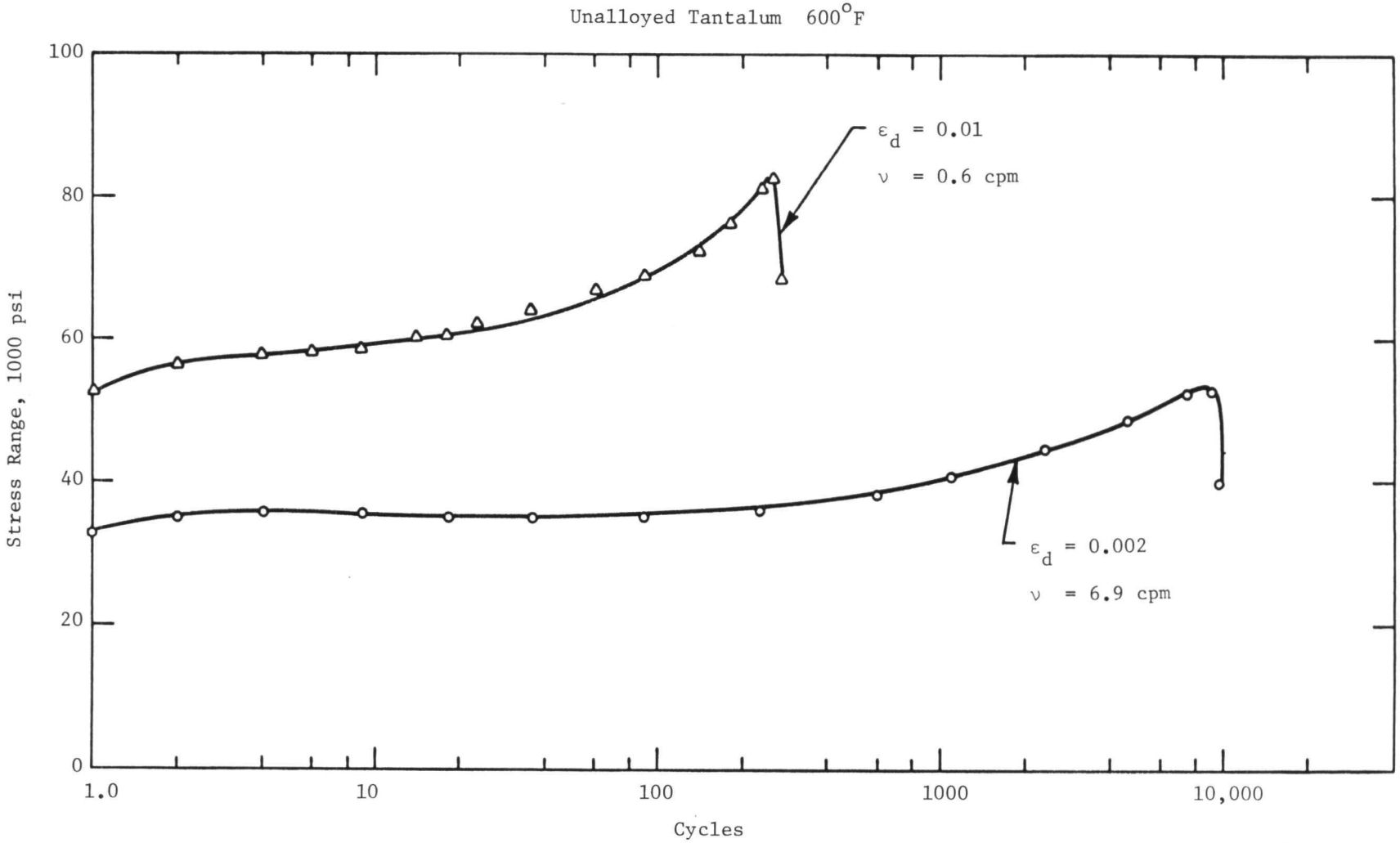

Figure 145. Stress range versus cycles for tantalum at 600° F.

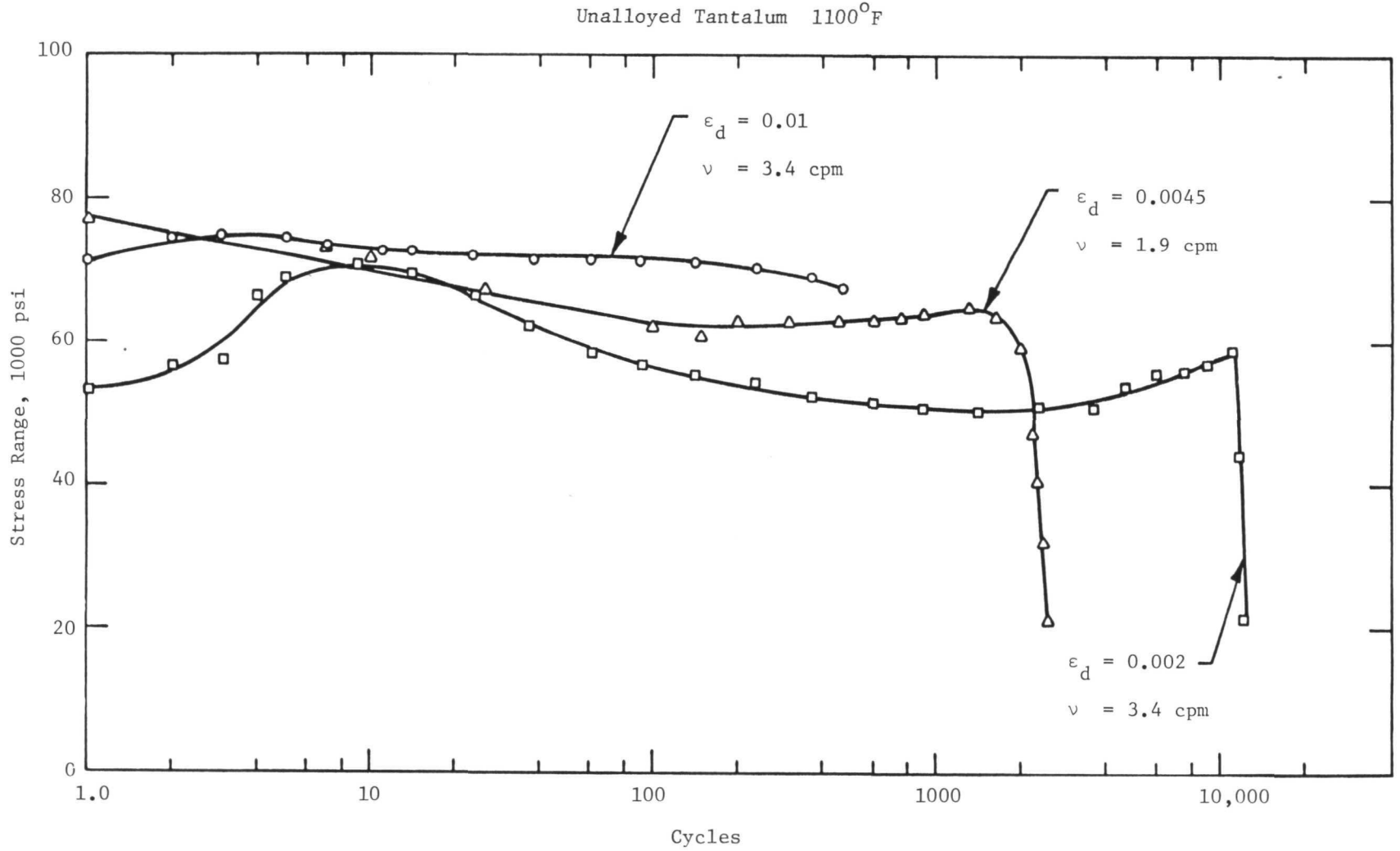

Figure 146. Stress range versus cycles for tantalum at 1100° F.

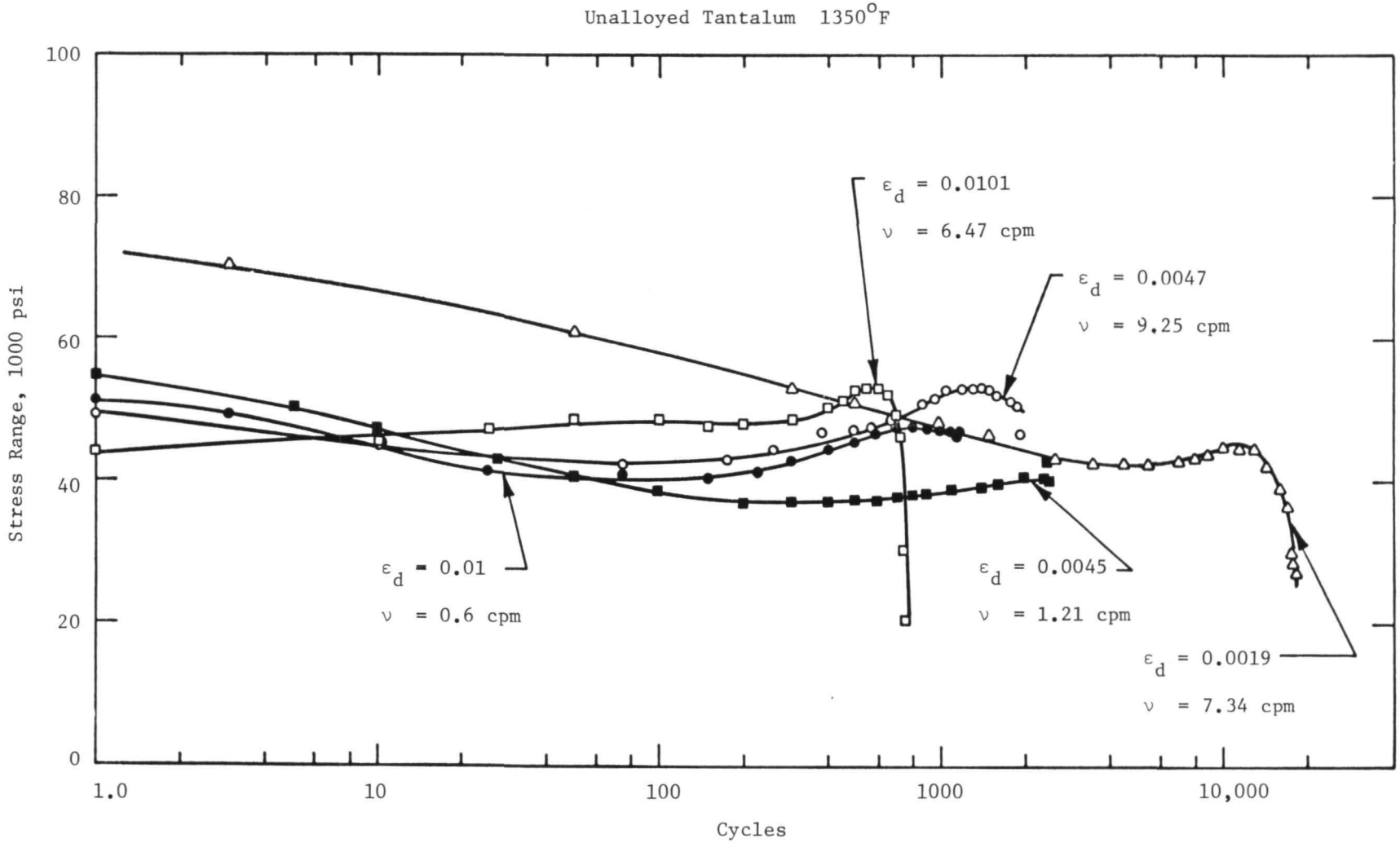

Figure 147. Stress range versus cycles for tantalum at 1350° F.

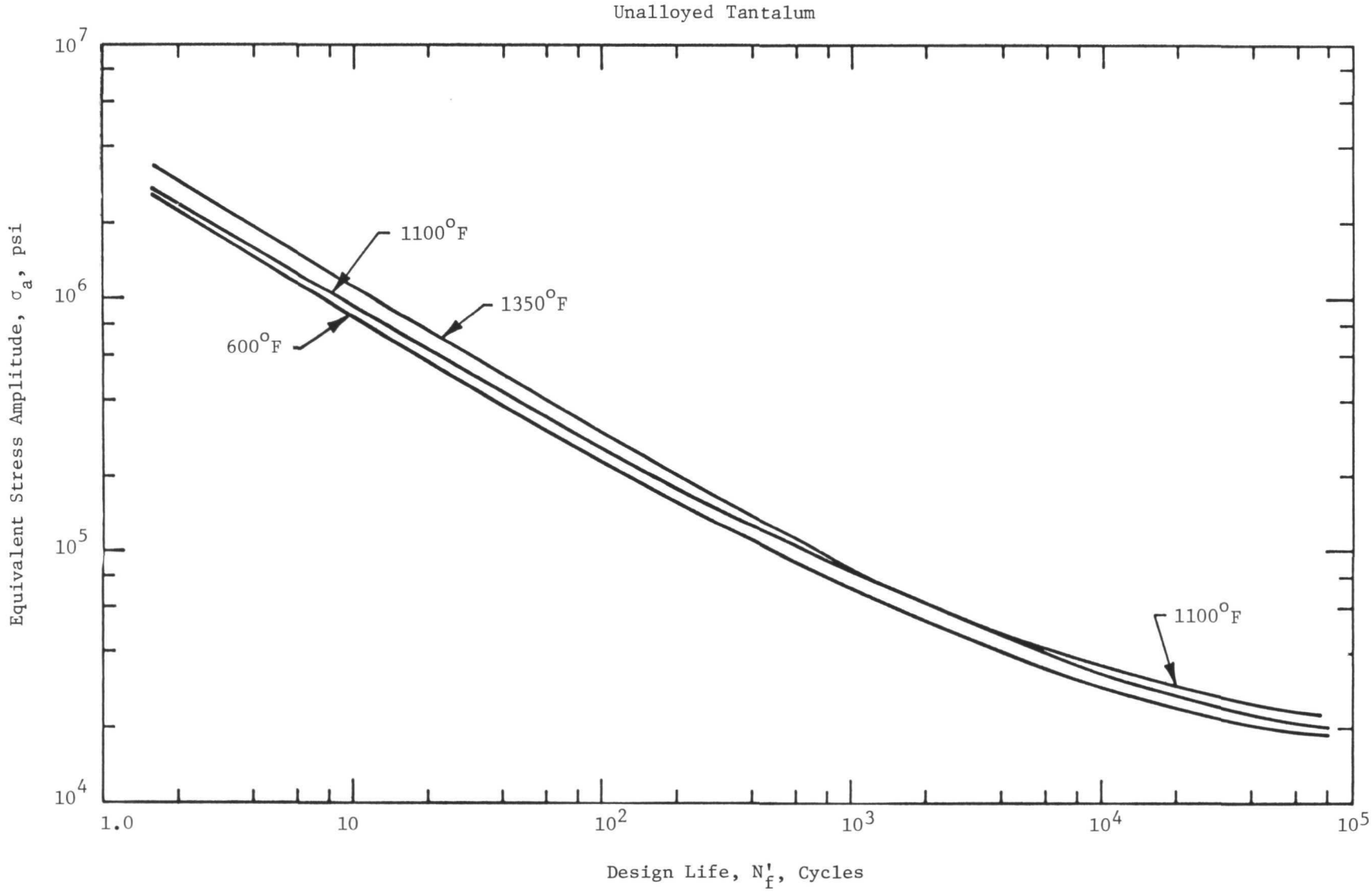

Figure 148. Equivalent stress amplitude versus design life of tantalum.

XII. SINGLE TUBE TESTS[15]

At the completion of the facility modification and while awaiting the delivery of boiler SN-1, it was decided to check out the facility with a single tube boiler, designed and built by GE-NSP using the heat transfer and two phase pressure drop relationship developed under previous NASA contracts NAS 3-2528 and NAS 3-9426. The application of these relationships led to a boiler which was 16 feet long as compared to the 35 foot boiler tube length based on non-wetting. Complete details on the design and testing of the single tube boiler may be found in a separate Topical Report, Reference 5.

The GE-NSP single tube boiler, shown in Figure 149, is different from previous single tube boilers in that instead of a plug followed by a wire coil, it contains a helical insert of P/D = 2.0 for 12 feet and a wire coil (P/D = 0.88) for the last 4 feet. The helical insert (Figure 150) has a tubular centerbody which is instrumented to permit measurement of local mercury temperatures thus giving some insight as to what is occurring within the boiler.

Initial operation of the boiler demonstrated immediate "wetting" and none of the conditioning problems previously reported. Test results which illustrate the performance of this boiler over the anticipated reactor temperature control band are shown in Figures 151, 152, and 153. These are boiler temperature profiles showing the measured temperature distribution on the shell and the measured local mercury temperature in the helix. In addition, the four basic heat transfer regimes have been denoted, namely, subcooled liquid, nucleate boiling, transition-film boiling and superheat. Note that superheated vapor is supplied to the turbine over the entire reactor control band and that the exit mercury vapor temperature remains within 30°F of the NaK inlet temperature as the NaK temperature varies 50°F. It is interesting to note that the stability of the boiler without the plug (Figures 154, 155, 156) meets the stability requirements for SNAP-8.[16] Shown in Figure 157 is a combined plot of a single tube data point with data from the multitube boiler test. The performance of the single tube boiler without the plug duplicates the multitube data.

These data are reported in Reference 15 but the primary significance is that the mercury boiler performance can be predicted and it is possible to shorten the length of the SNAP-8 refractory metal boiler and thus permit the design of a lighter, more compact boiler.

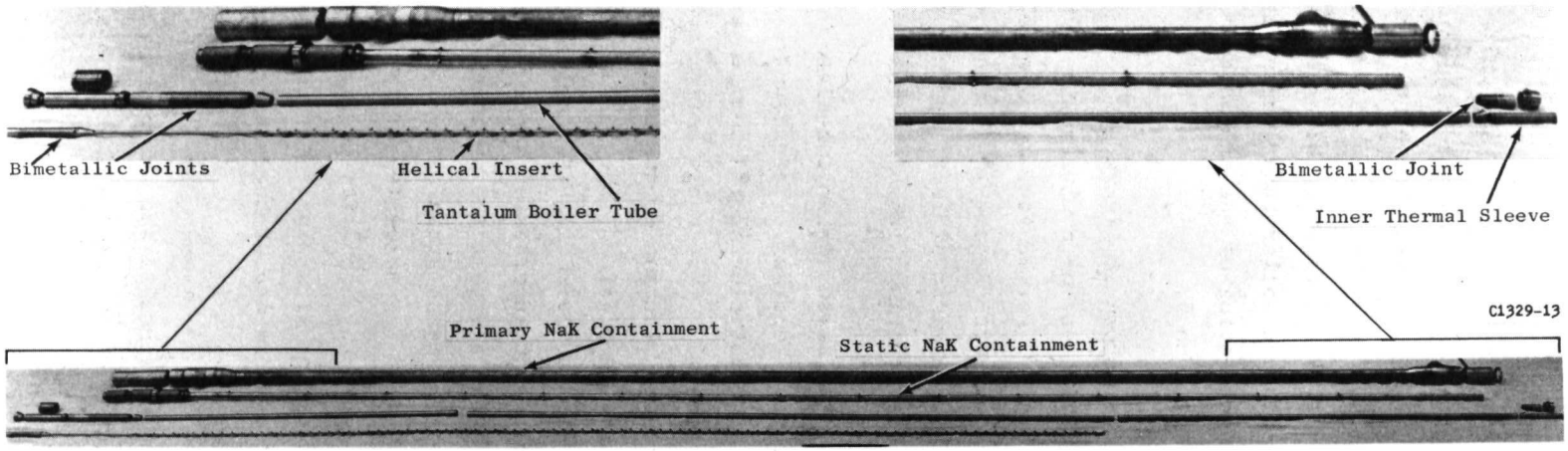

Figure 149. SNAP-8 single tube test boiler.

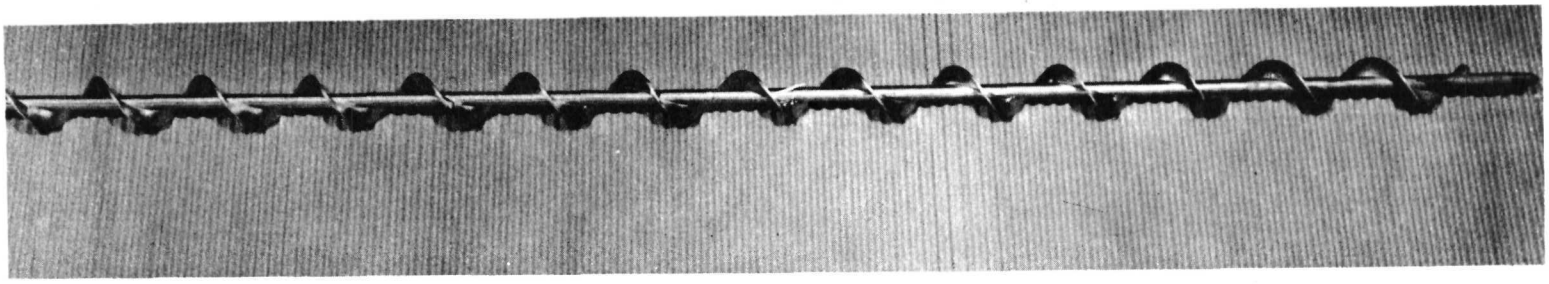

Figure 150. Helical insert P/D 2.0, 1/4-inch center body.

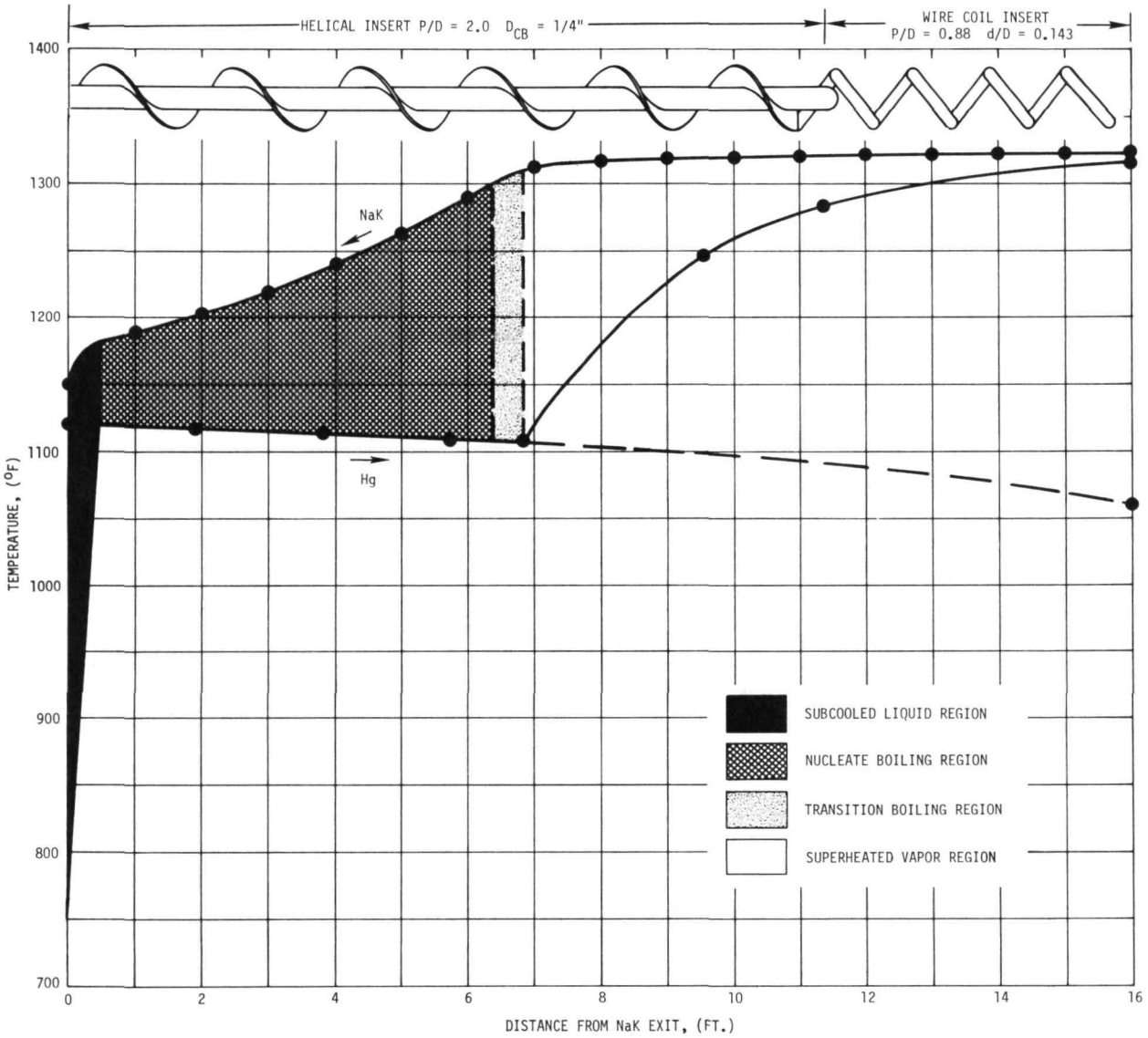

NaK SIDE

FLOW RATE	1.888	LB/SEC
POWER	65.9	KW
ΔT_{IB}	63	°F
ΔT_{EXIT}	5.6	°F
INLET TEMP.	1327	°F
EXIT TEMP.	1156	°F

MERCURY SIDE

LIQUID FLOW RATE	.469	LB/SEC
EXIT PRESSURE	254	PSIA
INLET PRESSURE	345	PSIA
PRESSURE DROP	91	PSI
EXIT SAT. TEMP.	1060	°F
INLET SAT. TEMP.	1120	°F
DEGREE OF VAPOR SUPERHEAT	256	°F

Figure 151. Single tube boiler test results.

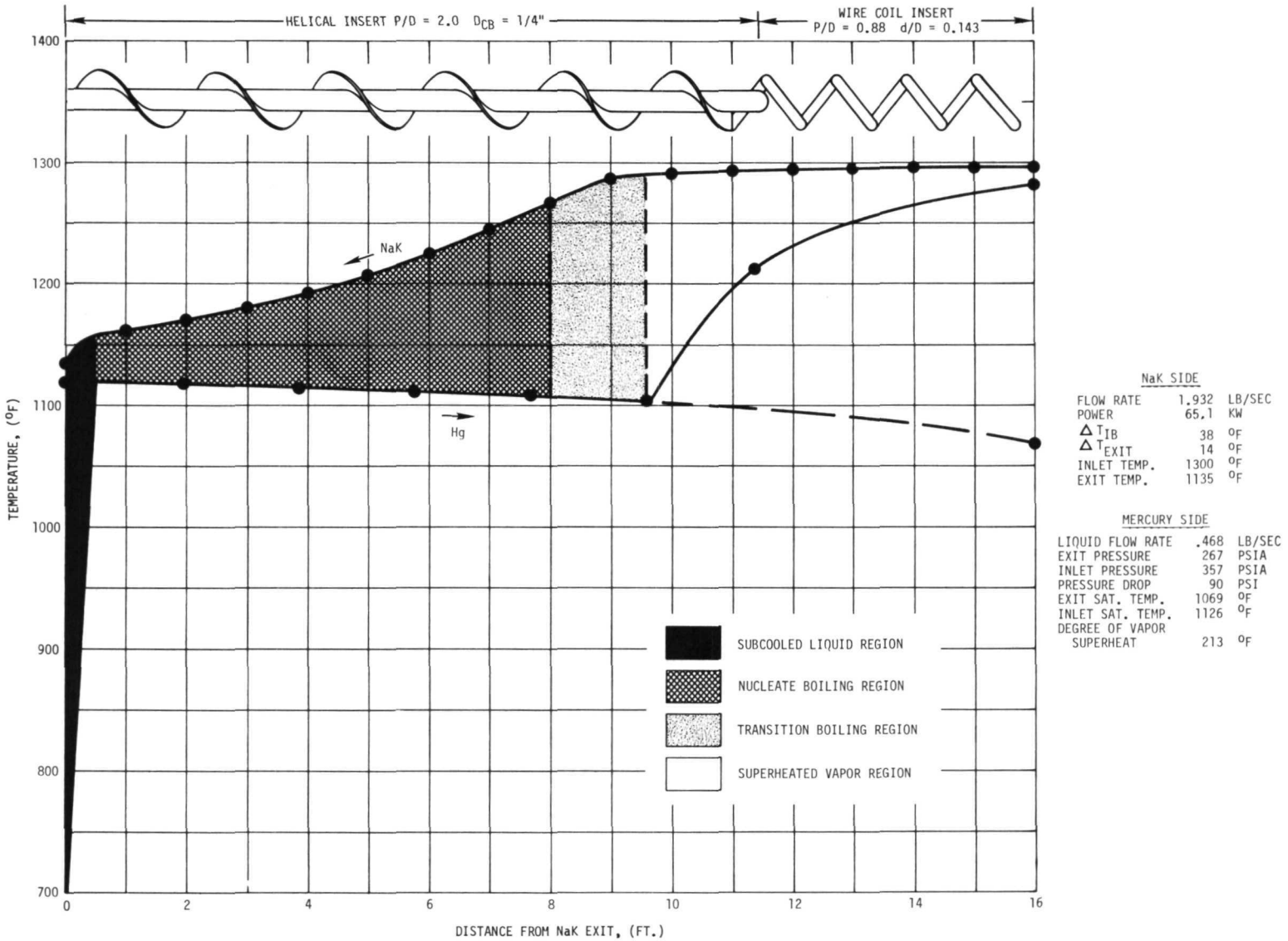

Figure 152. Single tube boiler test results.

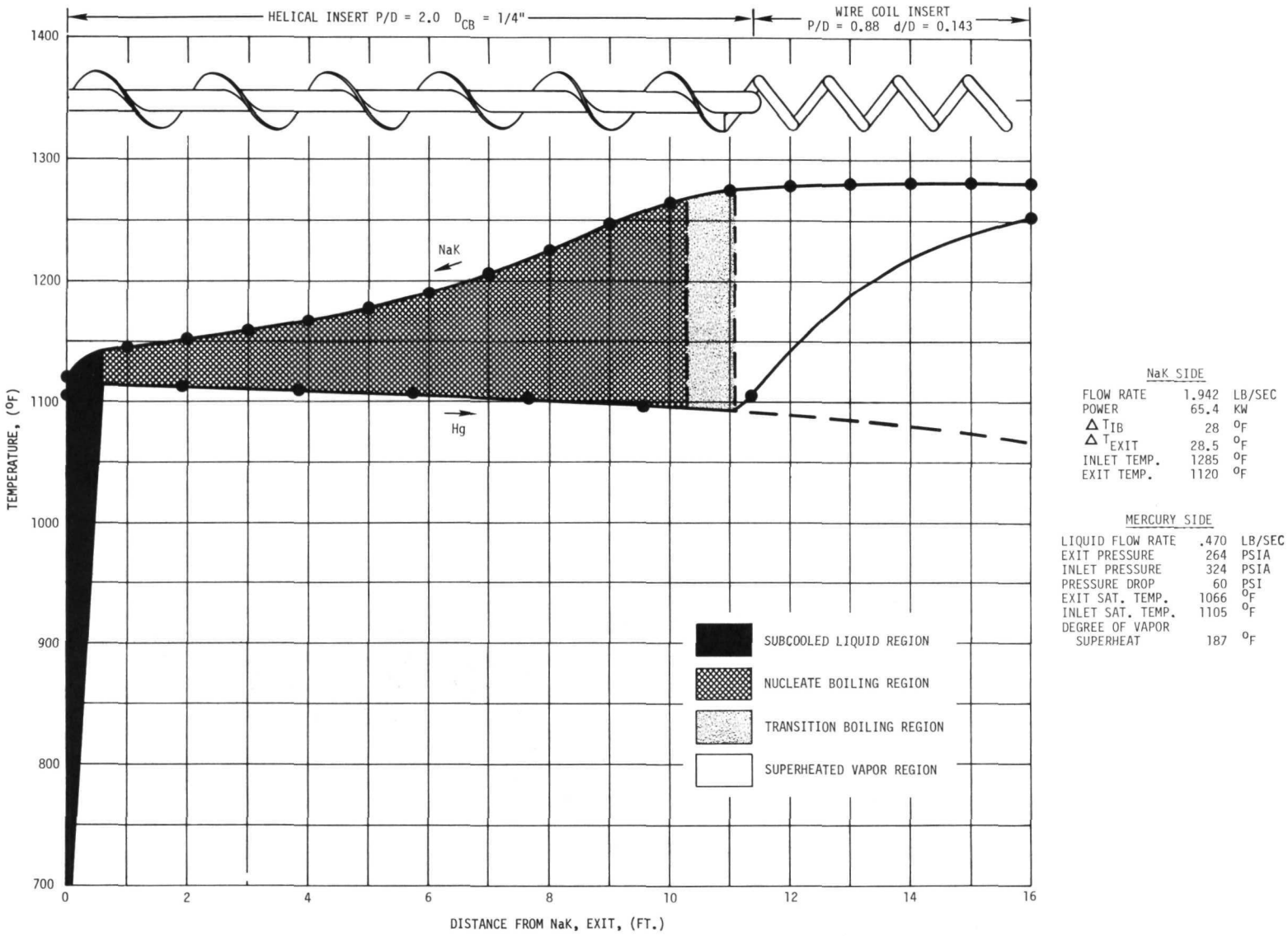

NaK SIDE

FLOW RATE	1.942	LB/SEC
POWER	65.4	KW
ΔT_{IB}	28	°F
ΔT_{EXIT}	28.5	°F
INLET TEMP.	1285	°F
EXIT TEMP.	1120	°F

MERCURY SIDE

LIQUID FLOW RATE	.470	LB/SEC
EXIT PRESSURE	264	PSIA
INLET PRESSURE	324	PSIA
PRESSURE DROP	60	PSI
EXIT SAT. TEMP.	1066	°F
INLET SAT. TEMP.	1105	°F
DEGREE OF VAPOR SUPERHEAT	187	°F

Figure 153. Single tube boiler test results.

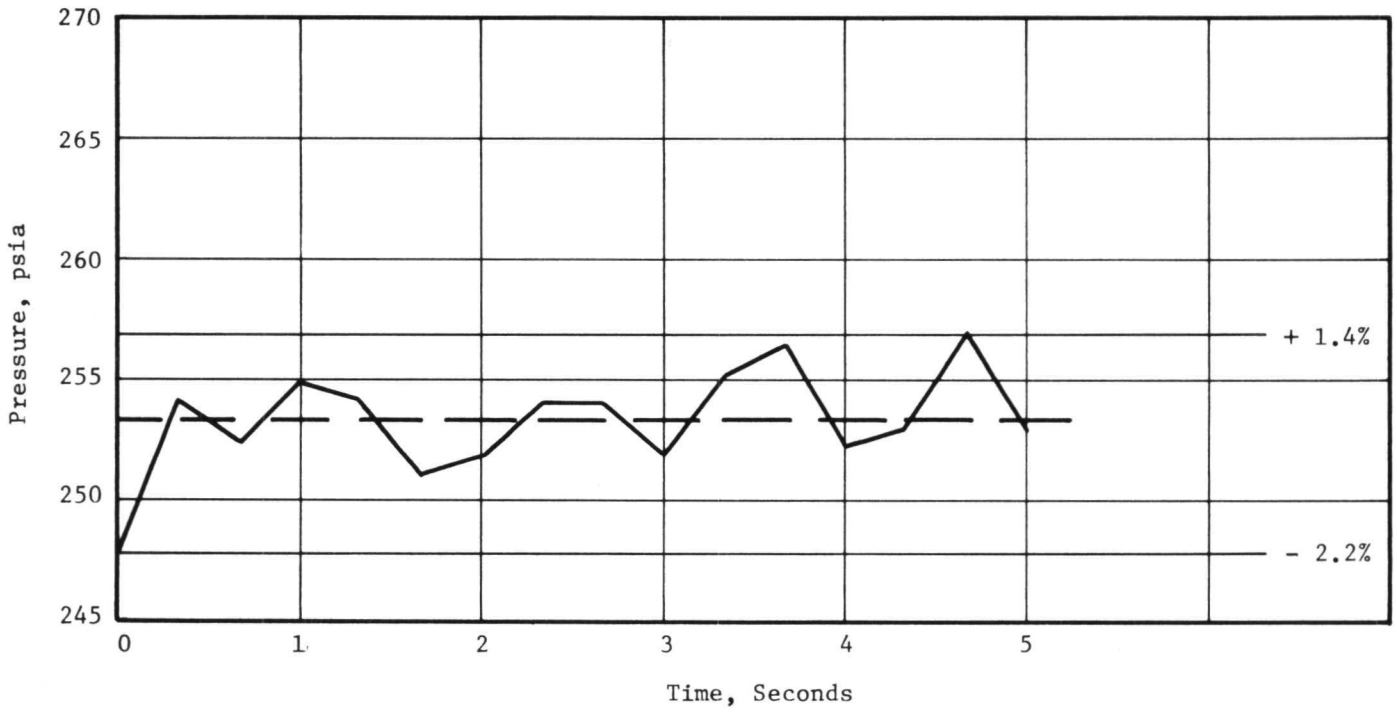

Figure 154. Pressure fluctuation vs time Hg exit.

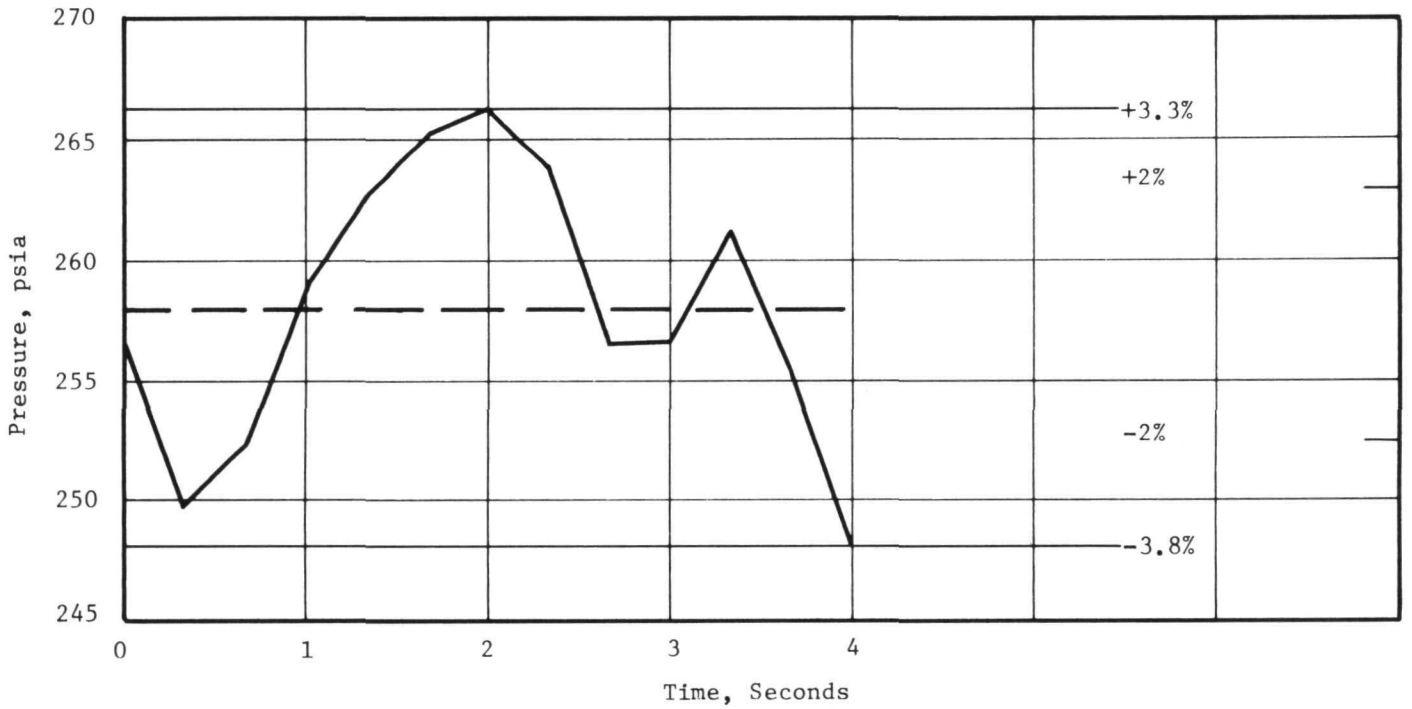

Figure 155. Pressure fluctuation vs time Hg exit.

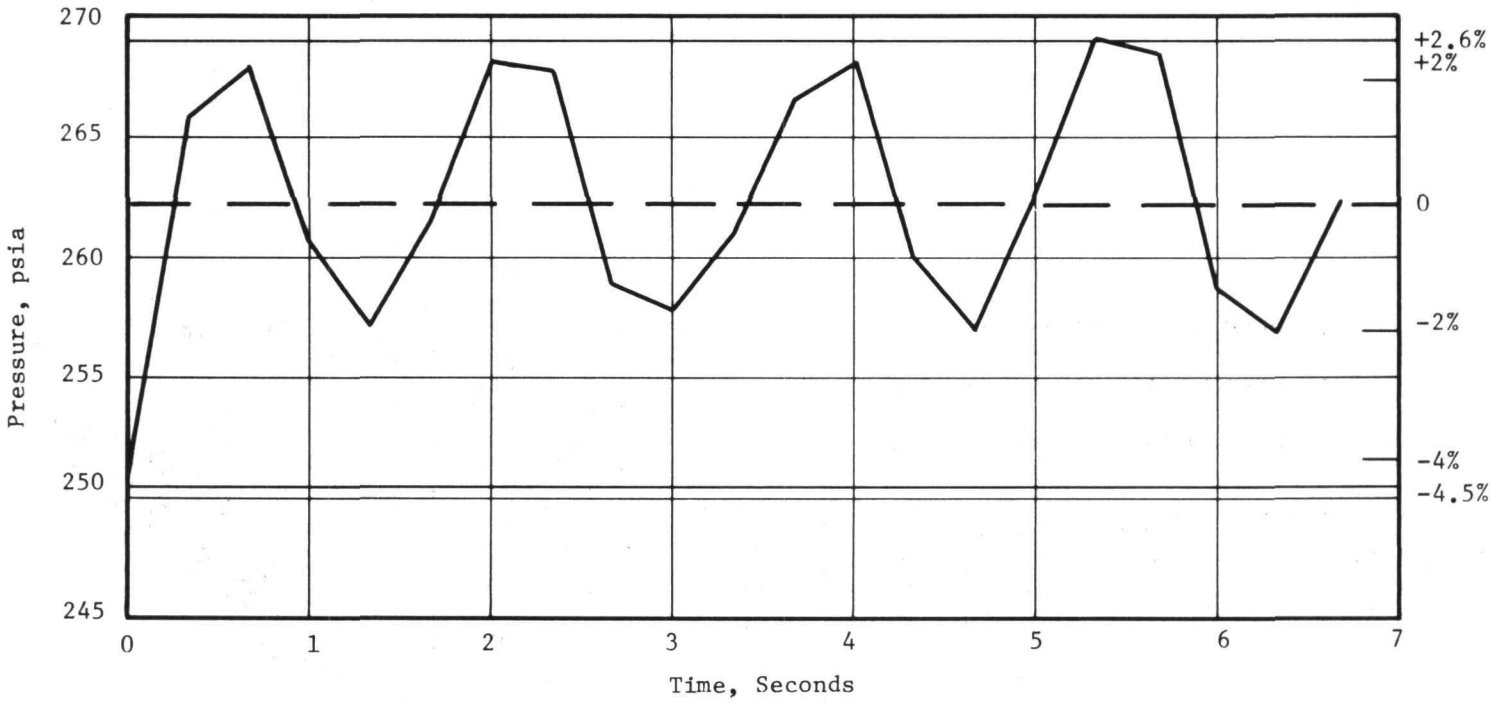

Figure 156. Pressure fluctuation vs time Hg exit.

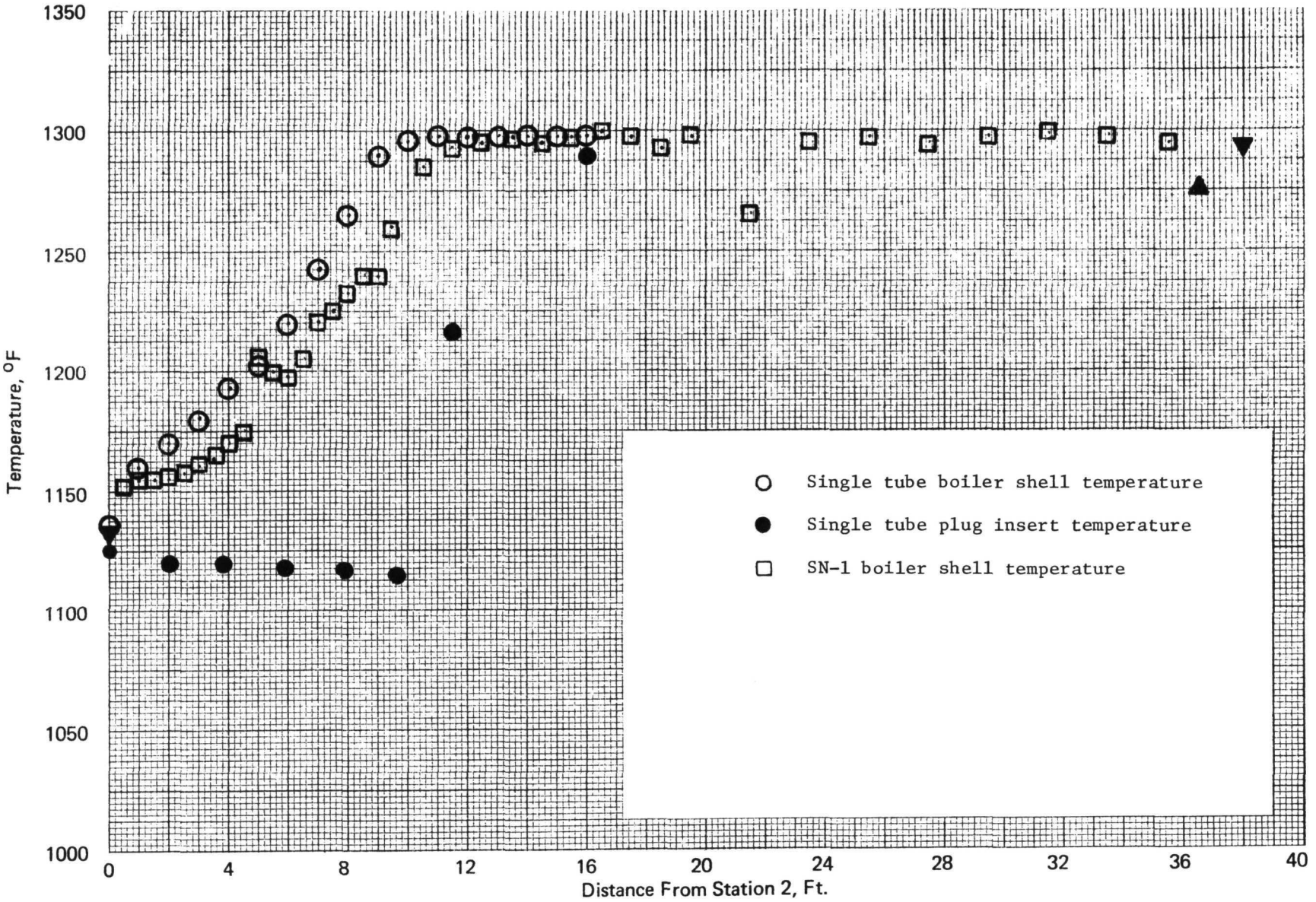

Figure 157. A comparison of SN-1 results with single tube results.

XIII. THE DEVELOPMENT OF AN ELECTROMAGNETIC PUMP FOR MERCURY[17]

An electromagnetic mercury pump was developed by General Electric for the SNAP-8 refractory boiler test to prevent the contamination of the refractory metals used in the boiler fabrication by the lubricating oils associated with the bearings of the SNAP-8 centrifugal pumps.

A total of 10 different pump ducts were designed, fabricated and tested. The results of these tests were used to design and fabricate the pump used in the test of the SNAP-8, SN-1 boiler. A pump duct design is shown in Figure 158 which shows the mercury entering the pump at the suction end and being accelerated to the outside wall where it spins until the vaned diffuser forces the mercury back to the core of the duct. The mercury is again accelerated to the outside wall where it spins through another diffuser and is accelerated back to the wall. The outlet of the pump consists of a flat plate welded to the straightening vanes located in the end caps with an annulus between the plate and the duct wall. The mercury passes through this annulus where it is straightened out and forced to the exit. The performance curve for this pump is shown in Figure 159.

Althouth this pump was not very efficient (approximately 1%) it thoroughly demonstrated the need for keeping the mercury side of the facility containment free.

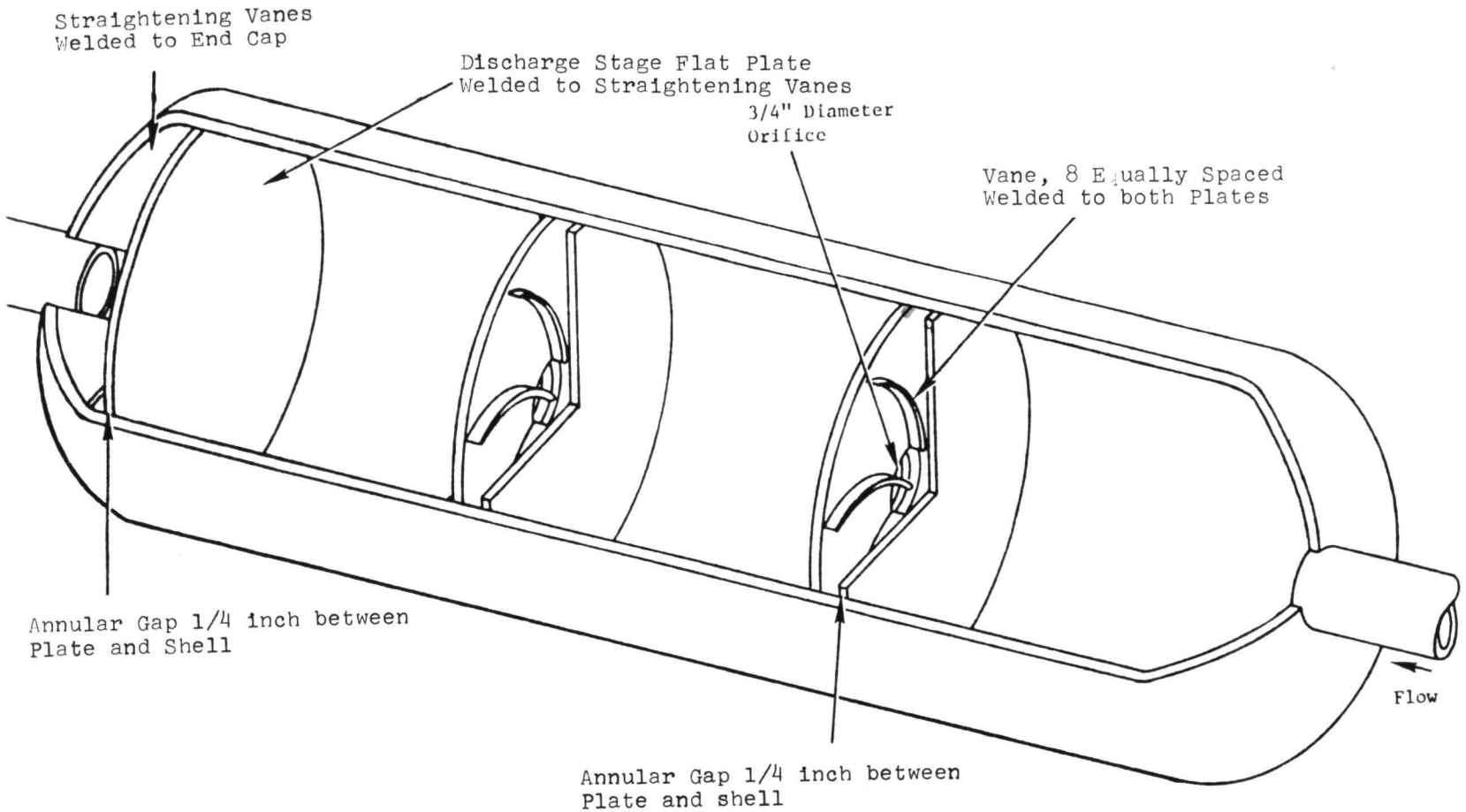

Figure 158. Pump duct - mercury centrifugal EM pump.

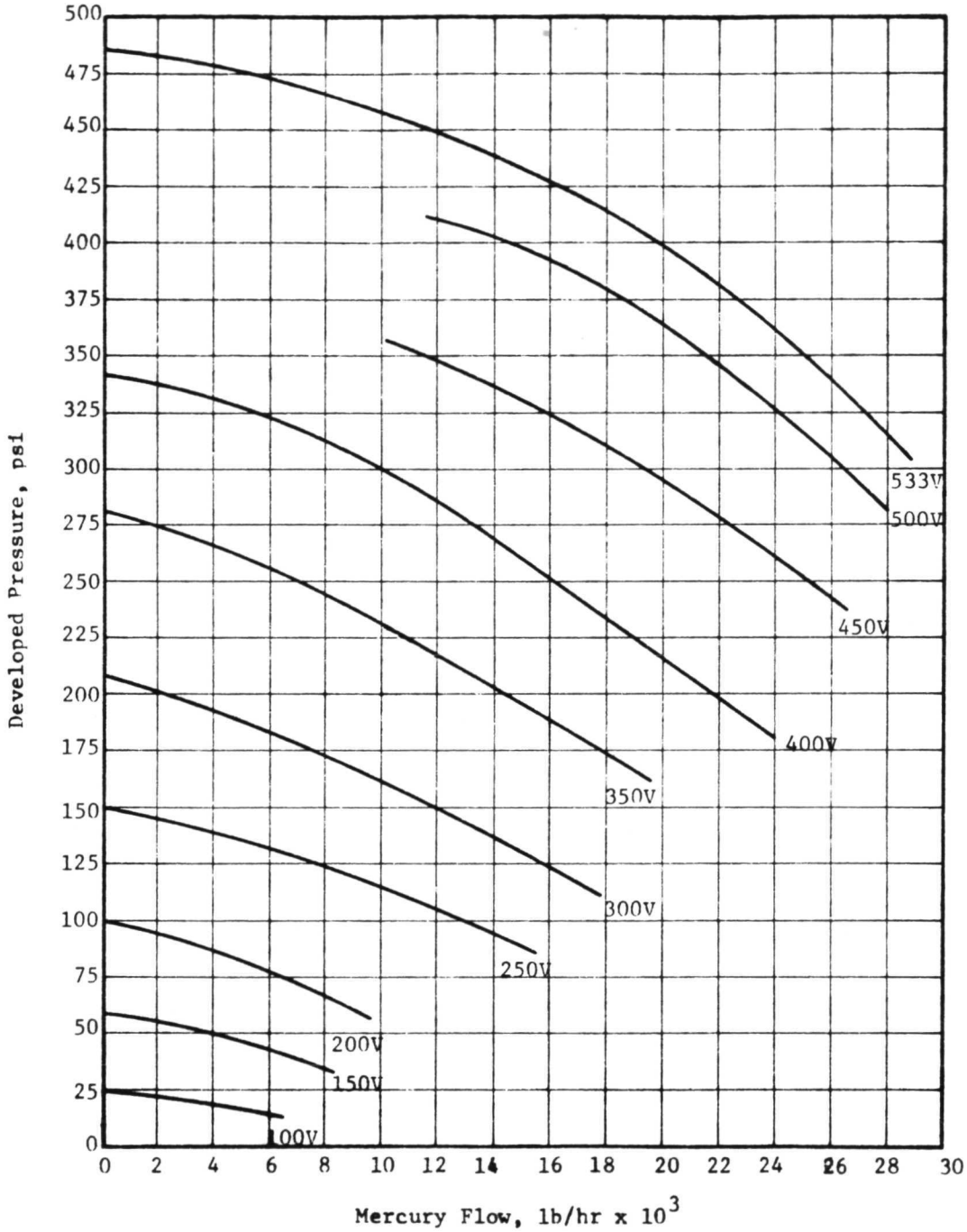

Figure 159. Performance curve - pump duct modification no. 9.

REFERENCES

1. Hackett, H. N., "Mercury for the Generation of Light, Heat and Power," Transactions of the ASME, Vol. 64, No. 7, Oct. 1942, pp. 647-656.

2. Sellers, A. J., "Evaluation of SB-1 Boiler Test Results and Proposed Design Modification," AGCTM-4921, 68-550, Aerojet Gen. Corp., Oct. 1968.

3. Fuller, R. A., Schnacke, A. W., "The Development of a Mercury Centrifugal Electromagnetic Pump," Proposed NASA Contractor Report.

4. Gertsma, L. W., Thollot, P. A., Medwid, D. W., and Sellers, A. J., "The Double Containment Tantalum - Stainless Steel SNAP-8 Boiler," Intersociety Energy Conversion Engineering Conference, Vol. 1, IEEE, 1968, pp. 363-369.

5. Brooks, R. D., "Summary of the February 17, 1968 SNAP-8 Refractory Metal Boiler Failure," GESP-118, April 1968.

6. Fuller, R. A., Zimmermann, W. F., "Summary of the May 31, 1968 SNAP-8 Refractory Metal Boiler Shell Failure, GESP-280, June 1969.

7. Fuller, R. A., Zimmermann, W. F., "Summary of the August 20, 1968 SNAP-8 Boiler Shell Failure," GESP-231, June 1969.

8. Harrison, R. W., "The Corrosion of Oxygen Contaminated Tantalum in NaK," Topical Report No. 1, GESP-138, Jan. 1969.

9. Engel, L. B., Jr., Harrison, R. W., "The Corrosion Resistance of Tantalum, T-111, and Cb-1Zr to Mercury at 1200° F," Topical Report No. 2, GESP-199, April 1969.

10. Harrison, R. W., Hendrixson, W. C., "The Evaluation of the SNAP-8, SN-1 Boiler," Topical Report No. 3, GESP-550 (NASA CR-72814), Nov. 1970.

11. Thompson, S. R., "Mercury Thermal Shock Testing of $2\frac{1}{2}$-Inch-Diameter Bimetallic Joints for SNAP-8 Applications," GESP-587 (NASA CR-72829), April 1971.

12. Hsia, E. S., Fuller, R. A., "The Shell Side Hydraulic Tests of a Full Scale SNAP-8 Multiple Tube Boiler," Topical Report No. 5, GESP-589 (NASA CR-72830), Jan. 1971.

13. Furman, E. R., Brooks, R. D., Harrison, R. W., "The Experimental Evaluation of Tantalum/Stainless Steel Mercury Boilers for the SNAP-8 System," Intersociety Energy Conversion Engineering Conference, Las Vegas, Nevada, Sept. 21-24, 1970, NASA TM X-52841, 1970.

14. Coffin, L. F., Jr., LaForce, R., Berning, R. F., "The High Temperature Low Cycle Fatigue Behavior of Tantalum," Topical Report No. 6, GESP-595, March 1971.

15. Hsia, E. S., "Analysis and Testing of a Single Tube Mercury Boiler," Topical Report No. 7, GESP-650 (NASA CR-72897), Sept. 1971.

16. Chalpin, E. S., "Final Design Review of BRDC Boiler Numbers 4 and 6 for PCS-G," Aerojet Gen. Corp., Oct. 1968.

NASA-Langley, 1974 E-7672

NATIONAL AERONAUTICS AND SPACE ADMINISTRATION
WASHINGTON, D.C. 20546

OFFICIAL BUSINESS
PENALTY FOR PRIVATE USE $300

SPECIAL FOURTH-CLASS RATE
BOOK

POSTAGE AND FEES PAID
NATIONAL AERONAUTICS AND
SPACE ADMINISTRATION
451

U.S.MAIL

POSTMASTER: If Undeliverable (Section 158 Postal Manual) Do Not Return

"The aeronautical and space activities of the United States shall be conducted so as to contribute . . . to the expansion of human knowledge of phenomena in the atmosphere and space. The Administration shall provide for the widest practicable and appropriate dissemination of information concerning its activities and the results thereof."

—NATIONAL AERONAUTICS AND SPACE ACT OF 1958

NASA SCIENTIFIC AND TECHNICAL PUBLICATIONS

TECHNICAL REPORTS: Scientific and technical information considered important, complete, and a lasting contribution to existing knowledge.

TECHNICAL NOTES: Information less broad in scope but nevertheless of importance as a contribution to existing knowledge.

TECHNICAL MEMORANDUMS: Information receiving limited distribution because of preliminary data, security classification, or other reasons. Also includes conference proceedings with either limited or unlimited distribution.

CONTRACTOR REPORTS: Scientific and technical information generated under a NASA contract or grant and considered an important contribution to existing knowledge.

TECHNICAL TRANSLATIONS: Information published in a foreign language considered to merit NASA distribution in English.

SPECIAL PUBLICATIONS: Information derived from or of value to NASA activities. Publications include final reports of major projects, monographs, data compilations, handbooks, sourcebooks, and special bibliographies.

TECHNOLOGY UTILIZATION PUBLICATIONS: Information on technology used by NASA that may be of particular interest in commercial and other non-aerospace applications. Publications include Tech Briefs, Technology Utilization Reports and Technology Surveys.

Details on the availability of these publications may be obtained from:

SCIENTIFIC AND TECHNICAL INFORMATION OFFICE

NATIONAL AERONAUTICS AND SPACE ADMINISTRATION

Washington, D.C. 20546